Geography of the Physical Environment

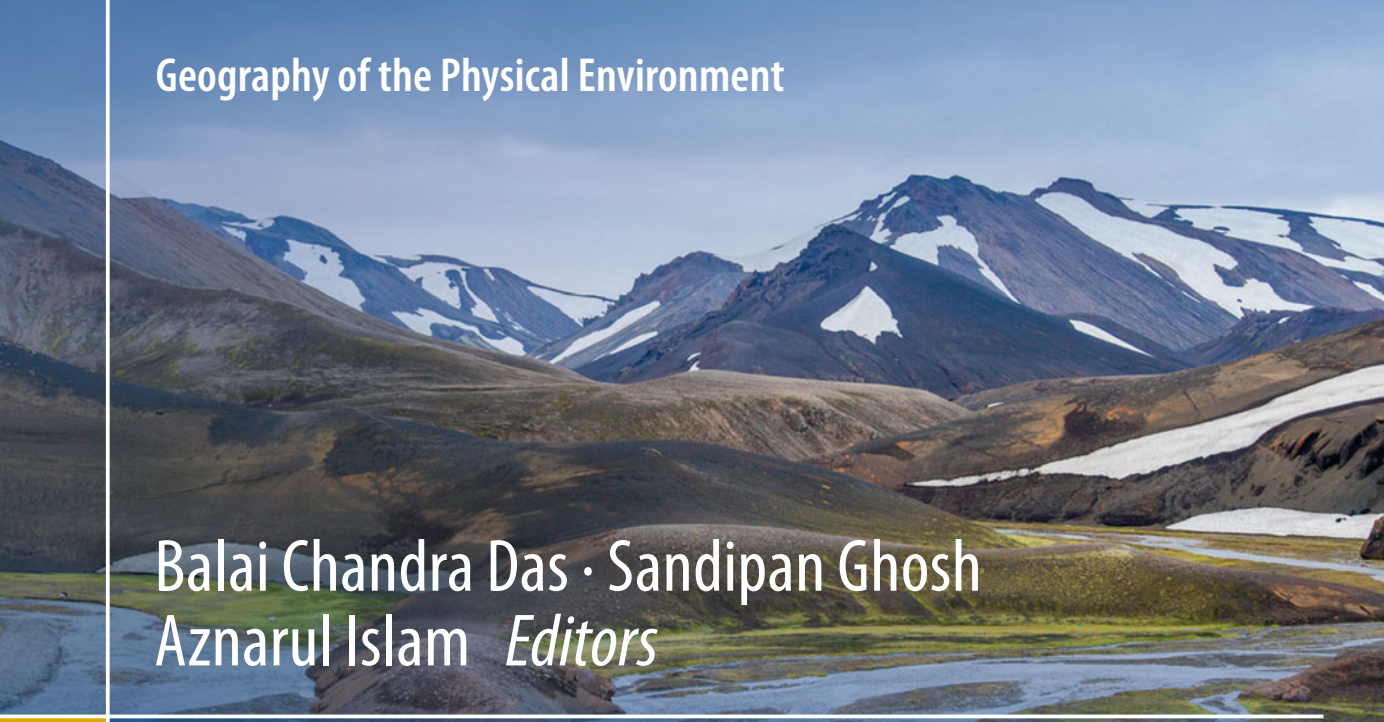

Balai Chandra Das · Sandipan Ghosh
Aznarul Islam *Editors*

Quaternary Geomorphology in India

Case Studies from the Lower Ganga Basin

Springer

Geography of the Physical Environment

The *Geography of the Physical Environment* book series provides a platform for scientific contributions in the field of Physical Geography and its sub-disciplines. It publishes a broad portfolio of scientific books covering case studies, theoretical and applied approaches as well as novel developments and techniques in the field. The scope is not limited to a certain spatial scale and can cover local and regional to continental and global facets. Books with strong regional focus should be well illustrated including significant maps and meaningful figures to be potentially used as field guides and standard references for the respective area.

The series appeals to scientists and students in the field of geography as well as regional scientists, landscape planners, policy makers, and everyone interested in wide-ranging aspects of modern Physical Geography. Peer-reviewed research monographs, edited volumes, advance and undergraduate level textbooks, and conference proceedings covering the major topics in Physical Geography are included in the series. Submissions to the Book Series are also invited on the theme 'The Physical Geography of…', with a relevant subtitle of the author's/editor's choice.

More information about this series at http://www.springer.com/series/15117

Balai Chandra Das · Sandipan Ghosh
Aznarul Islam
Editors

Quaternary Geomorphology in India

Case Studies from the Lower Ganga Basin

Springer

Editors
Balai Chandra Das
Department of Geography
Krishnagar Government College
Krishnagar, Nadia
India

Aznarul Islam
Department of Geography
Aliah University
Kolkata
India

Sandipan Ghosh
Department of Geography
Chandrapur College
Barddhaman
India

ISSN 2366-8865 ISSN 2366-8873 (electronic)
Geography of the Physical Environment
ISBN 978-3-319-90426-9 ISBN 978-3-319-90427-6 (eBook)
https://doi.org/10.1007/978-3-319-90427-6

Library of Congress Control Number: 2018939144

Cover image by Sonja Weber, München

Printed on acid-free paper

This Springer imprint is published by the registered company Springer International Publishing AG part of Springer Nature
The registered company address is: Gewerbestrasse 11, 6330 Cham, Switzerland

Preface

Welcome to '*Quaternary Geomorphology in India—Case Studies from the Lower Ganga Basin*'. This book presents a novel collection of field-based empirical studies on the quaternary geomorphology of the Lower Ganga basin. A wide range of topics in relation to the region is covered in this volume.

The journey of the volume started with the invitation before the geomorphologists all over India to contribute to 'Quaternary Geomorphology in India' in August 2015. We received huge response from authors. Hence, we are very much thankful to authors who contributed to this volume. Their thoughtful contributions made this volume possible. We are equally thankful to those compadre authors also, whose works are not appeared as chapters in this book but who made us blessed with number of articles rich in noesis. We express our deep gratitude towards our teachers, students and colleagues and family members. Lastly, we acknowledge our indebt to Springer International Publishing especially to Dr. Michael Leuchner the responsible editor of 'Geography of the Physical Environment' for association with us and providing their prestigious pages for manuscripts of our competent authors.

West Bengal, India
May 2018

Balai Chandra Das
Sandipan Ghosh
Aznarul Islam

Contents

Editors and Contributors

About the Editors

Balai Chandra Das holds a post-graduate degree in Geography from the University of Burdwan and a Ph.D. in Geography from the University of Calcutta, and has published more than 30 research articles in recognized international journals. He has served as an editorial board member for two international journals and as a reviewer for five more. He is the main editor of the book 'Neo-Thinking on Ganges–Brahmaputra Basin Geomorphology', Springer International Publishing, Switzerland. His current research focus is on fundamental geomorphology, in particular on rivers and lakes.

Sandipan Ghosh is an Applied Geographer with post-graduate and M.Phil. degrees in Geography from the University of Burdwan. He has published more than 40 international and national research papers in various geography and geoscience journals. He has authored a book entitled 'Flood Hydrology and Risk Assessment: Flood Study in a Dam-Controlled River of India' and edited a book entitled 'Neo-Thinking on Ganges–Brahmaputra Basin Geomorphology'. He is one of the editors of the Asian Journal of Spatial Science and has served as a reviewer for various international geoscience journals. He is a lifetime member of the International Association of Hydrological Sciences (IAHS), the Eastern Geographical Society (EGS) and the Indian Geographical Foundation (IGF). His principal research fields include various dimensions of fluvial geomorphology, flood geomorphology, Quaternary geology and laterite studies. Currently, he is working on the gully geomorphology and soil loss estimation on the lateritic

terrain of West Bengal and the Quaternary geomorphology and active tectonics of the Bengal Basin, West Bengal.

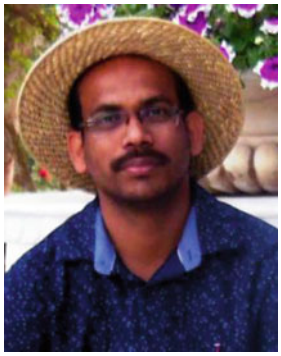

Dr. Aznarul Islam is an Applied Fluvial Geomorphologist with M.Sc. degree in Geography from Kalyani University, West Bengal and an M.Phil and Ph.D. in Geography from the University of Burdwan, West Bengal. He is currently an Assistant Professor at the Department of Geography, Aliah University, Kolkata. Previously, he was engaged in the West Bengal Education Service (WBES) in the Department of Geography, Barasat Govt. College, West Bengal. He has published more than 20 research papers in various national and international journals, edited volumes and conference proceedings. He co-edited the book 'Neo-Thinking on Ganges–Brahmaputra Basin Geomorphology', Springer International Publishing, Switzerland and has served as a reviewer for several geography and geoscience journals. Currently, he is editorial board member of several international and national journals. He is a life member of the Foundation of Practising Geographers (FPG), Kolkata, and National Association of Geographers, India (NAGI), New Delhi. He has served as an Assistant Convenor of the annual seminar of the Foundation of Practising Geographers since 2016. In addition, he is Project Director of the Indian Council of Social Science Research (ICSSR)-sponsored major research project 'Assessment of Socio-Economic Vulnerability of Flood Victims and Preparation of Community-Based Disaster Management Plan Using Social Engineering: A Study of Murshidabad District, West Bengal'. His principal areas of research include channel shifting, river bank erosion, floods and river decaying of the Ganga–Brahmaputra delta.

Contributors

Sunando Bandyopadhyay Department of Geography, University of Calcutta, Kolkata, West Bengal, India

Debika Banerji Department of Geography, Visva-Bharati University, Santiniketan, West Bengal, India

Suman Deb Barman Department of Geography, The University of Burdwan, Bardhaman, West Bengal, India

Subhankar Bera Department of Geography, University of Kalyani, Kalyani, Nadia, West Bengal, India

Sumantra Sarathi Biswas Centre for the Study of Regional Development, Jawaharlal Nehru University, New Delhi, India; Department of Geography, Sukumar Sengupta Mahavidyalaya, Keshpur, West Bengal, India

Balai Chandra Das Department of Geography, Krishnagar Government College, Krishnagar, West Bengal, India

Prasanta Kumar Ghosh Department of Geography, The University of Burdwan, Burdwan, West Bengal, India

Sandipan Ghosh Department of Geography, Chandrapur College, Barddhaman, West Bengal, India

Subhendu Ghosh Department of Geography and Disaster Management, Tripura University, Agartala, India

Sanat Kumar Guchhait Department of Geography, The University of Burdwan, Barddhaman, West Bengal, India

Aznarul Islam Department of Geography, Aliah University, Kolkata, West Bengal, India

Narayan Chandra Jana Department of Geography, The University of Burdwan, Burdwan, West Bengal, India

Nabendu Sekhar Kar Department of Geography, Shahid Matangini Hazra Government College for Women, Purba Medinipur, West Bengal, India

Sk. Mafizul Haque Department of Geography, University of Calcutta, Kolkata, India

Sunipa Mandal Department of Geological Sciences, Jadavpur University, Kolkata, India

Raghunath Pal Centre for the Study of Regional Development, Jawaharlal Nehru University, New Delhi, India

Subodh Chandra Pal Department of Geography, The University of Burdwan, Bardhaman, West Bengal, India

Padmini Pani Centre for the Study of Regional Development, Jawaharlal Nehru University, New Delhi, India

Priyank Pravin Patel Department of Geography, Presidency University, Kolkata, India

Suvendu Roy Department of Geography, Kalipada Ghosh Tarai Mahavidyalaya, Bagdogra, Darjeeling, West Bengal, India

Mehebub Sahana Department of Geography, Faculty of Natural Sciences, Jamia Millia Islamia, New Delhi, India

Haroon Sajjad Department of Geography, Faculty of Natural Sciences, Jamia Millia Islamia, New Delhi, India

Quaternary Geomorphology in India: Concepts, Advances and Applications

1

Balai Chandra Das, Sandipan Ghosh and Aznarul Islam

Abstract

This chapter deals with the critical review and summary of current advances and application of Quaternary geomorphology in Indian landscapes, specifically in the Lower Ganges Basin (LGB). Unfortunately, the LGB and Ganga–Brahmaputra Delta (GBD) perhaps are getting least attention by the practitioners of earth sciences and there is very little understanding of this Neogene–Quaternary morpho-stratigraphic unit from the perspectives of physical geography. Recently, the branch of Quaternary geomorphology has enough efficiency to analyse the Quaternary —Recent changes and records in the earth surfaces and the anthropogenic influence on the landforms and processes during recent times. Here, we have discussed and reviewed the key strengths of Quaternary geomorphology to re-explore the dynamic physical entities of the Ganges Basin, viz, Late Quaternary geomorphic, geological and climatic changes (e.g. palaeogeography, palaeoflood and fluvial response to climate, etc.), tectonic geomorphology (e.g. impact of active tectonics on the morphology of alluvial rivers and deltas, etc.), the links between fluvial processes and forms (e.g. variable fluvial regime and floodplain stratigraphy, channel shifting, fluvial geomorphology and arsenic contamination, gully erosion and sedimentation, etc.) and impact of anthropogenic activities on the rivers of LGB (e.g. embankment and bank erosion, dams and floods, groundwater contamination, etc.). The present volume, related to LGB, contains eleven significant chapters which are focused precisely on these above aspects using different geospatial techniques and quantitative analysis.

Keywords

Quaternary geomorphology · Anthropocene Active tectonics · Palaeoclimate · Ganga–Brahmaputra Delta · Lower Ganges Basin

B. C. Das
Department of Geography, Krishnagar Government College, Krishnagar, West Bengal, India
e-mail: balaidaskgc@rediffmail.com

S. Ghosh (✉)
Department of Geography, Chandrapur College, Barddhaman 713145, West Bengal, India
e-mail: sandipanghosh19@gmail.com

A. Islam
Department of Geography, Aliah University, Kolkata, West Bengal, India
e-mail: aznarulislam@gmail.com

B. C. Das et al. (eds.), *Quaternary Geomorphology in India*,
Geography of the Physical Environment, https://doi.org/10.1007/978-3-319-90427-6_1

1.1 Introduction

The term 'geomorphology' arose in the Geological Survey in the USA in the 1880s and was possibly coined by two great pioneers, J. W. Powell and W. J. McGee (Grapes et al. 2008; Sear and Newson 2010). Previously, the discipline of geomorphology was regarded as a part of geology which enabled the practitioners to reconstruct earth history by looking at the evidence of past erosion. Although geomorphology draws its roots from geology and hydraulic engineering and earth's physics, it differs from other earth sciences in that its focus is on the study of the processes of production, movement and storage of sediment with the landscape and on the characterization of the features these processes produce (Sear and Newson 2010). With course of time and development of earth sciences, geomorphology has changed greatly after Second World War, not least because of the plate tectonics paradigm, but due to the revolution in our knowledge of the Quaternary Period. That change was brought about by new dating techniques and environmental reconstruction of past, quantitative and statistical analysis of data, development of modelling and system thinking, appreciation of the importance of organisms, application of geomorphology to the study of palaeoclimatology, palaeohydrology, hazard, engineering problems and global environmental change. There is now a greater appreciation of the nature of micro-geomorphic processes and availability of a whole range of new technologies for the analysis of data and materials, the development of satellite remote sensing and exploration of space.

1.2 Important Concepts

'Quaternary' is the current and most recent period of the Cenozoic Era, having span from 2.588 ± 0.005 million years ago to the present (Cohen et al. 2015). The Quaternary is divided into two epochs—(1) the Pleistocene (2.588 million years ago to 11.7 thousand years ago) and (2) the Holocene (11.7 thousand years to today) (Cohen et al. 2015). This period is important because it is the geological period when the human evolution took place and it is also the geological period characterized by extraordinary changes in the global climate such as the Ice Ages (Singhvi and Kale 2009). The repeated climatic fluctuations (glacial and interglacial episodes) that have occurred throughout this latest chapter of earth history have given rise to a highly complex record of landforms, sediments, biological remains and assemblages of human artefacts (Lowe and Walker 2015).

Each aspect of the contemporary global environment including hydrogeomorphic processes is now modified or at least influenced by human activity during Late Holocene. The Quaternary record offers a foundational understanding of baseline conditions of earth system processes and responses and facilities increased confidence in evaluating the magnitude of past and future global climatic change and its diverse effects (Meadows 2016). The 'Anthropocene' (Crutzen 2002) represents an appropriate platform from which to inject the above perspective. Given the amplitude of human intervention on climate, environment and landscape, there are groups that now suggest the usage of term Anthropocene to demarcate the period from the times of the beginning of the industrial revolution, more correctly from 1610 to 1964 (Crutzen 2002; Singhvi and Kale 2009; Zalasiewicz et al. 2011; Lewis and Maslin 2015).

Geomorphology has enough efficiency to analyse the Quaternary changes and records in the earth surfaces and the anthropogenic influences on the landforms and processes during recent times. Quaternary geomorphology is the study of landscape changes during the recent Pleistocene and Holocene epochs (Goff 2017). While geomorphologists typically study landforms with a historical perspective in mind, Quaternary geologist focuses on the surficial sedimentary deposits, which provide a window into the past of earth's changing climate (Goff 2017). Therefore, 'Quaternary geomorphology' can be defined as a study of geomorphic processes (i.e. weathering, mass movements, erosion, transportation and deposition) and landform

evolution during the Early Quaternary Period to Anthropocene. We can correlate three fundamental concepts of geomorphology (Thornbury 1969) with the scope and approach of Quaternary geomorphology:

- *Little of the earth's topography is older than Tertiary and most of it not older than Pleistocene,*
- *Proper interpretation of present-day landscapes is impossible without a full appreciation of the manifold influences of the geologic and climatic changes during the Pleistocene and*
- *Geomorphic processes leave their distinctive imprint upon landforms and each geomorphic process develops its own characteristic assemblage of landforms.*

In recent years, Quaternary geomorphology has continued to grow as a discipline with emphasis on the quantitative data, experimentation and predictive modelling on the Late Quaternary geomorphic, geological and climatic changes (e.g. palaeoflood, fluvial response to climate changes, glacial deposits and global warming, etc.), tectonic geomorphology (e.g. impact of active tectonics on the morphology of alluvial rivers and deltas, etc.) and the understanding of links between process and form (e.g. variable fluvial regime and floodplain stratigraphy, fluvial geomorphology and arsenic contamination, gully erosion and sedimentation, etc.). The applications of Quaternary geomorphic study on these issues are discussed below.

1.3 Methodological Outlooks

Quaternary geomorphology has borrowed different methods and techniques of different disciplines of earth science, viz. fluvial geomorphology, sedimentology, alluvial geoarchaeology, palaeoclimatology, palaeohydrology, process geomorphology, geochronology, tectonic geomorphology, remote sensing and GIS (geographic information system), etc. The principal application of these methods is to explore the current and past geomorphic processes through in-depth study of recent landforms and diverse geological materials using sophisticated techniques. Mostly, our understanding about Quaternary geomorphology is concentrated on the fluvial archives, landforms and other geological parts of the Bengal Basin and different dimensions of useful methodology are briefly discussed as follows.

The pattern or configuration of a landscape is derived from its composition (the kinds of elements it contains), its structure (how they are arranged in space) and its behaviour (how it adjusts over time to various impulses or thresholds for change) (Fryirs and Brierley 2013). All the observations and interpretations in geomorphology should be framed in their spatial and temporal context. Currently, remotely sensed and modelled data using GIS provide a good guidance in our efforts to interpret fluvial landscapes; it is contended here that genuine understanding is derived from the field-based analyses. There is a general guideline to study each element of landform in a region (Fig. 1.1).

An inquiry into the process–form relationship implies that geomorphic landscape and its component form elements are in adjustment with contemporary process domains and process rates (Sharma 2010). Explanation of landforms also requires integration of time-dependent contemporary process data and historical process data reconstructed from signals of the past environment in the sedimentary record of landforms. The discipline of process geomorphology identifies those process domains and quantifies process rates for explaining the origin of landforms (Sharma 2010). It should be remembered that a change in any component of the landscape initiates a sequence of change in related form elements. The internal adjustment between process rates and from attributes is viewed in terms of critical conditions of landform stability called geomorphic thresholds (Schumm 1979; Sharma 2010). Impact of neotectonic activity on drainage patterns and morphology of alluvial rivers are also studied in the fluvial section of Quaternary geomorphology (Schumm et al. 2002). Therefore, the study of process geomorphology can

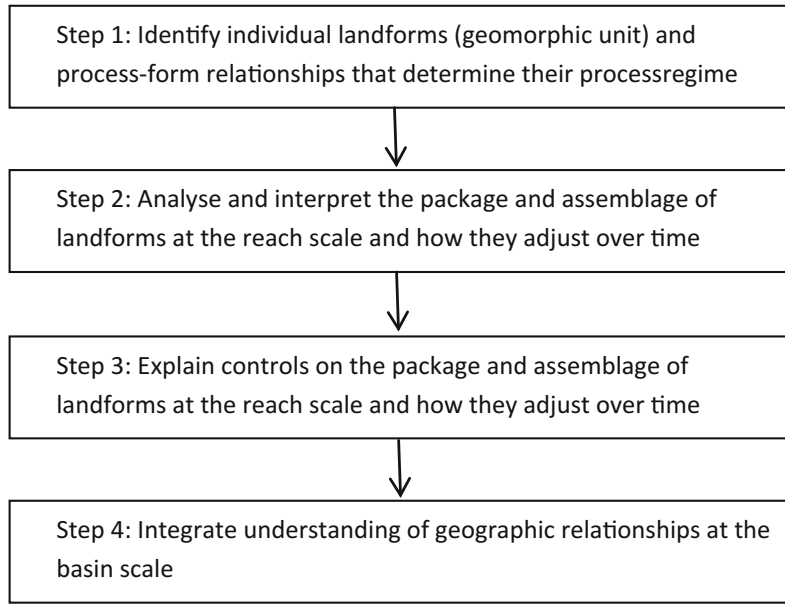

Fig. 1.1 Geomorphic approach to study the fluvial landforms and processes at basin scale (modified from Fryirs and Brierley 2013)

give insight into the evolution of landforms in relation to Quaternary environmental changes, because the external effects of climate change, tectonics and human activities disturb the established order of exchange of energy and material in the geomorphic systems, promoting landscape instability and responses.

Rivers are highly sensitive to environmental change: climate change, base level change (in relation tectonic activity) and anthropogenic activity (e.g. construction of large dams) (Tornqvist 2013). Any shift in external conditions instigates a rapid response from the fluvial system through changes in hydrogeomorphic processes and landforms (Ghosh and Islam 2016). So, the rivers are considered as excellent witness of the dynamics affecting earth surface systems by the Fluvial Archives Group (FLAG) which was framed in 1996 under the auspices of the British Quaternary Research Association (Cordier et al. 2017). FLAG is an independent international research group that affects the approaches of researchers involved in the study of past fluvial environment under two themes—(1) fluvial archives as templates for long terrestrial records and (2) fluvial environment and processes in relation to external and internal factors (Fig. 1.2).

Sedimentological and geoarchaeological aspects of Quaternary geomorphology are very much relevant to the environmental scientists and geographers because the vast majority of, if not all, contemporary floodplains have a greater or lesser degree been altered by human activity during the last 10,000 years (Brown 2001). Our ability to infer past conditions of Quaternary from the floodplain sediments comes from the analysis of hydrogeomorphic processes, river morphology, channel pattern analysis, sedimentation pattern, floodplain stratigraphy and other fluvial archives, i.e. present is key to the past. To reconstruct past hydrological conditions of human existence, the field geomorphic and stratigraphic evidences are explored at three timescales—the Late Pleistocene, the Holocene and the historical and instrumental period (i.e. Anthropocene) (Macklin et al. 2012). A change in the frequency and magnitude of floods is the main direct driver that determines the response of river systems to climate change and it reads the history of environmental changes in the form of sedimentary signals and sequences of landforms (Macklin et al. 2012) (Fig. 1.3). A reliable stratigraphic approach is essential to any palaeoenvironmental interpretation and it includes mainly lithostratigraphy (grain size,

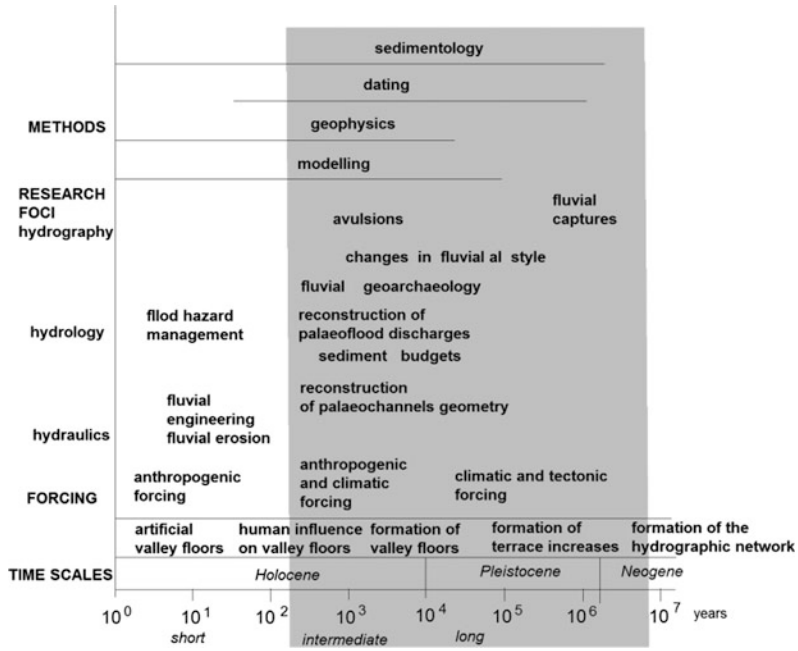

Fig. 1.2 Approach of FLAG to study fluvial environment of Quaternary (modified from Cordier et al. 2017)

grain shape, etc.), morphostratigraphy (sediment pattern in relation to surface form), biostratigraphy (use of pollen and mollusks), chronostratigraphy (identifying age of sediments by dating method) and pedo-stratigraphy (study of palaeosols and weathering properties) (Mather 2011).

From field excavations into the floodplain deposits, the following sedimentary characteristics can be recorded: grain size (texture), the arrangement of grain size variation (fabric), preferential orientation of particles (imbrication), small boundary—defining structures within units or beds, and the stacking and order of these units or beds (architecture) (Brown 2001). The fabric, structure and architecture all relate to the conditions of deposition. Miall (2014) provides a widely acclaimed procedure to identify and recognize the lithofacies of fluvial sediments based on their origin of development (Fig. 1.4).

Palaeoclimatology is a field of concern with study of past climate system activity with the help of proxies and it acts as a key discipline to explore Quaternary environment (Goff 2017). Several environment-sensitive proxy indicators are used for interpreting the type, magnitude and duration of environmental change (Sharma 2010). Depending upon the nature of indicator source, radiometric and thermoluminescence dating techniques find applications in the reconstruction of the Quaternary climate and environment (Fig. 1.5). The age of organic materials, such as wood, charcoal, bone and shell, is determined from the amount of radioactivity of ^{14}C they retain. The radiocarbon method is suitable for the reconstruction of events generally not more than 30 ka old (Sharma 2010). The optically stimulated luminescence (OSL) dating technique is routinely used for calibrating the age and palaeoclimatic environment of Aeolian sand and fluvial deposits (Singhvi and Kale 2009). Alongside palaeohydrology has grown as an earth science discipline to infer hydrological changes of Quaternary period in relation to changing fluvial processes (Schumm 1977). A more frequently used method has been the estimation of past velocity and formative discharge from the channel geometry and from sediments deposited by floods. The method of

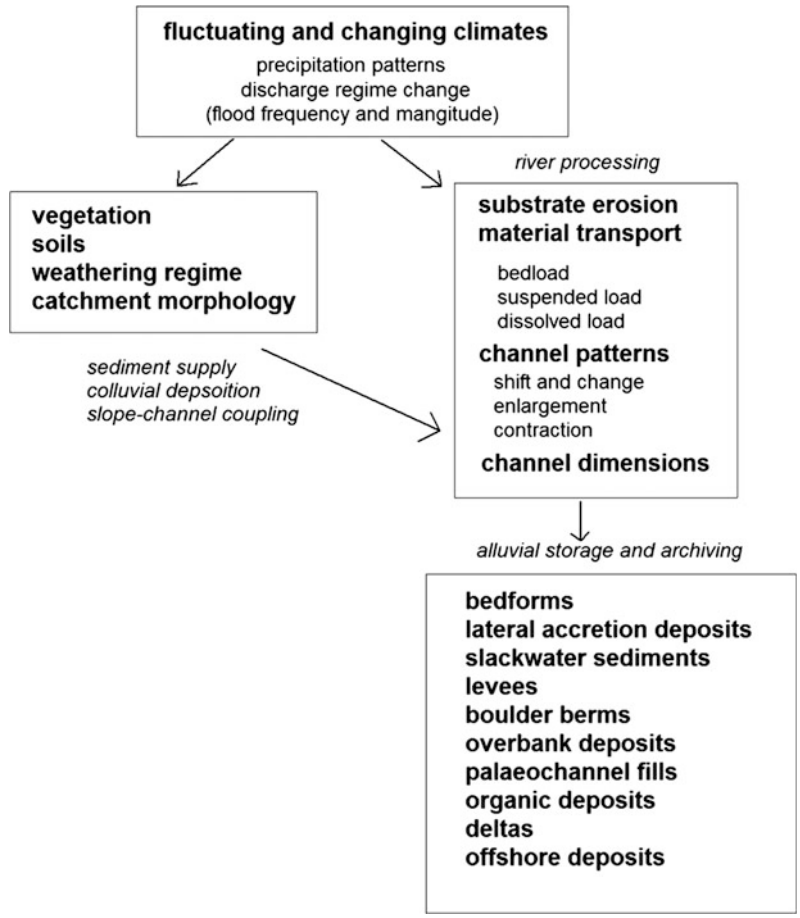

Fig. 1.3 Interaction between flood and Quaternary climate change, and resultant changes in process–form and storage of fluvial archives (modified from Macklin et al. 2012)

reconstructing palaeofloods from slack-water deposits in valley has used radiocarbon dating to provide a geochronology for the deposits and to infer environmental conditions of Quaternary (Brown 2001).

1.4 The Ganges Basin

Indian civilization grew up under the care of River Ganges for thousands of years, nourished for the generations by her generous bounties (Tare et al. 2013). The Ganges Basin is an important fluvial system of northern and eastern India and is a part of the Ganges–Brahmaputra–Meghna (GBM) River Basin, draining about 1,089,370 km^2 in Tibet (3.67%), Nepal (12.85%), India (79.20%) and Bangladesh (4.28%) (Tare et al. 2013; Rajmohan and Prathapar 2013). Central Ground Water Board (CGWB) of Ministry of Water Resources (under Government of India) recognized the basin map of lower Ganges River in India (Fig. 1.6). The river sub-basins of Mahananda, Ajay, Mayurakshi, Damodar, Bhagirathi-Hooghly, Ichamati, Jalangi , Kasai, Silai, Gandak, Kosi, Bagmati, Sone, Koel, etc. are within the domain of lower Ganges Basin (LGB). This part of basin is the world most populated region where 80% of people lives in the rural areas and depends on the agriculture. In 2011, the total population of LGB was 391.21 million (including Nepal and Bangladesh) which is 5.6% of the world population (6974 million) (Rajmohan and Prathapar 2013). The LGB receives above 1400 mm rainfall annually with high influence of tropical cyclones

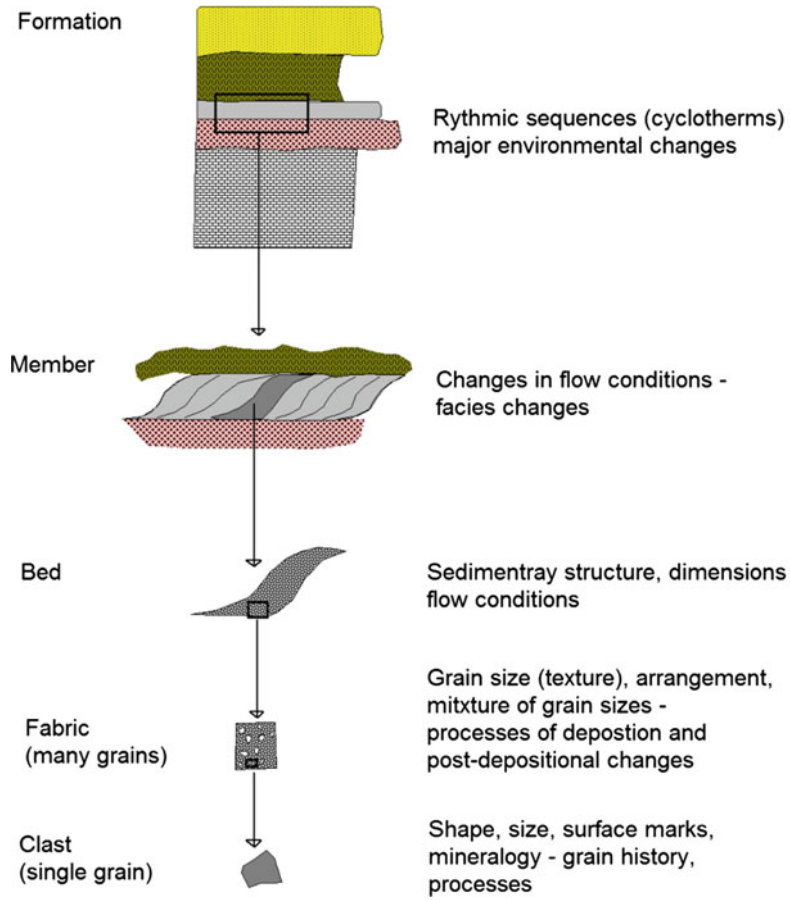

Fig. 1.4 Diagrammatic representation of fluvial geological approach to study lithofacies of Quaternary floodplain sediments (modified from Brown 2001; Miall 2014)

and rainstorms (that instigates periodic floods). Geomorphologically, LGB is associated with the crystalline, sedimentary and meta-sedimentary rocks of Himalayas, Late Quaternary alluvium of Ganges, Archean rocks of Chotanagpur Plateau, Gondwana sedimentary rocks of Damodar Graben, basalts of Rajmahal hills, unconsolidated alluvium and floodplain deposits of Late Quaternary and Recent deltaic deposits of Bengal Basin.

One of the most important parts of LGB is the Ganges–Brahmaputra Delta (GBD) which is an active and giant geomorphic unit of the Bengal Basin. Unfortunately, the LGB and GBD perhaps are getting least attention by the practitioners of earth sciences and there is very little understanding of this Neogene–Quaternary morpho-stratigraphic unit (Tandon et al. 2008). This part of delta is scored with variables tracks of palaeochannels and meander cut-offs which represent the various ancient channels scooped out with their lateral migration and channel shifting to form vast floodplains of lower Ganges and its tributaries and distributaries (Jha and Bairagya 2011). It is stated to be 736–800 million tonnes of suspended sediment loads in the River Ganges with average sedimentation rate of 0 ± 3 mm per year (Rudra 2010; Wilson and Goodbred 2015). The rivers of peninsular India (e.g. Mayurakshi, Ajay, Damodar, Kasai, etc.) formed the *Rarh* Plain and palaeofan-delta which are now appeared as Pleistocene terraces. The extreme palaeofloods of these rivers formed the vast Late Quaternary fertile floodplains with minerals rich coarse sediments of the Chotanagpur Plateau.

In the LGB as a result of a general lack of cohesive bank materials and a high mobility of

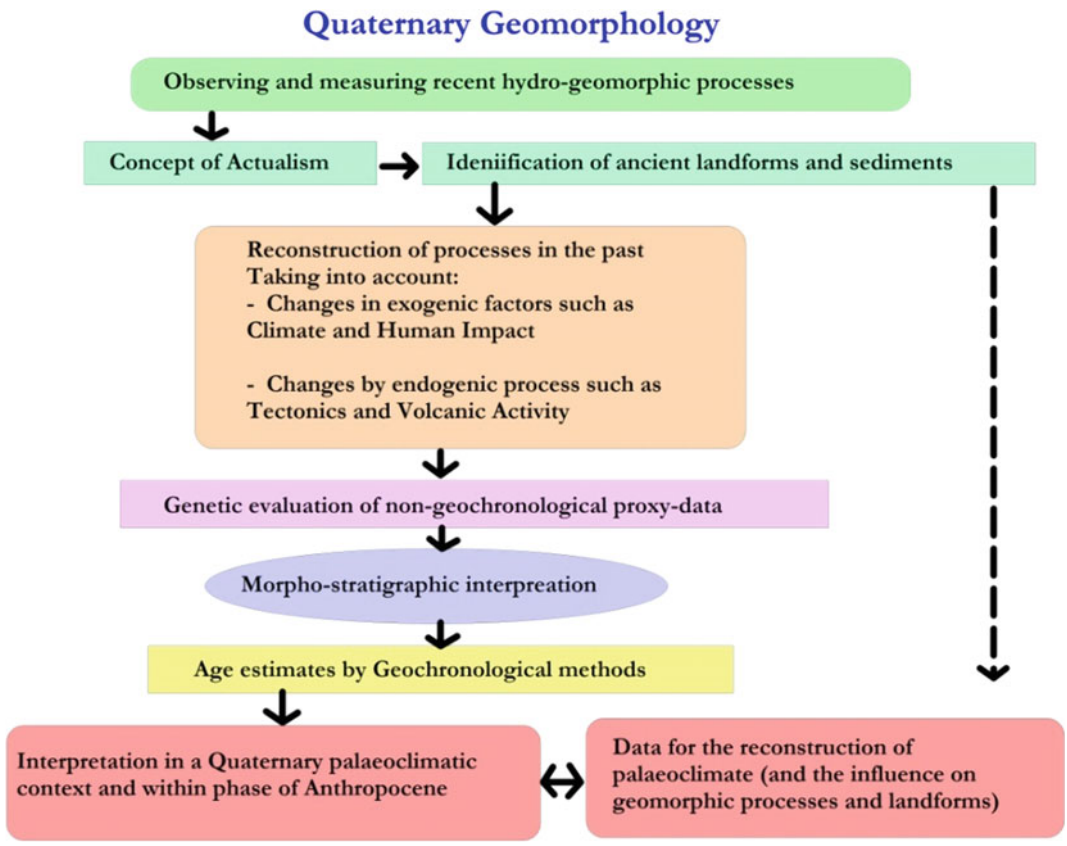

Fig. 1.5 Methodological flowchart of palaeoclimatic research in Quaternary geomorphology (modified from Bose 2014)

bed materials, the alluvial rivers respond to large changes in discharge and sediment load by shifting their courses and by dramatically changing their morphology and bedforms (Kale 2002). The LGB has preserved the fluvial archives of past and present environment as well as the signals of ongoing processes (mainly impact of different external factors and anthropogenic processes) of Anthropocene. The repetitive study of satellite images and historical maps has revealed that in the lower reaches of the Ganges River, natural as well as anthropogenic factors have influenced largely the fluvial dynamics after the formation of Farakka barrage (completed in 1975) (Sinha and Ghosh 2012). In this region, periodic monsoon floods, bank erosion, channel shifting, palaeochannels, active tectonics, land degradation, palaeo-weathering surfaces, dynamic deltaic landforms and arsenic contamination of groundwater are the key issues which can be analysed through the advanced methods of Quaternary geomorphology. The previous applied works of Quaternary study and geomorphology in the whole Ganges Basin (including LGB) are reviewed and summarized in the following section.

1.5 Issues, Advances and Applications of Quaternary Geomorphology

An exceptional book of the Geological Society of London (i.e. 'History of Geomorphology and Quaternary Geology') was published to cover the various aspects of the geomorphic processes of

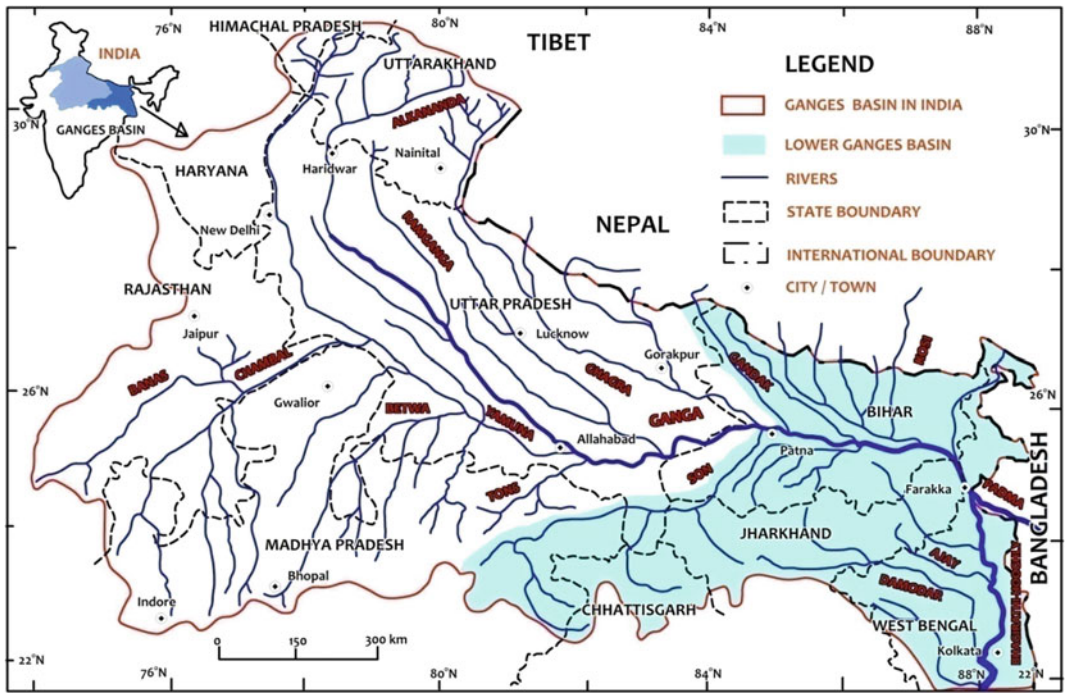

Fig. 1.6 Spatial extent of the Ganges Basin in India including Lower Ganges Basin

the Quaternary period in the different parts of the world (Grapes et al. 2008). In the Indian subcontinent, the landscapes, growth and demise of numerous civilizations and other anthropogenic phenomena are directly or indirectly related to the changes in climatic conditions of Early Quaternary–Anthropocene. The most important single factor is the monsoon that determines the lives, ecology and other physical environment in India (Singhvi and Kale 2009). The quest to understand the Quaternary climate change has become more intense in recent times largely and the researchers have quantified the variable responses of the earth system to changes in past and present climate (Kale et al. 2003; Tandon et al. 2008; Singhvi and Kale 2009). Some of the archives (e.g. fluvial sediments, marine sediments, Aeolian sediments, glacial moraines, etc.) and proxies (e.g. pollens, magnetic properties of minerals, plant macrofossils, isotopic composition, etc.) enable quantification of the changes in the past climate and reconstruction of monsoon variability in India (Singhvi and Kale 2009).

The new advances in Quaternary studies are strengthening with the introduction of chronometric techniques in the palaeoclimatic and palaeogeographic reconstruction. Radiocarbon dating (>60 to ~40,000 years age range), luminescence dating (10–10^6 years age range), Potassium/Argon–Argon dating (>10^6 years age range), dendrochronology (Recent to ~10,000 years) and sediment varves (up to a few thousand years range) are widely applied in the various domains of Quaternary geomorphology (Singhvi and Kale 2009). Charcoal, organic matter and mineral grains trapped in fluvial sediments are used to date the sediments using radiocarbon and luminescence techniques and the fossil remains of flora and fauna and archaeological evidences are widely used to indicate change in past environment of several Indian rivers, like the Ganges, Saraswati, Indus,

Sone, Sabarmati, Mahi, Luni, Narmada, Godavari, Krishna, Kaveri, Pennar and Bhagirathi-Hooghly (Rajaguru et al. 1993; Singh 1996; Sinha et al. 1996, 2005; Kale et al. 1997, 2000, 2003; Mishra et al. 2003; Kale 2007, 2008; Tandon et al. 2008; Singhvi and Kale 2009; Rajaguru et al. 2011a; Sridhar et al. 2014; Sarkar et al. 2016).

1.5.1 Fluvial Landforms, Archives and Palaeoenvironment

Quaternary floodplain landforms and sediments bear the imprints of past and present active environment, which affect the components and functions of fluvial system since Late Pleistocene. Channel pattern of a fluvial system is very dynamic in both space and time because it is controlled fundamentally by the distribution of erosive forces and resisting forces along channel boundaries (Brown 2001; Sharma 2010). It is found that slope, discharge and sediment load have great importance to develop straight, meandering and braided channel pattern, having variable geomorphic thresholds (Schumm 1979). Meandering channel pattern is widely observed in the floodplains of LGB and the point bar is the main depositional unit of meandering stream. So the fluvial archives of point-bar deposits have enough potential to unfold the past stratigraphic and climatic events which are the firm basis of Quaternary geomorphology of a region.

Particle size sorting and bedform development also produce the characteristic point-bar stratigraphy; a fining upward sequence from base to top; an erosional surface, channel lag deposits, coarse sand with large-scale cross-stratification (due to migration of ripples and dunes), progressively finer sands with ripple cross-laminae and at the top and silty-clay deposits (due to low fluvial regime) formed by overbank flow. Large floods may reverse this sequence, producing a unit with reverse grading (Brown 2001). The recognition of these reverse grading units is helpful in identifying periods of hydrological change and in particular slack-water deposits—palaeoflood indicators (Fig. 1.7).

Potholes are one of the most common, current and spectacular erosional features in the bedrock by rapidly flowing rivers. Kale and Joshi (2004) found that the potholes are formed in the man-made channels and pits (craved in mid-1940s) in the Indrayani River of Pune. It reflects the current rate of potholes formation in the bedrock channels where the energy levels of monsoon floods are higher by several orders of magnitude (Kale and Joshi 2004). Using N-type Schmidt rock hammer, Sengupta and Kale (2011) calculated the rock resistance along the locations of potholes in the Indrayani River. That study revealed that the dominant role played by hydraulics of flows and the factor of rock resistance in the erosion was getting less important because in a region of uniform lithology the ability of a river to erode in bedrock is largely controlled by the channel gradient and the amount of abrasive materials (Sengupta and Kale 2011).

The alluvial plains of Ganges basin preserved subsurface fluvial record (i.e. important continental archive) which is used for understanding the landscape development against a background of Late Quaternary to recent environmental changes driven mainly by the Himalayan tectonics, monsoonal dynamics and base level changes(Tandon et al. 2008; Sanyal and Sinha 2010). The LGB including GBD is a key spatial unit of past environmental changes which can be scientifically studied by Quaternary geomorphology. Available data from different parts of India and the Ganges Plain demonstrate a strong climatic influence on the stratigraphic development during the Late Quaternary (Fig. 1.8). Prominent changes in the monsoon rainfall in the Ganges Plain have been identified, viz., 45 ka BP—humid climate, 20–13 ka BP—low rainfall, 13–11.5 ka BP—high rainfall, 11.5–10.5 ka BP—low rainfall, 10.5–5.8 ka BP—high rainfall, 5.8–2.0 ka—low rainfall and 2.0–0 ka BP—high rainfall (Singh 1996). According to Sinha et al. (2005), the initiation of GBD formation began at ~11 ka when rising sea level led to back-flooding of lowland surface and the trapping of riverine sediments. It is learned that the humid phase of Early Holocene (~9000–

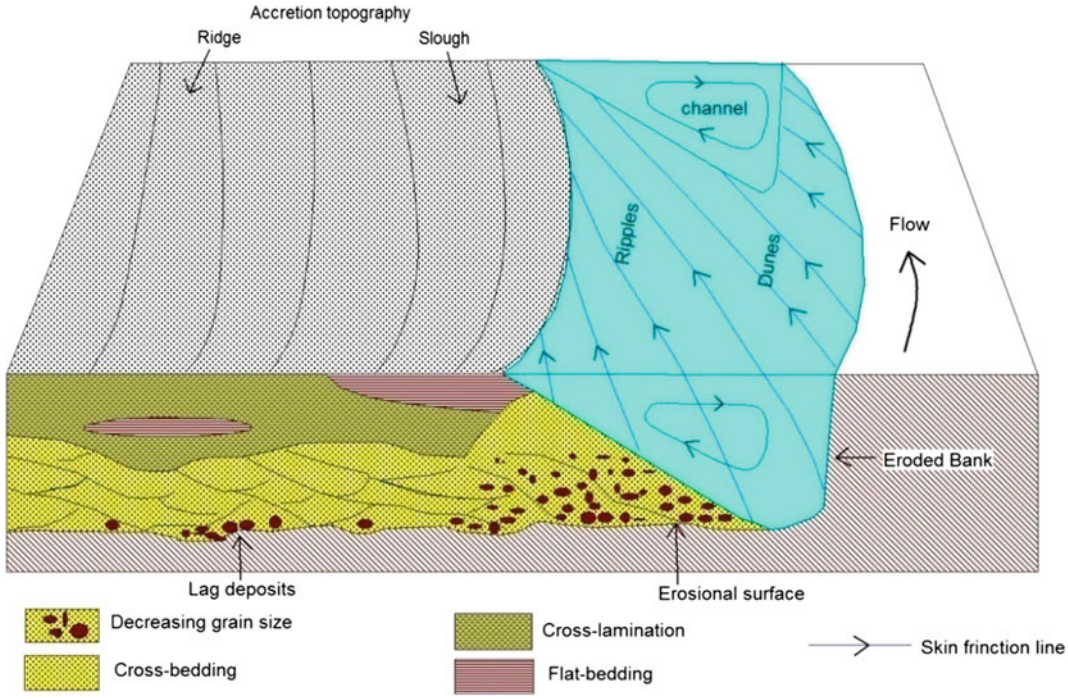

Fig. 1.7 Alluvial stratigraphy of point-bar deposits in a meandering channel (modified from Brown 2001)

6000 years BP) was characterized by revival of fluvial activity in the Indian subcontinent and the sediment discharge from the Ganges–Brahmaputra Rivers dropped significantly after 7000 years BP indicating weaker monsoon condition (Singhvi and Kale 2009). During the Holocene, the Ganges Plain experienced abandonment of river channels in response to changes in base level and climate (Singh 1996). Pollen, phytoliths and ^{13}C signatures of soil organic matter from the fluvial sedimentary sequences of the Darjeeling foothills, eastern Himalayas are used to portray palaeoclimatic oscillations (Ghosh et al. 2015). A comparatively low monsoonal activity and slight higher temperature was prevailed during 31 ka onwards. Later during 5.4–4.3 ka, a strong monsoonal activity was observed there (Ghosh et al. 2015).

Using historical records, maps, aerial photographs, DEM (digital elevation model), satellite images, DGPS (differential global positioning system) survey and GIS (geographic information system) techniques, the fluvial geomorphologists investigated the short- and long-term changes of river banks and flow paths (Fig. 1.9) in the GBD during the last 250 years (Rudra 2010, 2014; Sinha and Ghosh 2012; Bandyopadhyay et al. 2015). The spatio-temporal geomorphic study reveals that in recent times the rivers of LGB exhibit most common types of changes which include channel shifting owing to avulsion, alteration of flow direction, change in sinuosity and degree of meandering, channel widening, bank erosion, bar development and braiding, meander loop migration and abandonment of channels. The research reveals that within 39 years since 1975, four meander cut-offs were accomplished at an average rate of one in every 9.8 years (Fig. 1.3) (Bandyopadhyay et al. 2015). Several courses of the Kosi River have been identified that suggests episodic and progressive lateral shifting of the river by about 113 km in 228 years (Kale 2002; Sinha 2009; Chakraborty et al. 2010; Sinha et al. 2014). In the floodplains of LGB, one of the most critical environmental issues is the arsenic contamination

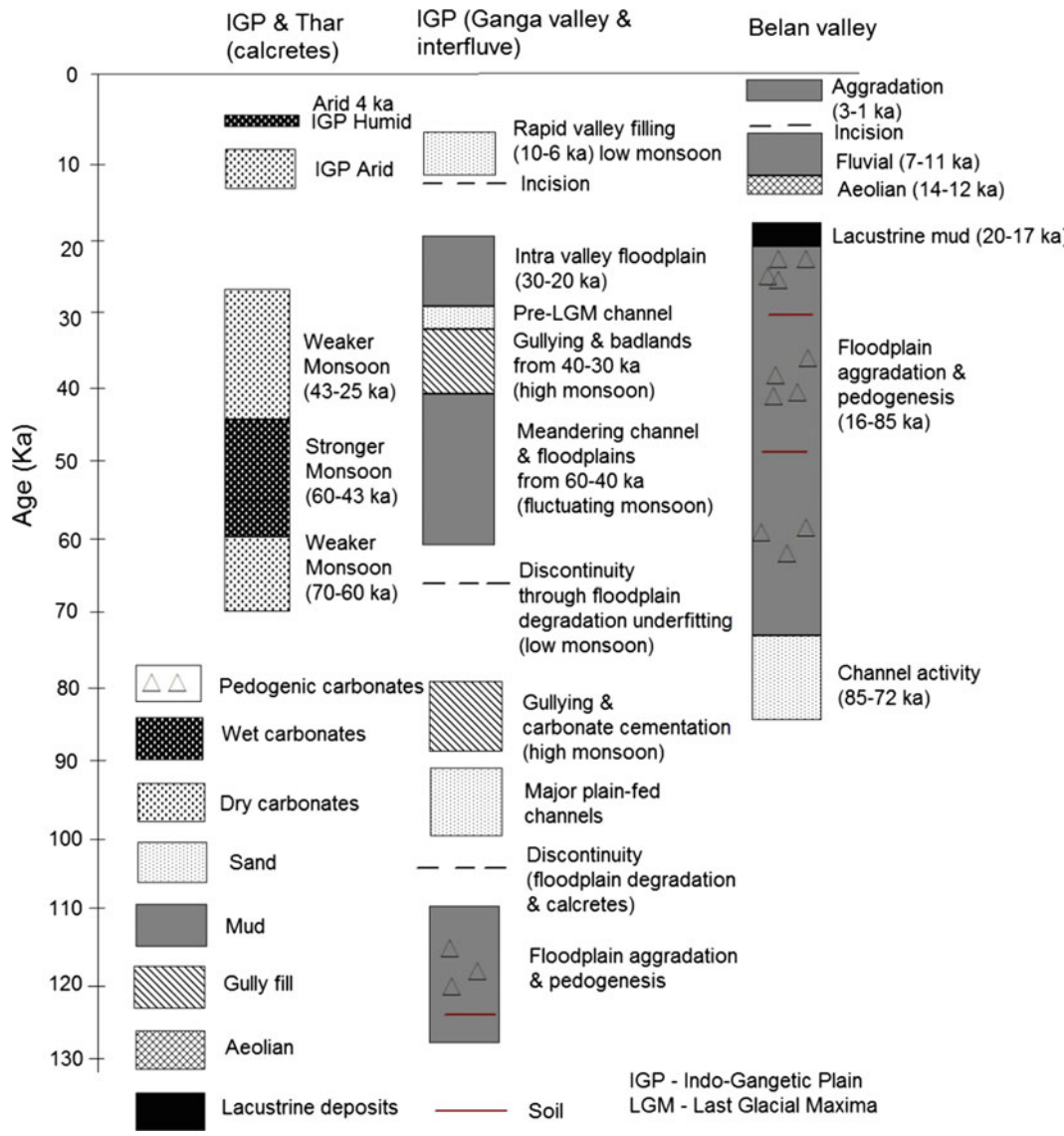

Fig. 1.8 Response of terrestrial systems to Late Quaternary monsoonal variability in India (modified from Sanyal and Sinha 2010)

of groundwater and sediments. From the study of fluvial geomorphology, Quaternary morphostratigraphy and XRD (X-Ray Diffraction) analysis, it is learned that arsenic contamination in GBD is confined to the Holocene Younger Delta Plain and the hydrated ferric oxide rich alluvium deposited around 10,000–7000 years BP, mainly in the abandoned channels, oxbow lakes, swamps, etc. (Pal et al. 2002; Acharyya and Shah 2007, 2010).

1.5.2 Geoarchaeology and Quaternary Climate

Detailed evaluation of Late Quaternary climate change and geomorphic event in the LGB can be done through the geoarchaeological study. In situ archaeological artefacts within the interfluves of GBD and Rarh Plain suggest two distinct periods of human occupation with occasional flood deposits in this region—5th century AD and 8th

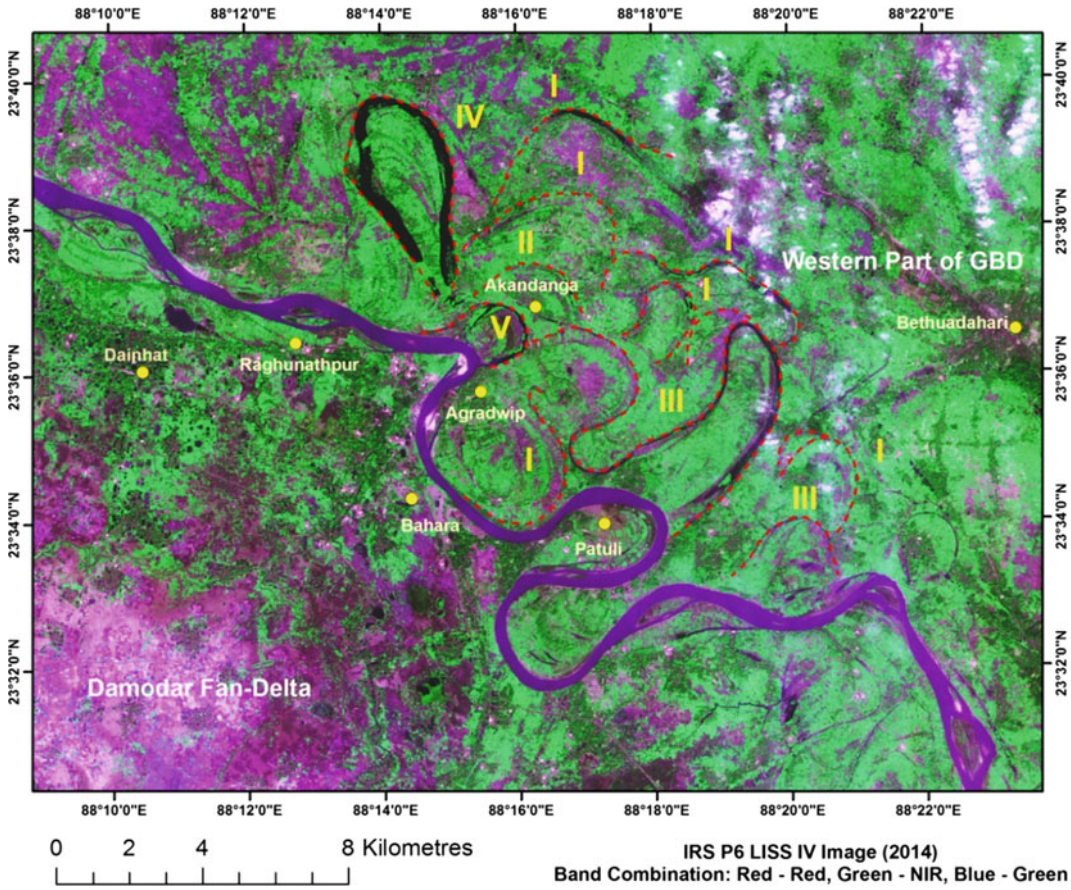

Fig. 1.9 Quaternary floodplain landforms (red dashed lines) of Bhagirathi in between Damodar fan-delta and western part of GBD, depicting different phases (I, II, III, IV and V) of meander cut-off formations and separation of oxbow lakes in LISS IV FCC base image of 2014, I—pre-1949 to 55, II—1949-55 to 1916-18, III—1916-18 to 1967, IV—1989 to 2000, V—2000 to 2014; *source* 1949–55—Atlas of India, 1916–18—SoI toposheet (79 A/2), 1967—Corona KH4A, 1989—Landsat-5 TM (path-138, row-44), 2000—Landsat-7 ETM+ (path-138, row-44), 2014—IRS P6 LISS IV (path, row) (modified from Bandyopadhyay et al. 2015; Guchhait et al. 2016)

to 12th century AD (Tandon et al. 2008). Rajaguru et al. (2011a) have found potential geoarchaeological sites in the GBD of West Bengal through optically stimulated luminescence (OSL) and radiocarbon dating. It is now understood that the alluvial rivers of GBD had changed their paths frequently in the extreme palaeofloods and it governed the locations of ancient settlements in the interfluves. The present morphology of GBD was achieved during the last 3.5 ka BP and the settlement started around 2.5 ka BP in this region (Rajaguru et al. 2011b). A recent study of oxygen isotope and archaeological data suggests that the pre-Harappans started inhabiting the area of Indus-Ghaggar-Hakra river valleys along the mighty Ghaggar-Hakra Rivers fed by intensified monsoon from 9 to 7 ka BP and weakening of the monsoon after ~5 ka BP is a strong contender for the Harappan collapse (Sarkar et al. 2016). It is attempted to reconstruct palaeomonsoon on the basis of geomorphology and geoarchaeology in western India (Rajaguru et al. 2011b) (Table 1.1).

Table 1.1 Reconstruction of palaeoclimate in relation to geomorphic signatures and geoarchaeological phases in western India

Geological period	Geomorphic signatures	Palaeoclimate	Cultural phase
Palaeogene (Eocene to Early Miocene)	Laterite regolith, littoral deposits	Humid Equatorial/Monsoon	Nil
Neogene (Late Miocene to Early Pleistocene)	Anomalous fluvial gravel affected by ferricrete and calcrete pedogenesis	Sub-humid to wet-arid	Nil
Early Pleistocene (1.5–0.8 Ma)	Hardpan calcrete with relief inversion; gravel with laterite clasts but without calcrete clasts; volcanic ash lens	Wet—semi-arid	Acheulian culture
Middle Pleistocene (>350 ka to 130 ka BP)	Colluvium–alluvial sediments; calcretised playas, dunes, sand sheets, palaeosols (calcisols) with animal fossils, littoral Milliolite	Dry—semi-arid with short spells of wet—semi-arid	Acheulian culture
Late Pleistocene (~25 ka to 10 ka BP)	Colluvium–alluvial calcretised sediments; palaeosols, dunes with palaeosols; playas, Milliolite formation	Arid (22–18 ka BP)—semi-arid with short spells of wet—semi-arid phases (25–100 ka, 60–30 ka)	Middle to Late Palaeolithic

Source Rajaguru et al. (2011)

1.5.3 Active Tectonics and Fluvial Reponses

Active tectonics is defined as those tectonic processes that produce deformation of the earth's crust on a timescale of significance to human society (Keller and Pinter 1996). The studies of long-term dynamics of fluvial systems and their responses to external or internal controls can play important roles in research concerning both global change and sequence-stratigraphy, as well as in studies of the dynamic interplay between tectonic activity and surface processes (Blum and Tornqvist 2000). In order to predict and to understand active tectonics, it must be studied within millions of years, which is the time span (post-Miocene) during which deformation is referred to as neotectonics (Schumm et al. 2002). Interestingly, fluvial system is very much sensitive to active tectonics which can change drainage pattern and processes of aggradation and degradation. The mapping and recognition of tectonic landforms and their quantitative measurements can give insight into the underlying seismic movement and resultant deformation or morphological changes on the surface. Ouchi (1985) had presented an adjustment of braided river and suspended load meandering river to anticlinal uplift and synclinal subsidence to understand the confined-river response to active tectonics (Figs. 1.10 and 1.11).

The Quaternary fluvial systems of India are a direct result of the uplift and erosion of mountains which are still active today, as convergence of known directions and rate is continuing (Sinha and Friend 2007). Due to the Indian–Eurasian collision, the Himalaya and its associated regions (GBD and Bengal Basin) are one of the most tectonically active regions of the world. Recently, a massive earthquake of 7.8 magnitude destroyed the Nepal Himalayas and Indian parts on 25 April 2015 (Bilham 2015; Witze 2015). In 2016, an important research reveals that an earthquake of 8.2–9.0 magnitude can hit the Bengal Basin and the Indo-Burman Ranges (Steckler et al. 2016). For this reason, it has attracted the attention of geomorphologists for several decades. Quaternary geomorphology can

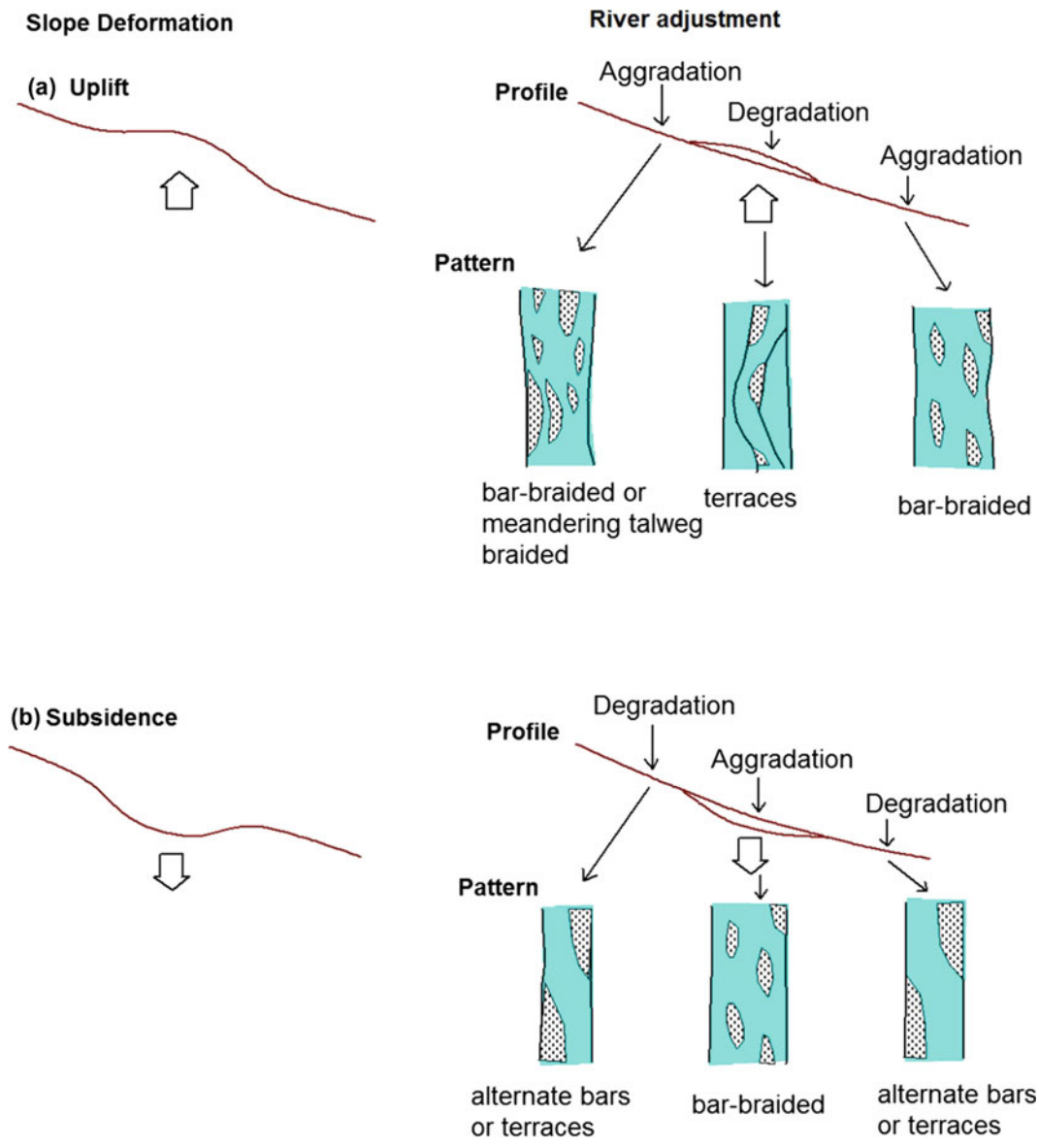

Fig. 1.10 Response of braided river to (**a**) anticlinal uplift and (**b**) synclinal subsidence (modified from Schumm et al. 2002)

examine the river response and adjustment to active tectonic movement and describe the process of adjustment. River morphology and channel behaviour are governed by the active tectonic movement (e.g. titling and faulting), influencing its pattern, landform evolution, sedimentary facies, processes of degradation and aggradation (Ouchi 1985). The interactions between tectonic uplift and subsidence, river erosion and alluvial deposition are fundamental processes which have acted to shape the landscape we see today (Holbrook and Schumm 1999; Schumm et al. 2002).

The study of tectonic geomorphology of Quaternary period reveals that fluvial sedimentary evidence for past tilting is traditionally based

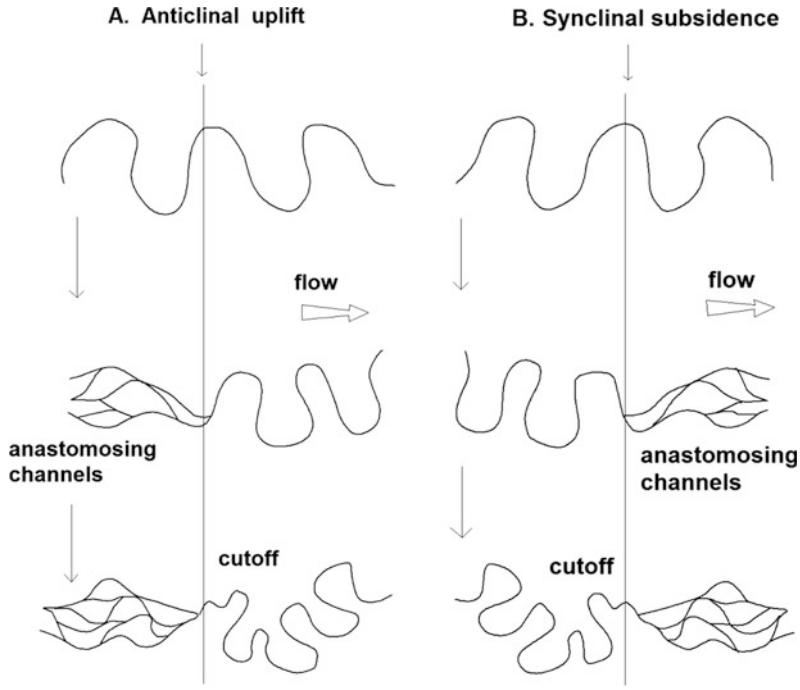

Fig. 1.11 Response of suspended load meandering river to (**a**) anticlinal uplift and (**b**) synclinal subsidence (modified from Schumm et al. 2002)

on the assumption that depositional features reminiscent of modern fluvial tectonic effects are evidence for past tectonic effects (Holbrook and Schumm 1999). Ouchi (1985) found that an experimental braided channel responded to anticlinal uplift across the channel with degradation and terrace formation in the central part of the uplift, and an experimental meandering channel responded to slope steepening with an increase in sinuosity. Using quantitative techniques of channel morphology, channel hydraulics, floodplain stratigraphy and estimation of rate of erosion and deposition, Schumm et al. (2002) studied the responses of alluvial rivers on active tectonic in the Neches River (Texas), Humboldt River (Nevada), Sevier River (Utah), Jefferson River (Montana), Indus River (India and Pakistan) and Nile River (Africa).

There are important Quaternary studies of fluvial response to active tectonics in the river basins of Himalaya and the Ganga Alluvial Plain. Jain and Sinha (2005) found that each tectonic block of Himalayan foreland basin is characterized by the associations of fluvial anomalies, viz. compressed meanders, knick point in longitudinal profiles, channel incision, anomalous sinuosity variations, distribution of overbank flooding, water-logged area, etc. Using satellite remote sensing, digital earth surface modelling, advanced morphometric techniques, gravity anomaly, seismo-tectonic maps and geographic information system (GIS), many practitioners studied the fluvial response to active tectonics and the geomorphic signatures of tectonic signals in the Sutlej River (northwestern Himalayas), Baghmati River (Himalayan foreland basin), Alaknanda River (Garhwal Himalaya), Sone-Ganga alluvial plain (Ganges Basin), Kosi River (Bihar) and Vatrak River Basin (Gujarat), etc. (Malik and Mohanty 2007; Sahu et al. 2010; Raj 2012; Sinha et al. 2014; Rana et al. 2016). A classic example of tilt-induced avulsion and channel migration during Late Quaternary is evolution of the Kosi mega-fan along the active faults of Late Pleistocene to Holocene surfaces (Chakraborty et al. 2010; Sinha et al. 2014). Due to re-activation of some basement faults of Bengal Basin and episodic uplifts the courses of

the Ajay, Damodar, Kasai, Ganges and Bhagirathi rivers were modified since Early Pleistocene (Singh et al. 1998; Sinha and Sarkar 2009; Roy and Chatterjee 2015).

1.5.4 Flood Geomorphology of Anthropocene

During Last Glacial Maximum (LGM), decreased monsoonal precipitation influenced more aggradation of major rivers of the Ganges Basin in between 27 and 90 ka (Sanyal and Sinha 2010). Then, increase precipitation during 15 to 5 ka was the period of monsoon recovery which increased discharges and promoted incision of interfluves and widespread badland formation (Sanyal and Sinha 2010). It is found that about three-fourths of the extreme floods of India have occurred during the excess monsoon periods between ~1840 and 2000 AD, implying a noteworthy link between the monsoon and flood (Kale 2012). During Anthropocene, the fluvial systems of Himalayas, Indo-Gangetic Plains and Peninsula are experiencing large-scale changes in their flow regime conditions, floods, sediment load, river morphology and behaviour due to increased human interference (e.g. development of large dams) and extreme rainfall events (Kale 2005).

The extreme floods, flash floods, process of braiding and meandering, sediment flux, formation of fans and avulsion, stream power, etc. are assessed through Quaternary geomorphology in the river basins of Ganges, Kosi, Yamuna, Gandak, Sabarmati, Narmada, Tapi, Krishna, Kaveri, etc. (Friend and Sinha 1993; Sinha et al. 1996; Kale 2002, 2003, 2005, Chakraborty et al. 2010; Kale et al. 2010; Sinha et al. 2014; Sridhar et al. 2014). Terrestrial records of extreme climatic events include 'slack-water flood deposits' (SWD) which is used to deduce the palaeoflood records (with the help of OSL dating) in the Narmada, Tapi, Godavari, Krishna, Pennar, Kaveri and Luni Rivers. This kind of study and geomorphic evidence suggests that the climate was dry during the end of Pleistocene in the central India (Rajaguru et al. 1993; Mishra et al. 2003). Kale et al. (2003) tried to assemble a 2000-year chronology of large floods on the Narmada River and a <500-year chronology of floods on the Tapi River using radiocarbon dating of floating charcoal, cultural hearths, shell and OSL dating of SWD. The study indicated that a series of extraordinary floods occurred during the Early Holocene humid phase and absence of large-magnitude floods during the Late Middle Age and Little Ice Age (700–400 years BP) in the Narmada River (Kale et al. 1997, 2003). The recent flood studies of Anthropocene reveal that flood-generating rainstorms and cyclonic systems are usually of 3-day duration and are confined to two major zones in India—(1) the Ganges Basin and (2) northern part of Indian Peninsula (Kale 2003). In the western part of GBD Mayurakshi, Ajay, Damodar, Kasai, etc. are the most flood-prone rivers and the peak discharge of monsoon period often exceeds 6000 m^3 s^{-1}. In this tropical monsoonal environment, large floods are important geomorphic agents that affect the forms and behavioural characteristics of these rivers and leave a lasting effect on the inhabitants of GBD (Ghosh and Guchhait 2016).

1.5.5 Palaeosols and Weathering

Floodplain soils are the important climate proxies that reflect patterns of Quaternary alluvial deposition, water regime, climatic optimum and vegetation distribution. The channel zone is associated with lithosols which may be gravelly or fine sediment, often laminated with inherited micro-aggregates and organic matter (Brown 2001). There is a gradation into floodplain flat soils which generally become finer and increase in organic matter away from the channel and towards groundwater gley soils which occur in the backswamps (Brown 2001). Higher occurrence of particular minerals can reflect the environment of formation and alteration of floodplain sediments (Table 1.2).

The presence of pedogenic carbonates or caliches and Fe–Al or Fe–Mn mottles in the floodplain soils can infer dry and wet episodes of

Table 1.2 Development of common minerals in floodplain sediments

Mineral	Chemical formula	Environment of formation
Gibbsite	$Al(OH)_3$	Wet tropical
Limonite	Fe_2O_3, H_2O	Temperate
Jarosite	$KFe_3(SO_4)_2(OH)_6$	Temperate—estuarine
Viviantite	Fe_2PO_4	Temperate
Calcite	$CaCO_3$	Semi-arid and arid
Halite	NaCl	Semi-arid

Source Brown (2011)

Quaternary. Micromorphology (rhizocretes, Fe–Mn features, pedogenic carbonate, etc.), weathering information and dating of palaeosol are very necessary to know the palaeoenvironment of the Ganges Basin. In the Ganges–Yamuna interfluves, the mature palaeosols represent a major stratigraphic break of 8000–10,000 years BP when prolonged pedogenesis occurred over large areas of the Ganges–Yamuna interfluves following regional degradation and local gullying in response to climate change from sub-humid to semi-arid conditions (Srivastava et al. 2010). The clay pedogenic features formed during earlier wet phase (13.5–11 ka) show degradation and speckled appearance in contrast with later phase of wet climate (6.5–4 ka) in the Indo-Gangetic Plains (Srivastava et al. 2015). Western upland of GBD overlain by the red soils, characterized by autochthonous origin (Late to Middle Pleistocene age), shows the ferrugination phase of development under tropical wet–dry climate and the soils of Old Fluvial/Deltaic Plains (6–3 ka) have argillic horizons and exhibit the fersiallitisation phase of development under sub-humid climate (Singh et al. 1998). The usefulness of ferricrete and weathered mottled and bleached zones as morpho-stratigraphic markers is strongly depended upon whether the laterite formation has been continual or episodic (Bournman 1993). Weathering profile of laterite reflects an episode of seasonally dry, humid, tropical climatic optimum and resultant product of intensive chemical weathering of rocks (Thomas and Kale 2011).

1.5.6 Soil Erosion

In Anthropocene, the soils have critical relevance to current global issues such as food and water security, climate regulation, land degradation and desertification. Soil erosion is an issue where the adage 'think globally, act locally' is clearly apropos (Toy et al. 2013). It is learned that soil resource is being lost from the land areas 10 to 40 times faster than the rate of soil renewal imperilling future human food security and environmental quality (Pimentel 2006; Pimentel and Burgess 2013). It is estimated from sediment yield modelling that soil erosion is taking place at average rate of 16.35 tonne ha^{-1} $year^{-1}$ in India and about 29% of total eroded soil is lost permanently to the sea and 10% of it is deposited in reservoirs (Narayana and Babu 1983). In the humid subtropical region of India, soil erosion (about 15 million tonnes per year) leads to low crop productivity and an annual loss of 13.4 million tonnes in the production of crops due to water erosion equivalent to about $2.51 billion (Bhattacharyya et al. 2007; Sharda et al. 2010; Sharda and Dogra 2013).

The extreme form of soil erosion is gully erosion (Fig. 1.12) which represents a major sediment producing process, generating between 10 and 95% of total sediment mass at catchment scale, whereas gully channels often occupy less than 5% of total catchment area (Poesen et al. 2003; Valentin et al. 2005; Poesen 2011). There are wide ranges of threshold conditions or values (viz., thresholds of hydraulic, rainfall,

Fig. 1.12 Intensive gully erosion in the lateritic terrain of Birbhum, West Bengal

topography, lithology, land use–land cover control, etc.) which are responsible for the initiation of gullies in different environments (Patton and Schumm 1975; Vandaele et al. 1996; Vandekerckhove et al. 1998; Moeyersons 2003; Morgan and Mngomezulu 2003; Poesen et al. 2003; Montgomery and Dietrich 2004; Valentin et al. 2005; Dong et al. 2013; Torri and Poesen 2014). In West Bengal, the geomorphic studies of gully erosion are solely concentrated on the erodible laterites which are the most vulnerable sites of soil erosion (Kar and Bandyopadhyay 1974; Basu 1992; Jha and Kapat 2009, 2011; Ghosh and Guchhait 2012; Ghosh and Bhattacharya 2012; Shit and Maiti 2014; Shit et al. 2015b). The importance of these researches is mostly concentrated on the processes, modelling, estimation and effects of rill and gully erosion. In the lateritic region of western Bengal Basin (about 7700 km^2), land degradation is acute because of aberrant weather, drought, ferruginous crusting, rill and gully erosion, NKP (Nitrogen–Potassium–Phosphorous) deficiency, low water holding capacity and wide range of land use conversion (Jha and Kapat 2009, 2011; Shit et al. 2015a).

1.6 A Brief Outline of the Contributions

The discussion contained in the above sections clearly indicates nature and development of geomorphological studies in the quaternary period. The present volume is the outcome of 10 chapters besides this introductory chapter. The first two chapters (2 and 3) have focussed on geomorphology on lateritic substrate; next three chapters (4–6) have discussed the geophysical control on the fluvial process–form relations and how active and paleochannels are controlled by geophysical controls. Chapter 7 contributes important technique of identification of paleochannels using historical tools. Chapters 8 and 9 applied GIS techniques for understanding of quaternary river morphology. Last two chapters (10 and 11) are concerned with the geomorphology of Sundarban and the active deltaic part of the lower Ganges Basin. The following section will illuminate the uniqueness of the present book.

Western fringe of Bengal basin is characterized by typical lateritic formation. Present volume analysed that fringe to address perennial unanswered questions—what are the different modes of lateritization to classify laterites? What types of climates produce laterites? When and where were the particular palaeoclimates that formed laterites? What can laterites tell us about palaeoenvironment, palaeogeomorphology and other global events of the past? What are the microstructures of rocks in lateritic lands? The field studies, detailed profile analysis of lithofacies, geochemical analysis and characterization of various ferricretes, fossil records and OSL dating have emphasized on the primary and secondary origin of laterites in West Bengal to find answers of those unanswered questions in Chap. 2 of this volume. Chapter 3 with tools of

deposited microstructure features in one of the lateritic pockets, soil samples from gully dominated badland topography and snaps of the microscopic view along with digital colour analysis of thin sections of samples assessed prevailed processes of palaeo-coastal development and its associated events of cross-bedding, ripple marks and shoreline retreat mechanism at Gangani region of Paschim Medinipur, West Bengal.

In Chap. 4, remotely sensed data and field investigation were used to illuminate the sensitivity of extra-channel geomorphology to the stimulus of quaternary faulting. Along with in-channel deformation, extra-stream area was also modified with extended swampy floodplain, unpaired terraces, large alluvial fans and palaeochannels. Strike-slip fault was auxiliary to shifting channel path and developed series of palaeochannels over the neotectonic time frame. Fault line along the channel made stream straight, narrow and incised, which helped in the formation of alluvial fan. Surface gravity anomaly is important to know the underlying rock density since it plays dominant role in the channel pattern adjustment. The technique of knowing how longitudinal profile, planform index, channel geometry and other fluvial forms of alluvial deltaic channels are controlled and deformed by Bouguer gravity anomaly and in turn by underlying rock density is illustrated in this volume. Bouguer gravity anomaly effectively and efficiently used in Chaps. 5 and 6 in this context. The streamlines are sharply controlled by the variation in underlying rock density, alignment of the subsurface faults. Neotectonic influence on the deformation of channel planform (Cox 1994; Jacques et al. 2014; Kale et al. 2014), channel patterns, the assessment of the stream asymmetry and identification of tilted drainage basin (Siddiqui 2014; Jacques et al. 2014) and channel dynamics are studied in these two chapters. Geophysical control on the fluvial process–form relations and how active and paleochannels are controlled by geophysical controls are highlighted here. Besides geophysical consideration, Chap. 7 contributes important technique of identification of paleochannels using historical and archaeological tools. Old religious texts and literatures, calibrated with the information of other old maps, have been aptly mingled in the study of morphology of the past, especially to delineate the course of paleo-river channels. Technique may be applied to the end in wider world.

Besides these vital issues of geophysical control over channel forms and processes and identification of paleochannels, some fundamental problems in river sciences have been explored in next two chapters (Chaps. 8 and 9). Chapter 8 raises an important issue of channel confluence morphology—a basic problem in fluvial hydraulics. Confluence of two participating rivers is very much unique in terms of channel morphometry as well as hydraulics as it neither represents the mainstream nor reflects the tributary. Methodologies applied in this volume made simple knowing of rivers confluence with the help of RS and GIS. The next chapter (9) of this volume is focused on basic morphological aspects of fluvial system. Computed hydraulic parameters of the Bakreshwar River along with planform channel images and land use maps are used to demarcate the river corridor within which several terrains and channel attributes are investigated and their interlinkages are highlighted. Stream reach classification after the Rosgen (1994) method is used to demarcate morphologically distinct channel stretches.

Last two chapters (10 and 11) concentrated their focus on southernmost active deltaic part (Sundarbans) of the Lower Ganga Basin. Sundarban is the home of world largest mangrove forest taken together with India and Bangladesh. Chapter 10 used Landsat MSS for 1975, Landsat Thematic Mapper (TM) images of 1990, 2000 and Landsat 8 OLI image of 2015 to assess Tidal-Fluvial Dynamic Of Deltaic Island And Estuarine Processes In Indian Sundarban Of Lower Ganga River Basin and land use/land cover change. In Chap. 11 of this volume, application of remote sensing and GIS has been employed exquisitely to portray the geomorphic landscapes. Satellite Standard FCC is used as an inventory for land use–land cover and landform identification. It has made a leap in the knowing

of Ganges delta with smart use of latest technology.

This volume has been materialized for post-graduate students, research scholars and faculties who are in keen need of detailed knowing of geology of particular area, stratigraphy of a particular sub-basin, processes and forms of a micro-region within lower Ganges basin or in search of newer methodologies applicable for study of two-way feedback mechanism between forms and processes.

References

Acharyya SK, Shah BA (2007) Groundwater arsenic contamination affecting different geologic domains in India—a review: influence of geological setting, fluvial geomorphology and Quaternary stratigraphy. J Environ Sci Health 42(12):1795–1805

Acharyya SK, Shah BA (2010) Groundwater arsenic pollution affecting deltaic West Bengal, India. Curr Sci 99(12):1784–1787

Bandyopadhyay S, Das S, Kar NS (2015) Discussion paper: 'Changing river courses in the western part of the Ganga-Brahmaputra Delta'. Geomorphology 250:442–453

Basu P (1992) Morphology of Silai River in Garbeta area and evolution of its gully basins with reference to lateritization. Geogr Rev India 54(2):47–52

Bhattacharyya T, Babu R, Sarkar D, Mandal C, Dhyani BL, Nagar AP (2007) Soil and crop productivity model in humid sub-tropical India. Curr Sci 93 (10):1397–1403

Bilham R (2015) Raising Kathmandu. Nat Geosci 8:582–584

Blum MD, Tornqvist TE (2000) Fluvial response to climate and sea-level change: a review and look forward. Sedimentology 47:12–48

Bose M (2014) From morphostratigraphy to chronostratigraphy—modern Quaternary geomorphology as a basic for climatic research. Quat Geomorphol 20 (4):303–306

Bournman RP (1993) Perennial problems in the study of laterite: a review. Aust J Earth Sci 40(4):387–401

Brown AG (2001) Alluvail geoarchaeology—floodplain archaeology and environmental change. Cambridge University Press, Cambridge

Chakraborty T, Kar R, Ghosh P, Basu S (2010) Kosi megafan: historical records, geomorphology and the recent avulsion of the Kosi River. Quatern Int 227:143–160

Cohen KM, Finney SC, Gibbard PL (2015) International chorono stratigraphic chart. ICS

Cordier S, Briant B, Bridge D, Herget J, Maddy D, Mather A, Vandenberge J (2017) The Fluvial Archives Group: 20 years of research connecting fluvial geomorphology and palaeoenvironments. Quatern Sci Rev 166:1–9

Cox RT (1994) Analysis of drainage-basin symmetry as a rapid technique to identify areas of possible Quaternary tilt-block tectonics: an example from the Mississippi Embayment. Geol Soc Am Bull 106:571–581

Crutzen PJ (2002) Geology of mankind. Nature 415:23

Dong Y, Xiong D, Su Z, Li J, Yang D, Zhai J, Lu X, Liu G, Shi L (2013) Critical topographic threshold of gully erosion in Yuanmou dry-hot valley in south-western China. Phys Geogr 34(1):50–59

Friend PF, Sinha R (1993) Braiding and meandering parameters. In: Best JL, Bristow C (eds.) Braided rivers. Geological Society Special Publications No. 75, London, pp 105–111

Fryirs KA, Brierley GJ (2013) Geomorphic analysis of river systems: an approach to reading the landscape. Wiley-Blackwell, Chichester

Ghosh R, Bera S, Sarkar A, Paruya DK, Yao Y, Li C (2015) A ~50 ka record of monsoonal variability in the Darjeeling foothill region, eastern Himalayas. Quatern Sci Rev 114:100–115

Ghosh S, Bhattacharya K (2012) Multivariate erosion risk assessment of lateritic badlands of Birbhum (West Bengal, India): a case study. J Earth Syst Sci 121 (6):1441–1454

Ghosh S, Guchhait SK (2012) Soil loss estimation through USLE and MMF methods in the lateritic tracts of eastern plateau fringe of Rajmahal Traps, India. Ethiop J Environ Stud Manag 5(4):529–541

Ghosh S, Guchhait SK (2016) Dam-induced changes in flood hydrology and flood frequency of Tropical River: a study in Damodar River of West Bengal, India. Arab J Geosci 9:1–26

Ghosh S, Islam A (2016) Quaternary alluvial stratigraphy and palaeoclimatic reconsyruction in the Damodar River Basin of West Bengal. In: Das B, Ghosh S, Islam A, Ismail M (eds) Neo-thinking on Ganges-Brahmaputra basin geomorphology. Springer, Switzerland, pp 1–18

Goff P (2017) Quaternary geomorphology and landscapes. In: Richardson D, Castree N, Goodchild MF, Kobayashi A, Liu W, Marston RA (eds) The encyclopedia of geography. Wiley, New York, pp 1–7

Grapes RH, Oldroyd D, Grigelis A (eds) (2008) History of geomorphology and quaternary geology. Geological Society Special Publication No 301, London

Holbrook J, Schumm SA (1999) Geomorphic and sedimentary response of rivers to tectonic deformation: a brief review and critique of a tool for recognizing subtle epeirogenic deformation in modern and ancient settings. Tectonophysics 305:287–306

Jacques PD, Salvador ED, Machado R, Grohmann CH, Nummer AR (2014) Application of morphometry in neotectonic studies at the eastern edge of the Paraná Basin, Santa Catarina State, Brazil. Geomorphology 213:13–23. https://doi.org/10.1016/j.geomorph.2013.12.037

Jain V, Sinha R (2005) Response of active tectonics in the alluvial Baghmati River, Himalayan foreland basin, eastern India. Geomorphology 70:339–356
Jha VC, Bairagya HP (2011) Flood plain evaluation in the Ganga-Brahmaputra Delta: a tectonic review. Ethiop J Environ Stud 4(3):12–24
Jha VC, Kapat S (2009) Rill and gully erosion risk of lateritic terrain in south-western Birbhum district, West Bengal, India. Rev Soc Nat 21(2):141–158
Jha VC, Kapat S (2011) Degraded lateritic soilscape and land uses in Birbhum district, West Bengal, India. Rev Soc Nat 23(3):545–556
Kale V (2012) On the link between extreme floods and excess monsoon epochs in South Asia. Clim Dyanmics 39:1107–1122
Kale VS (2002) Fluvial geomorphology of Indian Rivers: an overview. Prog Phys Geogr 26:400–433
Kale VS (2003) Geomorphic effects of monsoon floods on Indian rivers. Nat Hazards 28:65–84
Kale VS (2005) Fluvial hydrology and geomorphology of monsoon-dominated Indian rivers. Rev Brasil Geomorfol 6(1):63–73
Kale VS (2007) Fluvio-sedimentary response of the monsoon-fed Indian rivers to Late Pleistocene–Holocene changes in monsoon strength: reconstruction based on existing 14C dates. Quatern Sci Rev 26:1610–1620
Kale VS (2008) Palaeoflood hydrology in the Indian context. J Geol Soc India 71:56–66
Kale VS, Achyutha H, Jaiswal MK, Sengupta S (2010) Palaeoflood records from upper Kaveri River, southern India: evidence for discrete floods during Holocene. Geochronometria 37:49–55
Kale VS, Joshi VU (2004) Evidence of formation of potholes in bedrock on human timescale: Indrayani River, Pune district, Maharastra. Curr Sci 86(5):723–726
Kale VS, Mishra S, Baker VR (1997) A 2000-year palaeoflood record from Sakarghat on Narmada, central India. J Geol Soc India 50(3):283–288
Kale VS, Mishra S, Baker VR (2003) Sedimentary records of palaeofloods in the bedrock gorges of the Tapi and Narmada rivers, central India. Curr Sci 84 (8):1072–1079
Kale VS, Sengupta S, Achyuthan H, Jaiswal MK (2014) Tectonic controls upon Kaveri River drainage, cratonic Peninsular India: inferences from longitudinal profiles, morphotectonic indices, hanging valleys and fluvial records. Geomorphology 227:153–165. https://doi.org/10.1016/j.geomorph.2013.07.027
Kale VS, Singhvi AK, Mishra PK, Banerjee D (2000) Sedimentary records and luminescence chronology of Late Holocene palaeofloods in the Luni River, Thar Desert, northwest India. CATENA 40:337–358
Kar A, Bandyopadhyay MK (1974) Mechanisms of rills: an investigation in microgeomorphology. Geogr Rev India 36(3):204–215
Keller EA, Pinter N (1996) Active Tectonics: earthquakes, uplift and landscape. Prentice-Hall, Upper Saddle River
Lewis SL, Maslin MA (2015) Defining the anthropocene. Nature 519:171–180
Lowe J, Walker M (2015) Reconstructing quaternary environments. Routledge, New York
Macklin MG, Lewin J, Woodward JC (2012) The fluvial record of climate change. Philos Trans R Soc 310:2143–2172
Malik JN, Mohanty C (2007) Active tectonic influence on the evolution of drainage and landscape: geomorphic signatures from frontal and hinterland areas along the north western Himalayas, India. J Asian Earth Sci 29:604–619
Mather A (2011) Interpreting quaternary environment. In: Gregory KJ, Goudie AS (eds) The Sage handbook of geomorphology. Sage, London, pp 513–534
Meadows ME (2016) Geomorphology in the Anthropocene: perspectives from the past, pointers for the future? In: Meadows ME, Lin J (eds) Geomorphology and society. Springer, New York, pp 7–22
Miall AD (2014) Fluvial depositional systems. Springer, London
Mishra S, Naik S, Rajaguru SN, Deo S, Ghate S (2003) Fluvial response to late Quaternary climate changes: case studies from upland Maharastra. Proc Indian Natl Sci Acad 69:185–200
Moeyersons J (2003) The topographic thresholds of hillslope incisions in southwestern Rwanda. CATENA 50:381–400
Montgomery DR, Dietrich WE (2004) Landscape dissection and drainage area-slope thresholds. In: Kirkby MJ (ed) Process models and theoretical geomorphology. Wiley, New York, pp 221–246
Morgan RPC, Mngomezulu D (2003) Threshold conditions for initiation of valley-side gullies in the Middle Veld of Swaziland. CATENA 50:401–414
Narayana DVV, Babu R (1983) Estimation of soil erosion in India. J Irrig Drain Eng 109(4):419–434
Ouchi S (1985) Response of alluvial rivers to slow active tectonic movement. Geol Soc Am Bull 96:504–515
Pal T, Mukherjee PK, Sengupta S, Bhattacharyya AK, Shome S (2002) Arsenic pollution in groundwater of West Bengal, India—an insight into problem by subsurface sediment analysis. Gondwana Res 5:501–512
Patton PC, Schumm SA (1975) Gully erosion, northwestern Colorado: a threshold phenomenon. Geology 3:88–90
Pimentel D (2006) Soil erosion—a food and environmental threat. Environ Dev Sustain 8:119–137
Pimentel D, Burgess M (2013) Soil erosion threatens food production. Agriculture 3:443–463
Poesen J (2011) Challenges in gully erosion research. Landf Anal 17:5–9
Poesen J, Nachtergaele J, Verstraeten G, Valentin C (2003) Gully erosion and environmental change: importance and research needs. CATENA 50:91–133
Raj R (2012) Active tectonics of NE Gujarat (India) by morphometric and morphostructural studies of Vatrak River Basin. J Asian Earth Sci 50:66–78
Rajaguru SN, Deo SG, Mishra S (2011a) Pleistocene climate change in western India: a geoarchaeological

approach. http://www.ifr.res.in/ārchaeo/FoP/…/Rajaguru%20climate.pdf [21 June 2018]
Rajaguru SN, Deotare BC, Gangopadhyay K, Sain MK, Panja S (2011b) Potential geoarchaeological sites for luminescence dating in the Ganga-Bhagirathi-Hugli Delta, West Bengal, India. Geochronometria 38(3): 282–291
Rajaguru SN, Kale VS, Badam GL (1993) Quaternary fluvial systems in upland Maharastra. Curr Sci 11:817–821
Rajmohan N, Prathapar SA (2013) Hydrogeology of the Eastern Ganges Basin: an overview. IWMI Working Paper 157, New Delhi, pp 1–33
Rana N, Singh S, Sundriyal YP, Rawat GS, Juyal N (2016) Interpreting the geomorphometric indices for neo-tectonic implications: an example of Alaknanda valley, Garhwal Himalaya, India. J Earth Syst Sci 125 (4):841–854
Rosgen DL (1994) A classification of natural rivers. Catena 22(6):169–199
Roy AB, Chatterjee A (2015) Tectonic framework and evolutionary history of the Bengal Basin in the Indian subcontinent. Curr Sci 109(2):271–279
Rudra K (2010) Dynamics of the Ganga in West Bengal, India (1764–2007): implications for science-policy interaction. Quatern Int 227(2):161–169
Rudra K (2014) Changing river courses in the western part of the Ganga-Brahmaputra Delta. Geomorphology 227:87–100
Sahu S, Raju NJ, Saha D (2010) Active tectonics and geomorphology in the Sone-Ganga alluvial tract in mid-Ganga Basin, India. Quatern Int 227:116–126
Sanyal P, Sinha R (2010) Evolution of Indian summer monsoon: synthesis of continental records. In: Clift PD, Tada R, Zheng H (eds) Monsoon evolution and tectonic-climate linkage in Asia. Geological Society, London, pp 152–183
Sarkar A, Mukherjee AD, Bera MK, Das B, Juyal N, Morthekai P, Deshpande RD, Sinde VS, Rao LS (2016) Oxygen isotope in archaeological bioapatites from India: implications to climate change and decline of Bronze Age Harappan civilization. Nature Scientific Reports 6:1–9
Schumm SA (1977) The fluvial system. Wiley, New York
Schumm SA (1979) Geomorphic thresholds: the concept and its applications. Trans Inst Br Geogr 4(4):485–515
Schumm SA, Dumont JF, Holbrook JM (2002) Active tectonics and alluvial rivers. Cambridge University Press, Cambridge
Sear DA, Newson MD (2010) Fluvial geomorphology: its basis and methods. In: Sear DA, Newson MD, Throne CR (eds) Guidebook of applied fluvial geomorphology. Thomas Telford, London, pp 1–31
Sengupta S, Kale VS (2011) Evaluation of the role of rock properties in the development of potholes: a case study of Indrayani knickpoint, Maharastra. J Earth Syst Sci 120(1):157–165
Sharda VN, Dogra P (2013) Assessment of productivity and monetary losses due to water erosion in rainfed crops across different states of India for prioritization and conservation planning. Agric Res 4:382–392
Sharda VN, Dogra P, Prakash C (2010) Assessment of production losses due to water erosion in rainfed areas of India. J Soil Water Conserv 65(2):79–91
Sharma VK (2010) Introduction to process geomorphology. CRC Press, Boca Raton
Shit PK, Maiti R (2014) Gully erosion control—lateritic soil region of West Bengal. Indian Science Cruiser 28 (3):54–61
Shit PK, Nandi AS, Bhunia GS (2015a) Soil erosion risk mapping using RUSLE model on Jhargram subdivisional West bengal in India. Model Earth Syst Environ 1:28
Shit PK, Paira R, Bhunia G, Maiti R (2015b) Modeling of potential gully erosion hazard using geo-spatial technology at Garhbeta block, West Bengal in India. Model Earth Syst Environ 1(2). https://doi.org/10.1007/s40808-015-0001-x
Siddiqui S (2014) Appraisal of active deformation using DEM-based morphometric indices analysis in Emilia-Romagna Apennines, Northern Italy. Geodyn Res Int Bull 1(3):34–42
Singh IB (1996) Geological evolution of Ganga Plain—an overview. J Palaeontol Soc India 41:99–137
Singh LP, Parkash B, Singhvi AK (1998) Evolution of the lower Gangetic plain landforms and soils in West Bengal, India. CATENA 33:75–104
Singhvi AK, Kale VS (2009) Paleoclimatie studies in India: last ice age to the present. IGBP-WCRP-SCOPE-Report Series 4, Indian National Science Academy, New Delhi
Sinha R (2009) The great avulsion of Kosi on 18th August 2008. Curr Sci 97(3):429–433
Sinha R, Friend PF (2007) Quaternary fluvial systems in India. Quatern Int 159:1–5
Sinha R, Friend PF, Switsur VR (1996) Radiocarbon dating and sedimentation rates in the Holocene alluvial sediments of the north Bihar plains, India. Geol Mag 133:85–90
Sinha R, Ghosh S (2012) Understanding dynamics of large rivers aided by satellite remote sensing: a case study from Lower Ganga plains, India. Geocarto Int 27(3):207–219
Sinha R, Sarkar S (2009) Climate-induced variability in the Late Pleistocene–Holocene fluvial and fluvio-deltaic successions in the Ganga plains, India: a synthesis. Geomorphology 113:173–188
Sinha R, Sripriyanka K, Jain V, Mukul M (2014) Avulsion threshold and planform dynamics of the Kosi River in north Bihar (India) and Nepal: a GIS framework. Geomorphology 216:157–170
Sinha R, Tandon SK, Gibling MR, Bhattacharjee PS, Dasgupta AS (2005) Late Quaternary geology and alluvial stratigraphy of the Ganga Basin. Himalayan Geol 26(1):223–240
Sridhar A, Chamyal LS, Patel M (2014) Palaeoflood record of high-magnitude events during historical time in the Sabarmati River, Gujarat. Curr Sci 107(4): 675–679

Srivastava P, Aruche M, Arya A, Pal DK, Singh LP (2015) A micromorphological record of contemporary and reclit pedogenic processes in soils of the Indo-Gangetic Plains: implications for mineral weathering, province and climate changes. Earth Surf Proc Land 41(6):771–790

Srivastava P, Rajak MK, Sinha R, Pal DK, Bhattacharyya T (2010) A high-resolution micromorphological record of the late Quaternary paleosols from Ganga-Yamuna interfluve: stratigraphic and paleoclimatic implications. Quatern Int 227:127–142

Steckler MS, Mondal DR, Akhter SH, Seeber L, Feng L, Gale J, Hill EM, Howe M (2016) Locked and loading megathrust linked to active subduction on beneath the Indo-Burman Ranges. Nat Geosci. https://doi.org/10.1038/NGEO02760

Tandon SK, Singa R, Gibling MR, Dasgupta AS, Ghazanfari P (2008) Late Quaternary evolution of the Ganga Plains: nyths and misconceptions, recent developments and future direction. J Geol Soc India 66:259–299

Tare V, Roy G, Bose P (2013) Ganga river basin environment management plan: interim report. IIT Consortium. http://wrmin.nic.in/writereaddata/GRBEMPInterimReport.pdf

Thomas M, Kale V (2011) Tropical environment. In: Gregory KJ, Goudie AS (eds) The Sage handbook of geomorphology. Sage, London, pp 449–468

Thornbury WD (1969) Principles of geomorphology. Wiley, New York

Tornqvist TE (2013) Reponses to rapid environmental change. In: Elias S, Mock C (eds) Encyclopedia of quaternary science. Elsevier, New York

Torri D, Poesen J (2014) A review of topographic threshold conditions for gully head development in different environment. Earth-Sci Rev 130:73–85

Toy TJ, Foster GR, Renard KG (2013) Soil erosion: processes, prediction: Measurement and Control. Wiley, New York

Valentin C, Poesen J, Li Y (2005) Gully erosion: impacts, factors and control. CATENA 63:132–153

Vandaele K, Poesen J, Govers G, Wesemael B (1996) Geomorphic threshold conditions for ephemeral gully incision. Geomorphology 16(2):161–173

Vandekerckhove L, Poesen J, Wijdenes DO, Figueiredo T (1998) Topographic thresholds for ephemeral gully initiation in intensively cultivated areas of the Mediterranean. CATENA 33:271–292

Wilson CA, Goodbred SL (2015) Construction and maintenance of the Ganges-Brahmaputra-Meghna Delta: linking process, morphology and stratigraphy. Ann Rev Marine Sci 7:67–88

Witze A (2015) Major earthquake hits Nepal. Nature 10. https://doi.org/10.1038/nature.2015.17413

Zalasiewicz J, Williams M, Haywood A, Ellis M (2011) The Anthropocene: a new epoch of geological time? Philos Trans R Soc 369:835–841

2

Modes of Formation, Palaeogene to Early Quaternary Palaeogenesis and Geochronology of Laterites in Rajmahal Basalt Traps and Rarh Bengal of Lower Ganga Basin

Sandipan Ghosh and Sanat Kumar Guchhait

Abstract

The present research work deals with the geomorphic evolution of in situ (primary) and ex situ (secondary) types of laterites (in West Bengal, eastern part of India) which are found as distinct badland terrain and litho-stratigraphic unit, developed in between the eastern fringe of Chotanagpur Plateau (Rajmahal Basalt Traps, Gondwana sedimentary and Archaean rocks) and the western fringe of Bengal Basin (Rarh Bengal). These laterites are analyzed here to address perennial unanswered questions about their genesis. What are the different modes of lateritization to classify laterites? What types of climates produce laterites? When and where were the particular palaeoclimates that formed laterites? What can laterites tell us about palaeoenvironment, palaeogeomorphology and other global events of the past? The field studies, detailed profile analysis of lithofacies, geochemical analysis, characterization of various ferricretes, fossil records and OSL dating have emphasized on the primary and secondary origin of laterites in West Bengal. The primary laterites (Palaeogene to Neogene) are genetically related to parent rocks, viz., Rajmahal basalt and Gondwana sandstones, but the secondary laterites are re-cemented ferruginous materials of fluvial fan-deltaic depositions which are related to Early to Late Quaternary tectono-climatic evolution of north-western Bengal Basin. Here the geochronology of few secondary laterite profiles is determined by OSL dating method in three sample sites, representing Late Quaternary palaeogenesis of laterites and ferruginized sediments (150–35 ka), i.e. Late Pleistocene. The analysis of in situ and ex situ laterites signifies drifting of Indian plate through ideal tropics from Palaeogene to Early–Late Quaternary and widespread occurrence of basal chemical weathering under strong, optimum and seasonal tropical wet–dry climate than prevail today in this part of West Bengal. The litho-stratigraphic ferruginous unit of Rarh Bengal (formerly the palaeovalleys of ferruginous depositions) was developed as an inverted relief due to prolong gully erosion and neo-tectonic uplift in between the Chotanagpur Foot-hill Fault and Medinipur–Farraka Fault.

S. Ghosh (✉)
Department of Geography, Chandrapur College, Barddhaman 713145, West Bengal, India
e-mail: sandipanghosh19@gmail.com

S. K. Guchhait
Department of Geography, The University of Burdwan, Barddhaman 713104, West Bengal, India
e-mail: guchhait.sanat37@gmail.com

B. C. Das et al. (eds.), *Quaternary Geomorphology in India*,
Geography of the Physical Environment, https://doi.org/10.1007/978-3-319-90427-6_2

Keywords
Laterite · Inversion of relief · Palaeoclimate Palaeogeomorphology · Optically stimulated luminescence · Bengal basin

2.1 Introduction

Studies of long time-scales of landscape evolution are often considered less important in the geomorphology and Quaternary studies than those dealing now with processes and chronologically secure high-resolution sequences of Late Quaternary age (Rajaguru et al. 2004a, b). But this can be false dichotomy, as any landscape is a product of forms, materials of different origins and ages and the present day landscape has roots in relict and ancient environment with overprint of the Quaternary processes (Pappu and Rajaguru 1979; Sahasrabudhe and Rajaguru 1990; Rajaguru et al. 2004a, b; Mishra et al. 2007; Deo and Rajaguru 2014). The laterites of India are such geological unit which usually reflects relict weathered products of pre-Anthropocene palaeoenvironment, morpho-stratigraphic markers of past and unique paleogeomoprhic evolution since Palaeogene (Milnes et al. 1985). Laterites reflect a past geo-climatic environment which is not present in India and as well as in West Bengal, because many researchers agreed that existing laterites are clearly relics of geological antiquity (Sivarajasingham et al. 1962). The time span and ideal climate needed to create a fully developed laterite profiles is still unknown to many researchers. According to Bonnet et al. (2014) the ferruginous duricursts on the relics of palaeo-land surfaces in mostly cratonic domains results from successive long-duration chemical weathering and tectonic stability and such landforms represent morpho-climatic or climato-genetic fingerprints of tropical region. Here the genesis and geochronology of laterites and lateritization processes in north-western part of the Bengal Basin (eastern part of Chotanagpur Plateau or Peninsular Craton) are still needed to unearth in the light of palaeogeography of that region.

The term 'laterite' (from the Latin *later*, brick), is commonly attributed to Buchanan (1807) who described, in Malabar of Southern India, near-surface natural hard ferruginous materials used as brick (Tardy 1992). In a broadest sense the laterite include ferricrete, iron duricrust, mottled horizon, carapace, cuirasses, plinthite, pisolite or nodule bearing ferruginous materials and also kaolinitic lithomarge (Persons 1970; McFarlane 1976; Varghese 1987; Tardy 1992). Laterite can be defined as the reddish – brown coloured product of intense tropical weathering made up of mineral assemblages that may include iron or aluminum oxides, oxyhydroxides or hydroxides, kaolinite and quartz, characterized by a molar ratio, SiO_2:R_2O_3 (where, $R_2O_3 = Al_2O_3 + Fe_2O_3 + TiO_2$), and subjected to hardening upon exposure to alternate wetting and drying (Alexander and Cady 1962; Maignien 1966; McFarlane 1976; Tardy 1992). Nomenclature, classification, morphological and analytical characteristics, global distribution, lateritization processes and favourable conditions of laterites are precisely analyzed by Alexander and Cady (1962), Maignien (1966), Persons (1970), Paton and Williams (1972), Thomas (1974), McFarlane (1976), Young (1976), Aleva, (1985), Tardy and Nahon (1985), Tardy (1992), Ollier and Galloway (1990), Ollier (1991), Tardy et al. (1993) and Bourman (1993, 1996). In Indian context Roy Chowdhury et al. (1965), Pascoe (1964), Ray Chaudhuri (1980), Roy Chowdhury (1986), Babu (1981), Devaraju and Khanadali (1993), Achyuthan (1996), Widdowson and Cox (1996), Widdowson and Gunnell (1999), Achyuthan (2004), Ollier and Sheth (2008), Karlekar and Thakurdesai (2011) and Kale (2014) had been investigated the various profiles of Indian laterites and mentioned the in situ and ex situ origin of laterites in post-Late Cretaceous period, relating the drift of Indian plate and palaeoclimate. In West Bengal the detail regional and geomorphic descriptions of *Rarh* laterites are provided by Niyogi et al. (1970),

Niyogi (1975), Biswas (1987), Chatterjee (2008) and Chakraborti (2011). They have feebly emphasized on the onset of Neogene lateritization climate in relation to neo-tectonic activity of the north-western Bengal Basin. Importantly the litho-stratigraphic unit of ferruginous materials depicts a post-Cretaceous lateritization phase and marks distinct tropical wet-dry morphogenetic landforms between western Archaean–Gondwana of Peninsular Craton and eastern Quaternary alluvium of Bengal Basin.

In West Bengal the lateritic uplands or upland red soil groups (Singh et al. 1998) occur along a NE–SW trending belt parallel to the western margin of Bengal Basin. This unique geomorphic region (i.e. shelf zone of Bengal Basin) is designated as *Rarh* Bengal by Bagchi and Mukherjee (1983). The duricrusts, ferruginous gravels and kaolinite deposits (from Rajmahal Basalt Traps to Subarnarekha Basin) borders this province to make the transitional diagnostic tropical weathering surface and distinct sedimentary lithofacies in between the Archaean–Gondwana litho-unit at west and the Quaternary alluvial litho-unit of Bengal Basin at east (Niyogi et al. 1970; Niyogi 1975; Biswas 1987; Das Gupta and Mukherjee 2006). The information on stratigraphic or geomorphic relations, laterite–parent rock relationships, genesis of laterites and absolute age data are very scanty in this region. Basically the geomorphic evolution of laterites and exact age of duricrust are still not scientifically evaluated in West Bengal. To resolve the aforesaid problems and to depict the unique characterization and palaeogeography of laterites, this work is initiated to analyze the different laterite profiles of Rajmahal Basalt Traps (RBT) and *Rarh* Bengal.

2.2 Research Gaps and Needs

The laterite described by Buchanan (1807) is only one member of laterite families whose members have different properties but similar genesis. Laterites have raised controversy ever since the term was coined and disagreements over the definition of laterite have continued sporadically for 150 years (Thomas 1996). There has been renewal interest in the geochemistry, genesis and formation of laterites during the International Geological Correlation Programme (IGCP) project on 'Lateritization Processes' held in Trivandrum, India (1979). In spite of numerous publications and researches on laterites, much confusion, contradiction and controversies still proliferate in the available literatures on the genesis, distribution, classification, geological age, sub-surface profiling of laterites and present day lateritization process (Ghosh and Guchhait 2015). There are good and significant researches on the laterites of peninsular India (Roy Chowdhury 1986; Kumar 1986; Sychanthavong and Patel 1987; Ollier and Rajaguru 1989; Widdowson and Cox 1996; Rajaguru et al. 2004a, b; Ollier and Sheth 2008), but there are important research gaps to investigate the laterites of RBT and *Rarh* Bengal. To understand genesis and development of ferruginous laterites (mainly in RBT and *Rarh* Bengal) some imperative considerations, quires and research needs are born in mind.

(1) There is a question regarding source of ferrallitic material which contributed to make up reddish-brown duricrust of *Rarh*.
(2) Whether laterite and its variant are highly related to tropical chemical weathering of RBT and other rocks or western shelf deposits of Bengal Basin.
(3) Whether primary (in situ) or secondary (ex situ) origin of laterites (i.e. modes of formation) is observed in the region.
(4) Whether there is any possibility or potentiality of these laterites as an indicator of palaeoclimate and palaeogeomophic event (simultaneously tectono-climatic evolution).
(5) A key issue is raised about the exact age and geochronology of laterites in this region.
(6) There is a research need to understand the relation between drifting of Indian plate and establishment of lateritization climate.

Above all one basic question is borne in mind—what are reflected from the laterites to known about past environments and events?

Understanding above research needs and question, this work has set forth three prime objectives within the domain of palaeogeography:

- Analyzing the lithofacies of laterites to evaluate in situ and ex situ origin,
- Determining the possible time span of lateritization event, and
- Exploring the palaeoclimatic and palaeogeomorphic significance of laterites.

2.3 Materials and Methods

2.3.1 Study Area and Sample Sites

The west–central part of West Bengal is neo-tectonically influenced by the basin margin faults systems (i.e. Chotanagpur Foothill Fault, Garhmayna–Khandoghosh Fault and Pingla Fault) and the zone of laterites is placed in between the fault systems as an uplifted block. This region is geographically recognized as *Rarh*, i.e. 'land of red soil' (Bagchi and Mukherjee 1983; Sarkar 2004). The combined zones of primary and secondary laterites with Neogene gravel deposits is the main spatial unit of study, bounded by the latitude of 21° 30′ to 24° 40′N and longitude of 86° 45′ to 87° 50′E (Fig. 2.1). The distribution of laterites and ferruginous soils of *Rarh* is limited to eastern part of Chotongapur Plateau fringe, covering an approximate area of 7700 km^2 (comprising the districts of Murshidabad, Birbhum, Barddhaman, Bankura, Purulia and West Medinipur). A parallel west–east flowing (due to general west to east trending slope of underlying structure)peninsular drainage system (viz., Brahmani, Dwarka, Mayurakshi, Ajay, Damodar, Dwarkeswar, Silai, Kangsabati and Subarnarekha rivers) dissect the lateritic *Rarh* region into patches of badlands and tropical deciduous forests of West Bengal. This region bears the characteristics of a tropical sub-humid type of monsoon climate (mean annual rainfall of 1200–1400 mm) and tropical wet-dry morphogenetic landforms. Geologically this part of West Bengal was formerly developed as the stable shelf province of Bengal Basin which experienced severally marine regression and transgression since Miocene, related to climate change and neo-tectonic activity (Alam et al. 2003). Fringing the basalts of Early Cretaceous Rajmahal Basalt Traps, sandstones of Gondwana Formations (Permian–Silurian) and granite–gneiss of Archaean Formation at west and Late Quaternary Older Alluvium (Panskura and Sijua Formations) at east, the lateritic zone of *Rarh Bengal* is found at the north–western border of Bengal Basin. Detailed field investigations of weathering archives are conducted in the sample sites (covering study area) of Nalhati (24° 17′ 47″N, 82° 49′ 28″E), Pinargaria (24° 12′ 13″N, 87° 40′ 13″E), Ghurnee Pahar (24° 15′ 43″N, 87° 39′ 11″E), Dubrajpur (23° 47′ 12″N and 87° 25′ 19″E), Sriniketan (23° 41′ 31″N and 87° 40′ 31″E), Hetodoba (23° 26′ 45″N and 87° 32′ 07″E), Bishnupur (23° 05′ 28″N and 87° 16′ 15″E), Garhbeta (23° 05′ 28″N and 87° 16′ 15″E) and Rangamati (22° 24′ 42″N, 87° 17′ 55″E), covering the span of study area.

2.3.2 Methodology

2.3.2.1 Secondary Data Collection

To collect spatial information the topographical sheets (1:50,000 scale) of Survey of India (SOI, 72 P/12, 73M/3, M/4, M/6, M/10, M/11 and 73N/1) and GSI (Geological Survey of India) district resource maps of Birbhum, Barddhaman, Bankura and West Medinipur districts are severally used in research. The outline map of *Rarh Bengal* is prepared in ArcGis 9.1 with the help of a base-map prepared by Bagchi and Mukherjee (1983). With help of shape file format we have prepared thematic maps using option of subset in Erdas 9.1. To identify the lateritic zone we have applied NDVI (Normalized Difference Vegetation Index) and Iron Oxide Index in Erdas 9.1 imagine using post-monsoon GLCF (Global Land Cover Facility, http://glcf.umd.edu/data/landsat/). Landsat ETM+ images of 2000–2001

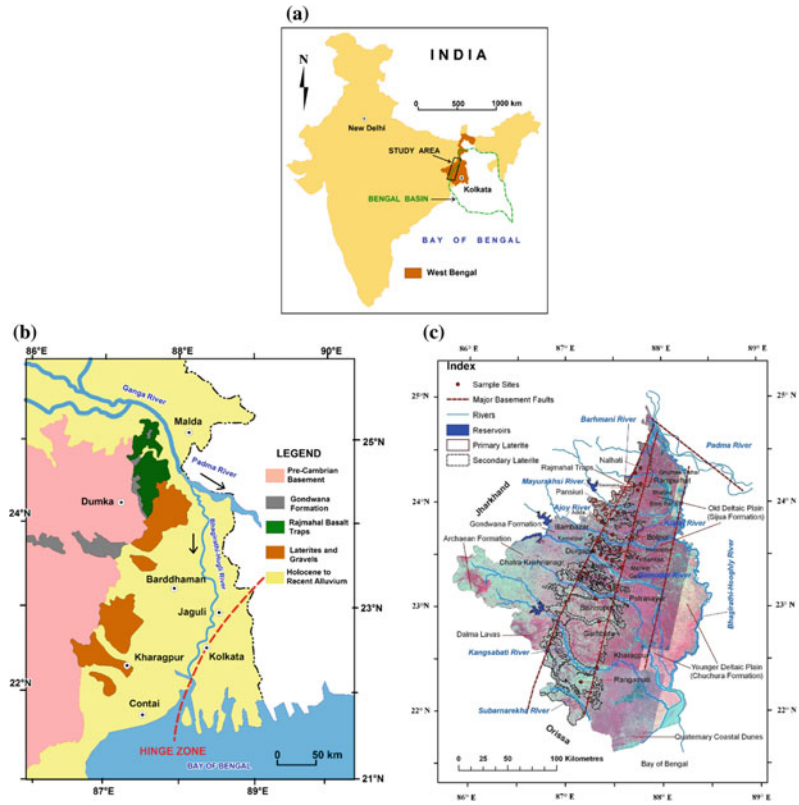

Fig. 2.1 **a** Location of study area and Bengal Basin in eastern part of India, **b** general surface geology of north-west part of Bengal Basin (modified from Das Gupta and Mukherjee, 2006), and **c** identified units of primary and secondary laterites (i.e. study area) with basement fault system in West Bengal, dissected by west–east flowing parallel rivers and merged with Older Deltaic Plain (Sijua Formation) of Bengal Basin at east (Ghosh and Guchhait 2015)

(path/row—138/43, 138/44, 138/45, 139/43, 139/44, 139/45 and 140/44). The ASTER (Advanced Space Borne Thermal Emission and Radiometer) elevation data with 30 m resolution of 2011 is collected from the website of Earth Explorer (http://earthexplorer.usgs.gov/). Alongside we have used the unpublished geological expedition reports of GSI, Eastern Region which are regularly provided in the official website (http://www.portal.gsi.gov.in). The total workflow of this work is depicted in flowchart (Fig. 2.2).

2.3.2.2 Geochemical Analysis

The lithosections of laterite profiles are investigated and analyzed on the basis of texture, colour, cementation, degree of mottling and bleaching, weathering front, iron–aluminum oxides assemblages and other petrograhic and geo-chemical properties. The chemical properties of laterite samples belonging to dismantled duricrust, ferricrete, clay horizons and saprolite zones are analyzed along the profile with depth to know the variable percentages of SiO_2, Al_2O_3, Fe_2O_3, MnO, MgO, CaO, Na_2O, K_2O, TiO_2 and P_2O_5. Then the molar ratio SiO_2/R_2O_3 (where, $R_2O_3 = Al_2O_3 + Fe_2O_3 + TiO_2$), suggested as an index of tropical weathering (Birkeland 1984; Singh et al. 1998), is used in the sample sites for increasing degree of leaching and Fe–Al segregations at the top. To know the degree of lateritization we have used Al_2O_3–Fe_2O_3–SiO_2triangular diagram (Schellmann 1986; Pain and Ollier 1995a; Meshram and Randive 2011) triangular diagram in this study. Chemical weathering strongly affects the mineralogy and major elements geochemistry of the bed rocks. The degree of weathering can be evaluated

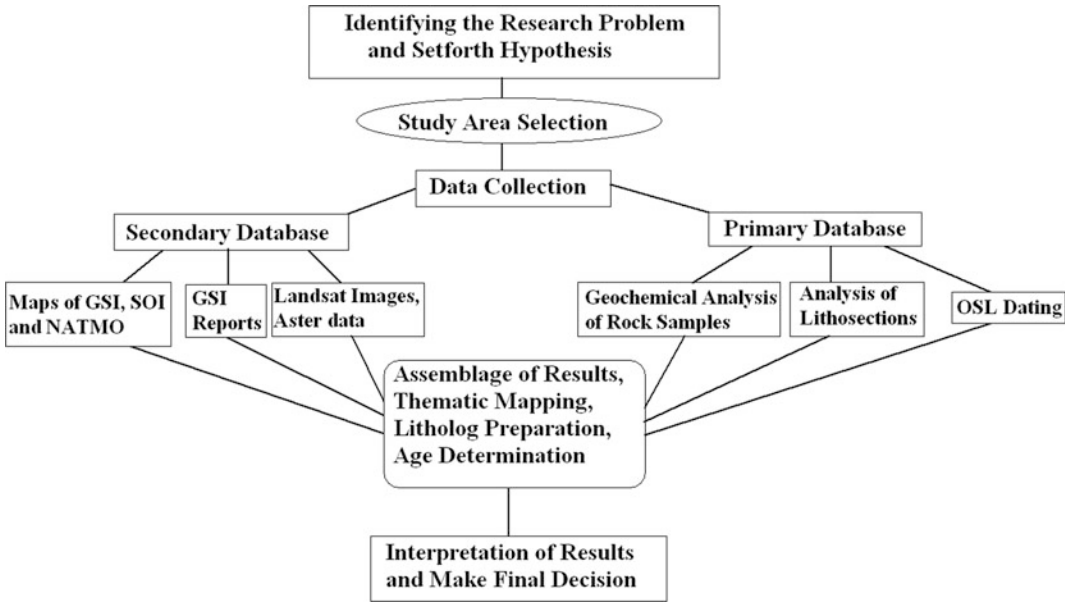

Fig. 2.2 Flowchart of adopted methodology used in this study

by quantitative measures using whole rock chemical analysis such as Chemical Index of Alteration (CIA) defined by Nesbitt and Young (1982) and Meshram and Randive (2011).

$$\mathrm{CIA} = 100\ \mathrm{Al_2O_3}/(\mathrm{Al_2O_3} + \ \mathrm{CaO} + \mathrm{Na_2O} + \mathrm{K_2O})$$

2.3.2.3 OSL Dating Method of Lithofacies

The choice of a particular proxy depends on the period for which palaeoclimate information is being retrieved, the site and availability of suitable material for extracting the proxy data. In general, any dating method can be understood by a simple example of a beaker being filled at a certain input drop rate or being emptied at a known rate (Singh et al. 1998; Singhvi and Kale 2009). Out of a number of dating tools, radiocarbon dating (^{14}C) is historically the most commonly used technique, but ^{14}C dating is limited to the environments where organic matter is preserved. As an alternative, optically stimulated luminescence (OSL) dating is applied here to find the accurate age of facies. OSL dating method uses minerals (quartz and feldspar) that are common in most environments making the technique applicable in the tropical landscapes of laterites. Fluvial sediments and fan deposits are the natural archives which have been used here in palaeoclimatic reconstruction (Ghosh and Guchhait 2014). The isotopic composition and mineralogical changes are the recommended climate proxies of various laterite profiles (i.e. primary and secondary laterites) which enables quantification of the change in climate in the past (Ghosh and Guchhait 2014).

Luminescence dating determines the age since burial of sediment by measuring the total amount of stored signal resulting from exposure of the sediment to a known annual dose of background radiation (Aitken 1998; Duller 2004; Preusser et al. 2008). OSL was introduced for dating by Huntley et al. (1985) and in geological dating, it is most important because the trapped electron component (Botter-Jensen 1997) is most likely to be emptied during transport prior to deposition and burial. The precise method of luminescence dating was reviewed, elaborated and used by Aitken (1998), Botter-Jensen (1997), Prescott and Robertson (1997), Wintle (1997, 2008), Stokes (1999), Murray and Olley (2002), Duller (2004), Preusser et al. (2008) and Rittenour

(2008). This dating method is successfully applied in the practical fields of geology, geomorphology, archeology and other palaeogeographic studies in India (Singhvi et al. 1982; Sankaran et al. 1985; Singh et al. 1998; Kale et al. 2000; Briant et al. 2006; Sridhar 2007; Singhvi and Kale 2009; Rajaguru et al. 2011; Metha et al. 2012). There is almost no research work to detect the age of lateritization in West Bengal using advanced dating methods. Here to unearth the geochronology of *Rarh* laterite and its palaeogeographic importance the Geological Survey of India (Chakraborti 2011) have effectively used OSL dating method using well known Risø TL/OSL-DA-15 reader using internal Sr/Y-90 beta source and a combination of Schott UG 11 and BG-39 filters. The detail measurements of luminescence characteristics and equivalent dose distributions in nine samples of Sriniketan, Bishnupur and Garhbeta (representative samples of *Rarh* laterites) are key elements of this research work. The key element for the success of OSL dating method is the validity of the assumption of closed system, i.e. the system had no unknown inputs or leakages during the time period under consideration and that the drop or leak rate remained constant throughout and, if they did change then the magnitude and the style of change through time was exactly known.

The energy stored increases with the amount of radiation to which a crystal is exposed and this provides a 'clock' that is the basis of all luminescence dating methods (Duller 2004). Typically, irradiation at ~500 nm/2.5 eV leads to emission at wavelength shorter than 400 nm/3.1 eV which can be isolated from the stimulating wavelength by optical filters (Prescott and Robertson 1997; Botter-Jensen 1997). This is commonly known as OSL which introduced for dating by Huntley et al. (1985). Luminescence dating determines the age since burial of sediment by measuring the total amount of stored signal resulting from exposure of the sediment to a known annual dose of background radiation. The concept of luminescence dating relies on defects in the crystal lattice of dosimeter minerals, most commonly quartz and feldspar, to trap energy produced during the interaction between electrons within the crystal and background radiation from the radioactive decay of uranium (U), thorium (Th) and potassium (K), and cosmic rays (Singh et al. 1998; Singhvi and Kale 2009). The principle is expressed in the 'age' equation (Aitken 1998), where equivalent dose is the radiation dose delivered to the mineral grains in the laboratory to stimulate luminescence and dose-rate is the rate at which ionizing energy is delivered from the background radiation. The acquired thermoluminescence at any time is related to the time elapsed since the burial. The basic equation thermoluminescence age is the ratio between total acquired thermoluminescence since burial and rate of thermoluminescence acquisition (Singh et al. 1998; Preusser et al. 2008; Singhvi and Kale 2009). The SI unit for dose is Gray (Gy) which is a measure of how much energy is absorbed by a sample in joules per kilogram (J kg^{-1}). The dose rate computation assumed a radioactive decay series. The measurement errors using the conventional error calculation method in these cases are computed to be 10–12% and a working estimate of total error should be taken as ±15%. Routine OSL dating of quartz can give ages from 10 ± 3 a to 150 ka (Stokes 1999; Duller 2004). Fluvial sediments and weathered lithologies, commonly dated as bleaching regimes in this environment, are relatively well understood. It has been demonstrated that when gravels are dominated by inert lithologies, sand within gravel matrix provides here reliable age estimates.

2.4 Results

2.4.1 Laterites of RBT

A well developed and well preserved laterite profile of about 11 m thick, will all its attributes of primary laterites is exposed at Nalhati hillock (24° 17′ 47″N, 82° 49′ 28″E) near Nalhati, Birbhum district (Fig. 2.3). Pisolitic hardcrust with residual ferruginous latosol varies in

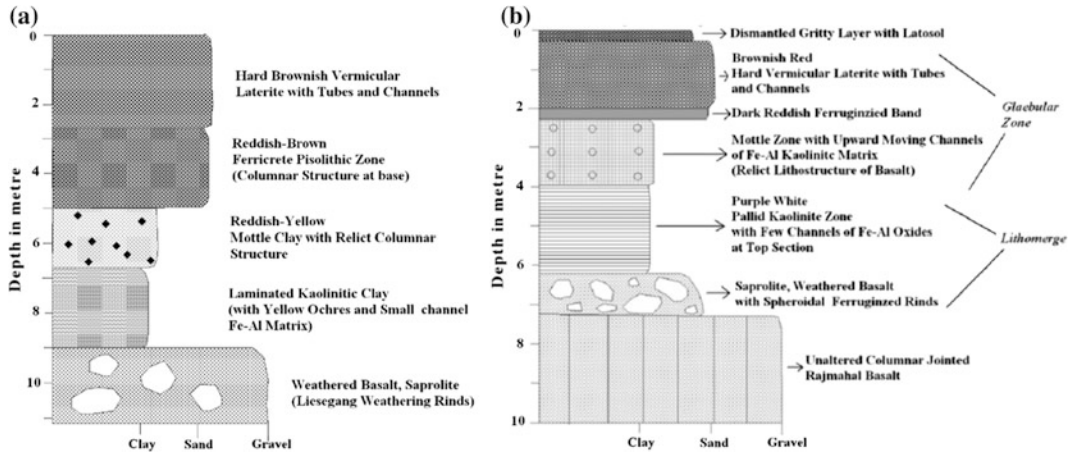

Fig. 2.3 **a** Well-developed sub-surface lithosection of primary laterite on the weathered Rajmahal Basalt in Nalhati, Birbhum and **b** in situ hard vermicular laterite profile of Pinargaria, Birbhum, having distinct zones of saprolite, kaolinte, mottle and ferricrete

thickness from 2.55 to 2.75 m. The broken pisolites show core to rim colour banding of limonitic to goethitic composition (i.e. gritty layer). About 2.75–4.0 m depth we have found ferricrete pisolite zone which is characterized by relict columnar structure of basalts. It corresponds to a progressive accumulation of iron and as a consequence, to a progressive development of hematitic iron nodules. The bleached zone is reduced in size, so that the yellow–white coloured domain decrease in size while the purple–red indurated domain enlarges and develops. A goethite cortex (concentric yellow brown) develops at the periphery of purple–red hematitic nodules. Below the hardcrust the thick mottle clay horizon with relict columnar structure (4.00–6.75 m) and laminated white kaolinite clay horizon with yellow ochre with small channels of Fe–Al oxides (6.75–9.00 m) are developed. Fe-mottles, mostly of a brown red colour, are diffuse glaebules and result in a concentration of iron which precipitates mainly as goethite and as hematite together with kaolinte matrix. The dominant minerals are secondary kaolinite $[Al_2Si_2O_5(OH)_4)]$ and ferruginous hydroxides in amorphous phase. This is followed by saprolite zone of weathered Rajmahal basalts having liesegang banding and weathering rinds (Fig. 2.4). These trap basalts are spheroidally weathered at base. It is constituted of plagioclase, pyroxene, opaque and glass with intergranular to intersertal texture. Ananalogous profile is found at an altitude of 227 m near Ghurnee Pahar, Birbhum (24° 15′ 43″N, 87° 39′ 11″E) (Table 2.1) and Pinargaria, Shikaripara, Jharkhand (24° 12′ 13″N, 87° 40′ 13″E) (Fig. 2.3).

2.4.2 Laterites of Gondwana

At the sample site of Dubrajpur, Birbhum (23° 47′ 12″N and 87° 25′ 19″E) the in situ residuum laterite profile is found over the Gondwana sandstone beds (Silurian age) with characteristic ferruginous residual soil, a loose murram horizon, hard crust, ferruginized sandstone and altered saprolitic sandstone (Fig. 2.5). The residual and partially developed soil generally forms a 25–35 cm thin soil cover consisting of relict ferricrete concretions and coarse sand grains. The presence of loose murram (i.e. dismantled horizon of ferricrete) over the duricrust is not a continuous phenomenon but wherever it is present, it occurs as 30–40 cm thick unit, constituting of ferricrete nodules, circular to amoeboid shaped concretions of iron and sand balls. Hard structured massive duricrust ranges in thickness from 2.0 to 2.65 m and may be divided into pisolitic ferricrete (up to 1.0 m depth) and

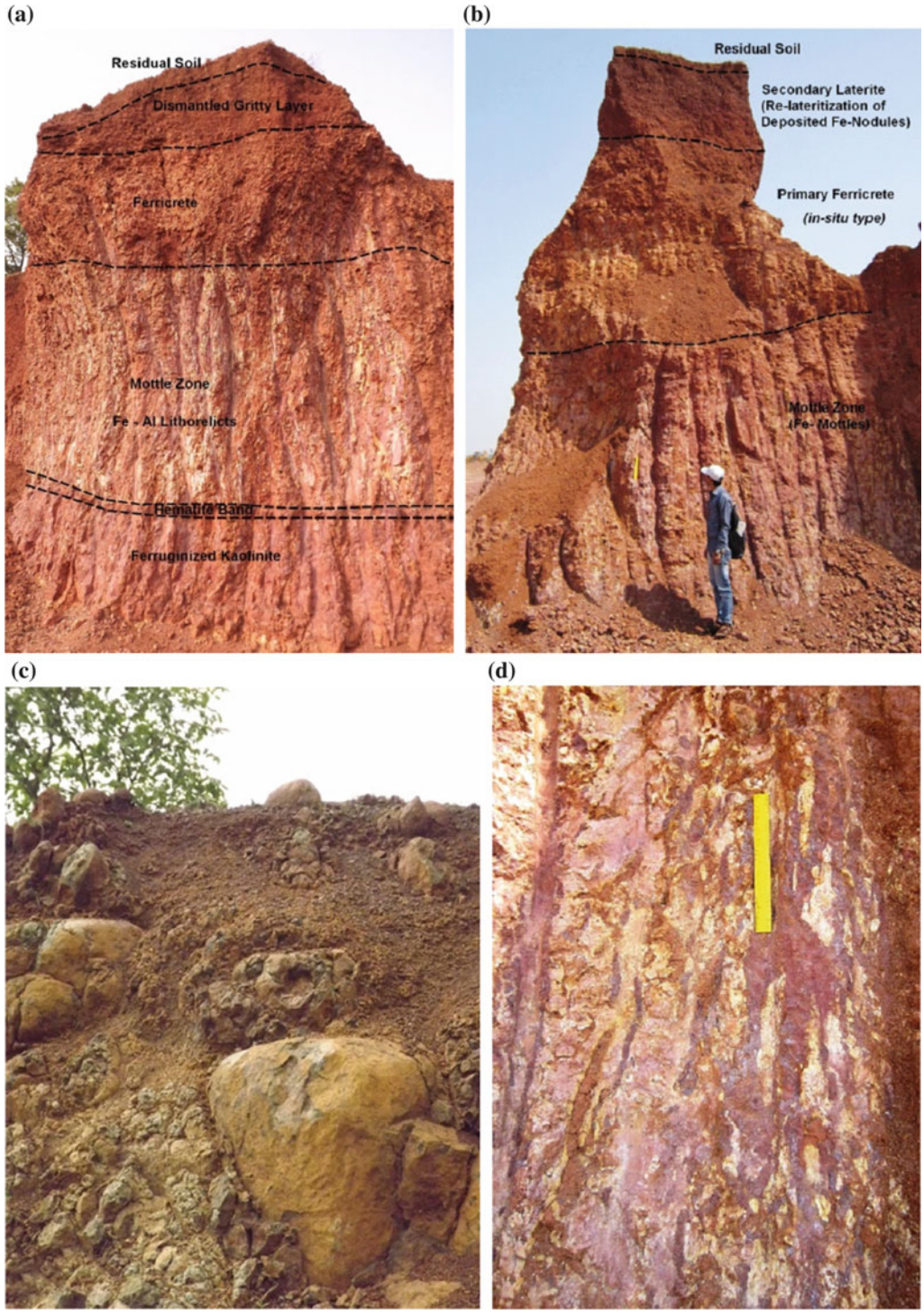

Fig. 2.4 **a** Lithosections of dismantled ferruginous layer, vermicular ferricrete and Fe–Al litho-relict mottles at Boro Pahari (24° 11′ 49″N, 87° 42′ 39″E), Birbhum, **b** development of secondary lateritic hard crust upon massive primary laterite profile at Bhatina (24° 10′ 02″N, 87° 42′ 25″E), Birbhum, **c** weathering rinds and core stones (saprolite) of Rajamahal basalts in weathered medium at Nalhati, Birbhum, and **d** channels of Fe-mottles (litho-relicts of weathered basalts) in kaolinite matrix at Bhatina, Birbhum (note: length of scale is 30 cm)

Table 2.1 Account of in situ laterite log profile at Ghurnee Pahar, Birbhum District

Profile depth in m	Lithological description of horizon
0–0.15	Dismantled gritty layer and slope wash with thin latosol
0.15–2.0	Vermicular hardcrust with tubes and channels, domination of hematite and goethite
2.0–2.15	Highly ferruginized pisolitic hematite band, reddish brown smooth colour
2.15–4.00	Mottle zone with upward moving channels of Fe–Al matrix in bleached purple red kaolintite medium, lithorelictual mottles, columnar structure
4.00–6.15	Purple to grayish yellow kaolinite clay, pallid zone with few channels of ferruginous to aluminous oxides, lithomarge
6.15–6.85	Saprolite, spheriodally weathered basalt, abundance of weathering rinds and liesegang banding, corestone like appearance in kaolinte clay
6.85–9.25	Unaltered basalts (quartz–tholeiites), columnar structure

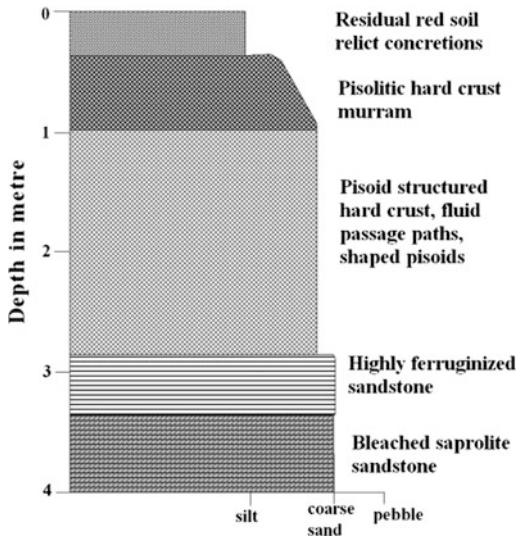

Fig. 2.5 Development of pisolitic hard crust on highly ferruginized sandstones of Gondwana Group in Dubrajpur, Birbhum

pisoid structured ferricrete (1.0–2.8 m depth). This part is characteristically rich in globular pisolites and fluid passage paths. The duricrust is underlain by very hard ironstone or highly ferruginized sandstone layer, varying thickness from 10 to 65 cm. This layer is underlain by altered sandstone or saprolitic sandstone of 45–50 cm thickness (exposed thickness).

2.4.3 Laterites of *Rarh* Bengal

2.4.3.1 Sriniketan Section

The ex situ laterite profile of Sriniketan, Birbhum (23° 41′ 31″N and 87° 40′ 31″E) is characterized by (1) pebble horizon (2.6–3.0 m depth), (2) ferruginized coarse sand (0.55–2.6 m depth) and (3) duricrust (up to 0.55 m depth) (Fig. 2.6 a). Pebble horizon is characterized by a lag deposits, constituting of pisoids, quartz pebbles and petrified woods of varying sizes set in a ferruginized matrix of sands. The thick layer of coarse sands constitutes gravels and pebbles of varying sizes and ferricrete pisolites which may be derived from distant locations of primary laterites. The thickness of duricrust generally varies from 30 to 50 cm and many a places absence of this layer is very common. This duricrust is nothing but a highly ferruginized or iron–cemented gravel and pebble horizon, constituting of quartz, ferricrete pisolite, petrified wood fragment and altered as well as fresh feldspar clasts. Basically it appears as a conglomerate ferricrete and Gmg (i.e. inverse to normal grading matrix-supported gravels) fluvial facies. Ananalogous profile of ex-situ laterite is observed in the Hetodoba village (23° 26′ 45″N and 87° 32′ 07″E) of Barddhaman district (Table 2.2).

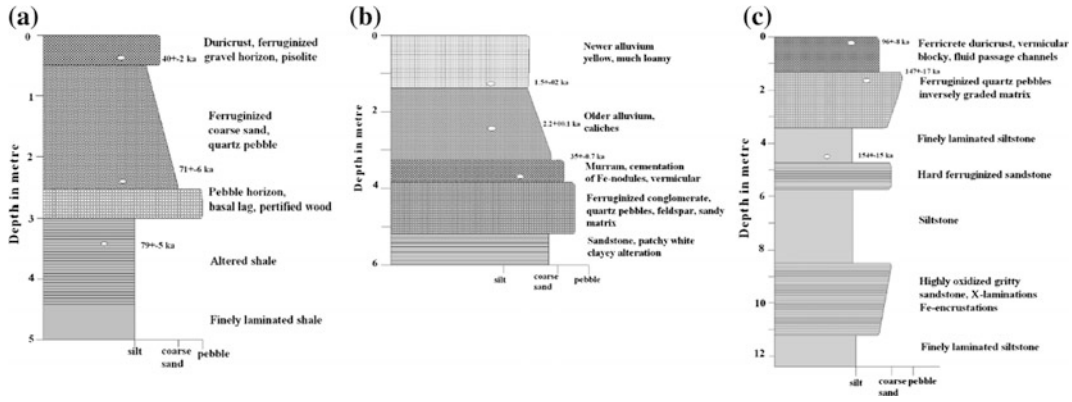

Fig. 2.6 **a** Formation of ex situ ferruginized duricrust with gravel horizons on finely laminated shale in Sriniketan, Birbhum, **b** successive lithofacies of newer alluviulm, older alluvium and vermicular ferruginous hard crust in Bishnupur, Bankura, and **c** development of Early Quaternary ferricrete and ferruginized quartz pebbles on finely laminated alternate siltstone and sandstone sequences in Garhbeta, West Medinipur (age in ka derived from OSL dating of samples)

Table 2.2 Development of ferruginous crust on Neogene gravels and pebbles at Hetodoba, Barddhaman

Profile depth in m	Lithological description of horizon
0–0.15	Ferruginized gravels and pebbles, cementation of hematite nodules
0.15–0.72	Murram with gravels, hardcrust, Gmg facies
0.72–1.2	Ferruginized clay bands, hard on exposure
1.2–3.1	Mottle zone with upward fining pebbles and gravels
3.1–4.15	Yellowish white kaolinite ochre with upward fining pebbles with dicotylendous fossil woods

2.4.3.2 Bishnupur Section

In the exposed profile of Bishnupur, Bankura (23° 05′ 28″N and 87° 16′ 15″E) one conglomerate ferruginous unit un-conformably overlies the grey coloured coarse sandstone unit (Fig. 2.6b). This conglomerate unit with murram at its upper part is overlain successively by older alluvium and newer alluvium sediments. The lowermost sandstone unit (5.2–6.0 m depth) is relatively more induarted and lithified than upper older and newer alluviums. It is relatively coarse grained and at places granular, yellowish–white in colour and characterized by white clayey alteration. The sandstone is sub-arkosic with feldspar content which is approximately 10–15% (with 80–90% quartz). This Paleogene sandstone unit is un-conformably overlain by a ferruginized conglomerate unit (3.8–5.1 m depth) which is oligomictic in character with pebbles of dominantly quartz and little feldspar. The matrix or groundmass is highly cemented by ferruginous cement (mainly limonite and goethite) which makes it very induarted. So it can be identified as modified ferricrete–duricrust of *Rarh Bengal*. The upper part of this conglomeratic ferricrete duricrust (3.2–3.8 m depth) is represented by murram with iron-stained quartz pebbles of 1–2 cm in size and ferricrete nodules in a ferruginized sand sized matrix (Gmg facies). This lower laterite unit is overlain by caliches impregnated, grey coloured and loamy sediment (Late Pleistocene to Early Holocene) which represent older alluvium and the yellowish–brown coloured sandy newer alluvium (Late Holocene to Recent) overlies the older alluvium.

2.4.3.3 Garhbeta Section

The right bank of Silai River, exposes a vertical profile of almost 12–14 m thick package of alternate sandstone–siltstone sequence with

overlying ferruginized sequence of fining upward fluvial sediments at Gongoni, Garhbeta of West Medinipur district (Fig. 2.6c). The exposed vertical section of about 12.5 m may be categorized into two geological units with distinctive characteristics. The lower lithofacies (3.5–12.5 m depth) is mainly constituted of Paleogene to Neogene alternate sandstone–siltstone lithofacies whose contacts at several levels are marked by thin but hard ferruginized sandstone layers of 4–8 cm thick. The lowermost siltstone lithofacies are very finely laminated yellowish–white and purple in colour and at places show whitish patchy clayey alteration. The ferruginized sandstone unit is generally grey in colour and towards the top portion of the sequence reddish in colour, coarse grained gritty in character and at places contain few quartz pebbles. It is found that the sandstone unit (8.5–11.7 m depth) is reddish in colour, highly oxidized and characterized by high degree of iron encrustation features. The highly ferruginized thin layers (4–8 cm thick) occurring in between sandstone and siltstone lithofacies are constituted of brown coloured iron oxide cemented quartz—a highly ferruginized quartz arenite. The top laterite is characterized by the topmost ferricrete duricrust followed by murram zone and lowermost quartz pebble horizon. These quartz pebbles are generally sub-angular to sub-rounded and vary in size from 2 to 4 cm and all of them are stained by iron solutions. The uppermost duricrust unit is vermicular, blocky in nature with numerous fluid passage channels. This lithounit is constituted mainly of finer quartz grains and cemented by goethite and limonite. This layer of duricrust with pebble horizon (1.5–3.3 m depth) un-conformably overlies the Neogene siltstone unit (3.3–4.8 m depth).

A detailed micro structural evidence of palaeo-coastal landform in the lateritic badland topography of Garhbeta Section is well illuminated in Chap. 3 of this volume.

2.4.3.4 Rangamati Section

In a murram quarry of Rangamati, West Medinipur (22° 24′ 42″N, 87° 17′ 55″E), a 11.7 m thick profile of laterite is developed over the

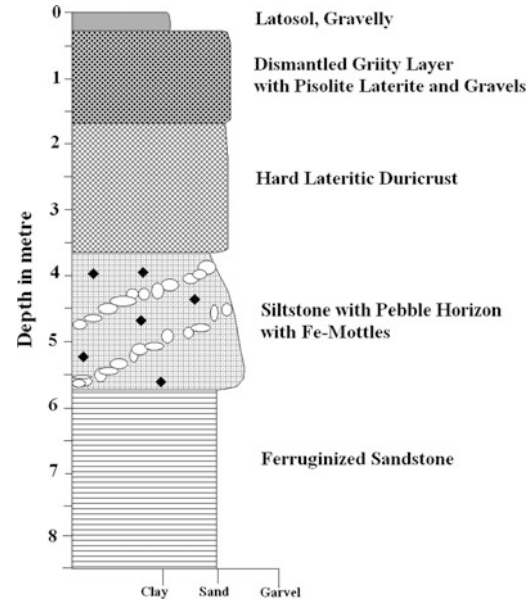

Fig. 2.7 Lithosections of secondary laterite with dismantled gritty pisolite ferricrete, vermiform hard crust, siltstone with pebbles and ferruginized sandstone in Rangamati, West Medinipur

Neogene sedimentary sequences which consist of alternate sandstone–siltstone lithofacies (Fig. 2.7). This unit is overlain by coarse pebble to sand sized quartz rich fining upward ferruginous sediments of Early Quaternary. But the ideal zone of lithomarge or weathered parent material is not readily observed in this profile. The base is sandstone units of Paleogene which is characterized by cross-bedding with forest dipping around 20° towards 125° (reddish purple colour) and shows high degree of ferruginization and iron-encrustation. The unit of siltstone varies in depth from 8.7 to 11.7 m and it successively merged with ferruginized sandstone (5.7–8.7 m depth) and pebble–siltstone bed with iron pisolits (3.7–5.7 m depth). This horizon shows some patchy alumina enrichment separated by a matrix supported, sparsely ferruginized multi layered gravel beds of thickness of about 25–25 cm. Towards top, gravel, large quartz and pebble horizon is ferruginized to a great extent through matrix supported medium, successively overlain by pisolitic porous murram zone and duricrust layer (0.2–3.7 m depth). The duricrust is about

1.5 m thick, vermicular type and constituted of re-cemented gravels, quartz grains and derived primary ferruginous nodules. This profile is overlain by 15–20 cm thick latosol which supports the deciduous vegetation like *Sal* (Shorea robusta) in this area. These types of gravely laterites are analogous to Early to Middle Pleistocene Lalgarh Formation in West Bengal.

2.4.4 Geo-chemical Properties and Lateritization Index

Five samples belonging to pisolitic hard crust (PL 1), ferricrete (PL 2), mottle clay and kaolinite (PL 3) and saprolite (PL 4 and 5) zones are analyzed to characterize the chemical variations along the Nalhati lithosection with depth. The result of geo-chemical analysis (Table 2.3) depicts that sample no. PL 1 belongs to pisolitic crust of Rajamahal Trap laterites and represented by high Al_2O_3 (36.7%), Fe_2O_3 (26.2%) and TiO_2 (4.77%) and very low SiO_2 (9.7%), low MgO (0.14%), CaO (0.17%), Na_2O (0.01%), K_2O (<0.02%) and P_2O_5 (0.11%) respectively. So it can be said that chemically the most mobile elements such as Si, Na, K, Mg and P has been removed from the upper part of laterite profile through leaching and solution system and enrichment of Fe, Al and Ti has been taken place in the top ferricrete zone.

Sample PL 5 represents saprolite or weathered basalt composition as reflected by SiO_2 (31.58%), Al_2O_3 (24.45%), Fe_2O_3 (25.33%) and TiO_2 (4.53%). The low values of other oxides may be the direct result of removal from the system during lateritization. The laterite samples from ferricrete pisolite zone (PL 2), clay horizon (PL 3), laminated clay horizon (PL 4) and saprolite zone (PL 5 and PL 6) indicate low fluctuations of SiO_2 (28.5–31.58%), Al_2O_3 (24.3–26.1%) and Fe_2O_3 (23.12–27.86%) which signifies intensive deep basal chemical weathering of Rajmahal basalt, forming the in situ primary laterite lithosection at Nalhati.

Four samples of Sriniketan lithosection are collected from different horizons of lateritized sediments and siltstone for chemical analysis (Table 2.4). Only the sample SL 1 shows some enrichment of Fe_2O_3 and lowering of SiO_2 relative to other sediments. High percentage of SiO_2 (60.83–73.39%) reflects low intensive leaching of silica from the profile. It can be interpreted that the sediments had not undergone any lateritization to develop ideal profile of laterites except ferruginization at the top with coarse sand and gravels. So this sediment profile with several inputs of earlier laterite represents a reworked secondary laterite lithosection. The ferruginous eroded mantles were fluvially derived from the upper primary laterite zones.

Table 2.3 Geo-chemical properties of primary laterite lithosection in Nalhati, Birbhum

Sample no.	PL 1	PL 2	PL 3	PL 4	PL 5	PL 6
Depth of sample from the top of profile (m)	0.65	3.70	5.85	8.25	9.15	9.60
SiO_2 (%)	9.70	28.50	31.46	29.61	31.58	37.67
Al_2O_3 (%)	36.71	26.10	26.42	24.3	24.45	31.15
Fe_2O_3 (%)	26.2	27.86	23.12	27.17	25.33	9.31
MnO (%)	0.29	0.33	0.11	0.12	0.10	0.03
MgO (%)	0.14	0.28	0.06	0.04	0.06	0.24
CaO (%)	0.17	0.07	0.16	0.11	0.18	0.21
Na_2O (%)	<0.01	<0.01	<0.01	<0.01	<0.01	<0.01
K_2O (%)	<0.01	0.02	<0.01	<0.01	0.01	<0.01
TiO_2 (%)	4.77	2.81	3.42	3.69	4.53	4.22
P_2O_5 (%)	0.11	0.11	0.19	0.26	0.09	0.07
Molar ratio	0.14	0.50	0.59	0.54	0.58	0.84

Table 2.4 Geo-chemical properties of secondary laterite lithosection in Sriniketan, Birbhum

Sample no.	SL 1	SL 2	SL 3	SL 4
Depth of sample from the top of profile (m)	0.35	1.50	3.10	4.45
SiO_2 (%)	60.83	73.39	60.01	58.79
Al_2O_3 (%)	8.88	15.74	20.94	18.44
Fe_2O_3 (%)	20.56	4.12	7.11	7.87
MnO (%)	0.42	0.03	0.03	0.03
MgO (%)	0.82	0.52	1.31	2.32
CaO (%)	0.01	0.20	0.36	0.47
Na_2O (%)	0.05	0	0.04	0.05
K_2O (%)	0.92	2.34	2.67	3.21
TiO_2 (%)	0.41	0.44	0.89	0.82
P_2O_5 (%)	0.09	0.02	0.03	0.04
Molar ratio	2.04	3.61	2.07	2.17

Under hot and sub-humid tropical climate the prime process of lateritization (i.e. tropical weathering) is the downward leaching of silica and bases (more mobile elements) and upward enrichment of Fe–Al oxides (less mobile elements). The molar ratio (Birkeland 1984), i.e. index of weathering, is applied here to depict the degree of leaching. There are marked difference of molar ratio in between the sections of Nalhati and Sriniketan. In Nalhati section the low value of molar ratio (0.14–0.84) signifies well developed leaching of silica and segregation of sesquioxides nodules throughout the profile. Molar ratio of ferricrete (sample from 0.65 m depth) is very low (0.14) due to prevalence of Al_2O_3 (36.71%) and Fe_2O_3 (26.20%) whereas it increases up to 0.58 in kaolinite horizon or lithomarge (sample from 9.15 m depth) due to dominance of SiO_2 (31.58%). Down the profile under acidic environment of tropics most of smectite and interstratified clay minerals have been transformed to kaolinite, iron oxides and minor amounts of gibbsite. On other side the high value of molar ratio (2.04–2.17) is found in Sriniketan section. The molar ratio of ferruginous crust (sample from 0.35 m depth) is very high (2.04) due to high amount of SiO_2 (60.83%) than Fe_2O_3 (20.56%). Below that crust layer (i.e. ferruginous coarse sand and pebbles at depth of 1.50 m) the molar ratio reaches up to 3.61 due to ample occurrence of SiO_2 (73.39%). In Sriniketan section the values of molar ratio suggest the relatively very low leaching of silica from the profile and low enrichment of sesquioxides. On the basis of molar ratio it can be said that the in situ intensive lateritization is observed in the lithosection of Nalhati and ex situ weak lateritization is observed in Sriniketan section. The triangular diagram (Schellmann 1986; Pain and Ollier 1996; Meshram and Randive 2011) shows a high degree of lateritization in the samples primary laterites (Nalhati, Birbhum) and very weak degree of lateritization (preservation of quartz fragments) in the samples of secondary laterites (Sriniketan, Birbhum) (Fig. 2.8). Getting amount of Al_2O_3, CaO, Na_2O and K_2O from the samples of laterite profiles we have found that CIA (Chemical Index of Alteration) for primary laterites (Nalhati, Birbhum) is greater than 99% which reflects higher rate of alteration in ferricrete zone, mottle zone and sparolite, and CIA for secondary detrital laterites (Sriniketan, Birbhum) varies from 83 to 93% which signifies good preservation of chemically altered minerals.

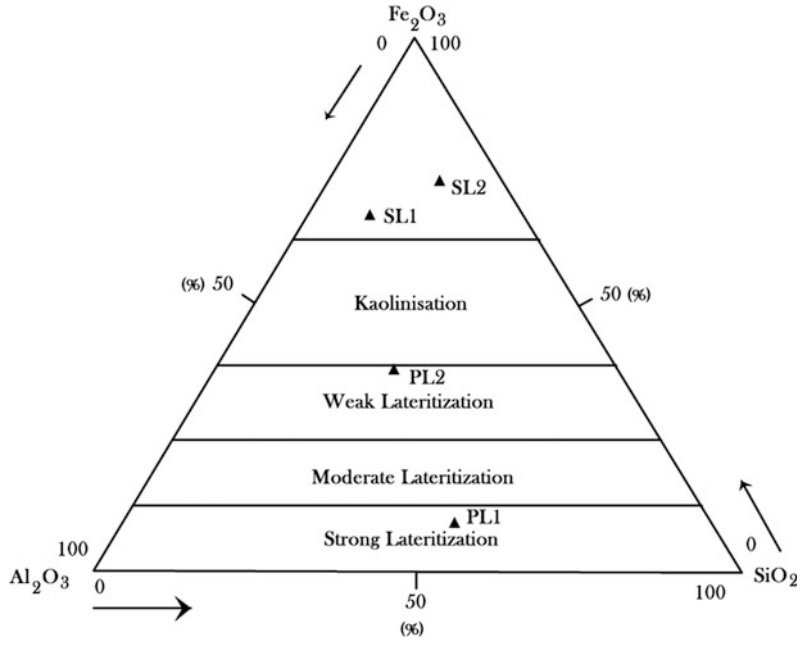

Fig. 2.8 Al_2O_3–Fe_2O_3–SiO_2 triangular diagram showing degree of lateritization in the study area

2.4.5 Age Determination of Laterites

2.4.5.1 Span of Lateritization Event in India

There are marked similarities in between the laterites of India and Australia because these continents have move from polar to tropical palaeolatitudes over the past 80 million years (Schmidt et al. 1983; Tardy et al. 1991; Retallack 2010). The optimum lateritization event was probably related to Late Oligocene to Early Miocene weathering event in India and Australia (Schmidt et al. 1976; Ollier 1988; Bourman 1993; Bird and Chivas 1993). Most of peninsular laterites have been magnetized over sufficiently long periods of time that reversals in the polarity of the geomagnetic field have been recorded (Schmidt et al. 1983). On the basis of pole positions and comparisons with the apparent polar wander paths age assignments have been made by Schmidt et al. (1983). It is concluded that the ages of Indian laterites are grouped as follows: Late Tertiary, Mid-Tertiary, Early Tertiary or Early Tertiary–Late Cretaceous (Schmidt et al. 1983). One interesting observation is the Palaeogene age assigned to laterites from the Deccan Traps which are Late Cretaceous in age. Similarly the high level primary laterites are found on the Early Cretaceous Rajmahal Basalt Traps (situated at north-western of study area, 24° 15′–24° 50′N, 87° 15′–87° 45′E) and the latitudinal position of this province is quite north of Deccan Traps (between 16° and 24°N, 73° and 80°E). So in respect of equatorial drift of Indian plate (Late Cretaceous–Early Palaeogene) this geologic unit of Rajmahal was getting early favourable climate for lateritization. The time taken for entry of Indian plate into the zone between 30°N and 30°S is about 65–75 million years from present (Kumar 1986). Therefore, the Rajmahal Basalts Traps (fringing north-west of *Rarh Bengal*) must have undergone through intensive lateritization after Early Cretaceous. The prevailing span of lateritization climate was found in between Late Cretaceous and Late Neogene in Indian peninsula (Schmidt et al. 1983). On the basis of palaeolatitudes and laterite magnetizations the favourable optimum climate of laterite formation was prevailed in India from Late Cretaceous to Late Neogene (Kumar 1986). Consequently, the laterites in the northern peninsula should be older than those in the south as per drifting of Indian plate. Complication of new and more accurate laterite and bauxite ages

reveals unusually widespread and intense laterite and bauxite formation during events of less than 100 k y duration at 2, 12, 16, 35, 48, 55 and 100 Ma (Retallack 2010). Globally the peak period of lateritization event was started in Neogene when the Indian plate was well established in tropical latitudes. In India numerous studies suggest that in situ ferricretes of plateaus were formed since Palaeogene to Neogene but ex situ detrital ferricretes of low slopes and valleys were occasionally formed in that time period and also in Early Quaternary due to erosion, re-deposition and re-lateritization (Pappu and Rajaguru 1979; Subramanina; Ollier and Rajaguru 1989; Sahasrabudhe and Rajaguru 1990; Achyuthan 2004; Rajaguru et al. 2004a, b; Mishra et al. 2007; Deo and Rajaguru 2014).

The earliest known latrites are those of the 2200 Ma profile near Sishen, South Africa but bauxites extend back to at least 3500 Ma, near Taldan in the Aldan Shield of Siberia (Retallack 2010). The earliest laterites of India were dated back to Early Palaeocene–Early Oligocene, found in Gujarat and Than desert (Sychanthavong and Patel 1987; Meshram and Randive 2011). According to the reconstruction of palaeolatitudes, it is found that southern India spent a longer time in the equatorial zone, i.e. between 53 million years and <32 million years. To assign a Cretaceous age of laterite formation is not plausible because at this juncture the Indian plate had just started drifting apart from its original position between latitudes 40°S and 60° S in the Gondwanaland (Sychanthavong and Patel 1987; Tardy et al. 1991). The lateritization event was probably related to a Late Oligocene to Early Miocene weathering event (Bourman 1993). The results of $^{40}Ar/^{39}Ar$ dating of laterite samples imply that Southern India was weathered to form laterite duricrust between ~36 and 26 Ma (Late Eocene–Oligocene) and may have been dissected mostly in Neogene (Bonnet et al. 2014). The high-level and low-level laterites of Western Ghats and Konkan Coast, India were developed in Early Tertiary and Mid-Tertiary respectively (Widdowson and Cox 1996). The plateau top laterites of Deccan Trap is dated back to Eocene–Miocene and detrital low level laterites with gravels and Acheulian artefacts indicates severe erosion of primary high level laterite cover during Early Pleistocene (Mishra et al. 2007). The transported laterites of southern India bears the imprints of Acheulian, Palaeolithic and Mesolithic artefacts, dated Early–Late Neogene Formation. According to Achyuthan (1996), Chakrabarti (2001), Rajaguru et al. (2004a, b) and Mishra et al. (2007) ferricrete surface is generally devoid of archeological evidence but the upper dismantled surface and ex situ laterites have bears the evidence of Acheulian (Early–Middle Pleistocene) to Mesolithic (40–150 ka) artefacts in India as well as *Rarh Bengal* (mainly in the districts of Birbhum, Barddhaman and Bankura). These archaeological evidences suggest an early to Middle Pleistocene origin of secondary detrital laterites.

2.4.5.2 Lateritization Age of RBT

The post-succession of Rajmahal Basalt Traps (adjoining to study area) is in situ laterites, gravel deposits and ferruginous sandstones on the stable shelf condition of Bengal Basin. The $^{40}Ar/^{39}Ar$ geochronological ages of Rajmahal basalts and basalts of Bengal Basin were dated back at ~118 Ma (Kent et al. 2002). So it is logical to establish that the development of in situ primary laterites on the Rajmahal basalts, Gondwana Formations and Archaean granite–gneiss is post-Cretaceous formation. According to Roy Chowdhury (1986) the ages of peninsular laterites ranges from Early Eocene to Recent and residual laterite caps (Lalgarh Formation of West Bengal) got formed during the Early Quaternary or Neogene.

In the history of plate drift through millions of years, those continents which travelled or had been travelled across tropics, must bear the imprints of laterites and bauxites. So the residual laterite profiles are the fossil type formed in past geological ages when climatic conditions were favourable for lateritization (Kumar 1986). In order to explain the origin of these laterites and

the accompanying thick tropical forests (found as Miocene to Eocene dicotyledonous fossils), we have to consider drift tectonics of the Indian Plate as it as moving across the equatorial zone from Cretaceous to Palaeocene times (Schmidt et al. 1983). The formation of secondary iron-oxides (hematite) by chemical weathering processes allows palaeomagnetism to be used to date ferruginous regolith material. The palaeomagnetic poles can be calculated from the remnant directions (during chemical Remnant Magnetization, CRM), which in turn are used to derive weathering ages by comparison with the trajectory of palaeomagnetic poles of known age. From the palaeomagnetic age detections and apparent polar wandering path of India (Schmidt et al. 1983; Kumar 1986) the high-altitude laterites have undergone a complex magnetic history during Late Creataceous and Palaeogene. The low-altitude laterites are Neogene in age. The accelerated northward drift into Koppen's 'A' zone between 65 and 53 Ma propelled India quite rapidly into the favourable zone of laterite formation (Kumar 1986). The age of lateritic weathering has also been roughly estimated on the basis of palaeomagnetic properties of iron-oxides formed in laterites around 16°N (Schmidt et al. 1983). Sankaran et al. (1985) have applied TL dating for age estimation of laterites and found that the age varies from 2.15 to 3.58 $\times$ 10^5 years. The OSL dating of collected samples of ex situ laterite sections, both lateritized and non-lateritized sediments, reveals that the lateritization process was started in Neogene and restricted within Middle to Late Pleistocene ($\sim$150 to 35 ka) and did not continue in Holocene times. This age data of secondary laterites suggests the prevalence of in situ trap laterites of Rajmahal prior to Early Quaternary, may be Eocene to Pliocene because we have found ample Miocene to Eocene dicotyledonous fossils and fragments of trap laterites found in the ex situ laterites (Fig. 2.10).

Crytomelane [$K_x\ Mn_{8\text{-}X}{}^{IV}\ Mn_x^{III}\ O_{16}$, n H_2O] is a major Mn-oxide of many lateritic Mn-ore deposits in south India (Bonnet et al. 2015a). This mineral is a suitable chronometer for of $^{40}Ar/^{39}Ar$ step heating dating of weathering processes in the lateritic soils including duricrusts and manganiferous ore deposits (Bonnet et al. 2014, 2015a, b; Beauvais et al. 2016). It has been learned that the peninsular India experienced six major phases of lateritic weathering, viz. $\sim$53 to 50, $\sim$40 to 32 and $\sim$30 to 23 Ma in the plateau tops and $\sim$47 to 45, $\sim$24 to 19 and $\sim$9 Ma in lowlands, pediments and valleys (Bonnet et al. 2015a; 2015b; Beauvais et al. 2016). The results of $^{40}Ar/^{39}Ar$ dating of laterite samples (Bonnet et al. 2014) and other dating information (Schmidt et al. 1983; Kumar 1986; Sychanthavong and Patel 1987; Tardy et al. 1991; Bourman 1993; Widdowson and Cox 1996; Rajaguru et al. 2004a, b; Mishra et al. 2007; Retallack 2010) imply that basalts of RBT were weathered intensively to form in situ ferricrete in between $\sim$36 and 26 Ma (Late Eocene–Oligocene) and may had been dissected mostly since Neogene under favourbale lateritization climate (becoming source materials of ex situ secondary laterites).

2.4.5.3 OSL Dating of *Rarh* Laterites

Niyogi et al. (1970) assigned Neogene and Early Pleistocene age for the lithomargic kaolinte clay and laterites respectively. The ferruginous soils of present study area are regarded as the oldest soils from Indian part of these plains (Singh et al. 1998). Niyogi (1975), Vaidyanadhan and Ghosh (1993) and Singh et al. (1998) have been assigned ages of 305–1000 ka, i.e. Early–Middle Pleistocene, reflecting autochthonous origin of ferruginous soils. Geoarcheological evidences suggest that the ferruginous landforms of peninsular India and *Rarh* Bengal is not sterile from the archeological viewpoint and these deposits have preserved Palaeolithic artifacts (stone-age tools) in the lateritic interfluves and badlands of Birbhum, Barddhaman and West Medinipur districts (Rajaguru et al. 2004a, b). In the lateritic gullies of Rampurhat, Maluti and Bhatina

Table 2.5 Summary of U, Th and K elemental concentrations, annual dose rate, equivalent dose and optical ages of ex situ laterite samples from the study area

Sl no.	Sample no.	Sample horizon	Depth in m	No. of Discs	U (ppm)	Th (ppm)	K %	Equivalent dose (avg) in Gray	Dose rate Gray/ka	Age (avg) ka
Sriniketan section										
1	OSLD 1	Hard Crust	0.4	45	1.94	11.93	0.88	78–2	1.9 ± 0.09	40 ± 2
2	OSLD 2	Ferruginized Sandstone—Pebble	2.5	45	1.17	8.56	1.63	153-9	1.1 ± 0.01	71 ± 6
3	OSLD 3	Siltstone	3.4	41	1.71	14.17	1.63	203-9	2.5 ± 0.01	79 ± 5
Bishnupur section										
4	OSLD 4	Younger Alluvium	1.6	12	2.95	17.04	0.95	35 + 0.4	2.33 ± 0.03	1.5 ± 0.2
5	OSLD 5	Older Alluvium	2.5	12	3.81	18.17	1.18	6.2 + 0.5	2.8 ± 0.01	2.2 ± 0.1
6	OSLD 6	Murram	3.9	42	3.56	37.59	0.65	12 + 2	3.4 ± 0.02	35 ± 0.7
Garhbeta section										
7	OSLD 7	Hard Crust	0.3	48	4.34	16.42	0.43	214–14	2.23 ± 0.01	96 ± 8
8	OSLD 8	Pebble Horizon	1.9	45	1.61	11.44	0.4	205–21	1.4 ± 0.08	147 ± 17
9	OSLD 9	Siltstone	4.8	36	1.63	13.71	0.68	264–21	1.7 ± 0.09	154 ± 15

Source Chakraborti (2011)

(south-east of RBT) we have found ample Acheulian artifacts (over secondary laterites) which dated back to Early Pleistocene (>40 ka to 1.2 Ma) (Rajaguru et al. 2004a, b; Mishra et al. 2007).

For accurate chrono-stratigraphic age detection, sampling for OSL (Optically Stimulated Luminescence) dating of sample laterite lithofacies in Sriniketan of Birbhum, Bishnupur of Bankura and Garhbeta of West Medinipur have been done. In Garhbeta section the samples have been taken from the hard crust (1.6 m depth), pebble horizon (2.5 m depth), loose murram layer (3.2 m depth) and siltstone unit (5.2 m depth). Sampling have been done from the upper three horizons of lateritized sediments including hard crust (0.3 m depth), ferruginized coarse sand–pebble horizon (1.9 m depth) and finely laminated siltstone (2.9 m depth) at Sriniketan section. Similarly numerous samples have also been collected from three layers—newer alluvium (0.9 m depth), older alluvium (2.2 m depth) and murram layer (3.4 m depth) at Bishnupur section (Table 2.5).

The possible age as determined by OSL method for the Sriniketan section, shows that the age of sedimentation or time of cut off from the sunlight for the hard crust (0.45 m depth) is 40 ± 2 ka. The age of ferruginized sandstone–pebble horizon (with petrified wood) is about 71 ± 6 ka. The age of laminated siltstone is 79 ± 5 ka. The un-conformably overlying ferruginized sandstone–pebble horizon definitely indicates its time of deposition in between 79 ± 5 ka and 71 ± 6 ka, i.e. well within Pleistocene epoch. The layer of ferruginous hard crust with gravels was probably developed in Late Pleistocene (well within ~125 ka to 10 ka BP). Similarly other ferruginous lithofacies of sandstone–pebble horizon and laminated siltstone are also assigned an age of Late Pleistocene.

The age as determined from the samples for Bishnupur section shows the age of sedimentation of the murram zone is more than 35 ± 0.7 ka as it was cut off from the sunlight at this date. Similarly the older alluvium is older than 2.2 ± 0.1 ka age and newer alluvium is older than 1.5 ± 0.2 ka. The ferruginous crust is again

assigned as age of Late Pleistocene and other above alluvium units is categorized as the lithofacies of Late Holocene to Recent.

The sedimentation age for the Garhbeta section shows that the lower siltstone unit (4.8 m depth) and pebble horizon (1.9 m depth) was cut off from the sunlight before 154 ± 15 and 147 ± 17 ka respectively. Interestingly both these units are intensively ferruginized under the tropical climate. Alongside the ferruginous hard crust (0.3 m depth) was cut off from the sunlight before 96 ± 8 ka. Yet again the laterite hard crust is assigned an age of Late Pleistocene. But the lower ferruginous lithofacies of pebbles and siltstone were developed in Middle Pleistocene (>350 to 130 ka). Based on the OSL dating data it can be said that climate for lateritization was prevailed at Middle Pleistocene and became intense in Late Pleistocene, forming lateritic hard crust.

2.5 Discussion

2.5.1 In Situ and Ex Situ Origin of Laterites

The in situ or primary lateritization processes on the basaltic bedrocks, at Nalhati (24° 17′ 47″N, 82° 49′ 28″E), Pinargaria (24° 12′ 13″N, 87° 40′ 13″E), Ichhanagar (24° 22′ 33″N, 87° 47′ 26″E), Chaukisal (24° 19′ 59″N, 87° 41′ 31″E), Mathurapahari (24° 03′ 03″N, 87° 36′ 39″E) and many other litho-sections along Rampurhat–Dumka Highway (NH, National highway 114A), are characterized by well developed laterite profiles (Fig. 2.4), starting from (1) saprolite of weathered basalts, (2) lithomargic clay or pallid zone, (3) mottled zone with litho-relicts of weathered basalts and (4) ferricrete. The primary laterites on the Chotanagpur gneiss and dolerite dykes are characteristically very thin and continued of poorly developed saprolite zone ferricrete hard crust. Laterites on the Gondwana sandstones, at Pansuiri (23° 46′ 39″N, 87° 16′ 47″E), Bhadulia (23° 48′ 42″N, 87° 13′ 44″E), Dubrajpur (23° 47′ 12″N and 87° 25′ 19″E), Ghutgaria (23° 25′ 09″N, 87° 15′ 11″E) and Saharjora (23° 24′ 36″N, 87° 14′ 32″E), often show ferruginous saprolite, ferruginous arenite and thick unit of pisolitic hard crust. A model of in situ development of laterite profile (development of alteration saprolite zone, glaebular mottle-ferricrete zone and the upper soft zone of Fe-nodules) is depicted in Fig. 2.9 to understand the complete formation of laterite layers. Under tropical wet-dry climate of Palaeogene to Neogene, the Rajmahal basalt was weathered to form lithomarge or fine saprolite (i.e. kaolinite) due to intense leaching of silica and chemical alteration of primary minerals and concurrently the secondary iron and aluminum oxides were cemented towards surface to form ferricrete. The relict structures of weathered basalt are found in the mottle zone, having elongated tubes and channels of hematite, Al-goethite and kaolinite (Fig. 2.4d).

The laterites developed over Neogene gravel sediments (mainly in the districts of Bankura and West Medinipur) also indicate in situ lateritization of lower conglomerate, i.e. pebble horizon–siltstone–sandstone units, not the upper older or newer alluvium. The indication of intensive tropical weathering and ferruginous transformation is evidenced from the spheroidal weathering, weathering rinds and lieseganag structures of basaltic saprolite (prominent in the lithosections of Nalhati, Ichhanagar, Chaukisal and Mathurapahari) which are characterized by reddish brown to yellow coloured fine grained clayey core and iron rich chocolate brown coloured rims. Occurrences of white kaolinte clay horizon (i.e. oxidized dots of opaque and mafic within pallid zone) and reddish or purple colour to yellow ochre clay (with ferricrete noudles and pisolites) is the direct product of lateritization process below the profile. At Nalhati and Ichhanagar sections, the development of very hard and compact iron rich pisolitic band (constitutes of feldspar, opaque and pisolites of iron concretions) signifies crudely weathered topmost surface of Rajmahal basalt, having litho-relicts of basaltic texture. The in situ ferruginous hard crust is generally thick vermicular type with well-developed rounded concretions of hematite and relict fluid passage paths. The zone of red

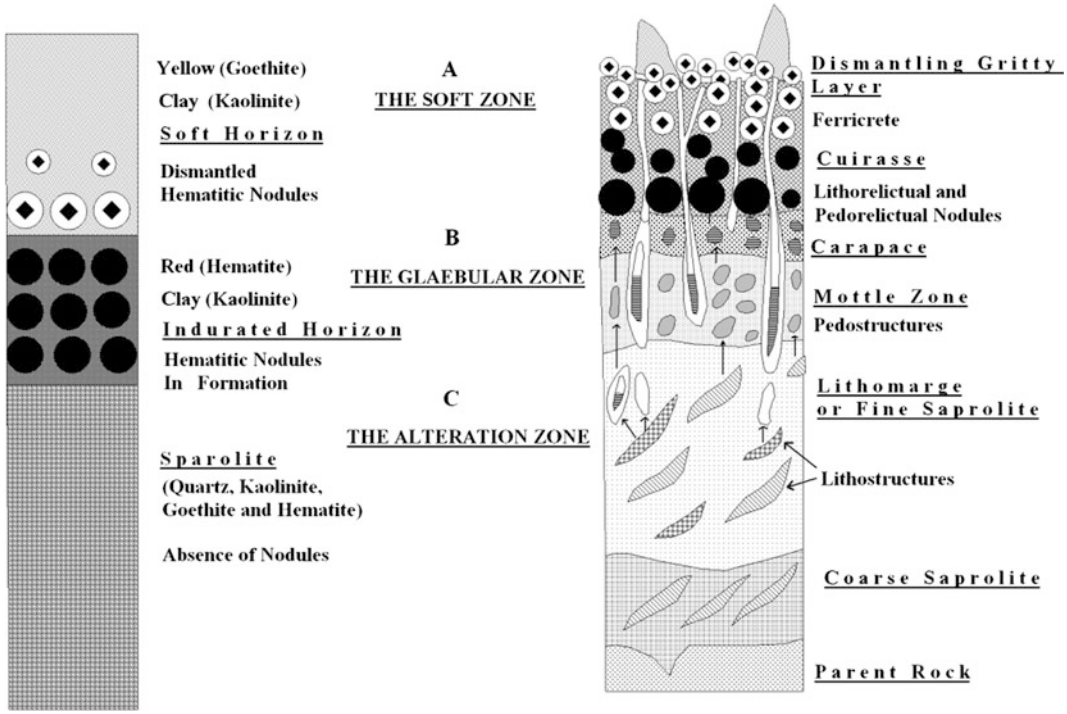

Fig. 2.9 An applicable schematic model (modified from Tardy, 1992) depicting in situ development of laterite profile with successive formation of coarse saprolite, lithomarge, mottle zone, ferricrete and gritty layer due to deep basal weathering of parent rock (similar signatures of lateritization found in the sections of Baramasia, Nalhati and Icchanagar)

pisolitic ferricrete with channels of mottles (1.5–1.75 m thick) at Ichhanagar lithosection represents a true in situ ferricrete of *Rarh Bengal*. The upper dismantled horizon of ferricrete consist of loosen globular to elliptical iron pisolites which show core to rim colour banding of limonitic to geothitic composition which reflects cortex development due to exposure of laterite mantle under the tropical wet–dry palaeoclimate. The pisoid structured ferricrete of Dubrajpur section (2–2.6 m thick) is very hard and compact in nature and continued of globular pisolites whereas the pisoid structured part is characteristically rich in pisoid and fluid passage paths and channels which acted as pathways for fluid or solution migration (leaching of silica) down the profile. In general the in situ hard crust nodules are circular to amoeboid shaped concretions of iron oxides (mainly hematite, limonite and goethite cortex) and sand balls. Centripetal accumulation of in-situ ferruginous materials to sub-nodules and to meta-nodules includes tropical dehydration of hematite, Al–hematite and Al–goethite at the surface in dry period (Birkeland 1984; Schellmann 1986). Observing the primary laterite lithosections of Nalhati and Rampurhat region we have found few interesting phenomenon about magnetite to hematite nodule formation along the profile. In saprolite zone, due to intense weathering under pressure, magnetite grains are altered to blood red coloured hematite at surfaces. In pallid zone, these grains are mostly altered to hematite pseudomorphs by oxidation around edges and along cracks (as channels or bands). In mottle zone, the biotic grains are completely replaced by goethite in the kaolinite medium and magnetite grains are replaced by hematite mottles, i.e. Fe-litho relicts (Fig. 2.4).

The re-lateritization of transported ferruginous materials (i.e. ex situ laterites) is mainly observed in the eastern part of *Rarh Bengal*, especially in the lithosections of in Bolpur (23° 40′ 18″N,

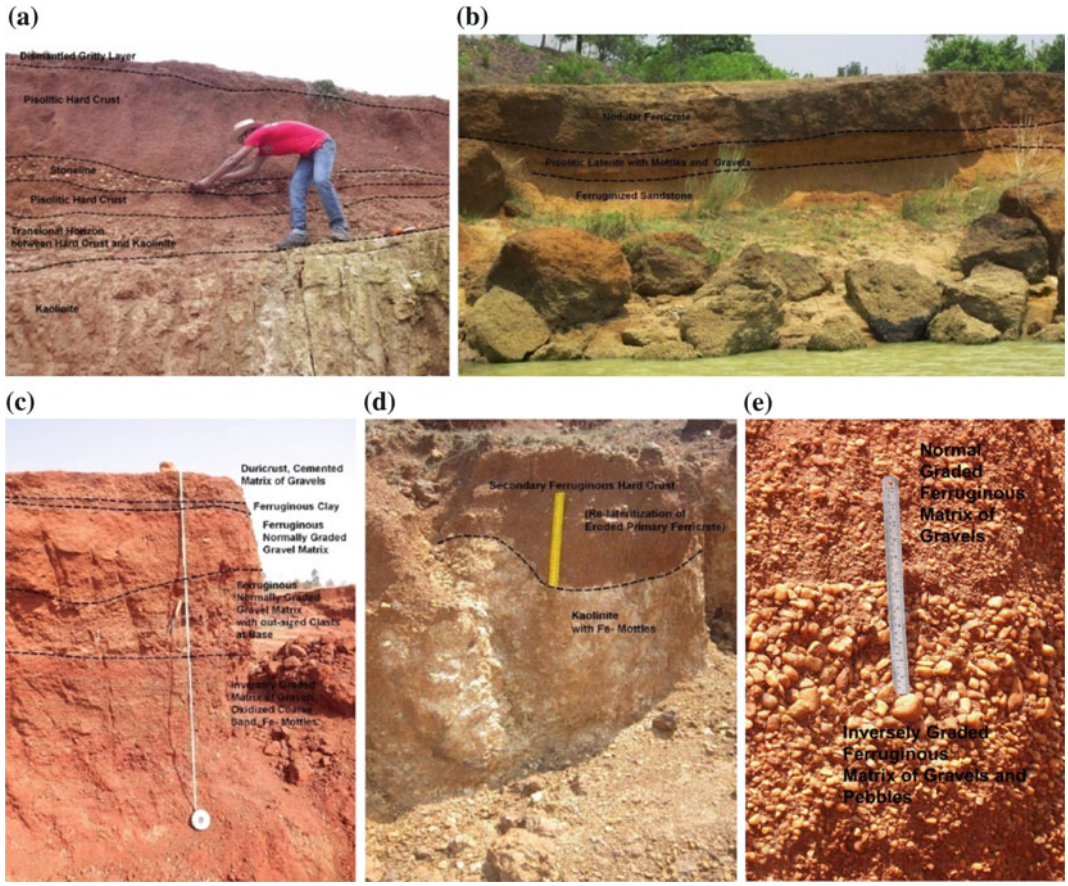

Fig. 2.10 **a** Development of pisolitic hard crust with stone lines of gravels and pebbles on kaolinite at Rampurhat, Birbhum, **b** nodular secondary ferricrete on left bank of Ajay River at Illambazar, Birbhum, **c** litho-facies of gravels and ferruginous hard crust at Hetodoba, Barddhaman, **d** formation of secondary lateritic hard crust on kaolinte at Bhatina, Bibhum, and **e** inversely to normal grading of ferruginized gravels and pebbles signifying palaeo fan-deltaic deposition at Hetodoba, Barddhaman (note: length of scale is 30 cm)

87° 39′ 10″E), Sriniketan (23° 41′ 31″N and 87° 40′ 31″E), Labhpur (23° 48′ 47″N, 87° 46′ 57″E), Rampurhat (24° 11′ 44″N, 87° 44′ 03″E), Illambazar (23° 36′ 56″N, 87° 32′ 07″E), Kanksa (23° 28′ 45″N, 87° 27′ 45″E), Panagarh (23° 27′ 10″N, 87° 31′ 51″E), Patryasayer (23° 12′ 35″N, 87° 31′ 17″E), Bishnupur (23° 05′ 28″N and 87° 16′ 15″E), Garhbeta (22° 51′ 34″ N and 87° 20′ 28″E), Khemsuli (22° 20′ 26″N, 87° 11′ 04″E), Rangamati (22° 24′ 42″N, 87° 17′ 55″E) (Fig. 2.10) etc. In Garhbeta section, alternative kaolinte clay and sandstone–siltstone sequences is overlain by some lenticular channel fill deposits, consisting of various size fragments of quartz grains, pisoids of in situ laterites and larger or out-sized clasts with petrified woods. The conglomeratic ferricrete hard crust with ample gravels (without horizon of mottle clay, pallid zone and saprolite) at Bishnupur sand Sriniketan sections reflects the secondary origin of laterites. At the section of Bishnupur Neogene sandstone facies is un-conformably overlain by a ferruginized conglomerate unit which is oligomictic in character with pebbles of dominantly quartz which is fluvially eroded remnants of primary in situ laterites. The crude large scale X-bedding sandstone unit of Bishnupur is almost a clast-supported conglomerate with ferruginized sand sized matrix of predominantly quartz and feldspar. These quartz

clasts are mostly well rounded to sub-rounded, smooth surface and flat without any striations which reflects fluvial origin. From the samples of ex situ secondary *laterites* it is observed that the matrix or groundmass is highly cemented by ferruginous oxides (limonite and goethite) which make it very induarted and the clasts show some iron staining on their surfaces (Fig. 2.10), signifying long-term retention in iron oxides medium. The clast composition and character indicate its provenance to be vein quartz and pegmatite bodies and it has suffered a long transportation. At Garhbeta and Rangamati sections the occurrences of ferruginized coarse sandstone (X-laminations and Fe-encrustation), quartz pebble horizon and topmost vermicular hard crust with quartz grains and clastic components again confirmed the re-lateritization episode of deposited materials up to Late Pleistocene. In the profile of Sriniketan section the degree of ferruginization increases upward and leads to ferruginized coarse sand whose lowermost part is almost free of ferrugination, signifying secondary weak lateritization with less leaching of silica. The variable pisoid shapes of secondary laterites are constituted by two elements—(1) a nucleus of variable nature surrounded by a cortex composed of concentric limonite and goethite and (2) pisoid of mono-nucleus and bi-nuclei composed of sand and clay. The large scale cross-bedding of ferruginous sandy unit with truncated top and asymptotic bottom indicate its sedimentary fluvial origin of the sediments, mostly in the palaeofan-deltaic sequences (Gmg facies). Lateritization climate of Paleocene, Eocene and post-Mio-Pliocene favoured good growth of broad leaf tropical and sub-tropical flora. The occurrences of large scale petrified dicotyledonous fossil woods (probably Miocene to Eocene age) (Fig. 2.11) with ferricrete nodules and channel lag deposits in the ex situ profiles bear the evidence of secondary lateritization up to Late Pleistocene (as OSL data suggested). Again this paleontological data suggests the primitive development of ferruginous crust (in situ laterite) in that period of Neogene.

2.5.2 Palaeoclimatic Inference

There is a perennial problem in the investigation of laterites, regarding the reliability of laterites and weathered zones as palaeoclimatic indicators and their usefulness as morpho-stratigraphic markers (Bourman 1993). Many of the researchers says that the formation of laterites and bauxites is restricted to Koppen's 'A' climate, a belt extending from about 30°N to 30°S latitude at present. Therefore, in the history of plate drift through millions of years, those continents which travelled or had been travelled across tropics, must bear the imprints of laterites and bauxites. So the residual laterite profiles are the fossil type formed in past geological ages when climatic conditions were favourbale for lateritization (Kumar 1986). These laterites were generally formed under an oxic atmosphere in the presence of abundant terrestrial biomass in an acidic environment (Retallack 2010), elevated atmospheric carbon dioxide, exceptional fossil wood preservation and intense deep basal weathering of basalts, dolerite, gneiss, sandstones and as well as Neogene gravelly sediments of West Bengal.

The most favourable climatic condition of laterite genesis is characterized by the contrasted seasons (wet – dry), high temperature throughout the year (28–35 °C), annual average relative humidity of the air nearer to 60 percent, annual rainfall lower than 1700 mm and long dry seasons during which a relatively low thermodynamic activity of water and atmospheric relative humidity decreases (McFarlane 1976; Tardy et al. 1991). While bauxites and aluminum enrichment can stand lower temperature (>22 °C) and are favoured by a higher thermodynamic activity of water and a higher relative humidity of the air (>80%) (Tardy 1992).

In order to explain the formation of these laterites and the accompanying thick tropical forests (found as Miocene to Eocene dicotyledonous fossils), we have to consider drift tectonics of the Indian Plate as it as moving across the equatorial zone (Fig. 2.12). It is now evidenced that

Fig. 2.11 Miocene to Eocenedated dicotyledonous fossil woods found **a** at a laterite quarry of Maluti, Shikaripara (Jharkhand) and **b** at a gully bed of Bhatina, Birbhum, **c** gravel lithofacies of ex situ ferruginous hard crust at Hetodoba, Barddhaman, and **d** progressive badland development on the terrain of secondary laterites and gravel litho-units at Kanksa, Barddhaman

climatic conditions were favourbale for lateritization from Cretaceous to Palaeocene times for during that period, the Indian continent crossed the zone between 30°S and 0° latitude (Schmidt et al. 1983; Kumar 1986; Tardy et al. 1991). After collision of India against Eurasian plate at the end of Miocene and upheaval of Himalayas, the palaeoclimate became more tropical to temperate but remained hot and humid with important dry season. The palaeoclimate of Eocene and Middle Oligocene was more favourable for the in situ type of laterite formation in peninsular India because in Eocene the equator was running across central Gujarat to southern West Bengal (Bardossy 1981).

As part of the global drift of plates, India also had drifted (average 2–3 cm year^{-1}) from relatively colder southern latitudes (between 37° and 53°S) to the present day tropical and monsoon-dominated climatic zone, commencing from about 70 million years (Sankaran et al. 1985). The Indian plate suddenly accelerated to 20 cm year^{-1} from Late Cretaceous to Early Eocene (Chatterjee et al. 2013). The Indian Plate was rotated in an anticlockwise direction since Palaeocene (Sychanthavong and Patel 1987),

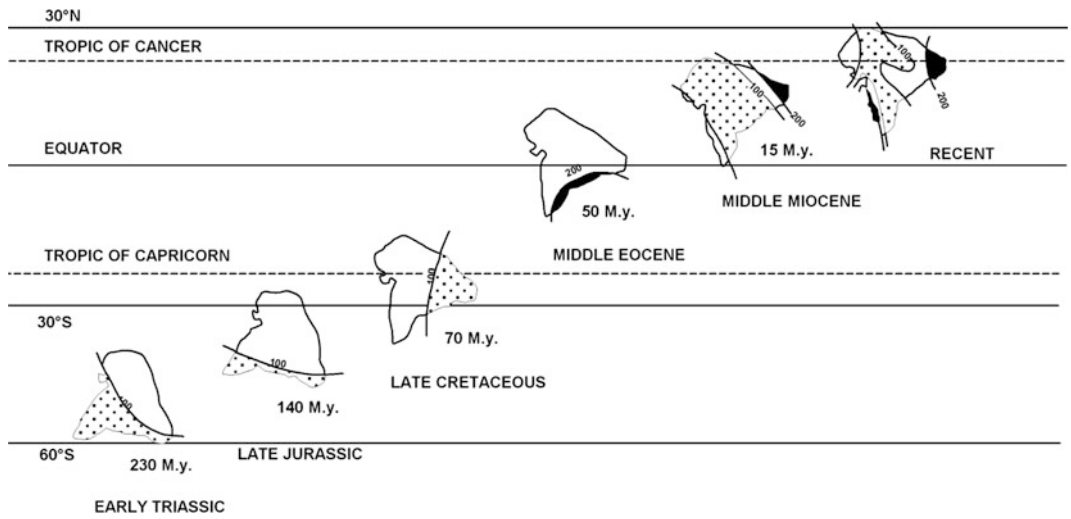

Fig. 2.12 Palaeogeographic reconstruction of Indian plate and its entry to the region of tropics since Early Triassic. Onset of lateritization process was started in Middle Eocene. Numbers shows the relative values of precipitation through geological times and no units are implied. Modified from Tardy et al. (1991), Alam et al. (2003)

after that particular linear laterite *Rarh* belt of NE–SW direction (formerly as E–W coinciding with the alignment of perfect tropical zone for lateritization) had crossed the equatorial zone while the total rotation was 50° in between Palaeocene and Present (Fig. 2.13). At that time span most of the primary laterites of *Rarh Bengal* (especially in the Rajmahal Basalt Traps) were developed. The laterite capping was observed over that Mio–Pliocene sandstones and it suggests continuation of favourbale climate to lateritization in the post-Pliocene times (Devaraju and Khanadali 1993).

During Oligocene (~30 Ma), the southern part of the subcontinent was in the Equatorial Rainy Belt whereas the northern part was extended into the Subtropical Arid Belt (Chatterjee et al. 2013). It is important to mention that mid-section of eastern Indian peninsula (i.e. our study area) had relatively dry episode (6–8 cm precipitation per month) and in rainy season the region experienced 10–26 cm precipitation per month (Chatterjee et al. 2013). It signifies noteworthy prevalence of wet–dry period in Oligocene, favouring lateritization. The results of $^{40}Ar/^{39}Ar$ dating of laterite samples suggest the Eocene climatic optimum of lateritization and the early beginnings of Asian monsoons at ~40 Ma (Bonnet et al. 2015a). The onset of laterite formation within tropics is commonly taken as evidence of a Great Oxidation Event (Retallack 2010). The presence of hematite (Fe_2O_3) and boehmite (AlO(OH)) are dehydrated minerals related to less humid and warmer tropical climatic conditions. Therefore the presence of *Rarh* laterites signifies a special warm and seasonal contrasted palaeoclimate which is not found in present decade throughout the study area. After this morphostratigraphic ferruginous unit Sijua Formation with caliches (Late Pleistocene–Early Holocene) and Chuchura Formation (Middle Holocene–Late Holocene) were developed without any development of ferruginous facies (Ghosh and Guchhait 2014). All ferricretes of *Rarh Bengal* are not subjected to ongoing transformations but these are the fossil laterites of Early Quaternary and that event of lateritization was episodic climate change in this part of West Bengal, related to equator drifting of Indian plate. These laterites were generally formed under an oxic atmosphere in the presence of abundant terrestrial biomass in an acidic environment (Retallack 2010), elevated atmospheric carbon dioxide, exceptional fossil wood

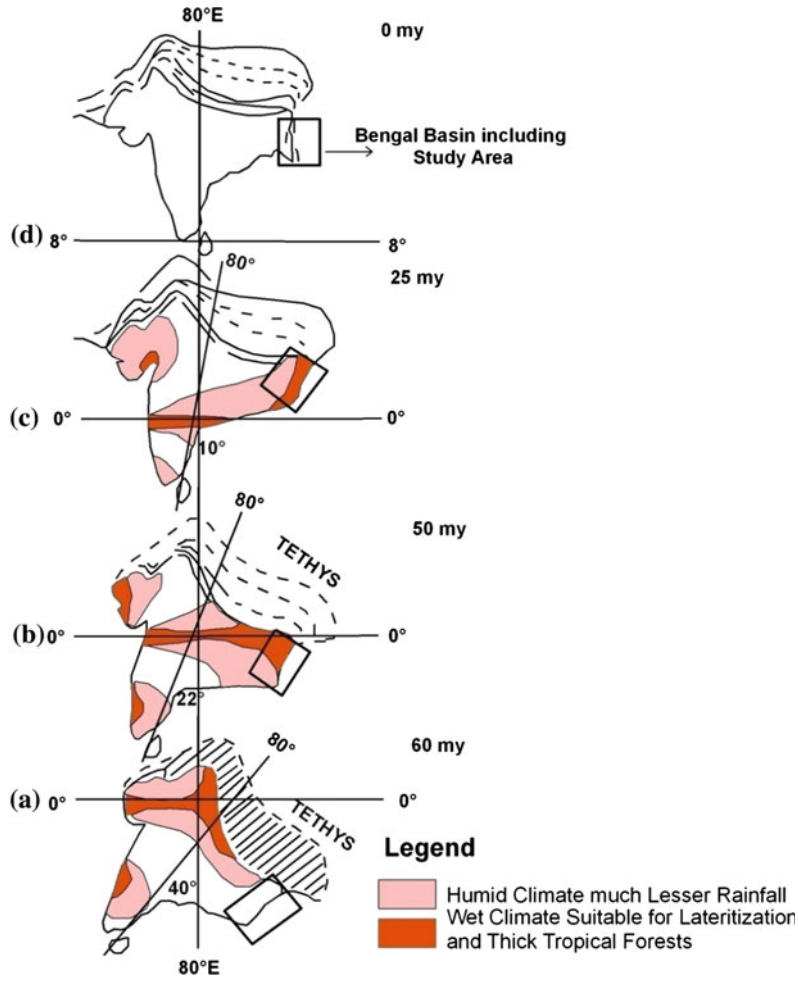

Fig. 2.13 A, B, C, and D, Palaeoclimatic reconstruction of the Indian Plate (including demarcated study area) and its rotation since Early Paleocene, during its course of drifting across the equatorial zone with the distribution of laterites. Modified from Sychanthavong and Patel (1987)

preservation and intense deep basal weathering of basalts, dolerite, gneiss, sandstones and as well as Neogene gravelly sediments of West Bengal. OSL dating of collected samples, both lateritized and non-lateritized sediments, from different sections reveals that the lateritization process (i.e. tropical weathering event) was started in Neogene and restricted within Late Pleistocene (Lalgarh Formation) and did not continue in Holocene times.

Fragments of fossil monocot wood (collected from ferruginous conglomerate bed at Bikaner, Thar Desert) reflect that during Late Neogene the climate was sub-humid to humid up to Rajasthan. An occurrence of hematite and boehmite in ferricretes is related to tropical climates with a marked dry season and relatively high temperatures (mean annual temperature 28 °C). During Paleocene the Indian plate crossed the zone between 30° S and 0° and climate was more favourbale for lateritization (Tardy et al. 1991). Alongside discovery of Pliocene–Eocene fossil algae from the NW Bengal Basin suggests a warm-humid climate and prevalence of estuarine condition in the shelf zone of Bengal Basin (i.e. now *Rarh* laterites). The palaeogeographic model of weather pattern for Eocene (Frakes and Kemp 1976) shows that India laid in low latitudes at that time, mostly to the south of the equator and it experienced high temperatures and

precipitation than today. From the model for Oligocene (Frakes and Kemp 1976) it is evident that by that time India had drifted mostly to the north of the equator and the hot and humid climate continued. Thus it is evident that by Eocene epoch, climate conducive for deep and sustained chemical weathering of rocks for the formation of laterite profiles had set in the peninsular India.

According to Rajaguru et al. (2011), the time span of intensive lateritization (i.e. development of in situ laterites) was started in Eocene and continued up to Early Miocene when the deep profiles of laterite regolith was widespread in peninsular India, signifying a strong wet–dry tropical palaeoclimatic condition. After that phase in between Late Miocene and Early Pleistocene the climate was changed to sub-humid to more wet condition. In that event the deposition of anomalous fluvial gravels–pebbles and lateritization of gravel facies were continued. It is now assume that the development of gravel facies (i.e. alluvial fan to fan-deltaic deposits) with lateritic clasts was occurred in Early Pleistocene. The overall tendency of increasing semi-arid to dry climate with intermittent wet phase (favourable for lateritization) from Neogene to Late Pleistocene had been observed through the occurrences of thin ferruginous crust or deposits in several levels of the lithosections. These ferruginous facies has re-confirmed the prevalence of lateritization climate in the *Rarh Bengal*, related to short-term climate change up to Late Pleistocene. Though the occurrences of colluviums–alluvial calcretized sediments and milliolite formation are carrying evidences of arid to semi-arid climatic phases in western India (Rajaguru et al. 2004a, b, 2011) but in the study area (i.e. eastern India or western part of Bengal Basin) the presence of ferruginous hard crust (mostly ex situ laterites) re-confirmed the dominance of tropical wet–dry palaeoclimate up to Late Pleistocene (96 ± 8 ka to 35 ± 0.7 ka). From the geoarcheological point of view (Deo and Rajaguru 2014) in the initial stage of Acheulian activity (~ 1 Ma) the climate was wet and it turned semi-arid around 0.8 Ma and later.

2.5.3 Palaeogeomorphic Significance

Niyogi et al. (1970) presented an organized thematic map of different lateritic lithofacies (Early Pleistocene to Late Holocene) in West Bengal in five classes (Fig. 2.14)—(1) in situ laterites on Rajmahal Basalt Trap, Archaean rocks, Gondwana sediments and Tertiary gravelly sediments, (2) mottled laterite clay on Pleistocene upland, (3) mildly mottled lateritic clay in river valleys, (4) faintly mottled lateritic clay in Kasai–Damodar deltaic plain, and (5) mildly lateritized soil in interfluves. The presence of iron hydroxide spots and mottles within Pleistocene alluvial sediments and similarity to the mottled clay zone of lateritic profiles suggest that the former lithofacies are derived parts of *Rarh* laterites and are affected by lateritization process in the western part of Ganga – Brahmaputra Delta up to Late Pleistocene. In most cases of *Rarh Bengal* the extensive mottling of brown iron hydroxides and aluminum clays found in B-horizon of soils, reflecting warm–humid palaeoclimate. The possible ages of B-horizons through TL dating (Singh et al. 1998) are 6.7 ka of Bhagirathi–Ajay Plain, 5.44 ka of Ajay–Silai Plain and 3.6 ka of Damodar Deltaic Plain respectively.

In the north-eastern India sub-continent the Bengal Basin evolved from a passive continental margin (pre-Oligocene) to a remnant ocean basin (beginning of Miocene) comprising three principal geo-tectonic provinces—(1) passive to extensional cratonic margin in the west, the Stable Shelf, (2) the Central Deep Basin and (3) the Chittagong–Tripura Fold Belt in the east (Alam et al. 2003; Bandyopadhyay 2007). The evolution of *Rarh* laterites is directly connected with the Stable Shelf Zone of Bengal Basin, experience maximum marine transgression, sediment depositions, tectonic uplifts and lateritization (Fig. 2.14a). Geomorphologically the

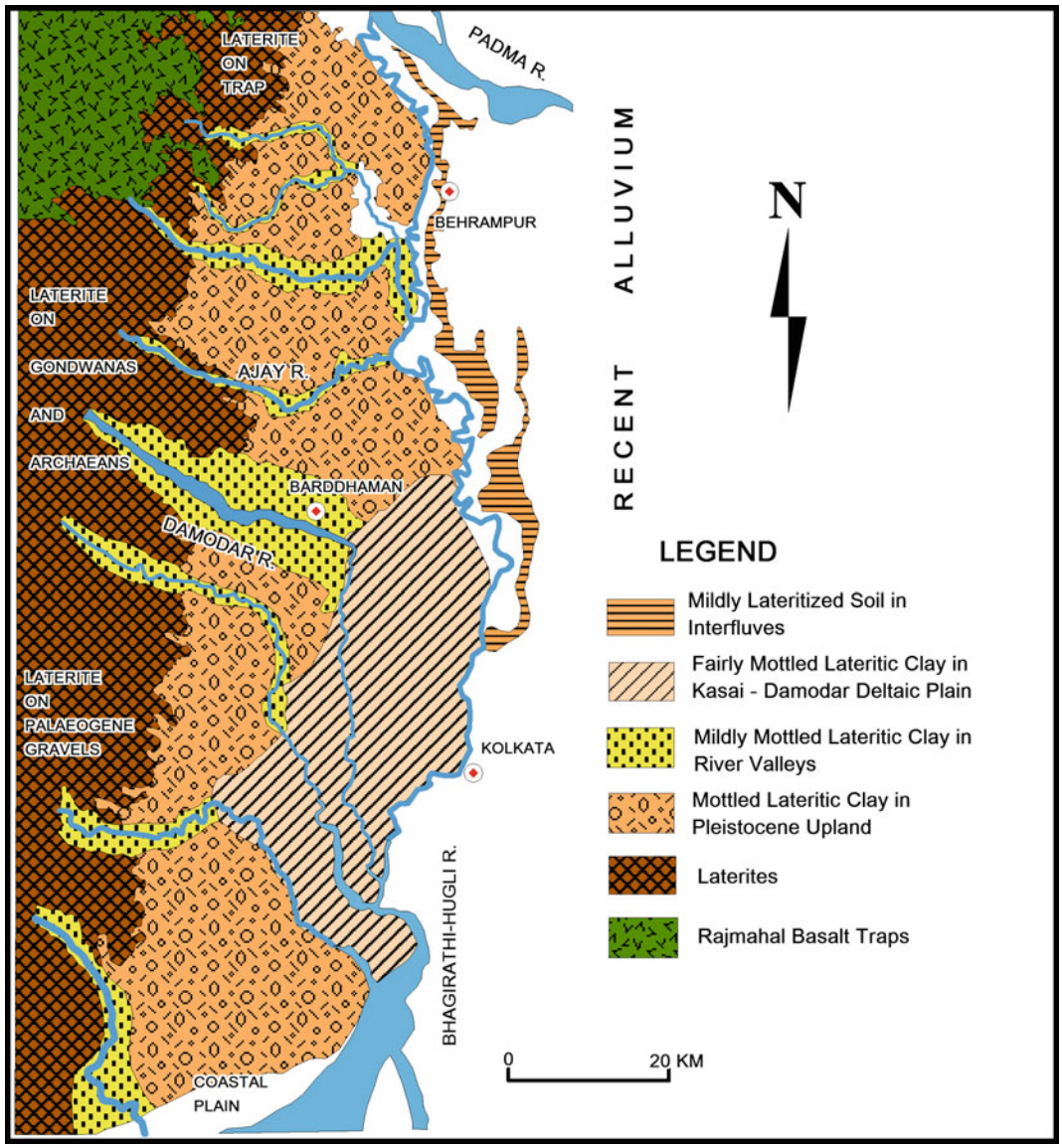

Fig. 2.14 Different units of laterites and lateritic sediments in the western part of Bengal Basin, West Bengal—(1) laterites on Rajmahal Basalt Trap, Archaean rocks, Gondwana sediments and Palaeogene gravelly sediments, (2) mottled laterite clay on Pleistocene upland, (3) mildly mottled lateritic clay in river valleys, (4) faintly mottled lateritic clay in Kasai–Damodar deltaic plain, and (5) mildly lateritized soil in interfluves. Modified from Niyogi et al. (1970)

laterites over Tertiary–Quaternary sequences are represented by degraded badlands which are dissected by drainage system of west to east flowing rivers of West Bengal. Only the primary laterites of Rajmahal Traps are preserved in butte type structures and under blanket of ferruginous soils. All laterites are topographically restricted within 35 to 115 m from mean sea level.

The whole of the present day Bengal Basin (including Stable Shelf) was under marine water until Mio–Pliocene epoch and the strandline grazed the eastern margin of Peninsular Shield,

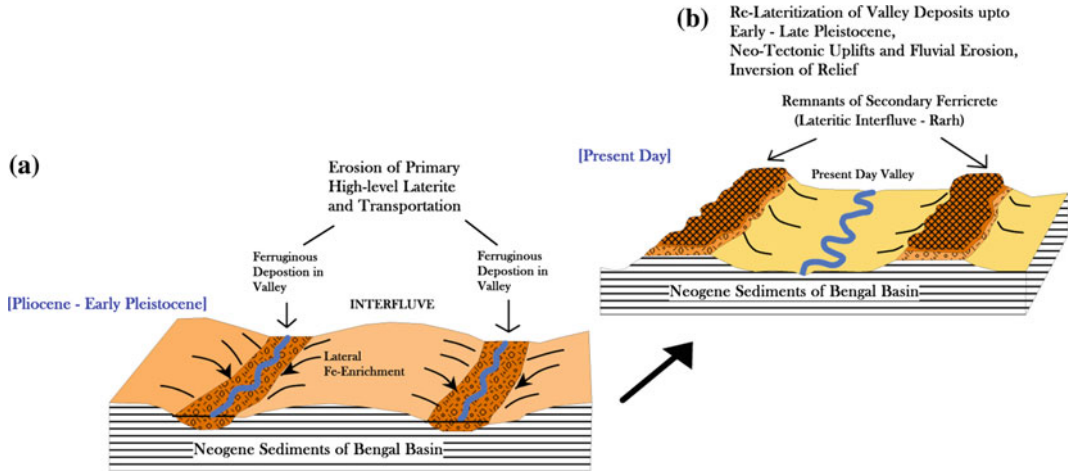

Fig. 2.15 A schematic model of secondary laterite evolution is proposed here, **a** showing the former valleys of ferruginous deposition and then re-lateritization of sediments, and **b** formation of ex situ ferricrete as present summit of mesas and present day valley, i.e. inversion of relief. Modified from Pain and Ollier (1995b), Ollier and Sheth (2008)

i.e. much inland (towards west of study area) from the present day Orissa–Bengal coastline (Vaidyanadhan and Ghosh 1993). The dominance of kaolinite clay with presence of hystrichospheriods (in the pores of clay beds) indicates lacustrine to fluvio-lacustrine condition of deposition in Neogene (Mukherjee et al. 1969). The Stable Shelf Zone is separated by the Chotangapur Foot-hill Fault (CFF) at west and the Medinipur–Farraka Fault (MFF, or called Pingla Fault) at east. Within this tectonic shelf the *Rarh* laterites of West Bengal (NNE–SSW axis) was developed when the sea finally transgressed from this region since LateNeogene. At that time, the Indian plate had been crossed the intense weathering zone of equatorial climate which was favourbale for lateritization.

The terrain of *Rarh* laterites are genetically linked with inversion of relief and active tectonics. Inversion of relief refers to an episode in landscape evolution when a former valley bottom becomes a ridge, bounded by newly formed valleys on each side (Pain and Ollier 1995b; Ollier and Sheth 2008). Inversion of relief occurs when materials on valley floors are, or become, more resistant to erosion than the adjacent valley slopes (Pain and Ollier 1995b). In the first model (Fig. 2.15) the lateral movement of water on hillsides carried weathering products from upper slopes to lower sites, when drainage was often impeded and so chemical precipitation was likely (Ollier and Sheth 2008). Gradually up to Neogene the valley with filled with ferruginous materials and prolong lateritization formed ferricrete within Late Pleistocene. The surrounding terrain was eroded to form next valleys and the present summits or interfluves of duricrusted mesas were formed. In the second model (Fig. 2.16) we reconstructed the event that up to end of Neogene the transported ferruginous materials (due to erosion of primary plateau laterites) re-deposited in the faulted Stable Shelf of Bengal Basin (under marine condition) by the drainage system of peninsular rivers as oldest fan-deltaic to para-deltaic formation in between CFF and MFF (Fig. 2.16). Since Early Pleistocene the sea started regressed from that region and those valley sites of sediment deposition were subjected to further lateritization up to Middle Pleistocene and forming duricrust at top of most of ex situ laterite profiles. The gradational occurrences of top lateritized and bottom un-lateritized gravel

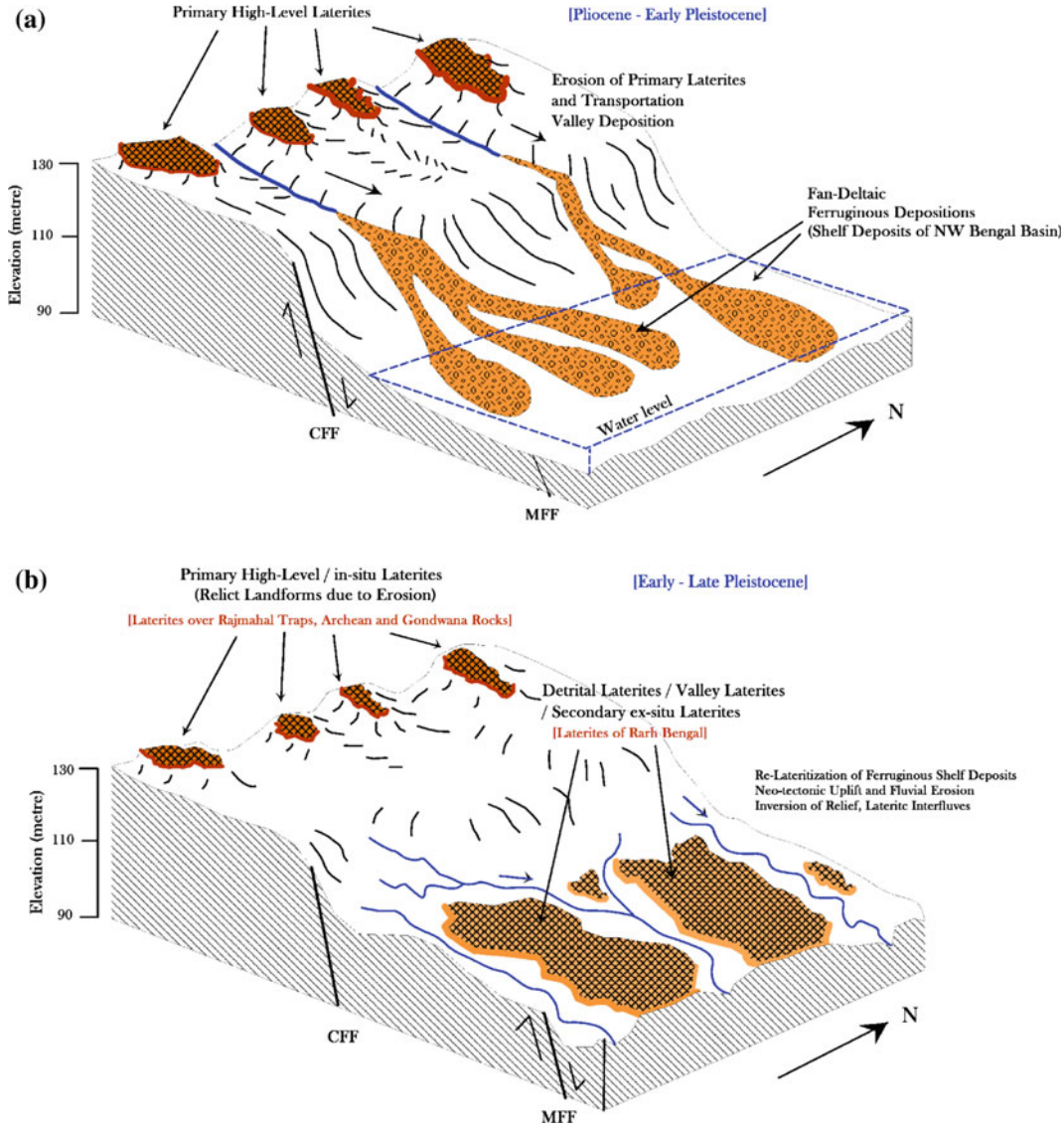

Fig. 2.16 A schematic model of *Rarh* laterite evolution, showing **a** erosion of primary laterites and ferruginous fan-deltaic depositions (modified from Mahapatra and Dana 2009) by rivers and stream in shelf zone of Bengal Basin in between Chotanagpur Foot-hill Fault (CFF) and Medinipur–Farakka Fault (MFF) up to Neogene, and **b** recession of sea, exposure of ferruginous sediments to lateritization climate (Early–Late Pleistocene), re-lateritization to form secondary *Rarh* laterites, neo-tectonic uplift, badland erosion to develop isolated summits of duricrusted mesas and inversion of relief

lithofacies (increasing fining towards the bottom) with numerous buried dicotyledonous fossil woods (Eocene to Miocene age) (Fig. 2.11) at the ex situ laterite sections (Late Pleistocene age) denote a gradual uplift and seismo-tectonic event of the area during the deposition of coarse sand and gravels with ferruginous materials in between Pliocene and Early Pleistocene. Additionally there was a marine regression and uplifts in this shelf zone of Bengal Basin (i.e. *Rarh Bengal*) after the end of Miocene-Pliocene. Since Early Quaternary the unit between MFF and CFF started to uplift

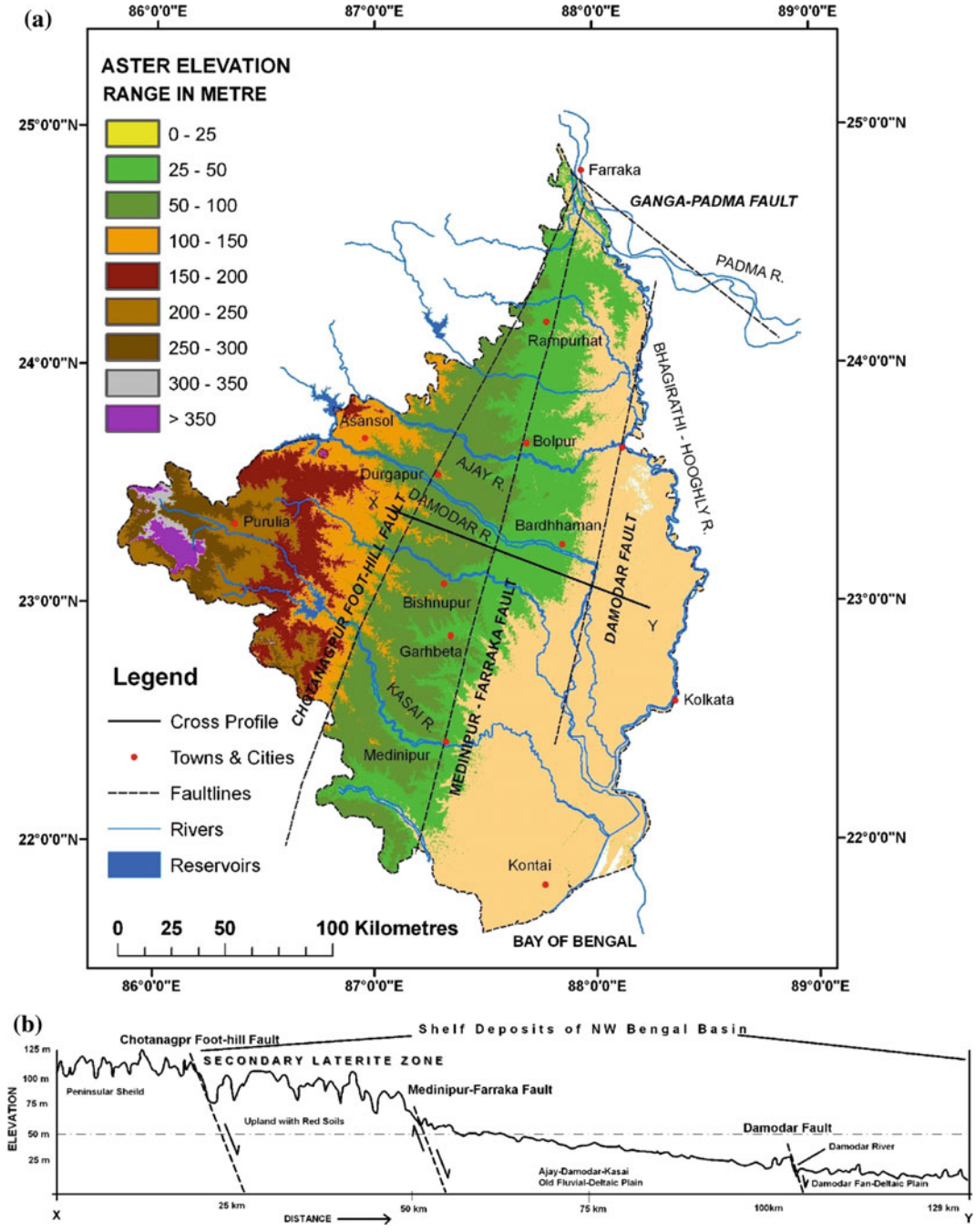

Fig. 2.17 **a** Distribution of laterites (see Fig. 2.1) in relation to topography and major basement faults of Shelf zone, viz., GPF (Ganga Padma Fault), CFF (Chotanagpur Foothill Fault), MFF (Medinipur Farraka Fault or Pingla Fault) and DF (Damodar Fault) (Ghosh and Guchhait 2015) in the north-western Bengal Basin (using Landsat ETM+ mosaic SFCC image, 2000–2001), and **b** west to east elevation cross profile (X–Y) with emplacement of faults and development of lateritic *Rarh* region (Ghosh and Guchhait 2015)

(Fig. 2.17) due to re-activation of basin basement faults during occasional Himalayan upheaval and active tectonics of Bengal Basin (Ghosh and Guchhait 2015). Then during 6–7 ka the eastern unit of Tectonic Shelf (between MFF and Damodar Fault) is subjected to subsidence (Singh et al. 1998) and the western lateritized unit (i.e. *Rarh Bengal*) is subjected to relief inversion (Ollier 1991; Pain and Ollier 1995b) due to neo-tectonic uplifts and consecutive fluvial erosion in Holocene times. Increased precipitation during the ~15 to 5 ka period of peak monsoon recovery probably increased discharge and promote incision and wide spread badland formation (Fig. 2.11) (Sinha and Sarkar 2009). As fluvial erosion proceeds, the valley floor becomes a ridge and interfluves (i.e. laterites of *Rarh Bengal*) bounded by newly formed Late Quaternary valleys on each side.

Due to episodic neo-tectonic uplifts, the reworked laterites with gravels are found at a distance from MFF or Pingla Fault at sites of Rampurhat, Mallarpur (24° 04′ 31″N, 87° 41′ 00″E), Labhpur, Bolpur, Guskara (23° 29′ 17″N, 87° 44′ 48″E), Khandoghosh (23° 12′ 51″N, 87° 41′ 30″E) and Kharagpur (22° 20′ 43″N, 87° 19′ 35″E), following the fault-line scarp of Pingla Fault. This tectonic upliftment of Stable Shelf (Singh et al. 1998) under tropical wet-dry palaeoclimate influenced the deep weathering of Fe-minerals, seasonal groundwater regime, sub-aerial exposure of valley sediments, intense leaching of silica to a depth, irreversible dehydration of Fe–Al oxides, well subsurface drainage and post-lateritization erosion. Geomorphologically the *Rarh* laterites (both in situ and ex situ) are now appeared as dissected interfluves having remnant covers of dry deciduous forest. Formerly the *Rarh Bengal* was the palaeovalleys of ferruginous depositions which are now appeared as the inverted relief due to duricrust formation and gully erosion (Bourman 1993; Ollier and Sheth 2008). It is now suggested that the Indian plate was rotated by 50° in an anticlockwise direction (Fig. 2.12) in between 60 and 0 my through the drifting (Schmidt et al. 1983). So the orientation of present north–south lateritic belt of West Bengal was more north-east to south-west (nearer and almost parallel to equator) in the period of Palaeogene (Late Oligocene to Early Miocene) when the lateritization weathering event was started to get more intensive in India.

In glacial and inter-glacial epochs of the Quaternary (particularly the Pleistocene, covering 1.5 million years) affected the *Rarh Bengal*, not only by strong fluctuations in climate, sea level and intermittent exposure of the western continental shelf of Bengal Basin to sub-aerial processes but also by appreciable perturbations in the rainfall patterns (Banerjee 1993). The linear belt of ex situ laterites on different parent rocks and in different topographic levels confirms an interest fact about the weathering engine of Last Glacial Maxima. Onset of interglacial epoch would re-establish the rainfall intensity of the humid tropics and the mildly acidic nature of the water table in silica-rich terrains, revive the bacteria and re-start the engine of lixiviation of rocks to generate laterite hard crust.

2.5.4 Palaeogeographic Reconstruction

From the above perspective of tectono–climatic evolution, basically the ex situ type of secondary *Rarh* laterites helps to reconstruct the geomorphic history and following palaeogeographic phenomena regarding the origin.

(1) Sea-level fluctuations in the glacial–inter-glacial epochs,
(2) Re-activation of basements faults due to isostatic disequilibrium of Bengal Basin (i.e. active passive continental margin of Indian Plate),
(3) Early–Late Quaternary episodic neo-tectonic uplifts, marine regression and aerial exposure of ferruginous sediments along the shelf zone of Bengal Basin,
(4) Groundwater fluctuation and leaching of silica under the prevalence of tropical wet–dry palaeoclimate, typical to lateritization,
(5) Episodic activation of fluvial erosion under more humid climate on the zone of primary laterites and fan-deltaic depositions,

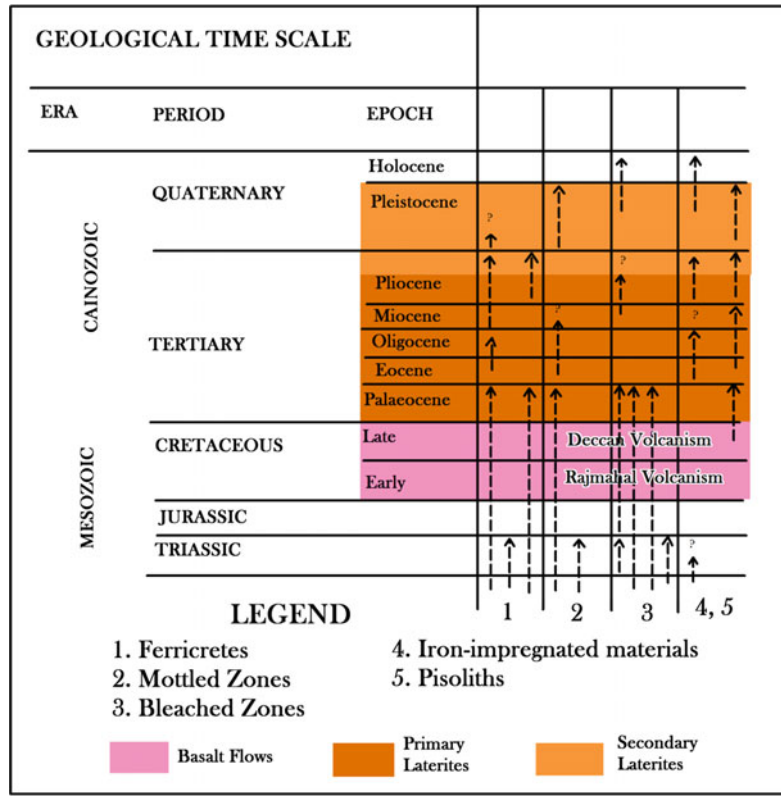

Fig. 2.18 Geological clock of laterite evolution in the study area, showing three phase major events since Cretaceous—(1) widespread volcanism in Cretaceous Period, (2) Paleocene to Mid-Pliocene in situ intense lateritization, and (3) Pliocene to Late Pleistocene ex situ re-lateritization. Modified from Bourman (1993)

6) Reversal of tropical weathering engine of lixiviation on the exposed detrital ferruginous sediments, and
7) Re-lateritization of ferruginous minerals as hard crust through formation of polyphased Fe-noudles up to Late Pleistocene.

If we reconstruct the geological clock of laterite evolution (Fig. 2.18), then we can categorized broadly three major events—(1) two widespread volcanisms in Cretaceous Period as Rajmahal Volcanism (~88 to 118 Ma) and Deccan Volcanism (~69 to 63 Ma), (2) Paleocene to Mid-Pliocene in situ intense lateritization and formation of primary high-level laterites (mostly occurred in ~36 to 26 Ma), and (3) Pliocene to Late Pliestocene ex situ lateritization of deposited ferruginous materials and formation of secondary low-level laterites (up to 35 ka). It has been found that formation of in situ ferricrete was stopped Early Pleistocene but the formation of iron-impregnated materials and pisoliths were still continued up to Late Holocene (Bourman 1993).

2.6 Conclusion

Based on the above geo-chemical and palaeogeographic analysis, the laterites of West Bengal (Birbhum, Barddhaman, Bankura and West Medinipur) are classified into two broad categories viz., (1) in situ or primary and (2) ex situ or secondary types. The primary laterites are genetically related to five types of parent rocks—(1) basalts of Rajmahal Traps, (2) sandstones of Gondwana sequence, (3) gneiss, (4) dolerite and (5) Neogene gravels. The ideal tropical weathering profile of primary laterites is found mostly in the province of Rajmahal Basalt Traps (north-western part of *Rarh Bengal*) where the ferricrete is pisolitic, massive and blocky, and it preserves the columnar structures and litho-relict of basalts. Other ferricretes are generally

vermicular and pisolitic type with glimpses of fluid passage like tubes.

On the other side, ex situ or transported secondary laterites were formed in the eastern part of *Rarh Bengal*, developing mainly in surroundings of Rampurhat, Bolpur, Labhpur, Guskara, Kanksa, Panagarh, Sonamukhi, Patrasyer, Garhbeta, Lalgarh, Kharagpur and Rangamati. These laterites are characterized by channel-fill deposits and petrified woods with ferruginous materials which were fluvially transported from the eroded province of high-level primary laterites (i.e. source of ferrallitic source materials). These laterites are geologically comparable with Early–Late Pleistocene Lalgarh Formation (West Medinipur), Kharagpur Formation (East Medinipur), Saltora Formation (Bankura), Worgram Formation (Barddhaman) and Illambazar Formation (Birbhum).

Very low molar ratio of primary laterites (0.14–0.84) signifies the excessive leaching and weathering parent rock to form thick ferricrete horizons. Very high molar ratio (2.04–2.17) reflects the improper leaching of silica from the secondary profile of laterites and weak development of ferruginous crust at the surface. CIA of primary laterites is more than 99% which signifies intensivebasal weathering and alteration of RBT to form deep laterite profiles.

Linked with other peninsular laterites, the lateritization age of RBT laterites, gneiss laterites and other primary laterites varies from Paleocene to Mid-Pliocene on the basis of Palaeomagnetism and $^{40}Ar/^{39}Ar$ dating. The region experienced six foremost phases of lateritic weathering and subsequent denudation (<5 to 25 m Ma^{-1}), viz. ~53 to 50, ~40 to 32 and ~30 to 23 Ma in the plateau tops and ~47 to 45, ~24 to 19 and ~9 Ma in lowlands, pediments and valleys. With the commencement of Asian monsoon the secondary lateritization was occurred in between Pliocene and Late Pleistocene. The calculated age of OSL data varies between 150 and 35 ka, thus indicating age of Quaternary lateritization (Middle to Late Pleistocene). The palaeoclimate of this period was characterized by the contrasted seasons (wet–dry), high temperature throughout the year (28–35 °C), annual rainfall lower than 1700 mm and long dry seasons. This ferruginous unit (reflecting more wet-humid palaeoclimate) is merged (erosional unconformity) with Late Pleistocene–Early Holocene Sijua Formation which has ample caliches (reflecting semi-arid palaeoclimate). Geomorphologically the ex situ laterites of *Rarh Bengal* now exhibit an inversion of relief with prolong gully erosion. This region is recognized as former palaeovalleys of ferruginous depositions (i.e. palaeofan-deltaic deposits in the western shelf zone of Bengal Basin) which were re-lateritized or re-cemented with gravels, pebbles and ferricrete nodules and developed secondary duricrusts up to Late Pleistocene.

Acknowledgements The authors are indebted to Prof. Cliff D. Ollier (School of Earth and Environment, University of Western Australia) for his encouragement, suggestions and help to execute this work. We are very much thankful to Suvendu Roy (JRF, Dept. of Geography, University of Kalyani), Subhankar Bera (JRF, Dept. of Geography, University of Kalyani) and Subhamay Ghosh (Researcher, Dept. of Geography, The University of Burdwan) for their rigorous all-round supports in the field study. The research is supported by the Department of Geography, The University of Budrwan. We are very much indebted to the Geological Survey of India (Eastern Region, Kolkata) for providing valuable reports regarding the morpho-genetic evolution of Indian laterites.

References

Achyuthan H (1996) Geomorphic evolution and genesis of laterites around the east coast of Madras, Tamil Nadu, India. Geomorphology 16:71–78

Achyuthan H (2004) Paleopedology of ferricrete horizons around Chennai, Tamil Nadu, India. Rev Mex Cienc Geol 21(1):133–143

Aitken MJ (1998) An introduction to optical dating. Oxford University Press, New York

Alam M, Alam MM, Curray JR, Chowdhary MLR, Gandhi MR (2003) An overview of the sediment geology of the Bengal Basin in relation to the regional tectonic framework and basin-fill history. Sediment Geol 155(3–4):179–208

Aleva GJJ (1985) Laterites—concepts, geology, morphology and chemistry. ISRIC, Wageningen

Alexander LT, Cady JG (1962) Genesis and hardening of laterite in soils. United States Department of Agriculture, Technical bulletin, 1281, Washington D.C., pp 1–90

Babu PVLP (1981) Laterite as an unconformity plane in the evolution of the Indian peninsula—a synthesis.

In: Proceedings of the international seminar on lateritization processes, Trivandrum, India, pp 302–307
Bagchi K, Mukherjee KN (1983) Diagnostic survey of Rarh Bengal (Part II). University of Calcutta, Calcutta
Bandyopadhyay S (2007) Evolution of the Ganga–Brahmaputra Delta: a review. Geogr Rev India 69 (3):235–268
Banerjee PK (1993) Quaternary tectonics and climatic record in tropical weathering profiles. Curr Sci 64(11–12):921–923
Bardossy GY (1981) Paleoenvironments of laterites and lateritic bauxites—Effect of global tectonism and bauxite formation. In: Banerjee P K (ed) Proceedings of the international Seminar on lateritisation processes, Trivandum, Geolog Survey India, pp 287–294
Beauvais A, Bonnet NJ, Chardon D, Arnaud N, Jayananda (2016) Very long-term stability of passive margin escarpment constrained by 40Ar/39Ar darting of K-Mn oxides. Geol Soc Am. https://doi.org/10.1130/G373031.1
Bird MI, Chivas AR (1993) Geomorphic and palaeoclimatic implications of an oxygen-isotope chronology for Australian deeply weathered profiles. Aust J Earth Sci 40(4):345–358
Birkeland PW (1984) Soils and geomorphology. Oxford University Press, New York
Biswas A (1987) Laterities and lateritoids of Bengal. In: Datye VS, Diddee J, Jog SR, Patial C (eds) Exploration in the tropics. K.R.Dikshit Felicitaion Committee, Pune, pp 157–167
Bonnet N, Arnaud N, Beauvais A, Chardon D (2015a) Deciphering post-Deccan weathering and erosion history of south India Archean rocks from cryptomelane ^{40}Ar–^{39}Ar dating. Geophys Res Abstr 17:9114
Bonnet N, Beauvais A, Chardon D, Arnaud N (2015b) Evolution of the south-west Indian continental divergent margin: constraints from ^{40}Ar–^{39}Ar dating of lateritic paleolandsurfaces. Geophys Res Abstr 17:9377
Bonnet NJ, Beauvais A, Arnaud N, Chardon D, Jayananda M (2014) First $^{40}Ar/^{39}Ar$ dating of intense Late Palaeogene lateritic weathering in peninsular India. Earth Planet Sci Lett 386:126–137
Botter-Jensen L (1997) Luminescence techniques: instrumentation and methods. Radiat Meas 27(5–6):749–768
Bourman RP (1993) Perennial problems in the study of laterite: a review. Austr J Earth Sci 40(4):387–401
Bourman RP (1996) Towards distinguishing transported and in-situ ferricretes: data from southern Australia. J Austr Geol Geophys 16(3):231–241
Briant RM, Bates MR, Schwenninger J, Wenban-smith F (2006) An optically stimulated luminescence dated Middle to Late Pleistocene fluvial sequence from the western Solent Basin, southern England. J Quat Sci 21 (5):507–523
Buchanan F (1807) A journey from Madras through the countries of Mysore, Kanara and Malabar (3 volumes). East India Company, London
Chakrabarti DK (2001) Archaeological geography of the Ganga Plain. Permanent Black, New Delhi
Chakraborti S (2011) Final report on Quaternary laterites in the western districts of West Bengal—their geomorphology, stratigraphy, genesis and implications for climate change. Geological Survey of India Eastern Region, Kolkata, pp 1–88
Chatterjee S, Goswami A, Scotese CR (2013) The longest voyage: tectonic, magmatic and palaeoclimatic evolution of the Indian plate during its northward flight from Gondwana to Asia. Gondwana Res 23:238–267
Chatterjee N (2008) Laterite terrains of the Chotanagpur Plateau fringe region (case study of the Mayurakshi Basin, eastern India). Indian J Landsc Syst Ecol Stud 31(1):115–130
Das Gupta AB, Mukherjee B (2006) Geology of N.W. Bengal Basin. Geological Society of India, Bangalore, pp 1–154
Deo SG, Rajaguru SN (2014) Early Pleistocene environment of Acheulian sites in Deccan upland: a geomorphic approach. In: Paddayya K, Deo SG (eds) Recent advances in Acheulian culture studies in India—ISPQS monograph 6. Indian Society for Prehistoric and Quaternary Studies, Pune, pp 1–22
Devaraju TC, Khanadali SD (1993) Laterite bauxite profiles of south western and southern India—characteristics and tectonic significance. Curr Sci 64(11–12):919–921
Duller GAT (2004) Luminescence dating of Quaternary sediments: recent advances. J Quat Sci 19(2):183–192
Frakes LA, Kemp EM (1972) Influence of continental positions on early tertiary climates. Nature 240 (5376):97–100
Ghosh S, Guchhait SK (2014) Palaeoenvironmental significance of fluvial facies and archives of Late Quaternary deposits in the floodplain of Damodar River, India. Arab J Geosci 7(10):4145–4161
Ghosh S, Guchhait S (2015) Characterization and evolution of primary and secondary laterites in northwestern Bengal basin, West Bengal, India. J Palaeogeogr 4 (2):203–230
Huntley DJ, Godfrey-Smith DI, Thevalt MLW (1985) Optical dating of sediments. Nature 313:105–107
Kale VS (2014) The laterite-capped Panchgani Tableland, Deccan Traps. In: Kale VS (ed) Landscapes and landforms in India. Springer, New York, pp 217–222
Kale VS, Singhvi AK, Mishra PK, Banerjee D (2000) Sedimentary records and luminescence chronology of Late Holocene palaeo-floods in the Luni River, Thar Desert, northwest India. CATENA 40:337–3587
Karlekar S, Thakurdesai S (2011) Coastal detrital laterites of Konkan Coast, Maharashtra. In: Sharma HS, Kale VS (eds) Geomorphology in India. Allahabad, Prayag Pustak Bhawan, pp 321–340
Kent RW, Pringle MS, Muller RD, Saunders AD, Ghose NC (2002) $^{40}Ar/^{39}Ar$ geochronology of the Rajmahal Basalts, India and their relationship to the Kerguelen Plateau. J Petrol 43(7):1141–1153

Kumar A (1986) Palaeolatitudes and the age of Indian laterites. Palaeogeogr Palaeoclimatol Palaeoecol 53:231–237

Mahapatra S, Dana RK (2009) Lateral variation in gravelly sediments and processes in alluvial fan—fan-delta setting, north of Durgapur. J Geolog Soc India 74(4):480–486

Maignien R (1966) Review of research on laterites. UNESCO, Paris, pp 1–148

McFarlane MJ (1976) Laterite and landscape. Academic Press, London

Meshram RR, Randive KR (2011) Geochemical study of laterites of the Jamnagar district, Gujarat, India: implications on parent rock, mineralogy and tectonics. J Asian Earth Sci 42:1271–1287

Metha M, Majeed Z, Dobhal DP, Srivastava P (2012) Geomorphological evidences of post-LGM glacial advancements in the Himalaya: a study from Chorabari Glacier, Garhwal Himalaya, India. J Earth Syst Sci 121(1):149–163

Milnes AR, Bourman, Northcote KH (1985) Field relationships of ferricretes and weathered zones in southern South Australia: a contribution to 'laterite' studies in Australia. Aust J Soil Res 23:441–465

Mishra S, Deo S, Rajaguru SN (2007) Some observations on the laterites developed on Deccan Trap: implications for the Post-Deccan Trap denudational history. J Geol Soc India 70:469–475

Mukherjee B, Rao MG, Karunakaran C (1969) Genesis of kaolin deposits of Birbhum, West Bengal. Clay Miner 8:161–170

Murray AS, Olley JM (2002) Precision and accuracy in the optically stimulated luminescence dating of sedimentary quartz: a status review. Geochronometria 21:1–16

Nesbitt HW, Young GM (1982) Early proterozoic climates and plate motion inferred from major element chemistry of lutites. Nature 299:715–717

Niyogi D (1975) Quaternary geology of the coastal plain in West Bengal and Orissa. Indian J Earth Sci 2:51–61

Niyogi D, Mallick S, Sarkar SK (1970) A preliminary study of laterites of West Bengal, India. In: Chatterjee SP, Das Gupta SP (eds) Selected papers physical geography (vol 1). 21st international geographical congress, Calcutta, National Committee for Geography, pp 443–449

Ollier CD (1988) The regolith in Australia. Earth Sci Rev 25:355–361

Ollier CD, Rajaguru SN (1989) Laterite of Kerala (India). Geogr Fis Dinam Quat 12:27–33

Ollier CD (1991) Laterite profiles, ferricrete and landscape evolution. Z Geomorphol 35(2):165–173

Ollier CD, Galloway RW (1990) The laterite profile, ferricrete and unconformity. CATENA 17:97–109

Ollier CD, Sheth HC (2008) The high Deccan duricrusts of Indian and their significance for the 'laterite' issue. J Earth Syst Sci 117(5):537–551

Pain CF, Ollier CD (1995a) Regolith stratigraphy: principles and problems. AGSO J Aust Geol Geophys 16(3):197–202

Pain CF, Ollier CD (1995b) Inversion of relief—a component of landscape evolution. Geomorphology 12:151–165

Pain CF, Ollier CD (1996) Regolith stratigraphy: principles and problems. AGSO J Australian Geol Geophy 16(3):197–202

Pappu RS, Rajaguru SN (1979) Early quaternary laterite around Anagwadi, Dist. Bijapur, Karnataka. Bull Earth Sci 7:41–43

Pascoe EH (1964) A manual of the geology of India and Burma (Volume 3). Geological Survey of India, Delhi

Paton TR, Williams MAJ (1972) The concept of laterite. Ann Assoc Am Geogr 62(1):42–56

Persons BS (1970) Laterite—genesis, location, use. Plenum Press, New York

Prescott JR, Robertson GB (1997) Sediment dating by luminescence: a review. Radiat Meas 27(5–6):893–922

Preusser F, Degering D, Fuchs M, Hilgers A, Kadereit A, Klasen N, Krbetschek M, Richter D, Spencer JQG (2008) Luminescence dating: basics, methods and applications. Quat Sci J 57(1–2):95–149

Rajaguru SN, Deo SG, Mishra S, Ghate S, Naik S, Shirvalkar P (2004a) Geoarchaeological significance of the detrital laterites discovery in the Karha Basin, Pune District, Maharastra. Man Environ XXIX(1):1–6

Rajaguru SN, Deo SG, Mishra S, Ghate S, Naik S, Shirvalkar P (2004b) Geoarchaeological significance of the detrital laterite discovery in the Karha Basin, Pune District, Maharastra. Man and Environment 31(1):1–6

Rajaguru SN, Deotore BC, Gangopadhyay K, Sain MK, Panja S (2011) Potential geoarchaeological sites for luminescence dating in the Ganga Bhagirathi–Hugli Delta, West Bengal, India. Geochornometria 38 (3):282–291

Ray Chaudhuri SP (1980) The occurrence, distribution, classification and management of laterite and laterite soils. Cah O.R.S.T.O.M. Ser Pedol 18(3–4):249–252

Retallack GJ (2010) Lateritization and bauxitization events. Econ Geol 105:655–667

Rittenour TM (2008) Luminescence dating of fluvial deposits: applications to geomorphic, palaeoseismic and archaeological research. Boreas 37:613–635

Roy Chowdhury MK (1986) Concepts on the origin of Indian laterite in historical perspective. Proc Indian Natl Sci Acad 52A(6):1307–1323

Roy Chowdhury MK, Venkatesh V, Anandalwar MA, Paul DK (1965) Recent concepts on the origin of Indian laterite. Proc Natl Acad Sci India Sect A Phys Sci 31A(6):547–558

Sahasrabudhe YS, Rajaguru SN (1990) The laterites of the Maharashtra State. Bull Deccan Coll Res Inst 49:357–374

Sankaran AV, Nambi KSV, Sunta CM (1985) Thermoluminescence of laterites: applicability in dating. Nucl Tracks 17(5):177–183

Sarkar PR (2004) Rarh-the cradle of civilization. Ananda Nagr Publication, Kolkata

Schellmann W (1986) A new definition of laterite. In: Banerjee PK (ed) Lateritisation processes. Geological Survey of India Memoir 120:11–17

Schmidt PW, Currey, Ollier CD (1976) Sub-basaltic weathering, damsites, palaeomagnetism and the age of lateritization. J Geol Soc Aust 23(4):367–370

Schmidt PW, Prasad V, Raman PK (1983) Magnetic ages of some Indian laterites. Palaeogeogr Palaeoclimatol Palaeoecol 44:185–202

Singh LP, Parkash B, Singhvi AK (1998) Evolution of the lower gangetic plain landforms and soils in West Bengal, India. CATENA 33:75–104

Singhvi AK, Kale VS (2009) Paleoclimate studies in India: last ice age to the present. IGBP–WCRP–SCOPE–Report Series 4:1–28

Singhvi AK, Sharma YP, Agrawal DP (1982) Thermoluminescence dating of sand dunes in Rajasthan. Nature 295:313

Sinha R, Sarkar S (2009) Climate-induced variability in the Late Pleistocene–Holocene fluvial and fluvio-deltaic successions in the Ganga Plains, India. Geomorphology 113(3–4):173–188

Sivarajasingham S, Alexander LT, Cady JG, Cline MG (1962) Laterite. Agronomy 14:1–56

Sridhar A (2007) A mid-late Holocene flood record from the alluvial reach of the Mahi River, western India. CATENA 70:330–339

Stokes S (1999) Luminescence dating applications in geomorphological research. Geomorphology 29:153–171

Sychanthavong SPH, Patel PK (1987) Laterites and lignites of northwestern India and their relevance to the drift tectonics of the Indian Plate. Curr Sci 56 (10):469–473

Tardy Y (1992) Diversity and terminology of laterite profile. In: Martini IP, Chesworth W (eds) Weathering, soils and paleosols. Elsevier, Amsterdam, pp 379–405

Tardy Y, Boeglin J, Novikoff A, Roquin C (1993) Petrological and geochemical classification of laterites. In: Proceedings of the 10th international clay conference, Adelaide, Australia, 481–486

Tardy Y, Kobilsex B, Paquet H (1991) Mineralogical composition of geographical distribution of African and Brazilian peri-Atlantic laterites: the influence of continental drift and tropical paleoclimates during the past 150 million years and implications for India and Australia. J Afr Earth Sci 12(1–2):283–295

Tardy Y, Nahon D (1985) Geochemistry of laterites, stability of Al–Goethite, Al–Hematite and Fe3 + Kaolinite in bauxites and ferricretes: an approach to the mechanism of concretion formation. Am J Sci 285:865–903

Thomas MF (1996) Laterites revisited. Progress Phys Geogr 20(1):113–121

Thomas MF (1974) Tropical geomorphology: a study of weathering and landform development in warm climates. MacMillan Press Ltd

Vaidyanadhan R, Ghosh RN (1993) Quaternary of the east coast of India. Curr Sci 31(6):231–232

Varghese T (1987) Laterite soils and their management. ISRIC–World Soil Information, Wageningan

Widdowson M, Cox KG (1996) Uplift and erosional history of the Deccan Traps, India: evidence from laterites and drainage patterns of the Western Ghats and Kankan Coast. Earth Planet Sci Lett 137:57–69

Widdowson M, Gunnell Y (1999) Lateritization, geomorphology and geodynamics of a passive continental margin: the Konkan and Kanara costal lowlands of western peninsular India. Spec Publ Int Assoc Sedimentol 27:245–274

Wintle AG (1997) Luminescence dating: laboratory procedures and protocols. Radiat Meas 27(5–6):769–817

Wintle AG (2008) Luminescence dating: where it has been and where it is going. Boreas 37:471–482

Young A (1976) Tropical soils and soil survey. Cambridge University Press, Cambridge

3 Microstructural Evidence of Palaeo-Coastal Landform from Westernmost Fringe of Lower Ganga–Brahmaputra Delta

Sk. Mafizul Haque and Subhendu Ghosh

Abstract

The largest delta of the world, i.e. Ganga–Brahmaputra (G-B) delta has been characterized by ample evidences of regional morphogenetic variations. The westernmost fringe of this G-B delta has long been influenced by both Chottonagpur upland as well as recent alluvium plain between the Cretaceous to early Quaternary period. Successively, the undulating Rarh topography that separates these two morphogenic units has been evolved as one of the relict terrains having the dominancy of ferrallitic soils. In this area, most of the sedimentary formations and pedogenesis processes have been performed during post-Pleistocene epoch. Here, all the features of this residual topography directed through hydro-morphogenetic origins had been performed over the remnant ocean basin, which are also treated as a product of Palaeo-marine deposition. Alterations as well as modifications of the ferrallitic–lateritic micro-features are also continuing through the changes of various hydro-meteorological components. The present chapter concentrates on the studies of deposited microstructure features in one of the lateritic pockets of Paschim Medinipur district, West Bengal. Few soil samples from Palaeo-coastal tracks in the gully dominated badland topography have been collected and the thin sectioning has been done for the assessment of prevailed process of Palaeo-coast development and its associated events. The snaps of the microscopic view along with digital colour analysis of samples depict the evidences of cross-bedding, to ripple marks and shoreline retreat mechanism in the study area.

Keywords

Palaeoclimate · Microstructure · Badland topography · Thin section · Digital technology

Sk. Mafizul Haque (✉)
Department of Geography, University of Calcutta, 35, B. C. Road, Kolkata 700 019, India
e-mail: mafi_haque@yahoo.co.in

S. Ghosh
Department of Geography and Disaster Management, Tripura University, Agartala 799 130, India
e-mail: subhendu_geo@rediffmail.com

3.1 Introduction

At present, various wings of environmental study are spreading through not only the means of searching the knowhow but also for the unknown facts of environmental dynamics that took place during the geologic past. Similarly, the study of

B. C. Das et al. (eds.), *Quaternary Geomorphology in India*,
Geography of the Physical Environment, https://doi.org/10.1007/978-3-319-90427-6_3

Palaeoenvironment is such type of platform which can investigate and evaluate the ancient imprints of the earth system. Although present environmental condition has been evolved from the early physical, chemical and biological events of the earth through the geological times, nature has the power of right justification by preserving the evidences of early events in the geological structures, stratigraphy, geoarchaeology, geomagnetic fields, ices, fossils, etc. Therefore, geology and geomorphology are the most important disciplines to demonstrate the facts of earth's history (Browne 2011). The *Bengal Basin* has long history of geologic evolution along with a wide range of geotectonic evidences considering the earlier Bengal Fan (Sarkar et al. 2009) to earliest progradation and basement geostructures (Allison et al. 2003). With the light of geotectonic settings, the entire area of Bengal Basin is surrounded by tectonic boundary which evolved from Upper Cretaceous to Upper Neogene (Roy and Chatterjee 2015). By the systematic investigation of those early evidences, many embroiled clues of early environmental conditions like isostatic balance, magnetism of the earth, tectonic processes, climatic condition, geomorphic processes and physicochemical changes of the earth system, etc. would be understood. On the other hand, the geomorphic agents create some small sculptures and designs in the sediment layers on the surface of the Quaternary landmass. These all small dimensional marks can be described as micro-geomorphic features. This term was initially used by Gardner and Helen in 1983 to explain the geomorphology of smaller parts of the earth surface. Though little has been discussed so far in the existing literatures of palaeo-coastal study is concerned, the significance of micro-geomorphic features can never be ignored in the study of Quaternary geomorphology (Ghosh 2013).

Regarding the units of micro-geomorphology, micro-features have a wide range of variations in temporal scale, i.e. a few hours to millions of years. The extent of this scale depends on the variability and efficiency of processes under specific environmental conditions. Bloom (2002) also accorded that generally smaller features of landform can be created and destroyed more rapidly than larger ones. According to Browne (2011), coasts are the chambers of prior facts of landforms and sediments. As per the Walther's Law, it can be concluded that each of the distinctive sedimentary environment has its own unique genetic characteristics (Chorley et al. 1984). Thus, imprints of ancient features with the regression and transgression of sea levels are more profound to prove their previous environment. These types of coasts having nature of past geologic genesis are generally known as palaeo-coasts. From that standpoint, the study of micro-geomorphology can be a very useful tool to the geomorphologists for advocating the palaeo-environmental condition of any "geomorphic units".

Microscopic investigation of soils, rocks or any morphological feature are considered as fascinating approach of profound practical importance in the sphere of system science (Radlinski et al. 2005), which are totally standing on two methodological pillars, first *microscopy and digital imaging* and second *image analysis and modelling*. Since 1970s, many outstanding contributions on soil or rock microstructure were published (as for example, Brewer 1976; Bale and Schmidt 1984; Katz and Thompson 1985; Wong et al 1986; Jacquin and Adler 1987; Hansen and Skjeltrop 1988; Van der Meer 1987, 1993; Van der Meer and Laban 1990; Menzies and Maltman 1992; Tardy et al. 1991; Bryant and Davidson 1996; Vernon 2004; Mamtani et al. 2007; Cashman et al. 2007; Dey et al. 2009, 2011; Roy and Chatterjee 2015), which proved the significance of high-quality small-scale imaging in this field of scientific research. Suttner and Dutta (1986) have interpreted the palaeoclimate and palaeoenvironment condition of Raniganj Basin based on mineralogical evidences (Ghosh 2002). Similarly, Cooper (1998), Lachniet et al. (1999) and Lachniet et al. (2001) discussed the complex impact of process on microstructure development by digital image analysis. Since the last half of the twentieth century, several research works have been carried out to focus a lot of arenas of the G-B delta. Considering the geomorphic micro-features as an

integral part of landform evolution, it is found that a few attempts have been put forward to investigate the palaeoenvironment. But the effort to explore the imprints of geo-structural history with the help of microscopic image analysis and reflectance visualization of grains is a different way of study. The main objective of this work is to understand the thin sections of samples (which have been shown in Figs. 3.5, 3.6 and 3.8) for the microstructural assessment of palaeo-morphogenetic environment in the western end of G-B delta, which assesses the older geomorphic processes and evidences through the analysis of Quaternary microstructures of the coastal to badland topographic evolution.

3.2 Palaeo-Geography of Ganga–Brahmaputra (G-B) Delta

In the view of large-scale geo-structural setting, the Bengal Basin is located on the eastern edge of Indian shield. This foreland basin has been adjusted through neotectonic changes (Chandra 1992) and bounded by Indian Peninsula Archanean Shield in west, Shillong Plateau in north and Indo-Burmese orogen in the east (Biswas and Agarwal 1992). The G-B delta, largest and siltiest delta of the world, is a product of Bengal Basin and has evolved from the part of the largest geosyncline during the Mesozoic–Cenozoic period (Evans 1964; Alam 1989; Kayal 2008). After the collision of India with Eurasia (soft collision performed in Paleocene and hard collision in Eocene), this part of the geosyncline gets to accumulate the huge amount of eroded loads. Progressively, the genesis of this delta has been controlled by plate movement, sediment accumulation, isostatic adjustment and land subsidence (Kuehl et al. 2004; Rogers 2012; Rudra 2014). Due to continuous spreading of Indian Ocean floor, Bengal basin has been characterized by hinge, en echelon fault and scarps in almost all sides (Paul 2002; Kayal 2008). Curray et al. (1982) advocated that continental shelf in the west and the geosynclinal facies in the east have been separated by Eocene Hinge Zone (Fig. 3.1) located in the western side of this basin territory. Here, eastward dipping and the asymmetrical depression of this basin area formulate some geo-structural units from west to eastward direction; these are—inner shelf, outer shelf or western basin marginal zone, shallow basin or stable shelf zone and deep basin area (Nandy 1994; Alam et al. 2003). During Pleistocene–Flandrian transgression of sea level, shelf zones have been totally uncovered and created widespread terrace and deep valleys in the entire basin area (Alam 1989; Paul 2002; Rudra 2014). But the formation of the western fringe of G-B delta, known as 'Rarh' is quite different than the other sections. This formation is basically exaggerated by palaeo-lobes and propagated by five eastward-flowing tributaries of Bhagirathi system.

Being a part of mature coastal plain, this 'Rarh' region is also active because of its basement geologic features. The western fringe of Bengal Basin is bounded by basic lava flow and Rajmahal formation in its basement (110 ± 10 Ma BP). During the fragmentation of Gondwanaland units of super-group exhibits lateral changes and deformation with tectonic performances. The long history of sedimentation in this area has a heterogeneous sequence influenced and dominated by continental sediments (Ghosh 2002). The nature of this deposition has been fully controlled by the fluvial and lacustrine environment during marine transgression (Shah and Shastri 1975). Area between Ajoy and Damodar River has tectono-sedimentary evolution with the enormous boundary fault and intra-basinal faults (Ghosh 2002). During the late Cretaceous ($\sim$65 Ma BP) period, the Indian peninsula encroached into the humid tropical region and experienced climatic maxima. In this situation, river system of eastern peninsular like —Subarnarekha, Kasai, Silai, Ajay, etc. carried enormous ferruginous coarse sediments and marine gradually transgressed. In this situation, the Neogene sedimentation has been buried as several lobes of fan-shaped para-delta. The river patterns located in the interfluves of River Kasai-Silabati have such types of adjustment which are prevailed on dome-shaped surface due to compactness of para-deltic basement geologic

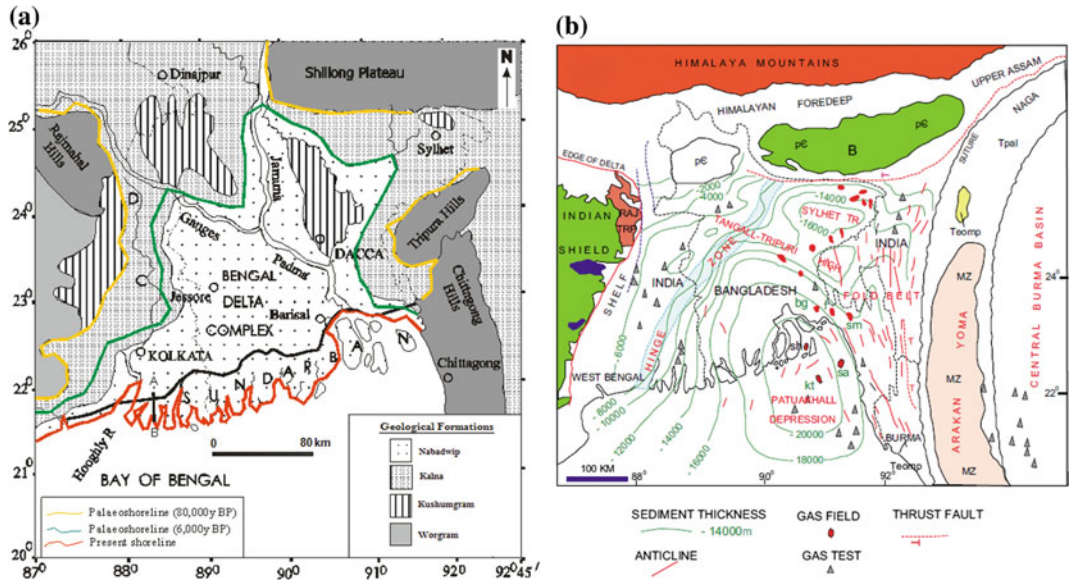

Fig. 3.1 **a** Location and temporal variation of different formations in coastal environment through geological ages (De 2014); **b** major geological features, sediment thickness of Bengal Basin and its surroundings (Shamsuddin and Abdullah 1997)

structure followed by 'Sijua formation'. Goswami (1997, 1999) illustrated that alternate sequence of greyish yellow sticky clay with caliches and nodules, grey to yellow, fine to coarse sand and gravel was engulfed in this river system at the time of marine regression (~18,000 YBP: Paul 2002). Garhbeta is situated in the northern end of this geo-stratigraphic setting, which was later reshaped by local subsidence, local transgression, marine regression and basement tectonics (Paul 2002).

3.3 Geographical Settings of the Study Area

The entire work has been carried out in a badland area, which has little span of economic utilization, less vegetation cover and almost no organic materials. The study area has developed through the marine siltation processes and experienced humid weathering condition (Sen et al. 2004). Besides the rugged nature of barren area along with local slope faces, numerous eroded features have been found prominently in this badland topography.

3.3.1 Location

This work shows the evidences of microstructures for the morphogenetic analysis of badland topography. For that purpose an area of ferrallitic–lateritic badland has been selected at Gangani region, locally known as *Ganganir Danga* (the 'land of fire'), is located in the right bank of Silai (Silabati) River (Sen et al. 2004). This is a transitional zone between G-B delta and Chottonagpur plateau fringe in its basement and covered by Quaternary sediment at the surface. Tectonically, this area is situated over the Midnapur Farakka Fault (MFF) line in the Bengal Shelf which is also known as 'basin margin fault' and characterized by gravity contours (Roy and Chatterjee 2015). The strategic location of the study area (Fig. 3.1) has also been advocated as a part of Palaeo-coastal belt of Bengal Basin by Niyogi (1970), Bera (1996), Paul (2002), Dey et al. (2009). From the administrative view Gangani is situated in the Garhbeta-I block under the jurisdiction of Paschim Medinipur District, West Bengal (Fig. 3.2). The latitude and longitude of this area 22° 51′ 19″N and 87° 21′ 27″E.

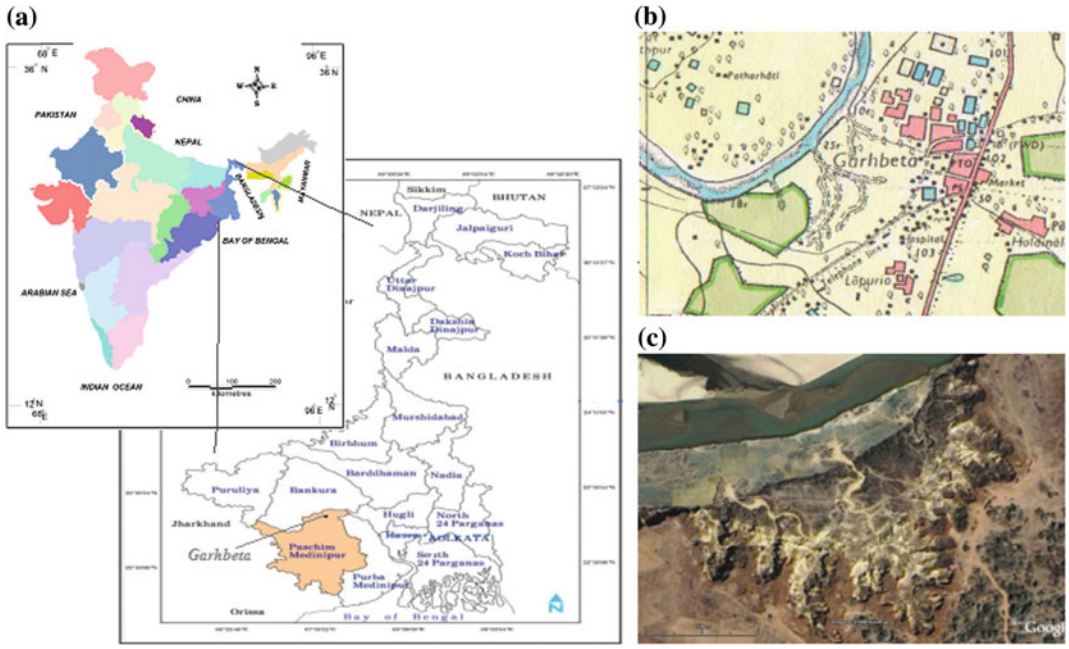

Fig. 3.2 Location map of study area—**a** administrative location; **b** spatial environment of Garhbeta region in SoI topographical map, 1931; **c** synoptic view of the study area, 2005

Gangani badland is rapidly extending by gully erosion and its hydro-meteorological setting develops the roughed topography covered with thick ferrigeneous laterite enduring.

3.3.2 General Geology

The study area has been experiencing humid type of climatic phenomena during middle Miocene era. Location shifting of gondwana land from hot and dry to hot and humid, shown in Fig. 3.3, is favourable for lateritization (Tardy et al. 1991). The formation of lateritic patches in the western fringe of G-B delta has mainly been found surroundings the lower basin area of the River Subarnarekha, Kasai, Silai and Ajay stretches from west to east (Fig. 3.4a). Tectonically, this is a part of the western geo-province of the Bengal Basin, i.e. having transitional location between shield (part of Gondwana land) and shelf area with a relatively high rainfall. Depositions of the above said rivers play the most vital role for the regional litho-morphogenic development during Tertiary and Quaternary periods (Fig. 3.1b). According to Wadia (1999), this region has evolved through the existence of hot cum humid monsoonal condition since late Tertiary era. Various geological evidences are preserved in this area which strongly support the existence of marine coastal environment of this landform which is now nearly 90–100 km away from the present day shoreline (Fig. 3.1a). Bera (1996); Ghosh and Majumder (1981) have furnished that Garhbeta is one of the youngest trace fossil assemblage zones in Bengal Basin dominated by the presence of *Ophiomorpha nodosa, Cylindricum* sp. *and Thalassinoides* sp. In this context, it has been established that all these traced components are the imprints of sandy coastal environment with oscillating meso-tidal processes (Seilacher 1964; Chiplonkar and Badve 1969; Frey et al. 1978; Ratcliff and Fagerstrom 1980). The quartzo-feldspathic cum ferromagnesian sand and lower clay layer are divided by two gravel beds. These sequences of formation have denoted the history of older to newer alluvium along with the existence of long

marine sedimentation. Presently, it is a gully dominated lateritic landscape which is characterized by some residual features along with few geomorphic imprints (Goswami 1980; Sen et al. 2004). In the northwest of the study area schists crop up from beneath the lateritic flats at some places, indicate the geological history of the formation of the study area during Quaternary period. The surface portion is mainly covered by hard crust with pebbles and the pallied layer extends at the base of river bank. According to Paul (2002), the uppermost layer was developed by the deposition of fluvial process in Pleistocene epoch and lowermost portion has been buried in shallow marine condition. Towards the farther north a grey and bluish-grey micaceous schists band with gneissose character has been found. Other important formation is quartzes grits. Frequently, nodular lateritic formations are found, some of which are cemented into a solid mass. This ferrigeneous laterite formation plays the vital role for the geomorphic understanding of Palaeo-coastal landform development of this area.

Most of the parts of this area are covered by deep lateritic soil which is infertile in nature. The process of laterite formation is most vividly manifested only under tropical condition such as found in this area (as found in Fig. 3.3). During this process, neoformation of iron chiefly as ferruginous-quartz concentrates within this form. They accumulate at different depths from the soil surface and form a layer of accumulation which further cemented by new supplies of iron into continuous layers of different thickness. The sharp range of temperature and humidity between summer and winter season play an important feedback on the landform modification over here (Sen et al. 2004).

Lithofacies of Gondwana laterites of Ganganir Danga is briefly illuminated under subhead 'Garhbeta Section' of Chap. 2 of this volume.

3.4 Methodology

The present study supports sedimentary analysis of bedding forms, trace fossils and other morphogenetic elements for the understanding of microstructure formation of Palaeo-coastal landforms. Besides, the textural analysis of soil, microstructure analysis effort has been done by the usages of digital technology like—(i) Micro-photography and (ii) Digital Colour Analysis (DCA) of images as proposed by Dey et al. (2009, 2011). For the purpose of micro-photography and DCA, six thin sections have been prepared in the laboratory. Attempts to investigate this work, have been done using the following methods.

3.4.1 Design for Texture Analysis

After the detail searching of existing literatures and maps from the secondary sources, extensive field surveys have been conducted during 2014–2015. The texture analysis of grains of seven soil samples (in Tables 3.1 and 3.2) collected from the intermediate portion of six thin section sample sites (Fig. 3.4b) have been performed. All the soil samples are collected separately to prevent any type of contamination. As the sample site has been exposed by the processes of slope development under the influence of gullies' advancement and river bank erosion, there is no change of manual deformation of grains' texture during the collection of samples. For the understanding of textural variation of grains, other soil parameters like colour, hardness and organic matter have also been examined. Other structural features from the surroundings of sampling point, for example, wood fossils, presence of conglomerate layers, bedding patterns, etc. have been considered for the understanding of the development process and dominated subsystems of the local area.

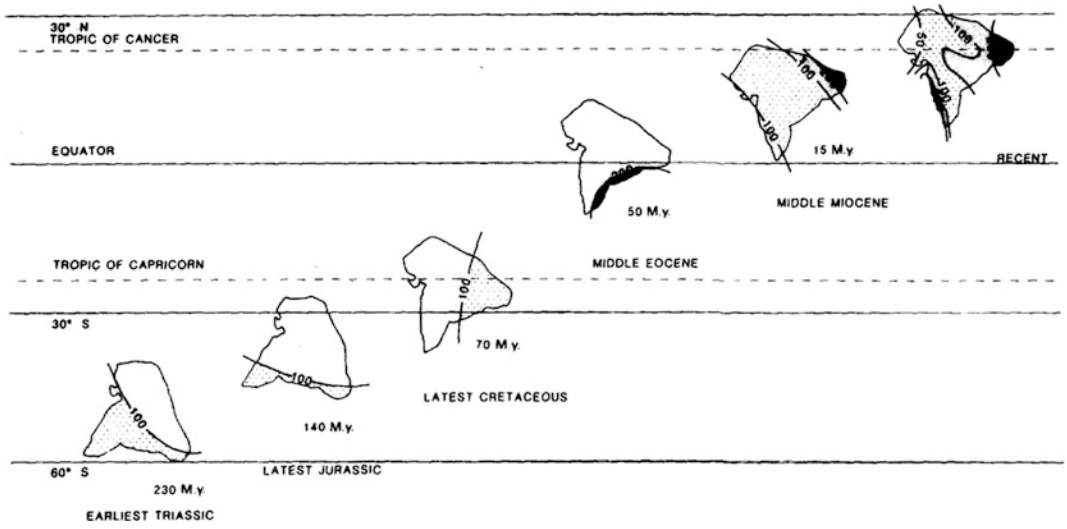

Fig. 3.3 Drifting of Indian Peninsular with the relative value of rainfall through Geological Time Scale (Tardey et al. 1991)

3.4.2 Design for Micro-Photography

High-resolution photographs of micro-geomorphic features and sediment depositions are taken into consideration during the field survey. All the photographs were processed and edited by computation technology in the laboratory for analysing the microstructure and micro-geomorphology. Regarding this, greyscale micro-images (covering 1 mm by 1 mm area on the surface) of deposited materials were prepared by polarized light microscope (Fig. 3.5). Raith et al. (2012) argued that the use of polarized light microscope are best attempts to analyse the solid components in nondestructive way to identify solid substance with a justified level of spatial resolution. Every pixel of this image product is considered here as a basic colour unit. In this work, the resolutions (surface area coverage/pixel) of these images are 50 µm. Two colour sets are taken for explaining ferruginous and non-ferruginous depositions. In Fig. 3.6, the dark colours are indicating ferruginous (low reflectivity or transmission) and light colours are indicating non-ferruginous (siliceous-medium reflectivity and micaceous very high reflectivity, glittering) materials.

3.4.3 Design for Digital Colour Analysis (DCA)

Micro-fabric study of the collected samples has been investigated by using *Digital Colour Analysis* (DCA) method. Finally, for the justification of grains' properties, Origin Lab 9.0 software was used through transmission level variation. Digital imaging of microstructure of the sediment layers is not a new experiment in systematic research of sedimentology. In this advancing study, the present authors attempted microstructural mapping by using reflectance quality of rock-forming minerals using greyscale variation which is influenced by the physical parameters of element. In the present work, an effort of image processing and slicing operation is made for the visualization of different kinds of rock-forming materials based on their brightness (t) and contrast (c) value. Regarding this 'reflectance' or 'transmission' value of each particle is an effect of t and c. In a normal primary colour composition, the good quality of visualization is found in an equal range of t:c ratio (Dey et al. 2011), i.e. 50:50. The final output of microstructure map has a thematic format which is helpful to interpret depositional

Table 3.1 Sediment status (experiment from collected sample in October 2014) at Gangani gully area of Garhbeta, West Bengal

Soil sample No.	Sample collected from (mbs)	Organic matter (%)	Nature	Colour	Texture (in %)		
					Clay	Sand	Silt
I	Surface	0.02	Hard	Reddish	5	15	80
II	0.035	0.03	Hard	Brown	10	30	60
III	1.50	0.03	Soft	Brown	25	75	0
IV	5.00	0.04	Soft	Brownish	30	70	0
V	10.0	0.05	Soft	Yellowish	10	80	10
VI	13.85	0.04	Soft	White	15	15	70
VII	19.0	0.07	Soft	White	10	90	0

Table 3.2 Sediment status (experiment from collected sample in October 2015) at Gangani gully area of Garhbeta, West Bengal

Soil sample No.	Sample collected from (mbs)	Organic matter (%)	Nature	Colour	Texture (in%)		
					Clay	Sand	Silt
I	Surface	0.04	Semi-hard	Reddish	08	02	90
II	0.035	0.05	Hard	Brown	20	30	50
III	1.45	0.05	Soft	Brown	90	10	0
IV	5.15	0.06	Soft	Brownish	95	05	0
V	9.75	0.06	Soft	Yellowish	70	30	0
VI	13.5	0.06	Soft	White	69	27	04
VII	19.15	0.05	Soft	White	77	18	05

pattern easily. In this work, all the samples are classified into nine classes through the natural grouping system of elements' t:c ratio with similar spectral ranges.

3.5 Results and Discussions

The samples were collected from the location where high range of local relief has been observed (about 22.5 m). These samples (considered as 1–6) are mainly composed of sandstone, mudstone, lateritic elements, etc. These components are common in this study area which was influenced by fluvial sediment and Palaeo-delta fan lobes in the monsoonal tropics. Basically, the shape of these elements is angular to subangular beside of some rounded shape rocks forming elements. Here, the authors studied six selected samples, which were collected after the rainy (post-monsoon) season, November in 2014 to know the major mineralogical composition by thin sectioning and its imaging process. The detail scenarios about these samples are discussed in the following section.

Sample-1 The sample collected from the top layer (0.73 cm below from surface or cmbs), is composed of ferrallitic–lateritic. The shapes of these rocks are angular to subangular; though some round shaped rock particles are also found in this sample. The maturity of this sample material is quite high due to the shape of the rock-forming elements. Very small amount of quartz mineral has also been observed in this sample.

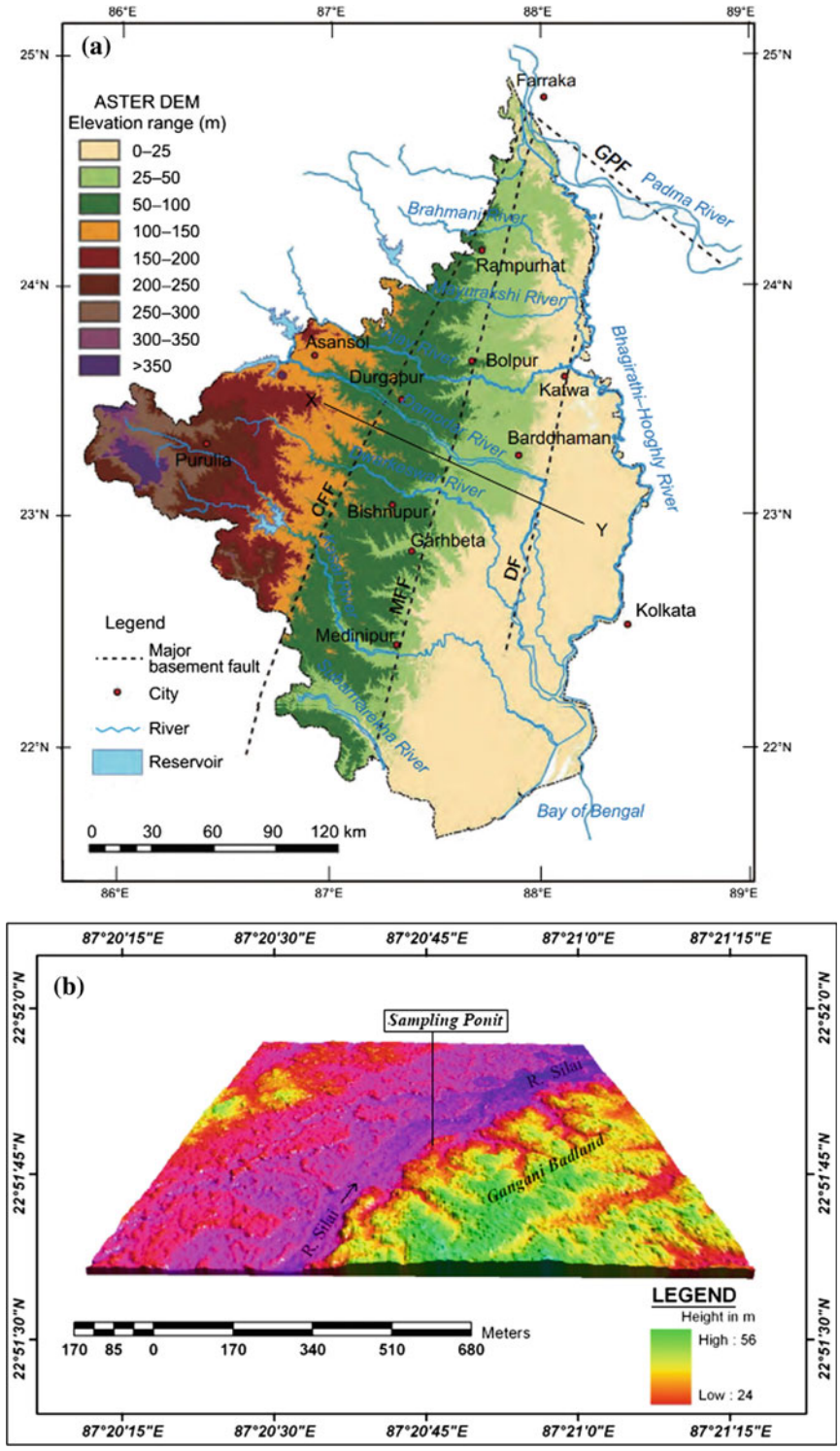

Fig. 3.4 **a** Physiographic and tectonic setting of *Rarh Bengal,* i.e. area in 50–100 m elevation (after Ghosh and Guchhait 2015); **b** DEM of Gangani and its surroundings based on LANDSAT-TM data, 2013 (Prepared by authors)

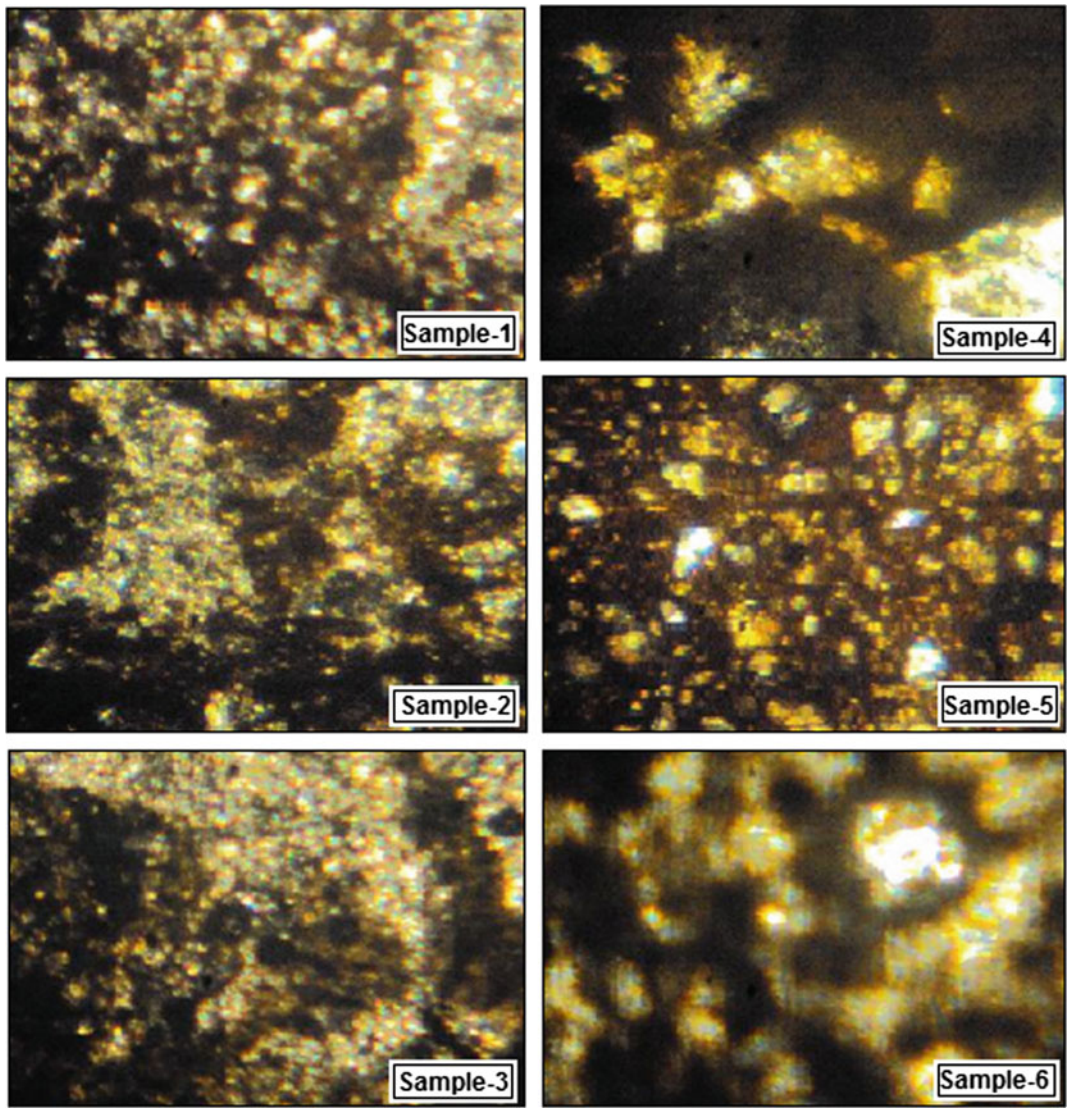

Fig. 3.5 Microscopic views of samples (1–6) in transmitted range and its textural variation in colour visualization

Sample-2 In this slide of sample (taken from 0.5 m below from the surface, i.e. mbs), few basic rock-forming minerals have been identified and these are silica, quartz particle and conglomerate. These are all cemented together and are also characterized by angular to subangular structure. Spots of dark tone indicate the presence of hard elements. The hardness of conglomerate grains' and its cemented properties advocates that its chances of erosion are less than the others particles. Thus, formation of '*duricrust*' has developed in the conglomerate dominated layer from where this sample has been collected.

Sample-3 The sample which is collected from the third layer at sample point (2.75 mbs) is characterized by major composition of sandstone and mudstone and composed by elements of finer grains texture namely silica, clay particles. Very high rate of translocation occurs in this layer due to the prevalence of relatively soft and fine-grained

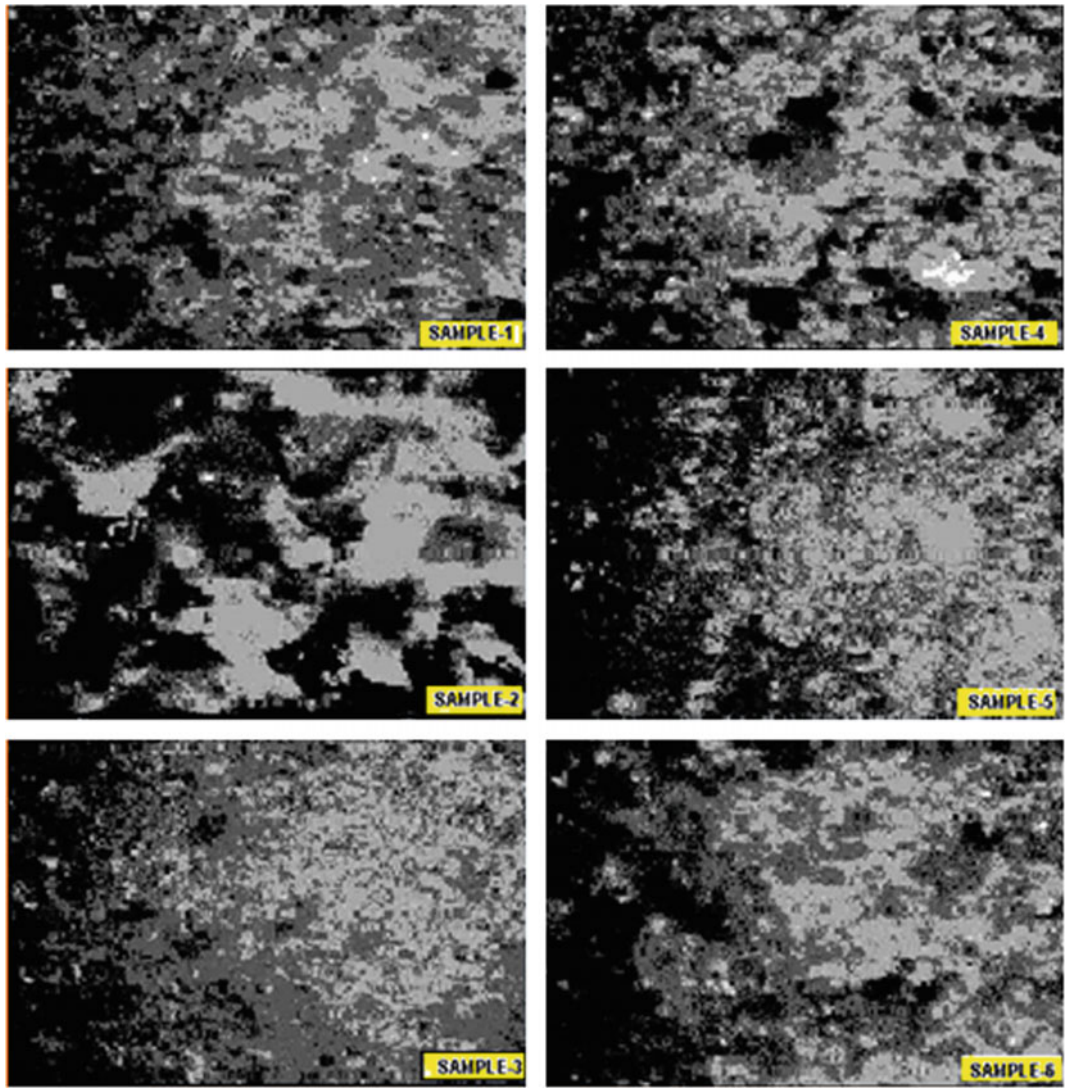

Fig. 3.6 Greyscale image of samples (1–6) in different layers

texture with their low cohesion nature. As a result, the free-faced slope segment turned into eroded and rugged surface, has clearly been noticed during field observation and sample collection.

Sample-4 The fourth sample, acquired from the light colour clay dominated layer at near about 7.75 mbs, is characterized by silica, quartz and iron oxide compact pattern has been observed in our laboratory. The shapes of these elements are angular to subangular and subangular to rounded shape. These samples are less erosive compared to previous one for its structural bonding with ferric components and hardness.

Sample-5 The fifth sample has been collected from 12.55 mbs, is composed of silica and iron oxide mainly. Characteristically, this sample has same properties as found in the sample-3. But the size of the textural particles is more and owing to the presence of ferric elements the nature of erosion is less than sample-3.

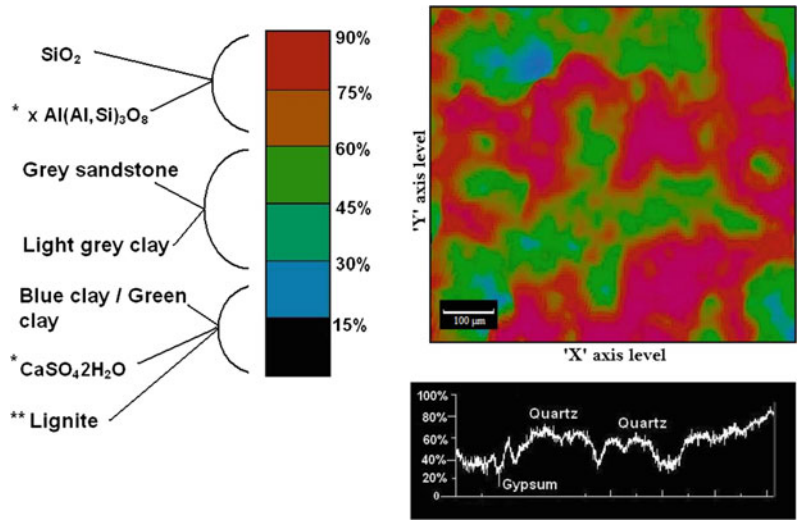

Fig. 3.7 Conceptual framework of visualizing reflectance of different mineral components and their transmission signatures

Sample-6 Minerals composition of this sample (taken from 15.85 mbs) is almost same as like the previous sample, i.e. sample-5. From the laboratory experiment, it has been observed that this sample is mature and contained lot of cemented particles. Clay and silica components are being observed in high percentage with the moderate nature of cohesion. So, the rate of erosion is less predominant in this particular layer of sample.

In Digital Colour Analysis (DCA), components of same chemical bonding and structure cluster displaying the same colour reflectance in the microscope. The colour reflectance and mineralogical combination have been shown in Fig. 3.7. Thus in the visualizing output, same mineralogical component illuminates with the single tone representation. Through this method heavy or light mineral component of sediments is examined for its categorization (Dey et al. 2011).

From the closed inspection at in situ laboratory setup, it is found that a wide range of diverse characteristics have been developed with dissimilar level of mineralogical reflectance. Rounded to angular structure of loosely nodular pisolitic and smother cone-shaped elements of silica components are clearly marked in sample-1 with high transmission level. From the Tables 3.1 and 3.2, it is found that this sample layer is mostly characterized by silica component in both 2014 as well as 2015. For the understanding of the sedimentary characteristics of the study area, sediment samples (considered as I–VII in Tables 3.1 and 3.2) are also collected from seven different layers. Bright (means high value of transmission) reflectance of yellow-reddish tone is responsible for quartz or silica components with ferrogeneous deposition in the sample, whereas darker tone, i.e. less reflectance (imaged by blue tone) depict the presences of blue-clay particles. The pattern of reflectance is found coarser which advocates the sharper surface of components that are also product of recent time morpho-climatic processes. Due to the presence of silica and quartz, the transmission of bright yellow-reddish predominates in the sample-2 with existence of hard components of conglomerates which transmit dark tone. The coarse texture of grains shows that the elements are mainly rounded with different diametres. The blue-clay particles are shorted in one direction having low transmission faces which is responsible for graded bedding formation. On the other hand, round shaped and smooth surface silica and quartz particle are seen in the sample-3 with random location. In this section, most of the grain particles are small in size compared to previous samples. Here, the sample has

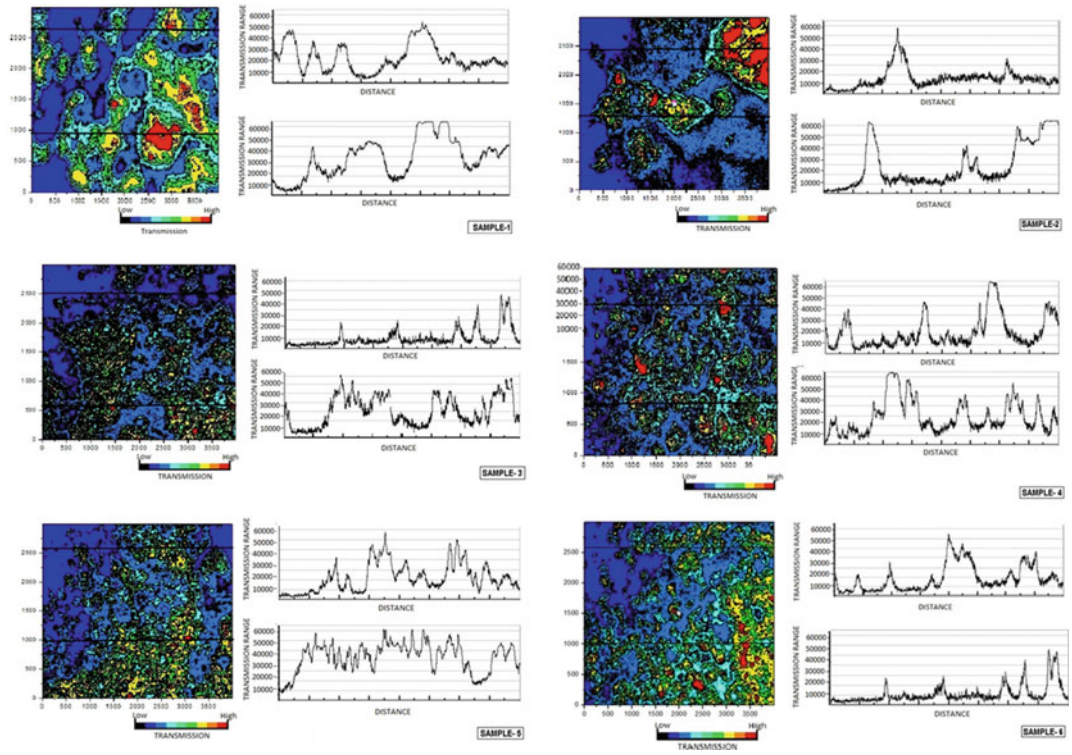

Fig. 3.8 Variability of microscopic output in different samples (1–6) and their transmission ranges

predominance of hard conglomerates particles showing dark and low reflectance of light while blue-clay components are very few. Random position of grains indicates the graded cum flamed structure bedding of deposition, presently the layer of this sample has been found with high experience of erosion process. Fine grain structure, low amount of cohesion and high consistency of similar materials portray the nature of short and extreme depositional events. Although the grain size in sample-4 is found almost same to sample no. 3, they are more shorted in colonies and silica particles are observed few in numbers with isolated position. During field observation, silt dominated cross-bedding (in soil sample VI in 2014), as well as plane bedding, has been clearly noticed which is responsible for the high energy-flow palaeo-coastal environment. Sharper cone with smoother surface finer grains have yellow dominancy transmission, which is recognized as aglitter particles like micaceous deposition for sample-5. In sample-6 the primacy of kaolinite clay (composed with aluminium hydroxide and silicon) along with a quartz component create bright signature, whereas the darker portions are responsible for heavy materials.

All the samples, because of the dominancy of blue transmission range, are mainly composed of blue-clay sediment particles under the marine condition. The microstructure of the tested samples shows that the coarser elements have more complex *micro-fabric pattern* in DCA than the finer, which indicate numbers of rapid fluctuations and alteration of deposition environment within a shorter duration of time in the study area. It is also noticed that the study area contains coarser particle at the upper layer, i.e. on surface portion, whereas bottom layer has finer depositions (Fig. 3.8).

3.6 Conclusion

The depositional patterns of the various materials at the bottom portion of the gully show the significant characteristics of a particular environmental condition rather its geological settings. But there is a sharp relationship between geotectonic controls of the study area and morphological regime. In this chapter, the microstructure observation by digital images shows that variation of process with different intensity is responsible for the characterisation of material components of deposition. So, in a particular environmental setting, this area achieved the domination of siltation process owing to different types of bedding and structures of material accumulation (Fig. 3.9). The presence of ripple marks strongly support that the condition of marine coastal wave dominancy did not prevail for a long time and the nature of inclined bedding of deposition also act as evidences of calm process environment with low to medium intensity of shoreline retreat. Accrual siliceous and micaceous elements at the bottom and silt dominancy at the upper layer indicates the meso-tidal to estuarine environment system (Fig. 3.9f). Whereas, the cross-bedding (Fig. 3.9d, e) strongly supports the alteration of geomorphic processes have occurred in this place in the geological past. The presences of ripples (both symmetrical and asymmetrical) are also strong evidences of tide dominating feedback in this study area. Finally, the primacy of ferrigeneous nodules (pisolitic materials) at the topmost layers shows the climatic extremity with hot and humid condition in Quaternary era.

The Palaeo-environmental condition of coast in this area remains very dynamic through the T-Q (Tertiary to Quaternary) period. Continuous lamina deposition (Fig. 3.9g) of fine to coarse sediment at present bottom portion of gully was placed under calm and quite environmental situation. Some changes of alongshore drift have also occurred, which are reflected by the differential texture of depositions with slightly tilted laminas. As this area is strongly influenced by gravity and magnetic anomalies (Singh et al. 2004; Roy and Chatterjee 2015), the evidence of tectonic movements which are found in the newly exposed gully bottom at this area, might be very important to investigate the change of the environmental consequences. Clear vertical displacement of sediment layer (Fig. 3.10a, d), cross lamina of siliceous depositions (Fig. 3.9d, e) show that tectonic activity took place during the early Quaternary Period. As the study area is situated on basement fault belt along with fractures lineament, this displacement might occur during the secondary effect sub-basement deformation. Another good evidence of alternation of sedimentary layers and crossed laminas, wood fossils' sample, etc. strongly supports that neo-construction of tectonism. Thus, there is ample scope of the further study on dating and micro-geomorphic structures with tectonic advancements to put forward the palaeo-environmental condition of this area.

However, this is also true that microstructure study is still considered as a small part of Structural Geology and has not become popular in the other branches of Geosciences, whereas the rock/sediment characters are studied for many purposes. At the same time, the arena of micro-scale analysis of geomorphic features in Engineering Science, Life Science, Material Science and Physical Sciences; it can be said that the study of rock microstructures has ability to play a pivotal role in earth system science if proper interest is shown by the future generation of researchers.

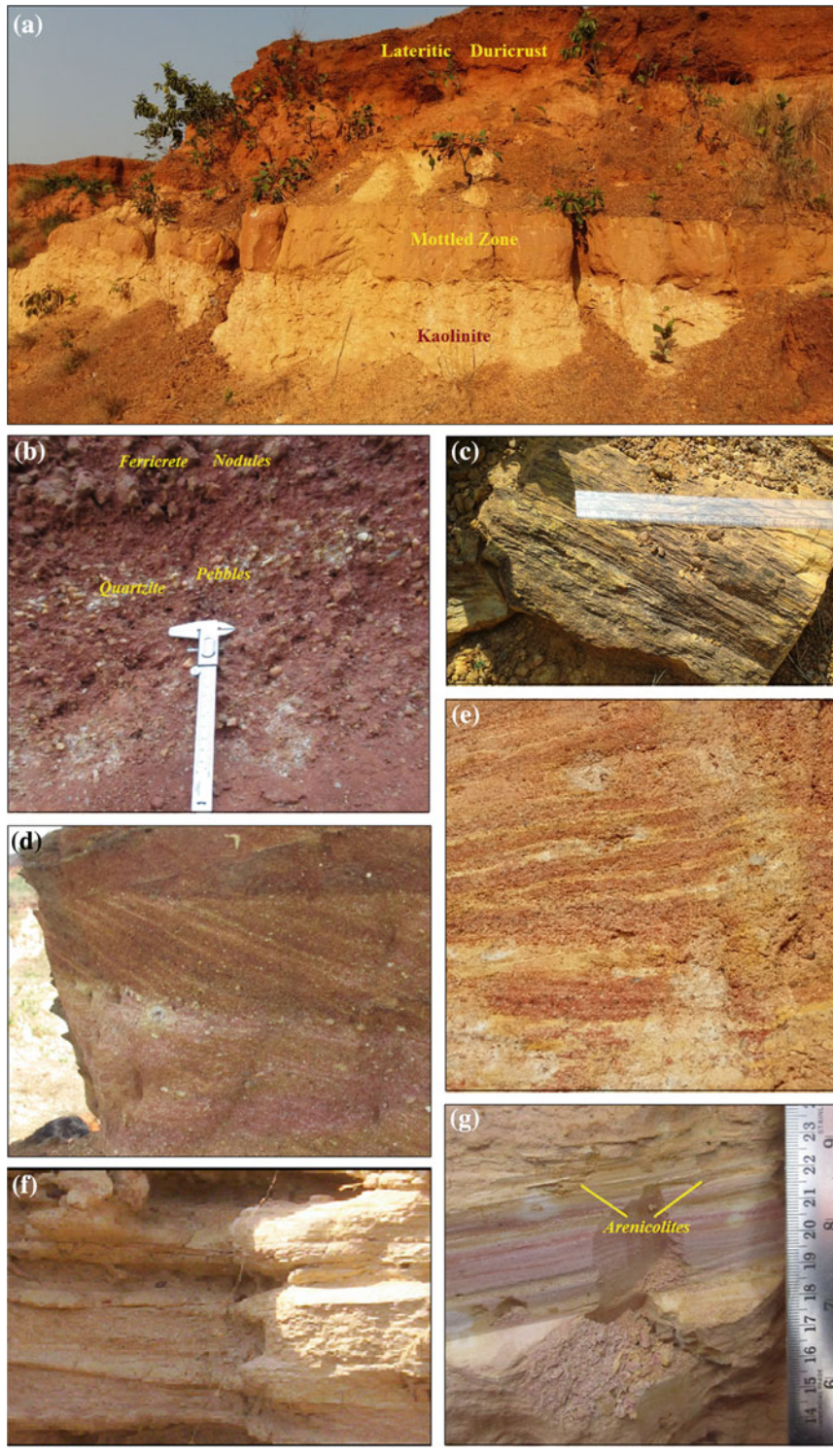

Fig. 3.9 Different types of micro-features found from top to bottom at the study area and its associated imprints: **a** profile of ferrigeneous dominated laterite, **d** stratum of oxide sediment with the presence of ferricrete and quarts, **g** fossil of petrified wood, **b** and **e** crossed lamina of old sediment deposition in different patterns, **f** plane bedding of clay deposition, **c** plane bedding stratum of sediment with *arenicolites*

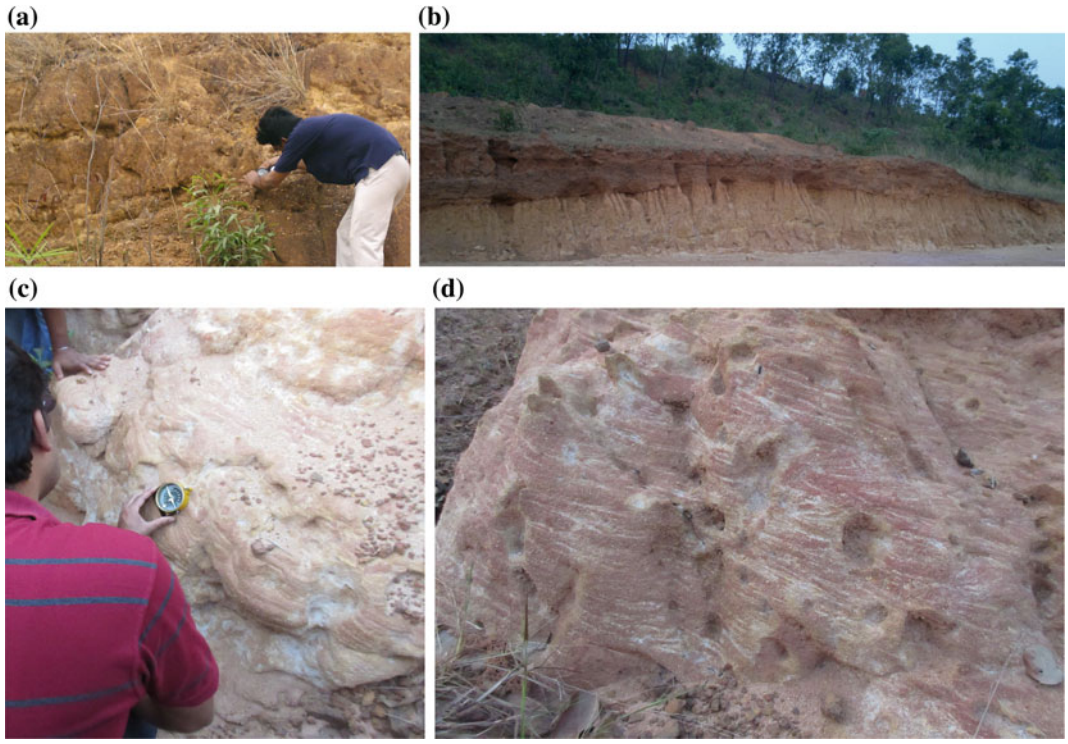

Fig. 3.10 Subsidence of lateritic ground: **a** and **b** subsidence and tilt surface at Gopegarh, southern location of Silai-Kasai interfluves; **c** and **d** inclined laminas of pallid zone at Gangani area

References

Alam M (1989) Geology and depositional history of Cenozoic sediments of the Bengal Basin of Bangladesh. Paleogeography, Paleoclimatology, Paleoecology 69:125–139

Alam M, Alam MM, Curray JR, Chowdhury MLR, Gani MR (2003) An overview of the sedimentary geology of the Bengal Basin in Relation to the regional tectonic framework and basin-fill history. Sedi Geol Elsevier 155:179–208

Allison MA, Khan SR, Goodbred Jr SL, Kuehl SA (2003) Stratigraphic evolution of the late Holocene Ganges–Brahmaputra lower delta plain. Sedi Geol 155:317–342

Bale HD, Schmidt PW (1984) Small-angle X-ray scattering investigation of submicroscopic porosity with fractal properties. Phy Rev Lets 53:596–599

Bera S (1996) Remarks on palaeo-environment from the trace fossils from surface and outcrop tertiary-quaternary sediments of the western part of Bengal Basin, India. J Geo Envt; Vid Uni; Midnapore 01:1–15

Biswas AN, Agarwal A (1992) Tectonic evoluation of the Bengal Foreland Basin since the early Pliocene and its implication on the dvelopment of Bengal Fan. Geol Surv Ind Spl Pub 29:5–19

Bloom AL (2002) Teaching about relict, no-analog landscape. Geomorphology 47:303–311

Brewer R (1976) Fabric and mineral analysis of soils. Krieger, Huntington, New York

Browne A (2011) Coarse coastal deposits as palaeo-environmental archives for storms and tsunamis. Ph.D. theses, Southern Cross University, Lismore, NSW, pp 15–19

Bryant RG, Davidson DA (1996) The use of image analysis in the micromorphological study of old cultivated soils: an evaluation based on a case study from the island of Papa Stour, Shetland. J Arcl Sci 23:811–822

Cashman SM, Baldwin JN, Cashman KV, Swanson K, Crawford R (2007) Microstructures developed by coseismic and aseismic faulting in near-surface sediments, San Andreas Fault. Geology 35:611–614

Chandra PK (1992) Some thoughts on Bengal Fan. Geol Surv Ind Spl Pub 29:1–13

Chiplonkar GW, Badve RM (1969) Trace fossil from the Bagh Beds. J Palaentological Soc India 14:1–20

Cooper MC (1998) The use of digital image analysis in the study of laminated sediments. J Palaeolimnology 19(1):33–40

Chorley RJ, Schumn SA, Sugden DE (1984) Geomorphology, Methuen & Co., 1st edn, Cambridge: 94

Curray JR, Emmel FJ, Moore DG, Raitt RW (1982) Structure, tectonics and geological history of the northeastern Indian Ocean. Edited by Nairn AEM, Stehli FG The Ocean Basins and Margins. The Indian Ocean. Plenum, New York, 6:399–450

De C (2014) Longest crab trackways from the Bay of Bengal Coast, India: their ecological and geotechnical applications; Palaeontologia Electronica, 17 (2,31A): 21

Dey S et al (2009) Some regional indicators of the tertiary-quaternary geodynamics in the palaeocoastal part of the Bengal Basin (India). Russ Geo Geops, Elsevier, Sci Direct 50:884–894

Dey S, Debbarma C, Sarkar P, Marfai MA (2011) Experiment on visualising micro-level surface characters of sediment sections: a methodological approach to reflectance based alternative petrographic image analysis. Ara J Geo. https://doi.org/10.1007/s12517-010-0122-5

Evans P (1964) The tectonic framework of Assam. J Geol Soc London 102:211–245

Frey RW et al (1978) Omphiomorpha: its morphologic, taxonomic and environmental significance. Palaeogeography, Palaeoclimatology Palaeoecology 23:199–229

Ghosh RN, Majumdar S (1981) Neogene-Ouaternary sequence of Kasai basin, West Bengal, India. In: Proceedings of Neogene/Quaternary boundary field conference. India, pp 63–73

Ghosh SC (2002) The Raniganj Coal Basin: an example of an Indian Gondwana rift. Sed Geol, Elsevier 147:155–176

Ghosh S, Guchhait, SK (2015) Characterization and evolution of primary and secondary laterites in northewestern Bengal Basin, West Bengal, India. J Paleog 4(2):203–230

Ghosh S (2013) Evolution and morphology of gully erosion of lateritic lands of Paschim Medinipur, West Bengal. unpublished Ph. D thesis, Dept of Geo & Dist Mang. Tripura University, India (revised in 2014)

Goswami AB (1980) Hydrology of lateritic terrain of Bankura and Medinipur Districts. In: Proceeding of international seminar on laterization process, Trivandrum, India, pp 407–410

Goswami AB (1997) A morphostratigraphic hydrologic and hydrochemical appraisal. Reprint of 8th National symposium on Hydrology, Jadavpur University, Calcutta, Medinipur coastal belt, WB, pp 30–40

Goswami AB (1999) Quaternary mapping concept constraints, aims and approaches with special reference to Bengal Basin. Workshop manual on coastal quaternary. Bengal Basin, Bose inst., Calcutta, 4–9(1):1–20

Hansen JP, Skjeltrop AP (1988) Fractal pore space and rock permeability implications. Phyl Rev 'B' 38:2635–2638

Jacquin CG, Adler PM (1987) Geometry of porous geological structures. Transp Porous Media 2:571–596

Katz AJ, Thompson AH (1985) Fractal sandstone pores: implications for conductivity and pore formation. Phyl Rev 'Letters' 54:1325–1328

Kayal JR (2008) Microearthquake seismology and seismotectonics of South Asia. Capital Publishing Company, New Delhi, pp 225–230

Kuehl SA, Brunskill GJ, Burns K, Fugate D, Kniskern T, Meneghini L, (2004) Nature of sediment dispersal off the Sepik River, Papua New Guinea: preliminary sediment budget and implications for margin processes. Cont Shelf Res 24:2417–2429

Lachniet MS, Larson GJ, Strasser JC, Lawson DE, Evenson EB (1999) Microstructures of glacigenic sediment flow deposits, Matanuska Glacier, Alaska. Edited by Mickelson DM, Attig JW Glacial Processes Past and Present, Geol Soc Ame, Special Paper 337, pp 45–57

Lachniet MS, Larson GJ, Lawson DE, Evenson EB, Alley RB (2001) Microstructures of sediment flow deposits and subglacial sediments: a comparison. Boreas 30:254–262. ISSN 0300-9483

Mamtani M, Mukharji A, Chaudhuri AK (2007) Microstructure in banded iron formation (Gua Mine, India). Geol Mag 144(2):271–287

Menzies J, Maltman AJ (1992) Microstructures in diamictons–Evidence of subglacial bed conditions. Geomorphology 6:27–40

Nandy DR (1994) Earthquake hazard potential of central and south Bengal Basin. Indian J. Earth Sci 21:59–68

Niyogi D (1970) Quaternary geology and geomorphology of Kharagpur-Digha area W.B. guide book for field trips: section of Geol and Geog, 57th session of Ind Sci Cong, Kgp, pp 1–8

Paul AK (2002) Coastal geomorphology and environment. ACB Pub. Kolkata, pp 1–137

Radlinski AP, Hinde AL, Rauch H, Hainbuchner M, Baron M, Mastalerz, M, Ioannidis M, Thiyagarajan P (2005) The microstructure of rocks and small-angle and ultra-small-angle neutron scattering: the coming of age of a new technique. Geop Rese Abs 7:03865. SRef-ID: 1607-7962/gra/EGU05-A-03865

Raith MM, Raase P, Reinhardt J (2012) Guide to thin section microscopy, 2nd edn. RRR, Germany, pp 3–134

Rogers KG (2012) Spatial and temporal sediment distribution from river mouth to remote Depocenters in the Ganga-Brahmaputra Delta, Bangladesh. Unpublished Ph. D thesis, Nashville, Tennessee

Ratcliffe BC, Fagerstrom JA (1980) Invertebrate lebensspuren of Holocene floodplain: their morphology; origin and palaeoecological significance. J Palaeontology 54:226–243

Roy AB, Chatterjee A (2015) Tectonic framework and evolutionary history of the Bengal basin in Indian subcontinent. Cur Sc 109(2):271–280

Rudra K (2014) Changing river courses in the western part of Ganga-Brahmaputra delta. Geomorphol Elsevier 227:87–100

Sarkar A, Sengupta S, McArthur JM, Ravencroft P, Bera MK, Bhushan R, Samanta A, Agrawal S (2009)

Evolution of Ganges–Brahmaputra western delta plain: clues from sedimentology and carbon isotope. Quat Sci Rev 28:2564–2581

Seilacher A (1964) Biogenic sedimentary structure, imbree and newell edited approaches to palaeo-ecology. Wiley, New York, pp 296–361

Sen J, Sen S, Bandyopadhyay S (2004) Geomorphological investigation of Badlands: a case study at Garhbeta, West Medinipur District, West Bengal, India; Edited by Sing S et al Geom and Envt, ACB Pub. Kolkata, pp 204–234

Shah SC, Sastry MVA (1975) Significance of early Permian fauna of Penninsular India. In: Cambell SSW (ed) Gondwana geology. Proceedings of 3rd gondwana symposium, Canada ANU Press, Canberra, pp 393–398

Shamsuddin AHM, Abdullah SKM (1997) Geologic evolution of the Bengal Basin and its implication in hydrocarbon exploration in Bangladesh. Ind J Geol 69 (2):93–21

Singh AP, Kumar N, Singh B (2004) Magmatic underplating beneath the rajmahal traps: gravity signature and derived 3-D configuration. Proc Indian Acad Sci (Earth Planet Sci) 113(4):759–769

Suttner LJ, Dutta PK (1986) Alluvial sandstone composition and palaeoclimate: I. Framework mineralogy. J Sedi Petrol 56(3):329–345

Tardy Y, Kobilsek B, Paquet H (1991) Mineralogical composition of geographical distribution of African and Brazilian peri-Atlantic laterites: the influence of continental drift and tropical paleoclimates during the past 150 million years and implications for India and Australia. J Afn Ear Sci 12(1–2):283–295

Van der Meer JJM (1987) Micromorphology of glacial sediments as a tool in distinguishing genetic varieties of till, Geol Sur Finland, special paper-III, pp 77–89

Van der Meer JJM, Laban C (1990) Micromorphology of some North Sea till samples, a pilot study. J Quat Sci 5:95–101

Van der Meer JJM (1993) Microscopic evidence of subglacial deformation. Quat Sci Rev 12:553–587

Vernon RH (2004) A practical guide to rock microstructure. Cambridge University Press, UK

Wadia DN (1999) Geology of India. Tata–McGgaw-Hill Co. Ltd., New Delhi, pp 130-268

Wong PZ, Howard J, Lin JS (1986) Surface roughening and the fractal nature of rocks. Phys Rev Lett 57:637–640

4 Influence of Faulting on the Extra-Channel Geomorphology of the Ajay-Damodar Interfluve in Lower Ganga Basin

Suvendu Roy

Abstract

The response of extra-channel geomorphology of an alluvial river system to the quaternary faulting has been presented here with remote sensing data and field investigation. In corresponding to the in-stream deformation, extra-stream area is also modified with extended swampy floodplain, unpaired terraces, large alluvial fans, and palaeochannels. Floodplain becomes waterlogged or swampy especially downstream section across the stream fault line. Strike-slip nature of fault helps to shift channel path and developed series of palaeochannels over the neotectonic time frame. Allocation of fault line along the channel makes stream straight, narrow and incised, which helps to generate favourable condition for development of alluvial fan.

4.1 Introduction

The neotectonic activities over the Ajay-Damodar Interfluve (ADI) have significantly influenced the fluvial system of this region, which have been accounted in previous works viz. Roy and Sahu (2015, 2016a, b). However, these publications have focused more on the tectonic sensitivity zoning and have explained in detail about the in-stream morphological alternation rather than extra-stream deformation. Therefore, the present study may call an extended version these research works to identify the extra-stream geomorphological processes and features, which are influenced by neotectonic activities and faulting in particular. The term 'extra-channel geomorphology' defines the different erosional and depositional processes and resulting landforms observed outside the active channel of any fluvial system (Wohl 2014). The prime observed landforms of this category are floodplains, terraces, alluvial fans, deltas, estuaries, palaeochannels and different minor landforms within those fluvial features (Wohl 2014). The amount and behaviour of water and sediment in channel are mainly controlling the fluvial processes and landforms (Leopold et al. 1964). Whilst, the lithological characteristics and faulting as a tectonic activity over a basin area are also significantly control the in-stream and extra-stream geomorphology (Keller and Pinter 1996; Jacques et al. 2014; Roy and Sahu 2015, 2016a). In general, tectonics enters into every aspect of earth science (Schumm et al. 2000). According to Summerfield (1991), active faulting has a dramatic impact on the fluvial system. Anomalies in the channel adjustment due to tectonics can be identified

S. Roy (✉)
Department of Geography, Kalipada Ghosh Tarai Mahavidyalaya, Bagdogra, Darjeeling, West Bengal 734014, India
e-mail: suvenduroy7@gmail.com

B. C. Das et al. (eds.), *Quaternary Geomorphology in India*,
Geography of the Physical Environment, https://doi.org/10.1007/978-3-319-90427-6_4

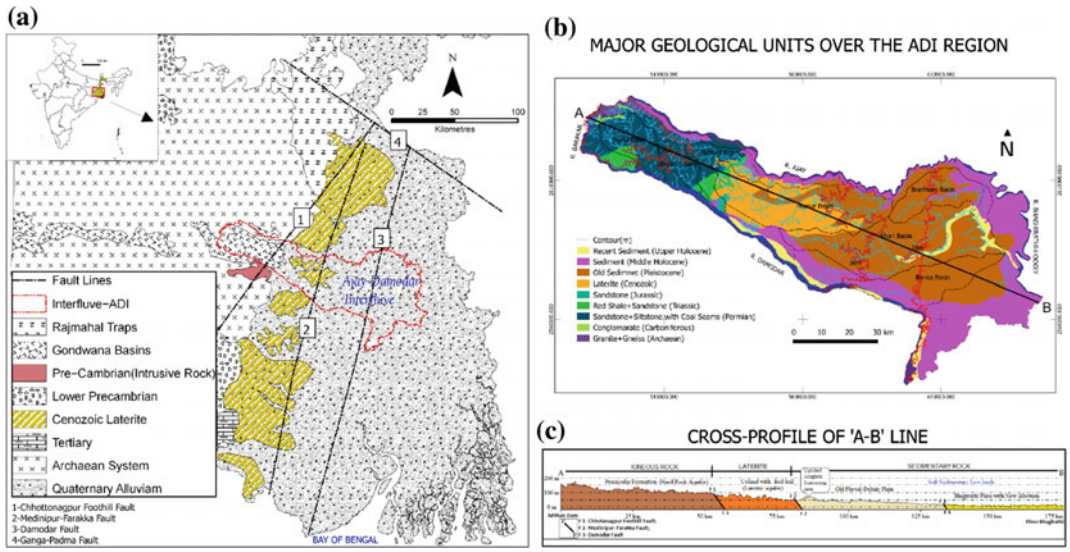

Fig. 4.1 **a** Simplified regional geology with the location of major fault lines (modified after Rao et al. 1999). **b** Geological detail of the Ajay-Damodar Interfluve with all sub-basins (GSI 2001). **c** Topographical cross-section of interfluve showing the geotactic blocks from west to east direction (Roy and Sahu 2016a)

through the local development of braiding or entrenched meandering, uncertain drainage pattern, offset river, creation of sag ponds, swampy areas, accumulation of alluvial fills or fan, river terraces and channel incision (Ollier 1981; Ouchi 1985; Summerfield 1991; Burbank and Anderson 2001; Roy and Sahu 2015, 2016a).

Several studied have investigated the role of tectonics in structural geomorphology, drainage pattern, channel morphology, river courses throughout the world. However, the effect on the extra-channel geomorphology is less focused. The present study focuses on the role of basement faults on the development and modification of floodplain environment, river terraces, alluvial fans and palaeochannels over the alluvial river system of an interfluve. From Quaternary geomorphological perspective, the region is a part of lower Gangetic plain (Bagchi and Mukherjee 1979) and experiencing significant neotectonic sensitivity and corresponding basement fault lines in different direction (Singh et al. 1998; Roy and Sahu 2015, 2016a). The present chapter especially focuses on the development of extra-channel geomorphological features in and around three sub-parallel basement fault zones e.g. Chhotanagpur Foothill Fault (CFF), Medinipur Farakka fault (MFF) and Damodar Fault (DF) (Fig. 4.1a). These faults are divided the ADI region into four geotectonic blocks in the NWW–SEE direction and figured up a step-like landscape along the entire region (Roy and Sahu 2015, 2016a) (Fig. 4.1c).

4.2 Study Area

The distinctive region between the two important rivers (Ajay and Damodar) of north-western Bhagirathi-Hooghly basin has been selected for the study of extra-channel geomorphology formed during the Quaternary period by neotectonic activities. The region has been termed as Ajay-Damodar Interfluve (ADI), which covers about 6174 km^2 area within the Barddhaman District (Purba and Paschim) of West Bengal in Eastern India (Fig. 4.1b). Topographically, the study area is experiencing the characteristics of plateau proper in the west (6%), plateau fringe in the middle (40%), and alluvial plain in the east (~54%) (Bagchi and Mukherjee 1979; Roy and Sahu 2016a), and across the region elevation is

ranging between 10 and 221 m. The north, south, east and west sides of the ADI are defined by Ajay River, Damodar River, Bhagirathi-Hooghly River, and Barakar River and Maithan Dam, respectively (Roy and Sahu 2015).

The geological detail of the ADI is showing that the north-western edge consists with the consolidated formation of high grade metamorphic Archaean Gneiss with a number of minor faults and lineaments (Roy et al. 1988). Surrounding the Asansol and Raniganj, the region is formed by semi-consolidated Gondwana series of rocks, and mainly comprises with thick coal seams and some sedimentary formation of sandstone, grit, conglomerate, shale and ironstone shale. Rest of the region is coming under Quaternary sediments of marine-estuarine-fluviatile origin, within which a significant amount of land is covered by Cenozoic Laterite as the upland in the middle of the region. The thickness of the alluvium increases towards east and southeast (Niyogi 1984).

The river system of this region is basically monsoon-fed and experiencing humid-tropical climatic characteristics with an average annual rainfall of 1400 mm and 26 °C as mean annual temperature (Roy and Sahu 2015). The drainage pattern of this region is dendritic in general, where six sub-basins have been demarked viz. Khari, Brahmani, Kunur, Tumuni, Nonia and Singaran. The typical drainage patterns in different parts these sub-basins have indicating the influence of neotectonic actions and faulting.

4.3 Materials and Methods

Topographical Maps of Survey of India have been used to generate the drainage map of the entire ADI region. The digital elevation map of Kunur Basin has been also prepared from these toposheets using contour values, spot heights, bench marks, triangulation points and relative values of '*r*' to get precision of this lowland region (Roy and Sahu 2016a). Satellite images from Landsat sensors of different time have been used to identify and preparing maps of geomorphic features. The unique band combination (457 of Landsat TM) and Normalized Difference Water Index (NDWI) technique of Gao (1996) have been applied to highlight the waterlogged or swampy land of floodplain areas and to identify the palaeochannels. In addition, intensive field investigation was also an important part of this work to identify and captures the photographs of interested landforms and landscapes.

4.4 Results and Discussion

4.4.1 Floodplain Characteristics

Being a monsoon-fed region of lower Gangetic plain, all major and minor rivers within the ADI region are experiencing frequent flood and characterized with extended floodplain in the downstream sections (Fig. 4.2). According to Fig. 4.2, a vast area of lower Ajay River basin is flooded frequently, whilst, no distinct swampy land has been observed in this region. Whereas, Fig. 4.3 has clarified that the downstream section of Khari River is experienced with a well developed extended swampy land, which is located immediately downstream of Damodar Fault line. The previous investigation of Roy and Sahu (2016a) has also identified this region as a tectonically active zone and fault guided region of ADI. The typical drainage pattern in the lower Khari Basin is the direct result of Damodar Fault line (Roy and Sahu 2015). The swampy land is also an indictable feature in the tectonically active area, as per Summerfield (1991).

In this region, an abrupt change in the flow direction of the lower Khari River near the Bhandardihi and Malamba villages helps to visualize the influence of faulting (Roy and Sahu 2016a) (Fig. 4.3). The east flowing Khari River takes a sudden bend towards the north (∼70°–80°) up to Palason (∼21 km) and thereafter taking a U-turn towards southeast up to the confluence point with the Bhagirathi-Hooghly River (Roy and Sahu 2015). Due to the incised and compressed meander of this section of Khari River, an extended swampy land (∼75.68 km^2) is developed due to frequent flooding (DDMP 2011–12) and also faces the

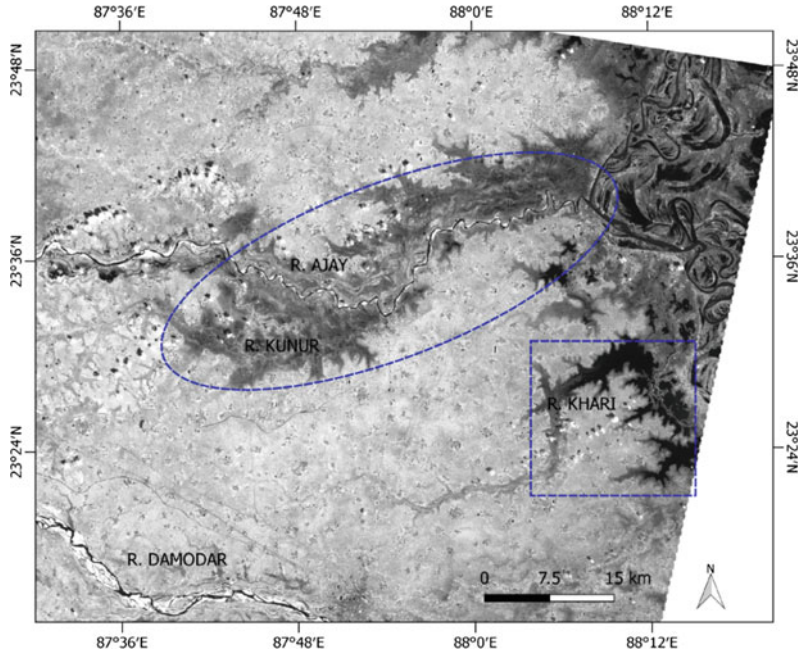

Fig. 4.2 Real-time satellite image of extended flooding condition (in dark colour) around the downstream section of rivers Ajay, Kunur, Khari, and Bhagirathi during a peak flood period of these rivers. *Source* Landsat 7, NIR Band, Date: 7th October, 2000

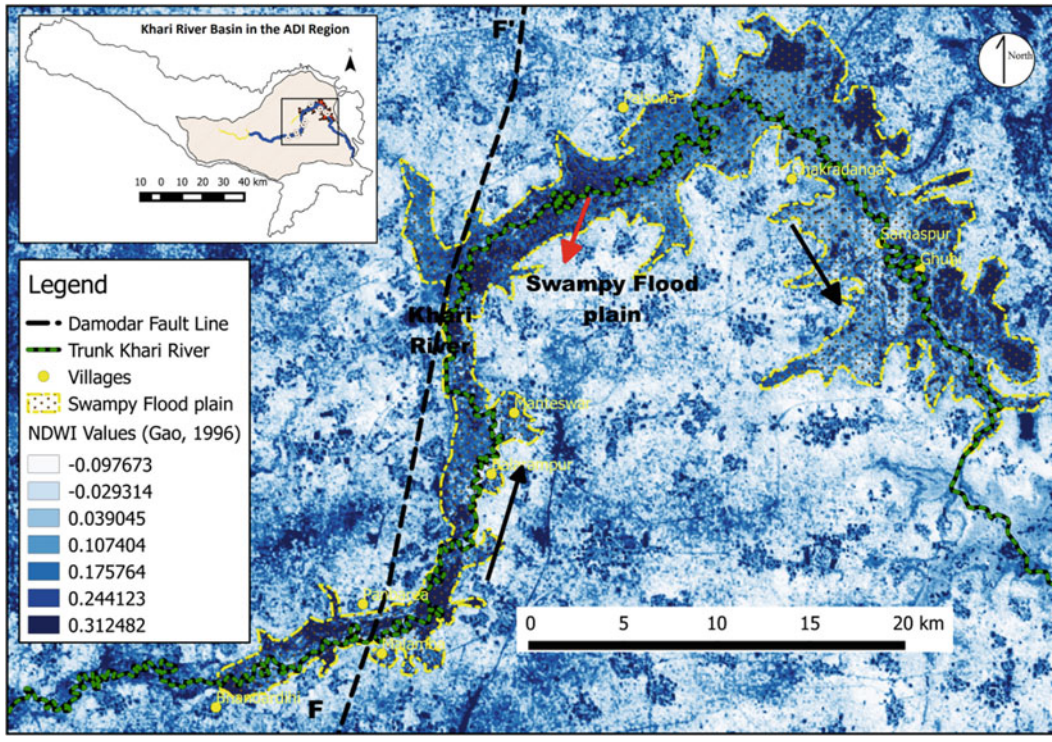

Fig. 4.3 NDWI map is showing the presence of extended swampy land around the fault guided reach of Khari River

severe problem of water-logging during the rainy season, as per the web map of NRSC (http://bhuvan5.nrsc.gov.in/bhuvan/wms) (Roy and Sahu 2015, 2016a).

4.4.2 Formation of River Terraces

Terraces are relict floodplains, sequence of terraces give the evidences of degradational and depositional stages of river's in past. The most important control on the evolution of terraces seems to be structural influences and fluctuations of sea level (Martins et al. 2009). Beside the climatic variability, tectonic upliftment is also an important factor to lead terrace formation (Bridgland 2000; Bridgland et al. 2004).

With an unpaired terrace landscape near Domra (23° 31′ 51″N; 87° 27′ 49″E), Kunur River highlights channel entrenchment due to structural control over there (Roy and Sahu 2015). The close location of Medinipur Farakka Fault (MFF) line might be the major cause of this landscape. Terraces mainly exist in the right bank with progressive inclination towards north-east of the river channel near Domra (Fig. 4.4). The thickness of sediment in terrace is basically control by the tectonics (Larue 2008). The thickness is increased where subsidence occurred. The thickness of T1 is less than one metre, but it is more than one metre for the T3 and T4.

4.4.3 Formation of Alluvial Fans

Alluvial fans are one of the distinctive cone-shaped fluvial depositional features in and around the breakpoint of stream gradient (Goudie 2004). According to Kale and Gupta (2001), the deposition of fans are poorly sorted, angular, coarse sediments and the helps to form a radially diverging system of stream channel, and display a multi-channel (braided) pattern. In addition, tectonically active areas favour the formation of fans and fault guided sedimentary basins provide optimum conditions for their development (Kale and Gupta 2001). As a result, the fault-guided section of lower Damodar River is also experiencing with similar fluvio-geomorphic features (Fig. 4.5a, b). A distinctive alluvial fan has been developed in the downstream of Damodar Basin, where river takes a sharp right angle turn towards south along the Damodar Fault.

This fan is also renowned as 'Damodar Fan-Delta' (Niyogi 1975; Acharyya and Shah 2007) and might also call it palaeo-alluvial fan

Fig. 4.4 Development of unpaired terrace at a reach of Kunur River (after Roy and Sahu 2015)

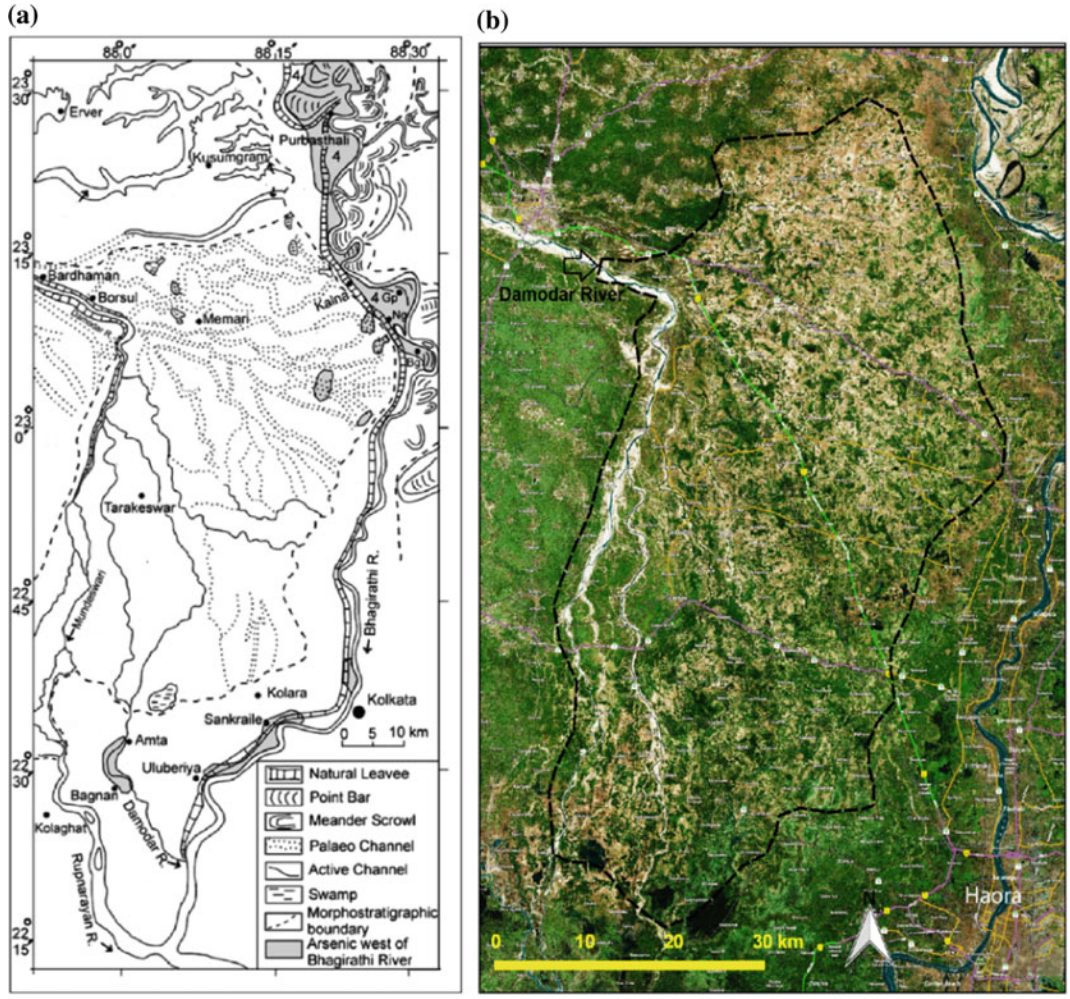

Fig. 4.5 **a**, **b** Extension of alluvial fan in the downstream of Damodar Basin with number of palaeochannels. *Sources* Acharyya and Shah 2007; Google Earth Image

for existence of huge tracks of palaeochannels as a radially diverging outlook (Fig. 4.5a). Acharyya and Shah (2007) reported that as per Mallick and Bagchi (1975), the geomorphic features of this part are revealed by the presence of abandoned channels bifurcating from Damodar, which was the apex of the Damodar fan-delta. In this part new yellowish sediments accumulate and spread radially outward on the plain, and formed a fan-shaped depositional alluvial tract, which is sharply identified from the colour contrast of hybrid satellite images (Fig. 4.5b). Behind the formation of the Damodar Fan-Delta, neotectonism plays a vital role here (Roy and Sahu 2015, 2016a). Due to the Damodar Fault the river takes a sharp right angle turn near Palla and Chanchai villages and runs in southward direction with shrinking width and carrying capacity (Bhattacharyya 2011).

For this distinctive morphological pattern of Damodar near these two villages, river channel is not capable to content huge suspended sediment accumulated flood water (~4011 cumec; Ghosh and Guchhait 2014) and spill-over on the eastern flood plain and temporally increased the thickness of alluvium deposits and expanded area of Damodar Fan-Delta. Back swamp, levee, mature point bar and palaeochannels are also

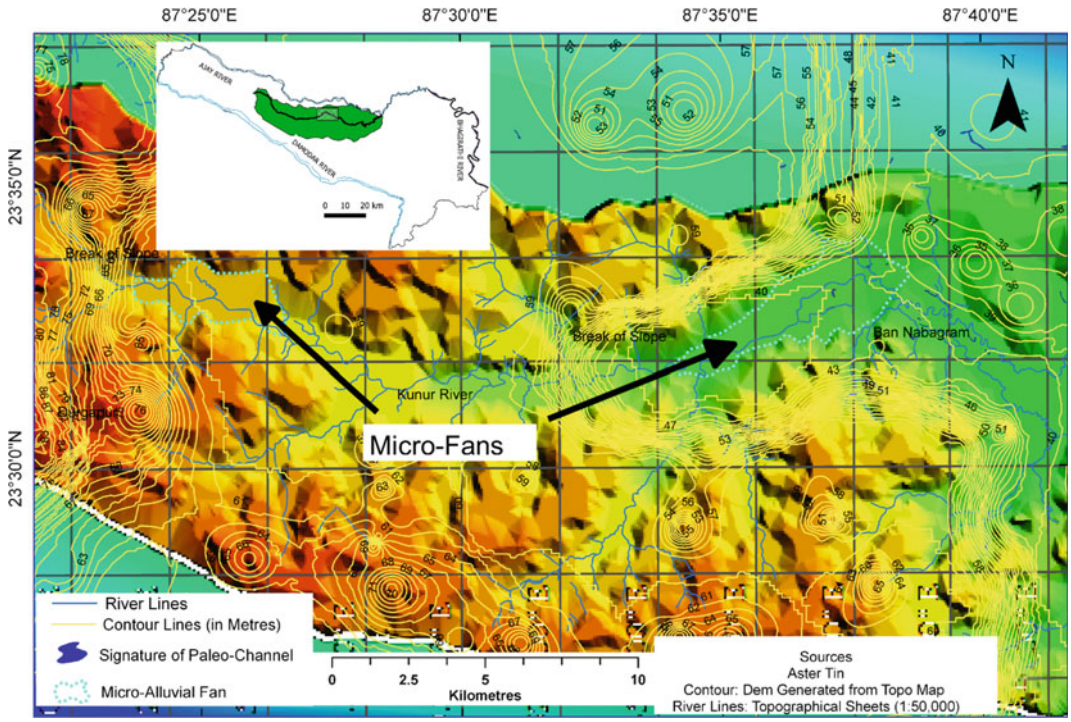

Fig. 4.6 Identified micro-fans of Kunur River, which are located immediately after the fault scarps (after Roy and Sahu 2015)

developed in this surface. In back swamp areas the upper clayey silt layer is about 4.5–6 m thick, whereas, in palaeochannels and point bar area, it is comparatively thin with thickness of about 2 m. The lower sandy layer at places contains pebbles and gravels of quartz and feldspar (Bhattacharya and Dhar 2005). According to Acharyya and Shah (2007, 2010) since middle of the eighteenth century, the Damodar River was flowing east to meet the Bhagirathi River, but after that track of the Damodar rotated and observed 128 km shifting of its mouth. This huge shifting of river track within a short temporal gap suggested the active tectonic influence at present in that region.

Some other micro-level alluvial fans are also identified in the ADI region. Within the Kunur River Basin, two micro-fans have been demarked in the tin map of this basin (Fig. 4.6) and the fundamental fact is that these two fans were developed just immediate downstream of the two knick points in the longitudinal channel slope of the Kunur River. This two knick points are the result of two active fault lines (Chhotanagpur Foot Hill fault and Medinipur Farakka Fault) passing across the basin.

4.4.4 Pattern of Palaeochannels

Typical shifting pattern of river also reveals the presence of tectonic influence on any region. As a result, a series of palaeochannel has been developed there and helps to understand the shifting pattern on Ancient River. Aerial images could help to identify them and several researches are also using satellite images to investigate about palaeochannels. In the study area, the satellite image shows a series of palaeochannel is the presence in the interfluve of Ajay and Kunur Rivers, which are diffused from the Ajay River just immediate downstream of the Medinipur Farakka Fault (MFF) line (Roy and Sahu 2016b) (Fig. 4.7). In respect to the present path of Ajay River, the shifting tendency is towards north-east in association with the direction of fault line and

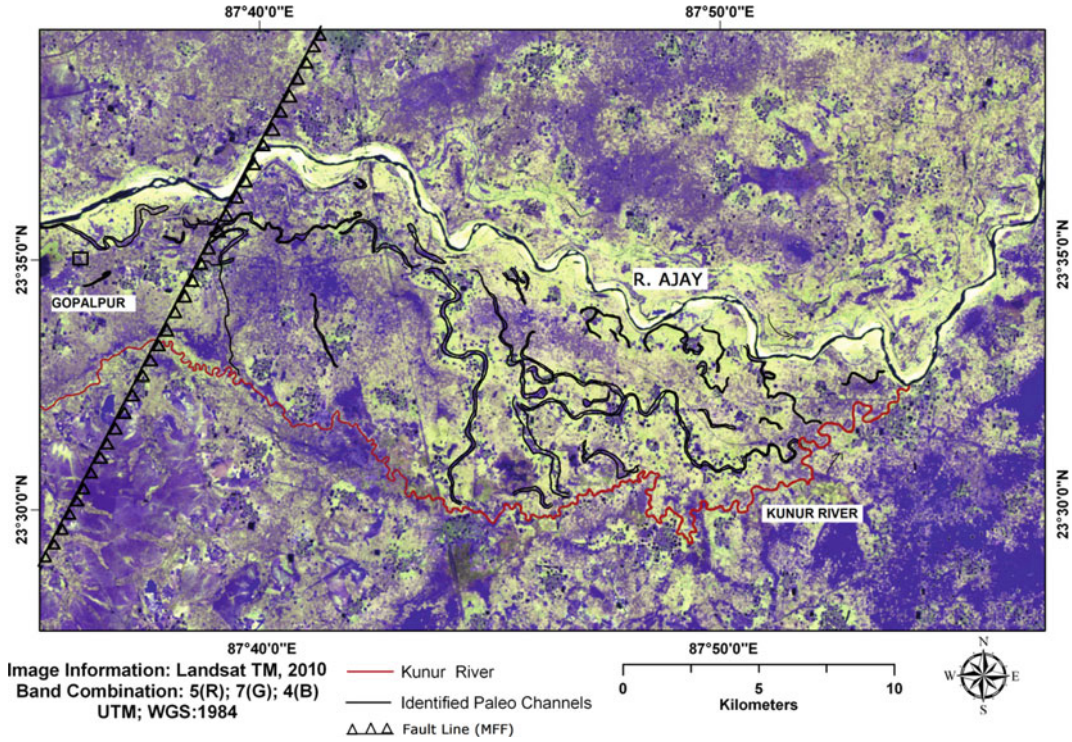

Fig. 4.7 Diffusion of palaeochannels of Ajay River below the Medinipur Farakka Fault line (after Roy and Sahu 2016b)

strike-slip nature of MFF might because of such scenario (Roy and Sahu 2015, 2016b).

4.5 Conclusion

Previous studies have claimed that the lower Gangetic Bengal is tectonically active with numbers of basement faults during the Quaternary period and fluvial geomorphology is directly influenced by it. Present study also successfully shows that those reactivated basement faults are also directly associated with the existing landscape and landforms developed over the extra-channel areas of ADI region. Remote sensing analysis and filed investigation have been helped to identify such features. Due to the presence of fault line, the width of active channel is reduced with deep channel incision, while the lateral width of floodplain has been increased in the downstream section of fault line. The extended swampy land and well developed alluvial fan immediate below the fault area are also revealed the influence of fault line on frequent flooding around the fault-guided stream reach. Role of structural fault on the development of palaeochannels has been also cleared from the palaeochannel maps of Damodar Fan and Ajay Kunur Interfluve. Alluvial terraces in the different section of studied streams are also influenced by nearby fault lines.

Geophysical controls on fluvial forms and processes of Kunur River and Khari River are illuminated more brightly in Chaps. 5 and 6 of this volume respectively.

References

Acharyya SK, Shah BA (2007) Arsenic-contaminated groundwater from parts of damodar Fan-Delta and west of Bhagirathi river, West Bengal, India: influence of fluvial geomorphology and quaternary Morphostratigraphy. Environ Geol 52: 489e501

Acharyya SK, Shah BA (2010) Groundwater arsenic pollution affecting deltaic West Bengal, India. Curr Sci 99(12):1787–1794

Bagchi K, Mukherjee KN (1979) Diagnostic survey of rarh Bengal, Part–I, morphology, drainage and flood: 1978. Department of Geography, University of Calcutta, Calcutta

Bhattacharya AK, Dhar N (2005) A report geo-environmental appraisal in Barddhaman urban agglomeration area and its environment for sustainable developmental activities. Geological Survey of India, Kolkata Eastern Region, pp 1–43

Bhattacharyya K (2011) The lower Damodar River, India (understanding the human role in changing fluvial environment). Advances in Asian human-environmental research. Springer, New York

Bridgland DR (2000) The characteristics variation and likely origin of the Buchan Ridge Gravel. In: Merrit JW, Connell ER, Bridgland DR (eds) The Quaternary of the Banffshire coast and Buchan. Quarternary Research Association, pp 139–143

Bridgland DR, Maddy D, Bates M (2004) River terrace sequences: templates for Quaternary geochronology and marine-terrestrial correlation. J Quat Sci 19:203–218

Burbank DW, Anderson RS (2001) Tectonic Geomorphology. Blackwell Scientific, Oxford

DDMP (2011–12) District disaster management plan. Burdwan District, Govt. of West Bengal, India

Gao BC (1996) NDWI: the normalized difference water index for remote sensing of vegetation liquid water from space. Remote Sens Environ 58:257–266

Geological Survey of India (GSI) (2001) District resource map: Barddhaman. Govt. of India, Kolkata

Ghosh S, Guchhait SK (2014) Analyzing fluvial hydrological estimates and flood geomorphology from channel dimensions using ASTER DEM, GIS and statistics in the controlled Damodar river, India. J Geomatics 8(2):232–235

Goudie AS (2004) Encyclopedia of geomorphology. Routeledge, London

Jacques PD, Salvador ED, Machado R, Grohmann CH, Nummer AR (2014) Application of morphometry in neotectonic studies at the eastern edge of the Paraná Basin, Santa Catarina State, Brazil. Geomorphology 213:13–23. https://doi.org/10.1016/j.geomorph.2013.12.037

Kale VS, Gupta A (2001) Introduction to geomorphology. Orient Longman Ltd., Calcutta

Keller EA, Pinter N (1996) Active tectonics: earthquakes, uplift and landscape. Prentice Hall, New Jersey

Larue J-P (2008) Effects of tectonics and lithology on long profiles of 16 rivers of the southern Central Massif border between the Aude and the Orb (France). Geomorphology 93(3–4):343–367

Leopold LB, Wolman MG, Miller JP (1964) Fluvial processes in geomorphology. W.H. Freeman, San Francisco

Mallick S, Bagchi TC (1975) Morphology and genesis of burried Sand of Mogra Pandua area, West Bengal India. Recent researches in geology. Hindustan Publisher Corporation, Delhi

Martins AA, Cunha PP, Huot S, Murray AS, Buylaert JP (2009) Geomorphological correlation of the tectonically displaced Tejo River terraces (Gavia˜o–Chamusca area, central Portugal) supported by luminescence dating. Quat Int 199:75–91

Niyogi D (1975) Quaternary geology of the coastal plain in West Bengal and Orissa. Indian J Earth Sci 2:51–61

Niyogi D (1984) Water resources of the Ajay basin: a geographical-hydrological Study. Ph.D. Thesis, Department of Geography, University of Calcutta

Ollier C (1981) Tectonics and landforms. Longman, London

Ouchi S (1985) Response of alluvial rivers to slow active tectonics movement. Geol Soc Am Bull 96:504–515

Rao IBP, Murthy PRK, Rao K, Murty P, Madhava Rao N, Kaila KL (1999) Structure of the lower crust revealed by one- and two-dimensional modeling of wide-angle reflections-West Bengal Basin, India. Pure appl Geophys 156:701–718

Roy RK, Ghosh BK, Ghosh DK (1988) Final report on quaternary geology and geomorphology of Ajay Basin, Bardhaman and Birbhum Districts, West Bengal with special reference to Geo-environmental studies. Published Report, Geological Survey of India, Eastern Region, Calcutta

Roy S, Sahu AS (2015) Quaternary tectonic control on channel morphology over sedimentary lowland: a case study in the Ajay-Damodar interfluve of Eastern India. Geosci Front 6(6):927–946. https://doi.org/10.1016/j.gsf.2015.04.01

Roy S, Sahu AS (2016a) Morphotectonic map generation using geo-informatics technology: case study over the Ajay-Damodar interfluve, West Bengal, India. Arab J Geosci. 9:183. https://doi.org/10.1007/s12517-015-2247-z

Roy S, Sahu AS (2016b) Palaeo-path investigation of the lower Ajay River (India) using archaeological evidence and applied remote sensing. Geocarto Int 31 (9):966–984. https://doi.org/10.1080/10106049.2015.1094526

Schumm SA, Dumont JF, Holbrook JM (2000) Active tectonics and alluvial rivers. Cambridge University Press, New York

Singh LP, Parkash B, Singhvi AK (1998) Evolution of the lower gangetic plain landforms and soils in West Bengal, India. CATENA 33:75–104

Summerfield MA (1991) Global geomorphology. Prentice Hall, England

Wohl E (2014) Rivers in the landscape: science and management. Wiley Blackwell, Oxford

5 Geophysical Control on the Channel Pattern Adjustment in the Kunur River Basin of Western Part of Lower Ganga Basin

Suvendu Roy and Subhankar Bera

Abstract

Surface gravity anomaly is important to know the underlying rock density and basement structure since they are playing dominant role in the channel pattern adjustment. Over the Western Bengal Basin (WBB), EW-tending and NS-tending garbens are actively controlled the gravity anomaly and adjacent variation in basement structure and lithology. The streamlines of Kunur River Basin (KRB) and rivers in surrounding are sharply controlled by the variation in underlying rock density, alignment of the lineaments and subsurface faults. Medinipur–Farakka Fault (MFF) and Garhmayna–Khandaghosh Fault (GKF) lines make prominent deformation in longitudinal profile, planform index, channel geometry and other fluvial forms of Kunur River. High Transverse Topographic Symmetry Factor (TTSF) values (>0.40) around the fault lines and high Drainage Basin Asymmetry (AF-index) values (64.40) also positively reveal the neotectonic sensitivity over the basin.

Keywords

Channel pattern · Bouguer gravity anomaly MFF line · TTSF · AF-Index · Neotectonic

5.1 Introduction

The term 'gravity' deals with the force that attracts a body towards the centre of the Earth (Mallick et al. 1999, 2012). The departure (anomalies) of uniform gravitational field is expressing the anomalous of density distribution over the outer part of Earth's surface, i.e. lithosphere (VijayaRao et al. 2006; Mandal et al. 2015). Bouguer gravity anomalies alternatively may call density anomalies below the Earth's surface (Marotta et al. 2006). The gravity directly controls the rate of mass wasting and related erosional processes. Among the obtained gravity data from geophysical estimations, Bouguer gravity data have appeared to be more accurate and aid to maintain the standard in geologic interpretation of land (USGS 1997). According to Verma (1985), an area underlying by masses with relatively higher

S. Roy (✉)
Department of Geography, Kalipada Ghosh Tarai Mahavidyalaya, Bagdogra, Darjeeling, West Bengal 734014, India
e-mail: suvenduroy7@gmail.com

S. Bera
Department of Geography, University of Kalyani, Kalyani, Nadia, West Bengal 741235, India
e-mail: subhankar.geo@gmail.com

B. C. Das et al. (eds.), *Quaternary Geomorphology in India*,
Geography of the Physical Environment, https://doi.org/10.1007/978-3-319-90427-6_5

density, Bouguer anomalies are reflected by higher gravity and vice versa. Bouguer anomalies are negative over the elevated region and it shows an inverse relationship with topography (Mandal et al. 2015). The most important unknown source of gravitational anomaly is the effect of the irregular underground distribution of different density rocks (USGS 1997). According to McKenzie (1977), if the gravity anomaly is well defined, the excess or missing mass can be computed directly from the gravity data. The exercise would be helpful for river science also to interpret the asymmetry in channel planform due to underlying litho-stratigraphy.

The Bengal Basin (BB) is always a complex region for geoscientists, in terms of its typical underlying structural geology, stratigraphy and alignment of surface river lines (Bagchi and Mukherjee 1979; Singh et al. 1998). Although the explanation of underlying geology is satisfactory (Alam et al. 2003; Goodbred et al. 2003; Mukherjee et al. 2009; Mallick and Mukhopadhyay 2011; Nath et al. 2014), the scientific explanation of typical arrangement of river lines are still not clear properly. Bhattasali (1941), Bhattacharya (1959), Banerjee and Chakraborty (1983), Bandyopadhyay (1996), Bandyopadhyay and Bandyopadhyay (1996), Bandyopadhyay et al. (2014, 2015) and Rudra (1987, 2010, 2014) all have explained well about the temporal shifting history of some rivers using historical maps and recodes, field observation and remote sensing images. However, introduction of the geophysical causes behind these channel shifting can increase the level of precision in the reconstruction palaeo-fluvio landscape. The present work has focused on the role of such geophysical parameters (gravity anomaly, active tectonic) on channel pattern adjustment over a small catchment (i.e. Kunur River Basin) in Lower Gangetic Plain.

5.2 Methods and Materials

5.2.1 Study Site

A 30 km long channel reach has been selected for the special focus within the Kunur River Basin (KRB) (Fig. 5.1). KRB is a major right bank tributary basin of the Ajay River and covers about 916.40 km^2 of area. The river originates near Jhanjira village of Ukhra Gram Panchayat on the western upland of the Barddhaman District at an altitude of 125 m. It runs for a distance of 114 km towards east direction. The elevation ranges from 20 to 131 m throughout the basin coverage. Over the region, annual average rainfall observed is 1380 mm and mean temperature is 25.8 °C during last 100 years (IMD 2014). The basin may discharge $\sim$200 m^3/s of water during its peak flood season (Roy and Mistri 2013). Average width of the study reached is $\sim$30 m.

Geologically, the entire reach is flowing over the Quaternary series of formation, where the Sijua formation (late Pleistocene to middle Holocene) has covered the downstream area and represents the oldest alluvial formation covering the floodplain of Kunur River (Bhattacharya and Dhar 2005). The exposed surface layers of this formation comprise a top soil of brown silty loam underlain by compact sticky clay in khaki or grey colour with greenish tinge impregnated with caliches nodules varying in size from 0.5 to 3.0 cm (Roy and Banerjee 1990). The reach has been selected for its typical pattern of channel planform in corresponding to the abrupt change in the Bouguer Gravity values (Fig. 5.1).

5.2.2 Geophysical and Geomorphological Data Acquisition

The present study has followed an integrated approach based on fluvial geomorphology, morphotectonics, geophysical parameters and digital topography, i.e. ASTER GDEM (30 m), multispectral imagery (Landsat 8and LISS IV) and field mapping. The regional gravity anomaly reading (Bouguer Gravity Anomaly) has been mapped by the National Geophysical Research Institute or NGRI (1978), Hyderabad, India composed with the interval of 5 mGal isolines. The map has been used here after converting into raster database using Q-GIS to extract gravity

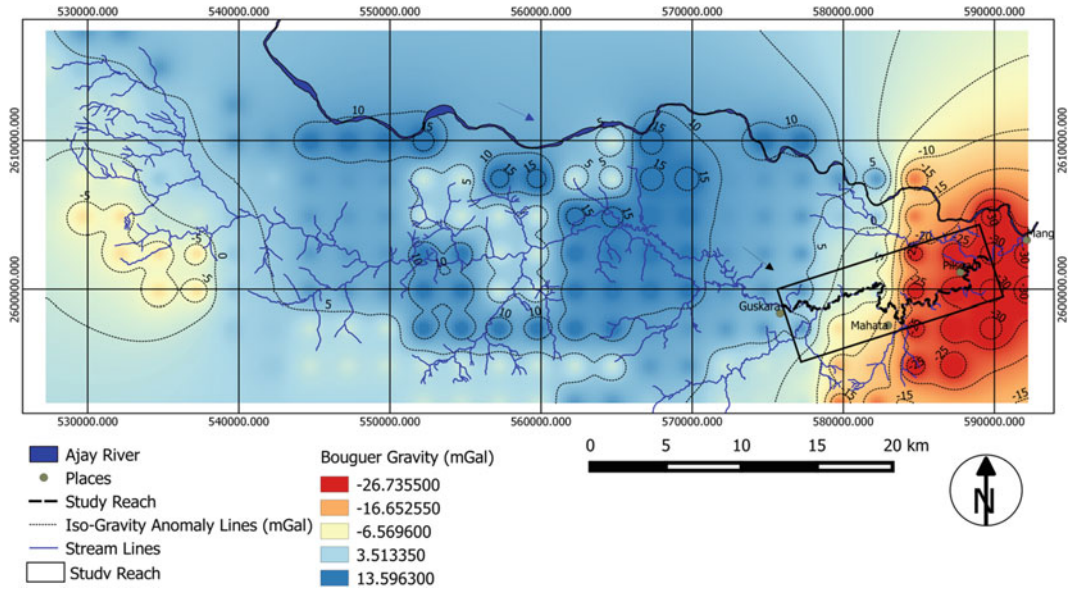

Fig. 5.1 Location map of the study reach (in Black Rectangle Box) within the Kunur River Basin. The background corresponds to the Bouguer Gravity Anomaly Map including gravity contours at 5 mGal interval

anomalies in the study. The basin boundary and river lines have been delineated using topographical maps of Survey of India (SoI) (73 M/6, M/7, M/10, M/11, M/14 and M/15 of 1:50,000) and LISS IV images. The geomorphological features related to morphometric indices have been digitized from topographical maps. In addition, online mapping using 'Plug-in layer tool in Q-GIS software' with 'Google Satellite Image' becomes a useful technique in extraction and upgrading of linear features related to relief and linear geomorphology. Online enable mapping technique has been followed using the 'Layer from WM(T)S server' mapping tools in Q-GIS to get the arrangement of lineaments from the recently updated web enable data (http://bhuvan5.nrsc.gov.in/bhuvan/wms) in thematic map services of National Remote Sensing Centre (NRSC), India. The lithological condition has been investigated through borehole data collected from secondary sources.

5.2.3 Morphotectonic Indices

Transverse Topographic Symmetry Factor (TTSF or T-index) and Drainage Basin Asymmetry Factor (AF-index) have been applied to the Kunur River Basin (KRB) to explain the neotectonic influence on the deformation of channel planform (Cox 1994; Jacques et al. 2014; Kale et al. 2014) and the assessment of the stream asymmetry, and identification of tilted drainage basin (Siddiqui 2014; Jacques et al. 2014). TTSF values range from 0 to 1. The value near to '0' means symmetric basin and value more than or far from '0' indicates asymmetric basin (Cox 1994). T-index has been computed for 35 reaches of the trunk Kunur River with equal interval of 2 km by using Eq. (5.1).

$$\mathrm{TTSF} = D_a/D_d, \tag{5.1}$$

where D_a is the distance from the longest channel to the basin midline (measured perpendicular to a

straight line segment fit to the channel) and D_d is the distance from the basin boundary.

AF-index evaluates the active tectonic tilting within the drainage basin and to determine the direction of tilting (Cox 1994; Sarma et al. 2013; Siddiqui 2014; Kale et al. 2014). It is suitable for large extended area and is sensitive to tilting perpendicular to the direction of the trunk stream (Keller and Pinter 1996). AF for the Kunur basin is defined by the Eq. (5.2).

$$\mathrm{AF} = A_r/A_t, \tag{5.2}$$

where A_r is the area of the basin to the right of the trunk stream, A_t is the total area of the drainage basin. AF-index value close to 50 indicates none or a slight tilting and value above or below 50 suggests a significant tilting of the drainage basin.

5.3 Result

5.3.1 Adjustment of Channel Attributes with the Fall of Bouguer Gravity

The Bouguer gravity anomaly varies from −35 to +15 mGal over the KRB (Fig. 5.1). The minimum gravity (−35 mGal) has been observed over the extreme eastern part of the basin with a concentrated elliptical depression near the confluence zone with Ajay River. The downstream reach of the Kunur River faces a certain fall in Bouguer gravity values, i.e. within ten kilometres gravity has fallen from −30 to +10 mGal. The result implies a huge change in the underlying rock density and mass. To adjust such geophysical condition, the channel of Kunur River has also changed its geometry (Fig. 5.2). As per the Fig. 5.2, the certain fall in the gravity value starts near the distance of 10,000 m and continue up to 20,000 m, where the distance value indicates a cumulative increase towards the confluence of KRB. Significant fluctuation in slope value has been observed within this definite zone (10,000–20,000 m), which varies from ∼1.2° to ∼3.6°. The increasing slope may also correspondingly increase the flow velocity and Kunur River follows a straight pattern with low sinuosity index (<1.1). However, the value of sinuosity index has rapidly increased (>1.35) just immediately after the definite zone of gravity anomaly (10,000–20,000 m). However, no typical change has been observed in the river bank elevation, although this map may be affected by coarse resolution digital elevation data (ASTER, 30 m). Nevertheless, the longitudinal profile of entire Kunur River (∼114-km) shows two certain falls in the bed elevation (i.e. Knick Point) at ∼98 and ∼74 km, respectively from the confluence point (Fig. 5.3). Near the second knick point, i.e. ∼74 km from confluence, the Kunur River faces about 5–7 m fall in bed elevation and bankfull channel width (Fig. 5.3).

For further knowledge of geophysical control on channel pattern adjustment at different sub-basin levels, one may go through Chap. 6 of this present volume with title ‘imprints of neotectonism on the evolutionary record along the course of Khari river in Damodar fan delta of lower Ganga basin’.

5.3.2 Lithological Adjustment with the Changing Pattern of Bouguer Gravity

The panel diagram using 12 boreholes data has fairly defined the lithological adjustment of the region with the spatial variation in Bouguer gravity and associated distribution of underlying rock density and thickness (Fig. 5.4a). In reference to the higher positive anomaly in the western part (near Kuldihi, Daradanga borehole point), the lithology consists of high-density rock, e.g. sandstone, calcareous shale and limestone with less amount of granular materials

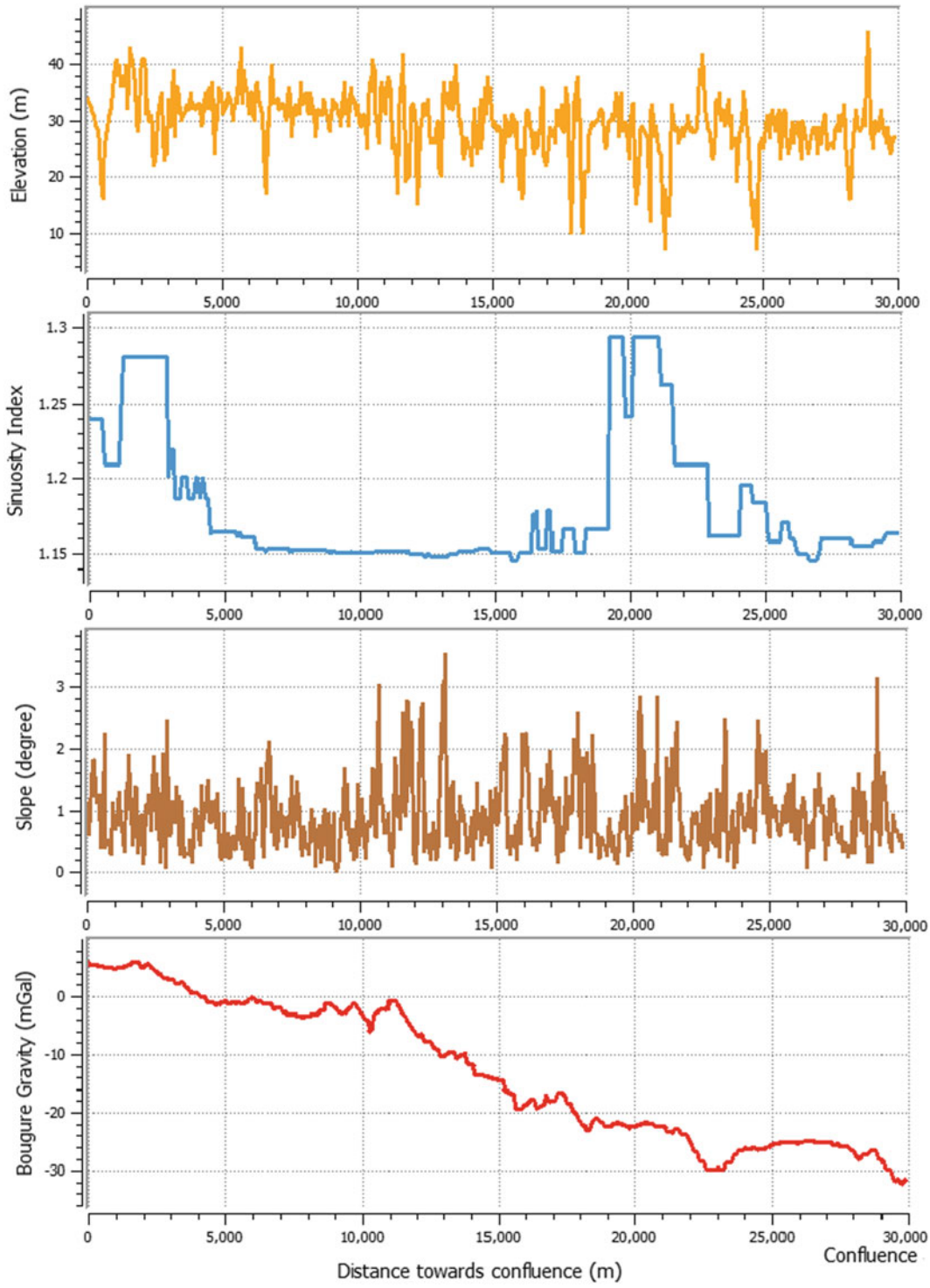

Fig. 5.2 Adjustment of channel attributes (Slope, Sinuosity Index, and Bed Elevation) with the certain fall of Bouguer gravity values (10,000–20,000 m) in the downstream of Kunur River

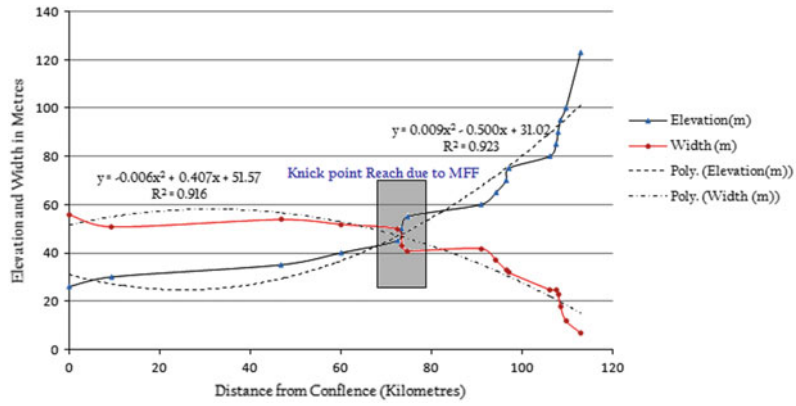

Fig. 5.3 Longitudinal profile of the entire Kunur River and associated bank full channel width

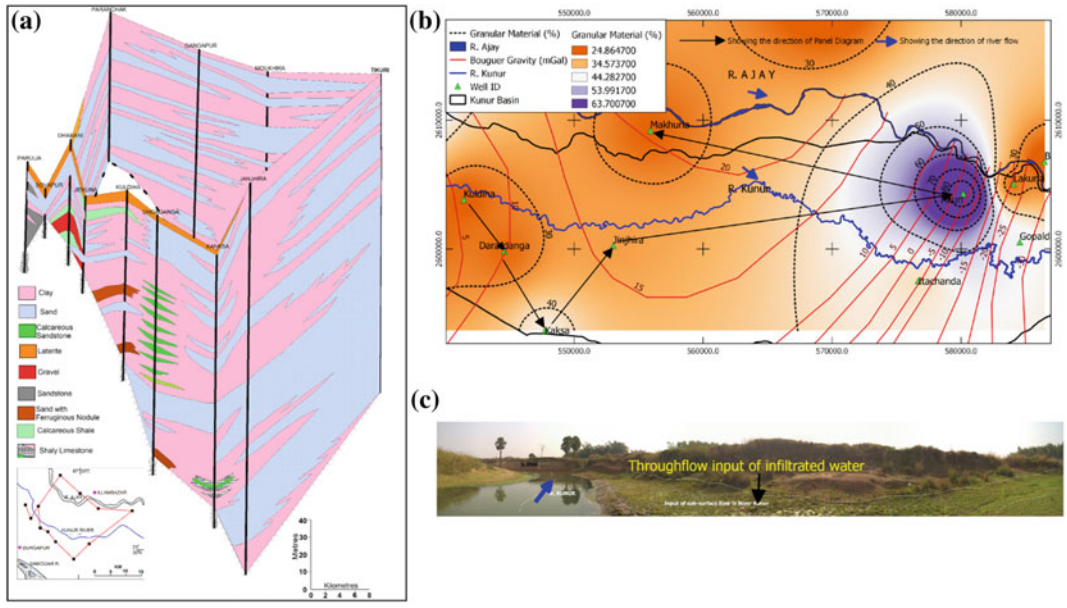

Fig. 5.4 **a** Panel diagram showing the lithological condition in the interfluve region of Ajay and Kunur Rivers (modified of Niyogi 1985); **b** distribution of underlying granular material in the downstream of Kunur Basin; **c** lithological influence on subsurface flow condition and steep bank indicates the active stream flow

or sandy layer (<20%). However, the eastern part consists of more than 60–80% of granular materials or sandy layer (at Tikuri 85.50%) and suggests major cause behind the high negative anomaly over here (Fig. 5.4b). The panoramic view of Kunur River, captured from this negative anomaly zone, also shows that the layer of granular materials works as a permeable layer (Fig. 5.4c). As a result, the infiltrated water from the upland area effluents in the channel of Kunur and maintain its base flow near Mahata village.

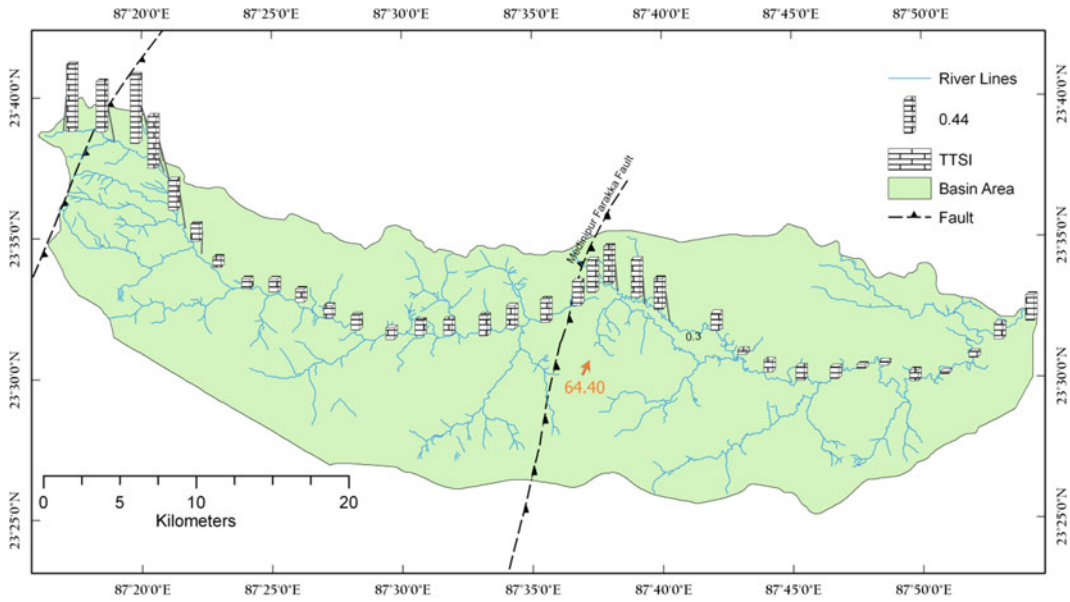

Fig. 5.5 Reach scale (~2 km) variation of TTSF index along the Trunk River of Kunur River inclosing the alignment of two major subsurface faults

5.3.3 Basin Asymmetry and Channel Planform Adjustment

There is a prominent northward tilting of the KRB with high AF-index (64.40), whereas reach wise (~2 km) TTSF values of the basin are ranging from 0.02 (purely symmetrical) to 0.93 (very highly asymmetrical). Therefore, Kunur River migrates towards north-east; however, the migration rate is not uniform in this direction along its all segments. Maximum rate of migration has been observed in the surrounding of predefined subsurface fault zones (Fig. 5.5). Hence, low TTSF values in the focused reach reveal the lower rate of migration, whereas the channel makes steep vertical erosion and configured an incised meandering planform due to steep slope and low density of underlying materials (Fig. 5.4c).

5.4 Discussion

Being an oldest tectonic block Western Bengal Basin (WBB) is still marked as active tectonic region since its beginning because of the marginal areas are still sinking as oblique manner and subsidence of the Central Bengal Basin (Steckler et al. 2016). The formation of WBB has begun as an intercratonic rift basin of the Gondwanaland during the late Carboniferous period before the apparent splitting of Gondwana in the Jurassic and early Cretaceous period (Krishnan 1982). The underwater sedimentation in the basin started during late Mesozoic Era (~205 Ma) as fluvio-deltaic formation with the opening of Bengal Basin through the splitting of Gondwanaland (Valdia 2001) when the Australia and India were separated and slipped along 90° east longitude (Alam 1989). At the same time, crystalline basement of Archean gneissic complex is also underlined by the Singhbhume group of metavolcanic rock and the Deep Seismic Sound (DSS) profile from north to south (CD) shows the depth of the basement varies from ~4.9, ~6.8 and ~6.3 km at Kandi, Kusumgramand Palashi, respectively (Figs. 5.6 and 5.7a) (Murty et al. 2008). In addition, another DSS profile in the west to east (AB) direction also shows the depth of Singhbhume basement that also varies significantly and the maximum depth (~6.3 km) of basement has been encountered in the middle of the profile, which also coincides with the deepest part at

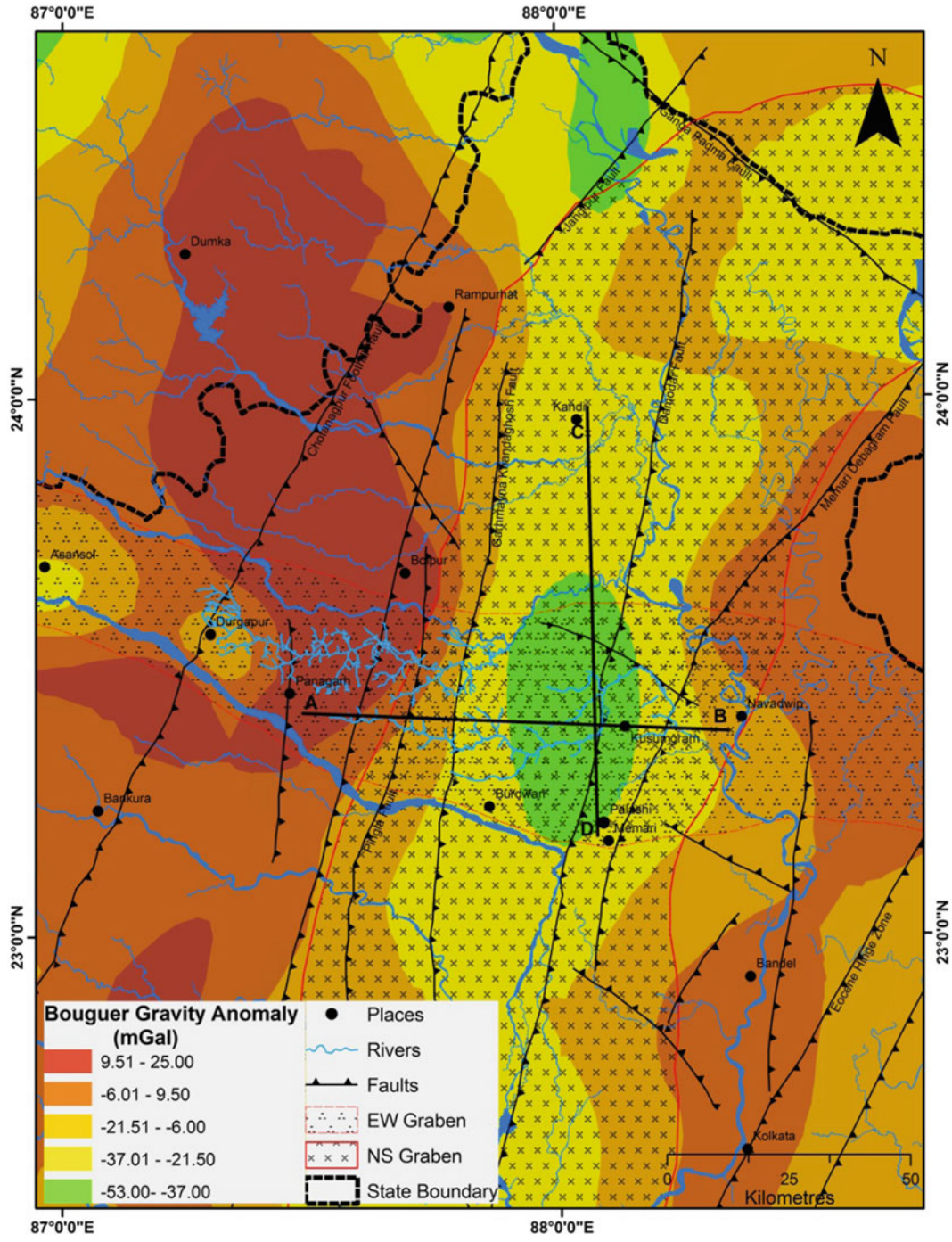

Fig. 5.6 Neotectonic map of the Western Bengal Basin (WBB) has been superimposed over the observed Bouguer gravity data (NGRI 1978), where two important Gondwana grabens (EW-tending and NS-tending) have been delineated with the mark of two DSS profiles. *Source* Based on Choudhury and Datta (1973), Verma and Mukhopadhyay (1977), Reddy et al. (1993), Murty et al. (2008), Rajasekhar and Mishra (2008), Roy et al. (2010), Banerjee et al. (2013)

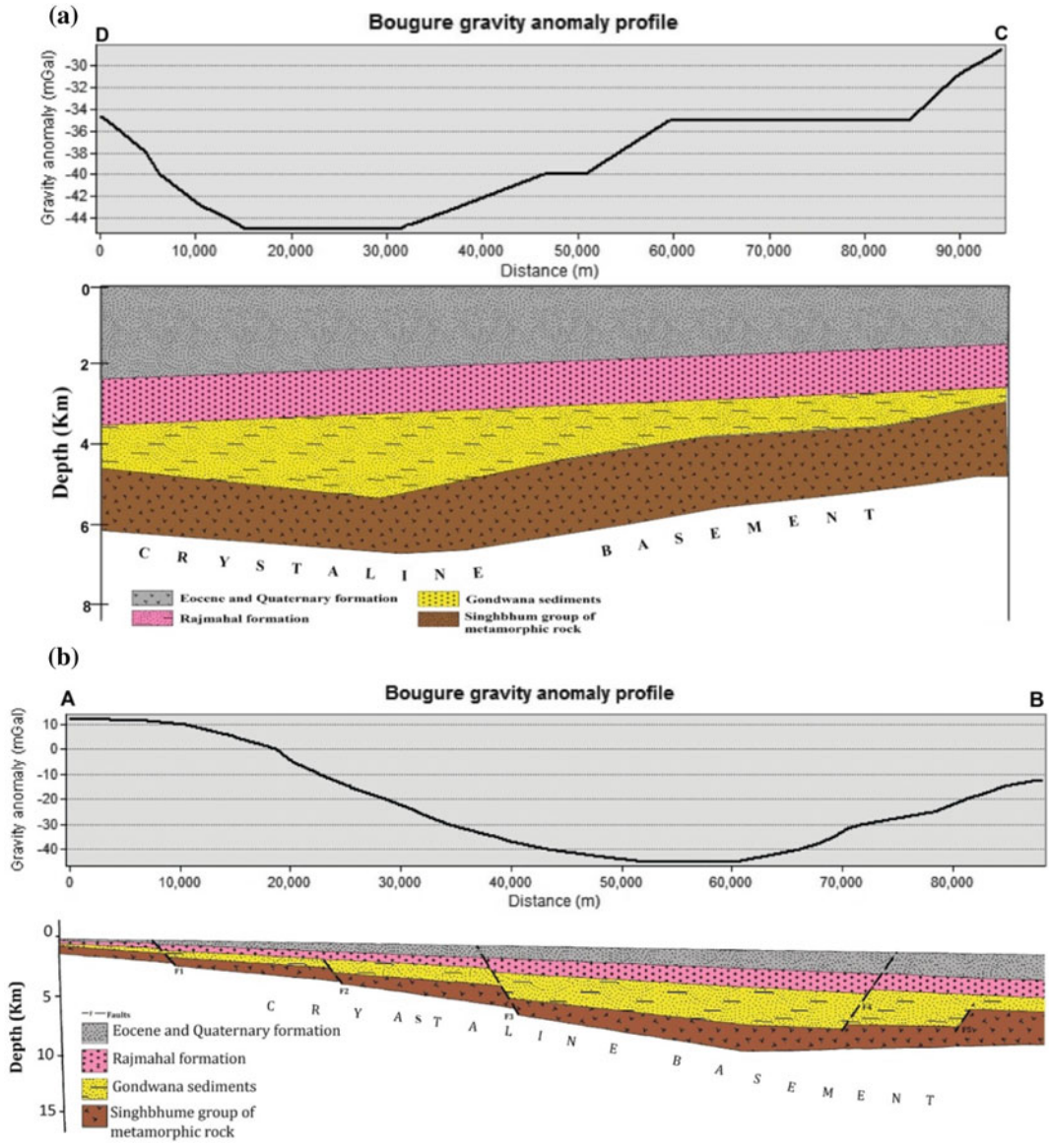

Fig. 5.7 Basement configuration and subsurface structure has been delineated through integrated interpretation of travel-time inversion of wide-angle seismic sounding reflection data and gravity data. **a**, In particular, profile CD shows north–south depression in Bouguer gravity values, where maximum depression has been observed over the interfluve of Ajay and Damodar Rivers (lower part); **b** and profile AB shows variation in gravity value and basement depth with successive formation and different fault lines (F_n): F1 = Mednipur–Farraka Fault or Basin-Margin Fault, F2 = Pingla Fault, F3 = Garhmayna–Khandaghosh Fault, F4 = Damodar Fault and F5 = Memari–Debagram Fault. *Source* Modified after Choudhury and Datta (1973), Verma and Mukhopadhyay (1977), Reddy et al. (1993), Murty et al. (2008), Rajasekhar and Mishra (2008), Roy et al. (2010), Banerjee et al. (2013)

Kusumgram in the north–south profile (Figs. 5.6 and 5.7b).

Both tectonic troughs are termed as EW-tending Gondwanagraben and NS-tending Gondwanagraben (McDougall and McElhinny 1970; Murty et al. 2008; Banerjee et al. 2013). The variation in basement depth of both grabens have also been influenced to make different depths of Gondwana sedimentation. The EW-tending graben, identified as 'Damodar Graben' (DG) in eastern Peninsula, was subsequently filled with thick Gondwana sedimentation during early Carboniferous to Triassic period (359–201 Ma) (McDougall and McElhinny 1970; Murty et al. 2008; Banerjee et al. 2013). The DG has been extended eastward up to the Bengal shelf zone, which is revealed by the presence of coal-bearing strata cover by several kilometres thick Quaternary alluviums (Krishnan 1982). Another graben in the north–south direction is bounded by the Basin Margin Fault (BMF) or Medinipur–Farakka Fault (MFF) to the west and Memari–Debagram fault on the east and filled by very thick depositions (Choudhury and Datta 1973; Reddy et al. 1993; Banerjee et al. 2013). The intersection zone of these two grabens can be marked as a deepest Gondwana structural depression in the WBB with thick column of sedimentation and called as sink zone.

In the regional Bouguer gravity maps, both grabens are also prominent with deep elliptical depression in gravity values (Fig. 5.6). Maximum negative anomaly (−45 mGal) has been identified at the intersection zone near Kusumgram. The spatial variation in the depth of basement rock (i.e. Singhbhume group) and associated thickness of Gondwana sedimentary layer is the major cause behind the typical gravity anomaly over the region. The Kunur River is also running through the northern boundary of this sink zone, where the graben is sedimented by Talchir formation (boulder bed succeeded by shales and sandstone) overlie by Barakar formation (sandstone and grits with occasional conglomerates), Raniganj formation (sandstone and shale with coal seams) and Panchet formation/Super-Pachet formation (micaceous and feldspathic sandstone shales) of Gondwana sediments which are sequentially exposed over surface at the western side of KRB (Krishnan 1982). Subsequently, this formation is roofed by Triassic Rajmahal Trap formation, which is also overlain by thick layer of Tertiary and Quaternary alluvium formation. Nature of this alluvium is soft and unconsolidated oxidized sand, silt and clay with caliche concretion (Table 5.1 and Fig. 5.7b) (GSI 2001). Hence, there is no significant variation in the thickness of Rajmahal Trap and Quaternary deposition (Fig. 5.7b). However, the basement complex and overlie sediments have been warped by strike-slip faulting during late Paleozoic and late Mesozoic Era which was tectonically reactivated during late Eocene (Alam et al. 2003).

Previous studies have delineated two strike-slip faults across this region, e.g. Chhotanagpur Foothill Fault (CFF) and Medinipur–Farakka Fault (MFF), which are the key controller of channel geomorphology of this region (Singh et al. 1998; Roy and Sahu 2015a, b, 2016). The two defined knick points in the Kunur River are also directly corresponding with these two fault lines. According to Roy and Sahu (2015a, b), the identified palaeo-channels within the interfluve of Ajay and Kunur (AKI) Rivers were also developed due to north-eastward shifting of Ajay River induced by neotectonic actions and the present lower reach of Kunur is basically a palaeo-path of Ajay River. Therefore, a direct control of underlying rock density has been observed on the planform of lower Kunur River. Roy and Sahu (2015a) have also identified the changes of sinuosity index along with the planform of Kunur and Khari Rivers (Fig. 5.8). It is clear to see that how the straight reach of both rivers become meandering and incised immediately after the MFF line. Inserted field photos (P1–P4) are also showing reach scale changing shape of Kunur River channel. A huge deformation near Mahata has been also marked in the same figure (Fig. 5.8).

Table 5.1 Generalized litho-stratigraphic chart of the Western Bengal Basin (WBB) along the AB profile in Fig. 5.6

Formation	Age	Average density (g/cc)	Depth of base from surface (km)	Velocity of seismic sound (kms^{-1})	Lithological description	Environment
Alluvium deposits	Quaternary (2.6 Ma–Resent)	2	0.30–0.75	1.95	Clay alternating with silt and sand, clay with caliche concretion and laterite patch	Fluvial and fluvio-marine
Shale	Pliocene (5.3–2.6 Ma)	2.31	0.50–1.70	2.86		
Sylhet limestone	Late Cretaceous to Eocene (100–33.9 Ma)	2.37	1.70–1.90	3.7		
Unconformity						
Rajmahal trap	Jurassic to Early Cretaceous (201–100 Ma)	2.8	1.70–2.40	4.6	Basalt (continental tholeiites) trap wash with intertrapen	Fissure type volcanic eruption
Unconformity						
Gondwana sediments	Carboniferous to Triassic (359–201 Ma)	2.4	2.40–5.80	4	Greenish sandy shale with boulders at base, very coarse to medium-grained dark grey to white sandstone, soft feldspathic sandstone and coal seam	Fluvial and glacio-fluvial
Unconformity						
Singhbhume group of metavolcanic rock	Proterozoic (2500–541 Ma)	2.61	5.80–6.80	5.5	Granite, Granodiorite	–
Crystalline basement	Archean (>2500 Ma)	2.71	Undefined	6.1		

Source Modified after Choudhury and Datta (1973), Verma and Mukhopadhyay (1977), Reddy et al. (1993), Murty et al. (2008), Rajasekhar and Mishra (2008), Roy et al. (2010), Banerjee et al. (2013)

The high negative gravity values have indicated the presence of low-density materials with higher thickness of basement sediment below the AKI region. This gravitational depression might be the result of underneath sandy or unconsolidated sediment with higher percentage of granular material (Sahu and Saha 2014). Underlying heavy dense rock and lower depth of basement have been perceived in the middle of the basin from the maximum positive gravity anomaly. Lithological condition of this region has been revealed by the panel diagram (Fig. 5.4a). Roy and Chatterjee (2015) have also delineated the western margin fault of Bengal Basin based on the zone of crowding of gravity contours; where the fault line marked along the neutral gravity value, i.e. 0 mGal. Similar crowding of gravity contours including 0 mGal have been also observed in the focused study region, where the Garhmayna–Khandaghosh Fault (GKF) has been

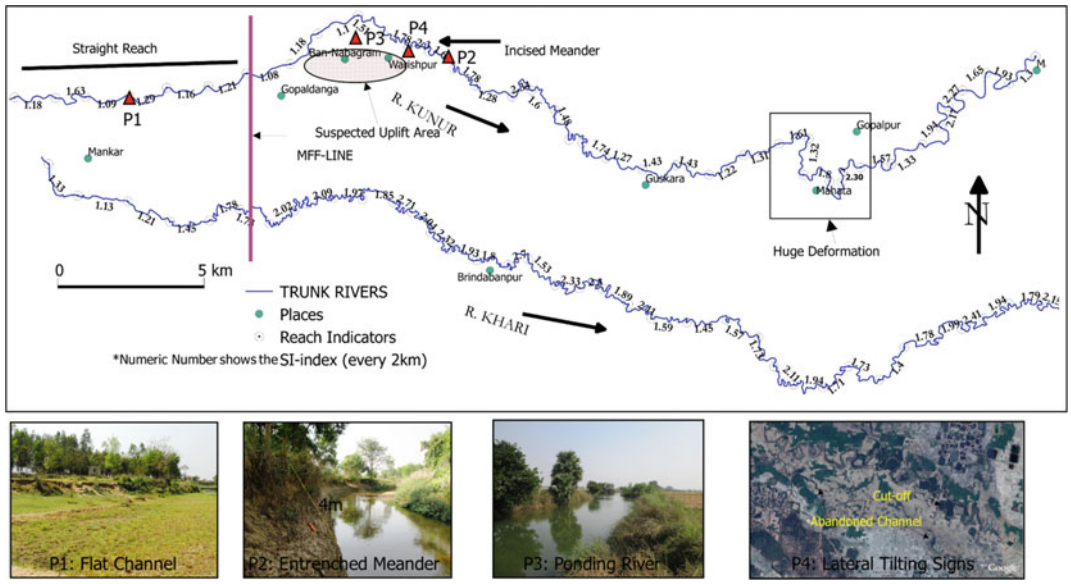

Fig. 5.8 Adjustment of channel sinuosity index and local fluvial features of Kunur and Khari rivers with tectonic controls (after Roy and Sahu 2015a)

marked by Geological Society of India in their 'Seismotectonic Atlas' (Fig. 5.6). The GKF is the major cause of the typical channel pattern in the study reach formed by the certain change in underlying structure. In the perpendicular direction of study reach, similar asymmetric in channel pattern has been observed for the Khari River also, where GKF also crosses the river Khari (Fig. 5.6). In addition, at the intersection part of both graben with maximum gravity anomaly (in negative), Khari River also takes a sharp right angle turn towards north near Kusumgram and runs almost 21 km with steep sidewall and developed extended mushy land over its floodplain (Roy and Sahu 2015a).

Channel side exposed strata also carry the evidences of active hydraulic actions in past due to active tectonic and geophysical actions around the focused channel reach. The buried soil layer of Sijua formation contents upward coarser materials (from coarse sand to gravel), which explains the presence of higher flow action during the late Pleistocene to middle Holocene (Fig. 5.9). According to Singh et al. (1998), the western part of lower Gangetic plain has number of subsurface faults which are reactivated during the early Pleistocene epoch. In connection with this, it may conclude that this part of Kunur Basin also experienced by the reactivation of GKF and tilting during this period. The factors related to asymmetry indices also allow the determination of general tilt of the basin landscape irrespective of the whether the tilt is local or regional. The unpaired terraces around the MFF line again exemplify the role of geotectonic control over the Kunur Basin (see Fig. 6a in Roy and Sahu 2015a).

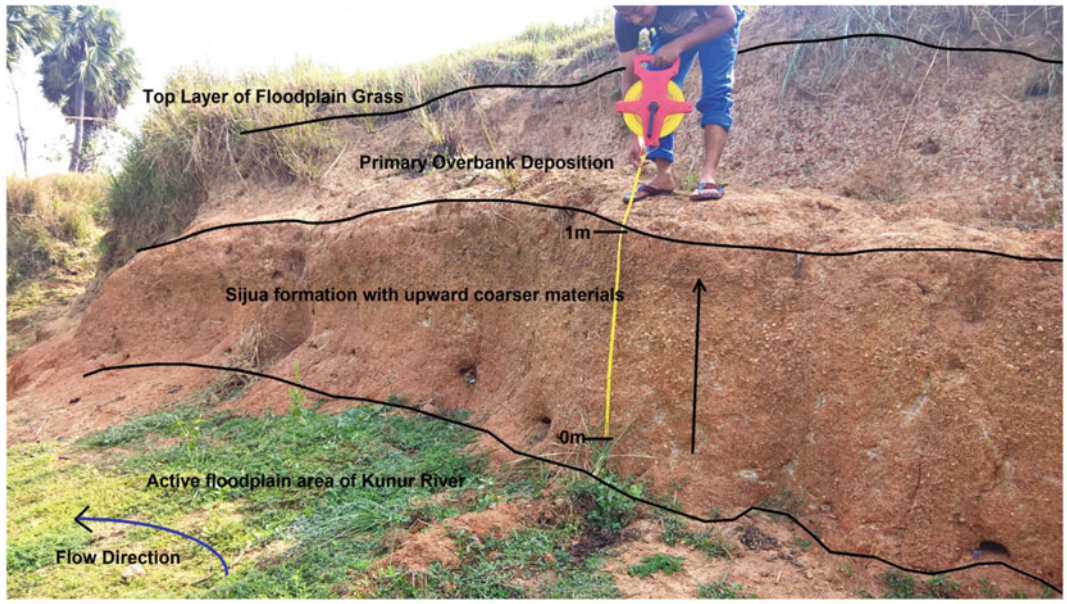

Fig. 5.9 Lithological evidence of high hydraulic action during early Pleistocene epoch, upward coarser layer of Sijua formation indicates the presence of high flow action over here

5.5 Conclusion

The overall attempt has been made to correlate the role of subsurface lithology, defined by gravity anomaly, on the explanation of anomalous drainage behaviour and drainage patterns of Kunur Basin and rivers in surroundings. The study has confirmed that the typical pattern of Kunur River, in its downstream area, is a combined result of underlying geology, i.e. variation of density and thickness of sedimentation and neotectonic movements. Tectonically formed grabens are the major sources of gravity anomaly over the WBB and the intersection zone featured with maximum negative anomaly and typical arrangements of surface river lines and their geometry. However, the resolution of Bouguer gravity anomaly is coarse but the data have played a valuable role in the combined interpretation of channel geomorphology and help to uncover the underlying causes behind the channel pattern adjustment. The subsurface lithological configuration helps to discriminate the variation of Bouguer gravity values and associated geology of this region. TTSF and AF indices also assist to define the presence neotectonic actions within the basin and field photographs provide valuable support in this interpretation.

N.B. for special understanding on influence of faulting on the extra-channel geomorphology, readers may go through Chap. 4 of this volume

References

Alam M (1989) Geology and depositional history of Cenozoic sediments of the Bengal Basin of Bangladesh. Palaeogeogr Palaeoclimatol Palaeoecol 69:125–139

Alam M, Alam MM, Curray RJ, Chowdhury MLR, Gani MR (2003) An overview of the sedimentary geology of the Bengal Basin in relation to the regional tectonic framework and basin-fill history. Sed Geol 155:179–208

Bagchi K, Mukherjee KN (1979) Diagnostic survey of Rarh Bengal, Part–I, morphology, drainage and flood: 1978. Department of Geography, University of Calcutta, Calcutta

Bandyopadhyay S (1996) Location of the adi ganga palaeochannel, S. 24 Parganas, West Bengal: a review. Geogr Rev India 58(2):93–109

Bandyopadhyay S, Bandyopadhyay MK (1996) Retrogradation of Western Ganga—Brahmaputra—Delta: possible reason. Nat Geogr 31(2):105–128

Bandyopadhyay S, Das S, Kar NK (2015) Discussion: 'Changing river courses in the Western part of the Ganga-Brahmaputra Delta' by Kalyan Rudra (2014). Geomorphology 227:87–100. Geomorphology 250:442–453. https://doi.org/10.1016/j.geomorph.2015.02.037

Bandyopadhyay S, Kar NK, Das S, Sen J (2014) River systems and water resources of West Bengal: a review. Geol Soc India (Spec Publ) 3:63–84

Banerjee B, Mara IA, Biswas AK (2013) Subcrop Gondwana of Bengal basin and their reservoir characteristics. J Geogr Soc India 81:741–754

Banerjee SN, Chakraborty P (1983) Some observation on recent trends of shifting pattern of the ganga between Rajmahal and Ganga. J Geol Soc India 24:318–320

Bhattacharya AK, Dhar N (2005) A report geo-environmental appraisal in Barddhaman Urban agglomeration area and its environment for sustainable developmental activities. Geological Survey of India, Kolkata Eastern Region, pp 1–43

Bhattacharya K (1959) Bangladesher Nad-Nadio Parikalpana (in Bengali). Bidyadoya Library Ltd., Calcutta

Bhattasali NK (1941) Antiquity of the Lower Ganges and its courses. Sci Cult 233–239

Choudhury SK, Datta AN (1973) Bouguer gravity and its geological evolution in the Western part of the Bengal Basin and adjoining area, India. Geophysics 38 (4):691–700

Cox RT (1994) Analysis of drainage-basin symmetry as a rapid technique to identify areas of possible quaternary tilt-block tectonics: an example from the mississippi embayment. Geol Soc Am Bull 106:571–581

Goodbred SL, Kuehl SA, Steckler MS, Sarkar MH (2003) Controls on facies distribution and stratigraphic preservation in the Ganges-Brahmaputra delta sequence. Sed Geol 155:301–316

GSI (Geological Society of India) (2001) District resource map: Barddhman. Eastern Region, Kolkata

IMD (2014) District wise normals. Indian Meteorological Department, Govt. of India, Barddhaman

Jacques PD, Salvador ED, Machado R, Grohmann CH, Nummer AR (2014) Application of morphometry in neotectonic studies at the eastern edge of the Paraná Basin, Santa Catarina State, Brazil. Geomorphology 213:13–23. https://doi.org/10.1016/j.geomorph.2013.12.037

Kale VS, Sengupta S, Achyuthan H, Jaiswal MK (2014) Tectonic controls upon Kaveri River drainage, cratonic Peninsular India: inferences from longitudinal profiles, morphotectonic indices, hanging valleys and fluvial records. Geomorphology 227:153–165. https://doi.org/10.1016/j.geomorph.2013.07.027

Keller EA, Pinter N (1996) Active tectonics: earthquakes, uplift and landscape. Prentice Hall, New Jersey

Krishnan MS (1982) Geology of India and Barma. CBS Publishers & Distributors, India

Mallick K, Sharma KK, Rao VK (1999) A new gravity interpretation: a case study from Pahute Mesa, Nevada test site. Current Sci 76:1495–1498

Mallick K, Vasanthi A, Sharma KK (2012) Bouguer gravity regional and residual separation: application to geology and environment. Springer Publication, Netherlands

Mallick M, Mukhopadhyay D (2011) An analysis of GPS-derived velocities in the Bengal basin and the neighbouring active deformation zones. Current Sci 101(3):1–4

Mandal A, Gupta S, Mohanty WK, Misra S (2015) Sub-surface structure of a craton—mobile belt interface: evidence from geological and gravity studies across the Rengali Province—Eastern Ghats Belt boundary, eastern India. Tectonophysics 1–13. http://dx.doi.org/10.1016/j.tecto.2015.01.016

Marotta AM, Spelta E, Rizzetto C (2006) Gravity signature of crustal subduction inferred from numerical modelling. Geophys J Int 166:923–938. https://doi.org/10.1111/j.1365-246X.2006.03058.x

McDougal I, McElhinny MW (1970) The Rajmahal trap of India, K-Ar ages and palaeomagnetism. Earth Planet Sci Lett 9:372–378

McKenzie D (1977) Surface deformation, gravity anomalies and convection. Geophys J R Astr Soc 48: 211–238

Mukherjee A, Fryar AE, Thomas WA (2009) Geologic, geomorphic and hydrologic framework and evolution of the Bengal basin, India and Bangladesh. J Asian Earth Sci 34:227–244

Murty ASN, Sain K, Prasad BR (2008) Velocity structure of West-Bengal Basin, India along the Palashi-Kandi profile using a travel-time inversion of wide-angle seismic data and gravity modeling—an update. Pure Appl Geophys 165:1733–1750

Nath SK, Adhikari MD, MaitiSK DevarajN, SrivastavaN MohapatraLD (2014) Earthquake scenario in West Bengal with emphasis on seismichazard micro zonation of the city of Kolkata, India. Nat Hazards Earth Syst Sci 14:2549–2575. https://doi.org/10.5194/nhess-14-2549-2014

NGRI (1978) NGRI/GPH-1 to 5: gravity maps of India scale 1: 5,000,000. National Geophysical Research Institute, Hyderabad, India

Niyogi M (1985) Groundwater resource of the Ajay Basin. In: Chatterjee SP (ed) Geographical mosaic–Professor K. G. Bagechi Felicitation. Manasi Press, Calcutta, pp 165–182

Rajasekhar RP, Mishra DC (2008) Crustal structure of Bengal Basin and Shillong plateau: extension of Eastern Ghat and Satpura mobile belts to Himalayans fronts and seismotectonics. Gondwana Res 14: 523–534

Reddy PR, Venkateswarlu N, Prasad ASSSRS, Rao PK (1993) Crustal density model across West Bengal basin, India: an integrated interpretation of seismic

and gravity data. Proc India Acad Sci (Earth Planet Sci) 102(3):487–505

Roy AB, Chatterjee A (2015) Tectonic framework and evolutionary history of the Bengal Basin in the Indian subcontinent. Curr Sci 109(2):271–279

Roy BC, Banerjee K (1990) Quaternary geological and geomorphological mapping in Parts of Barddhaman and Bankura Districts (And preliminary assessment of sand deposits suitable for construction and other allied purposes). Published Report. Geological Survey of India, Eastern Region, Calcutta

Roy DK, Ray GK, Biswas AK (2010) Overview of overpressure in Bengal Basin, India. Geol Soc India 75:644–660

Roy S, Sahu AS (2015a) Quaternary tectonic control on channel morphology over sedimentary lowland: a case study in the Ajay-Damodar interfluve of Eastern India. Geosci Front 6(6):927–946. https://doi.org/10.1016/j.gsf.2015.04.01

Roy S, Sahu AS (2015b) Palaeo-path investigation of the lower Ajay River (India) using archaeological evidence and applied remote sensing. Geocarto Int. https://doi.org/10.1080/10106049.2015.1094526

Roy S, Sahu AS (2016) Morphotectonic map generation using geo-informatics technology: case study over the Ajay-Damodar Interfluve, West Bengal, India. Arabian J Geosci. https://doi.org/10.1007/s12517-015-2247-z

Roy S, Mistri B (2013) Estimation of peak flood discharge for an ungauged river: a case study of the Kunur River, West Bengal. Geogr J 2013(214140):1–11. https://doi.org/10.1155/2013/214140

Rudra K (1987) Quaternary history of the lower Ganga distributaries. Geogr Rev India 49(3):37–38

Rudra K (2010) Banglar Nadikath (in Bengali). Shahitto-Sangsad, Kolkata

Rudra K (2014) Changing river courses in the Western part of the Ganga-Brahmaputra Delta. Geomorphology 227:87–100. https://doi.org/10.1016/j.geomorph.2014.05.013

Sahu S, Saha D (2014) Geomorphologic, stratigraphic and sedimentologic evidences of tectonic activity in Sone-Ganga alluvial tract in Middle Ganga Plain, India. J Earth Syst Sci. 123:1335–1347

Sarma JN, Acharjee S, Murgante G (2013) Morphotectonic study of the Brahmaputra basin using geoinformatics. Geophys Res Abs 15: EGU2013-14001

Siddiqui S (2014) Appraisal of active deformation using DEM-based morphometric indices analysis in Emilia-Romagna Apennines, Northern Italy. Geodyn Res Int Bull 1(3):34–42

Singh LP, Parkash B, Singhvi AK (1998) Evolution of the lower Gangetic plain landforms and soils in West Bengal, India. Catena 33:75–104

Steckler MS, Mondal DR, Akhter SH, Seeber L, Feng L, Gale J, Hill EM, Howe M (2016) Locked and loading megathrust linked to active subduction beneath the Indo-Burman Ranges. Nat Geosci. https://doi.org/10.1038/NGE02760

United State Geological Society (1997) Introduction to potential fields: gravity. FS-239–95.http://pubs.usgs.gov/fs/fs-0239-95/fs-0239-95.pdf. Accessed 13th Dec 2014

Valdia KS (2001) HIMALAYA emergencce and evolution. University Press Limited, India

Verma RK (1985) Gravity field, seismicity, and tectonics of the Indian peninsula and the Himalayas (Solid earth sciences library). D. Reidel Publishing Company, Holland. https://doi.org/10.1007/978-94-009-5259-1

Verma RK, Mukhopadhyay M (1977) An analysis of the gravity field in northeastern India. Techtonophysics 42:283–317

VijayaRao V, Kalachand S, Reddy PR, Mooney WD (2006) Crustal structure and tectonics of the northern part of the Southern Granulite Terrane, India. Earth Planet Sci Lett 251:90–103. https://doi.org/10.1016/j.epsl.2006.08.029

6 Imprints of Neo-tectonism in the Evolutionary Record Along the Course of Khari River in Damodar Fan Delta of Lower Ganga Basin

Suman Deb Barman, Aznarul Islam, Balai Chandra Das, Sunipa Mandal and Subodh Chandra Pal

Abstract

Neo-tectonism affected the evolution of landscape across the earth since post-Miocene. The Khari river in Lower Damodar fan delta in West Bengal similarly portrayed the imprints of neo-tectonism in the forms of rapidly changing meander geometry, deformation in long profiles, unpaired terraces, soft sediment structures (fluid escape structure and convolute), etc. The study of meander geometry considering 142 loops (upper—92, middle—38 and lower—12) for the years 1972 (Survey of India topo-sheet) and 2017 (Google Earth images) portrayed rapidity in channel evolution in the middle and the lower stretches of the river compared to its upper counterpart as shown by the changing sinuosity index during 1972 and 2017 (upper: 0.1, middle: −0.4 and lower: −0.42), radius–wavelength ratio (upper: 0.01, middle: −0.06 and lower: −0.04), meander shape index (upper: −0.05, middle: −0.09 and lower: −0.01), and meander form index (upper: −0.02, middle: −0.17 and lower: −0.13). We found this kind of meander behaviour to be correlated with the negative Bouguer anomaly (−45 to −30 m Gal) in the middle reach. Similarly, based on SRTM DEM (30 m), we detected a break in the long profile at the middle reach underlain by a sub-surface fault. In addition, we observed unpaired terraces in the middle reach. Besides, our extensive field survey guided us to identify long continued fluid escape structure and convolute along the banks of the river and a typical sedimentary facies which proved to be tectonically controlled.

Keywords

Neo-tectonism · Paleogeography · Meander geometry · Stream-length index · Unpaired terrace · Facies analysis · Soft sediment structure

S. D. Barman · S. C. Pal
Department of Geography, The University of Burdwan, Bardhaman, West Bengal, India
e-mail: sdbarman1993@gmail.com

S. C. Pal
e-mail: geo.subodh@gmail.com

A. Islam (✉)
Department of Geography, Aliah University, Kolkata, India
e-mail: aznarulislam@gmail.com

B. C. Das
Department of Geography, Krishnagar Government College, Nadia, West Bengal, India
e-mail: balaidaskgc@rediffmail.com

S. Mandal
Department of Geological Sciences, Jadavpur University, Kolkata, India
e-mail: sunipam@gmail.com

B. C. Das et al. (eds.), *Quaternary Geomorphology in India*,
Geography of the Physical Environment, https://doi.org/10.1007/978-3-319-90427-6_6

6.1 Introduction

Neo-tectonism is the most recent jerk in the geological history of the earth operating since post-Miocene to recent (AGI 2009). Most of the neo-tectonic movements and resultant landforms belong to Quaternary period which reveals the youthfulness of the topography (Ashley 1931). Virtually all geomorphological landscapes across the world owe their origin to neo-tectonism of Quaternary period. Therefore the issue of neo-tectonic movements or Quaternary controls over the evolution of landscape is overwhelmingly explored by the geoscientists. The neo-tectonic features have been studied by five complementary approaches—lineament analysis, drainage analysis, comprehending volcano morphology, use of geo-spatial tool especially images and DEM and field exploration (Rosenau 2014). However in most cases drainage analysis coupled with assistance from field and geo-spatial science has been popularly used by scholars to unveil the neo-tectonic mysteries. The studies of drainage network (Štěpančíková et al. 2008), channel pattern (e.g Lahiri 1996; Perucca et al. 2013), channel morphology (e.g. Goswami 2011), nature of fluvial incision (e.g. Cunha et al. 2005), river sinuosity (e.g. Timar 2003; Zámolyi et al. 2010), deformation in long profiles (e.g. Radoane et al. 2003), changes in valley floor width(e.g. Bil 2002), channel capture (Sinha-Roy 2001) in relation to neo-tectonics are common in literature. Besides these specific approaches, channel changes and basin evolution regarding tectonic forcing (e.g. Latrubesse and Franzinelli 2002; Cremon et al. 2016; Sougnez and Vanacker 2011; Shukla et al. 2009; Agarwal et al. 2002; Dar et al. 2013; Silver et al. 2015; Mats et al. 2000) have been focused all over the world. The drainage evolution of Ganga-Brahmaputra (GB) delta is largely a response to neo-tectonic movements in Quaternary period (Akter et al. 2016; Sarkar et al. 2009). The major rivers of this delta including Ganga, Brahmaputra and their major tributaries like Ajay, Damodar have well been explored in the context of morpho-tectonic setting from the mega-scale approach (Goodbred 2003; Goodbred and Kuehl 2000a, b). But the small tributaries like Khari, Kuye, Banka have drawn very little attention for the tale-tell lack of micro-scale survey. Though some scholars (e.g. Sen 1976, 1978; Roy and Sahu 2015) worked on few streams during the last few decades, the advances in knowledge is still very meagre to comprehend the drainage evolution and hydro-geomorphic instability in the micro-geomorphology of the Lower Ganga basin especially in the Damodar fan delta (DFD). Khari river being a part of DFD is still least explored in terms of revelation of landforms, drainage characteristics and geological features. Thus, the goal of the present contemplation is to understand the mode of evolution of the present basin in the context of palaeogeography and to search the occult imprints of neo-tectonism on landform, drainage and sedimentation in the alluvial plain of Damodar valley encompassing Khari river.

6.2 Study Area

Khari River, a right bank tributary of the Bhagirathi-Hooghly system, originates from Maro village near Budbud and flows in the eastern portions of the Bardhhaman district traversing an area ~2342 km^2 in Ajay-Damodar Interfluves (ADI) between 23° 10′ 10″N to 23° 38′ 52″N and 87° 23′ 39″E to 88° 20′ 45″E (Fig. 6.1). Geologically this area belongs to the Bengal Basin and geomorphologically it is a mature delta sloping towards east-south east with a minimum elevation of 5 m and a regional maximum of 60 m from msl (Fig. 6.2a). Regional stratigraphy reveals three Quaternary formations—Sijua, Chuchura and Hooghly formation (Fig. 6.2b) besides a Cenozoic Laterite formation (Ghosh and Islam 2016). Sijua formation, being the oldest unit (Upper Pleistocene to lower Holocene) represents an undulating surface comprised of fairly oxidized clay with alternate layers of 'caliche' and ferruginous concretions. Chuchura formation, the intermediate unit in sequence (Middle Holocene to upward Holocene) depicts natural levee, back swamp, paleo-channels, point bar and cut-off meander. Lithologically this unit is characterized by

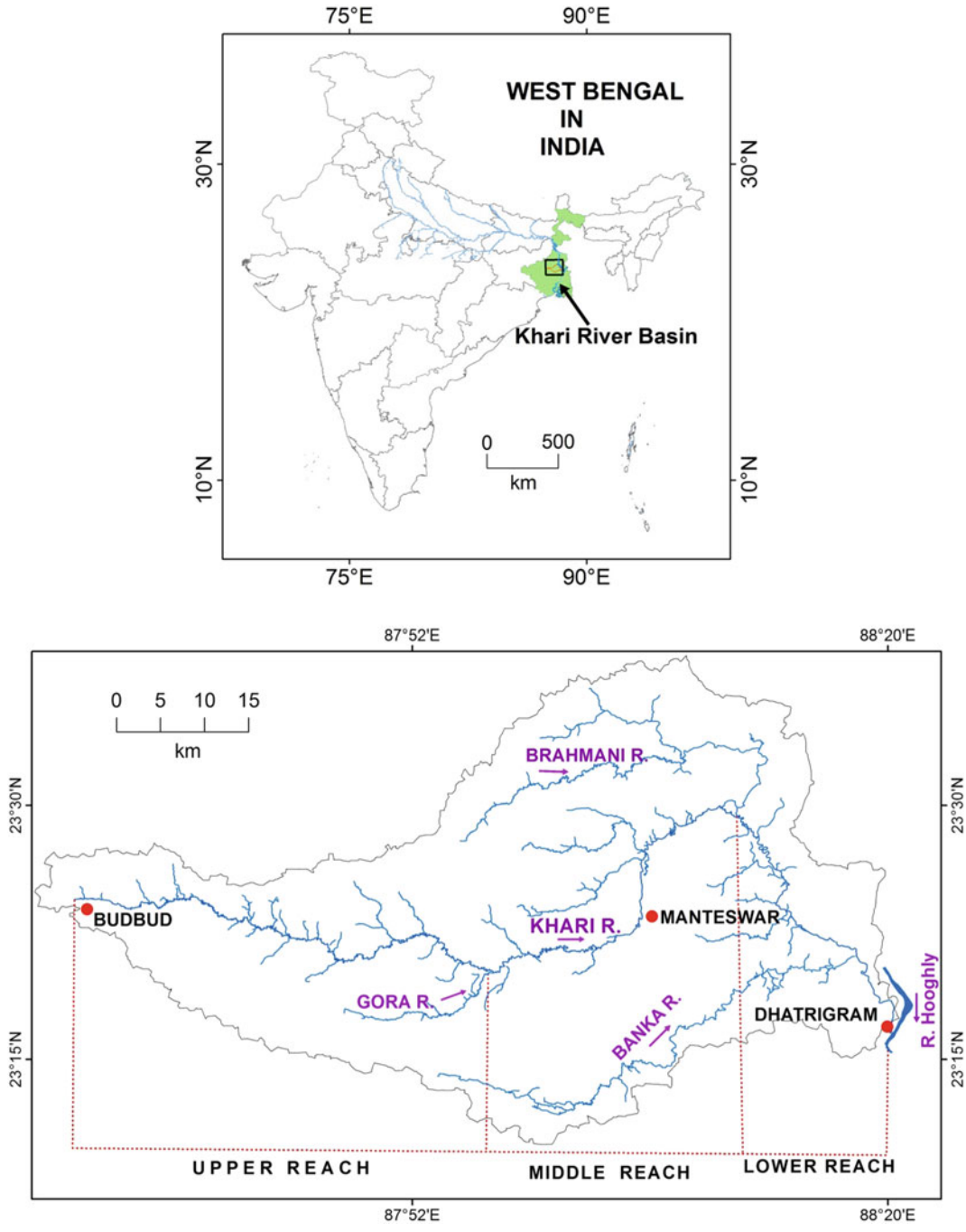

Fig. 6.1 Location of the study area

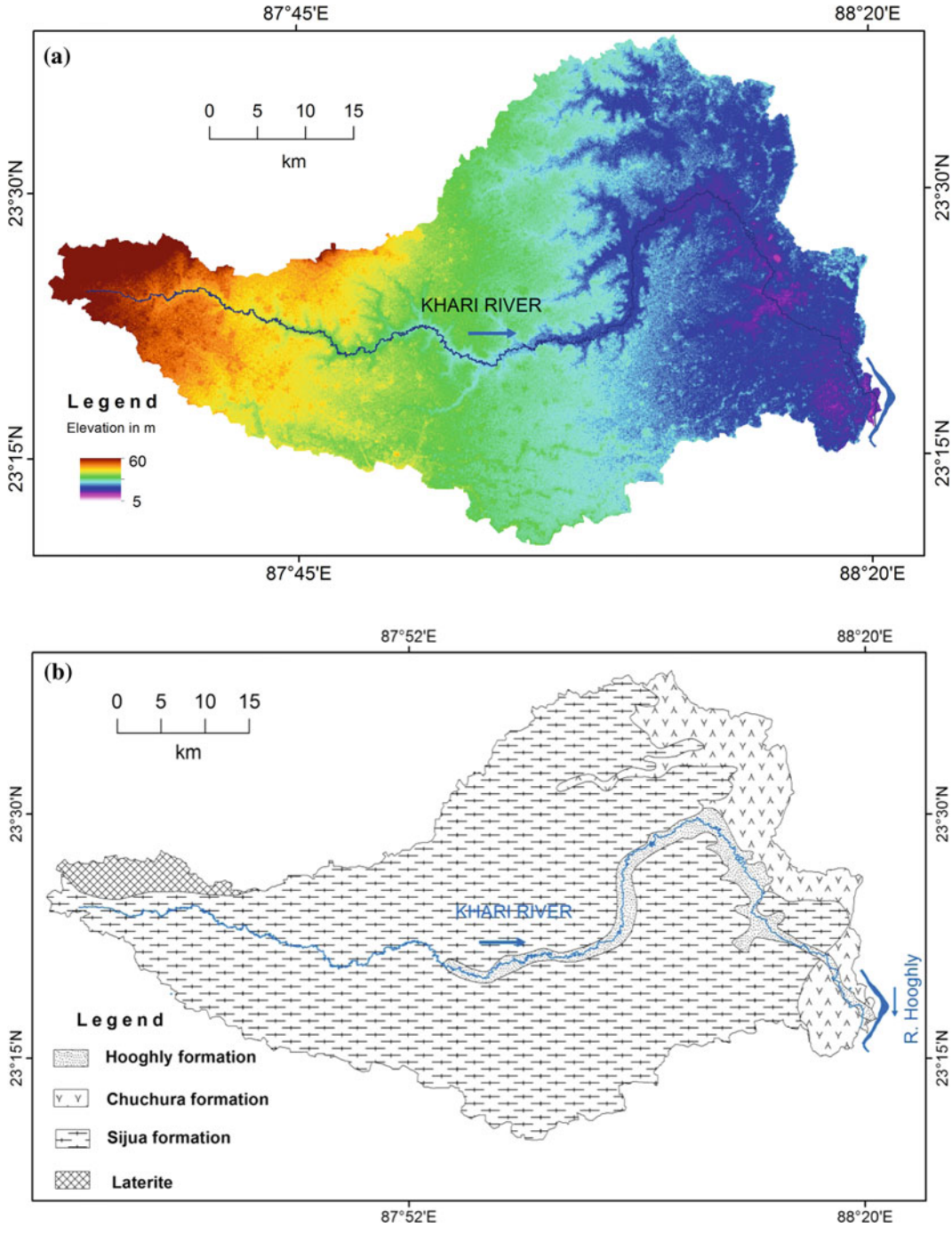

Fig. 6.2 **a** SRTM DEM of the study area. **b** Morpho-stratigraphic units of Khari river Basin (Barddhaman District Resource Map, GSI 2000)

sparsely oxidized sand, silt and clay with fining sequence. Hooghly formation, the youngest in age (Upper Holocene) is dominated by Point bar, and river terrace comprised of fine to coarse sand and silt with little clay.

6.3 Methodology

The present work has been carried out following a systematic methodology starting with the selection of the problem ultimately leading to unveiling the reality through a number of stages (Fig. 6.3).

6.3.1 Collection of Data

For conducting the present work, data have been collected from both the primary and secondary sources. Primary data have been collected on lithology, soft sediment structures (e.g. fluid escape, convolute), unpaired terrace, from field visit. The dimensions of the beds were measured by tape and the textural composition was determined in field by feel method. Soft sedimentary structures were excavated along the bank of river using geological hammer and normal trowel. The collection of field data was profusely helped by digital camera and normal Global Positioning System (GPS). Secondary data have been collected from Survey of India (SOI) Topographical maps of 1972 (79M/11, 79M/15, 79M/16 and 73A/2, 73A/3, 73A/6, 73A/7), Seismo-tectonic atlas (SEISAT-24) of India prepared by Geological Survey of India (GSI) , District Resource Map of Barddhaman prepared by GSI (2001), Shuttle Radar Topography Mission (SRTM) Digital Elevation Model (DEM) of 30 m resolution of United States Geological Survey (USGS) Earth explorer (https://earthexplorer.usgs.gov/) and Google Earth image (2017).

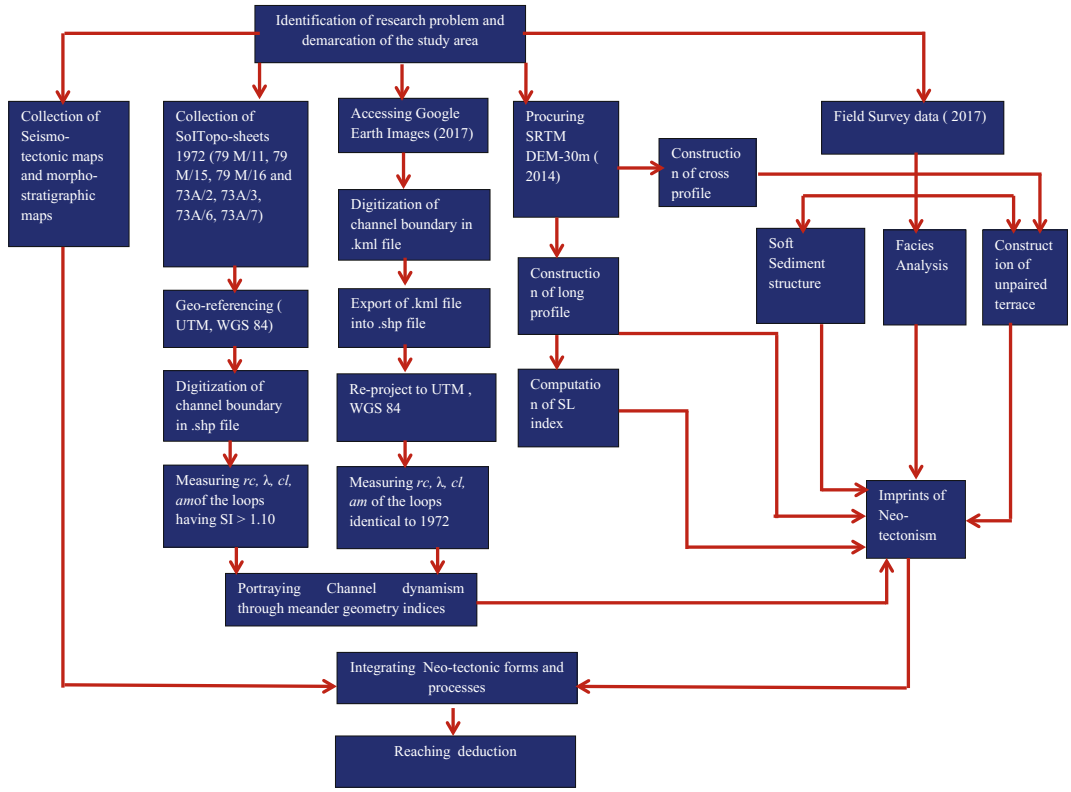

Fig. 6.3 Flow chart of methodology

6.3.2 Analysis of Meander Geometry

6.3.2.1 Selection of Loops

Meander loops have been selected according to their SI. Following Rosgen (1994), Zámolyi et al. (2010), Dey (2014), Islam and Guchhait (2017), those loops having SI > 1.10 in the 1972 topo-sheets have been considered for the present analysis. Thus, a total of 142 loops (Upper 92 taking 46 on each bank; Middle reach 38 taking 19 on each bank; and Lower Reach 12 talking 6 on each bank). The loops identical to 1972 have been selected for 2017 images irrespective of their SI for tracking any subtle changes in the loop geometry during 1972 and 2017.

6.3.2.2 Indices on Meander Geometry

(a) **Sinuosity index (SI)**

Sinuosity index (SI) is the most common and widely used measure of the intensity of meander or degree of convolution of a stream. There are several forms of sinuosity indices formulated by Leopold and Wolman (1957, 1960), Schumm (1963), Leopold et al. (1964), Leopold and Langbein (1966), Brice (1964, 1984), Stolum (2013). In this present study, sinuosity index (SI) was calculated using formulae devised by Leopold and Langbein (1966) as a simple ratio between channel length and wave length.

(b) **Radius-wavelength ratio *(r/λ)***

It is the ratio between radius of curvature (r) of a meander bend and wavelength (λ) of that meander and is defined as r/λ. If width of the channel is ignored, the ratio for a sine generated curve is 1:4 when centre of the curvature is on the m_{ax}. This ratio is a good measure to the intensity of meander. If centre of curvature and apex of loop is on opposite sides of the m_{ax}, intensity or degree of convolution of a meander is inversely proportional to the ratio. On the other hand, if centre of curvature and apex of loop is on the same side of the m_{ax}, intensity or degree of convolution of a meander is directly proportional to the ratio indicating the loop approaching towards neck cut-off.

(c) **Meander Shape Index *(S_mI)***

It is the dimension less measure of bend tightness and defined as the ratio between radius of curvature (r) and amplitude (a_m) of meander and expressed as follows:

$S_mI = r/a_m$ (Das 2014).
If wavelength λ is constant, intensity or degree of convolution of a meander is expressed by the value of the S_mI. Lesser the S_mI, more intense is the meander. When
$S_mI > 1$, it is open meander,
$S_mI = 1$, it is regular meander,
$S_mI = 0.5$, it is intense meander,
$S_mI < 0.5$, it is acute meander.

(d) **Meander form index (F_mI)**

It is the measure of degree of intensity or degree of curvature of a meander. It is defined as meander-amplitude (a_m) divided by wavelength (λ) and expressed as

$F_mI = a_m/\lambda$

If r remains constant, F_mI is proportional to the degree of intensity and curvature of meander. If

$F_mI < 0.25$, meander is open,
$F_mI = 0.25$, meander is regular sine curve,
$F_mI = 0.50$, meander is intense,
$F_mI = 1$, meander is acute,
$F_mI > 1$, meander is more acute towards neck cut-off.

(e) **Combined index of meander intensity (CIMI)**

In S_mI and F_mI, λ and r is conditional for understanding of the indices. Therefore, incorporation of conditional variables may strengthen

the measure. Therefore combined index of meander intensity (CIMI) is formulated as

$$\begin{aligned}\text{CIMI} &= \text{SI} \times \frac{1}{S_{\text{m}}I} \times F_{\text{m}}I \\ &= \frac{l}{\lambda} \times \frac{1}{\frac{r}{a_{\text{m}}}} \times \frac{a_{\text{m}}}{\lambda} \\ &= \frac{l}{\lambda} \times \frac{a_{\text{m}}}{r} \times \frac{a_{\text{m}}}{\lambda} \\ &= \frac{la_{\text{m}}^2}{r\lambda^2}\end{aligned}$$

6.3.3 Construction Long and Cross Profiles

Long profile and cross profiles both have been drawn from SRTM DEM data in ArcGIS. For long profile, first the entire stream length (~195 km) has been sub-divided into 100 m steam segments. Second, each 100 m segment has been converted into point feature. Third, point data have been interpolated from SRTM DEM. Finally a long profile has been graphed for Kari river taking 1996 elevation points (z). For cross profiling, an 'interpolate line' has been drawn followed by 'profile graph'.

6.3.4 Stream-length (SL) Index

A more celebrated methodology to determine stream-length index (Hack 1973a, b) or stream gradient index (Seeber and Gornitz 1983; Burbank and Anderson 2001), however, takes measurements in successive equal contour intervals ignoring directional variability along the river course.

$$\text{SL} = \left(\frac{\text{d}H}{\text{d}L}\right)L$$

where dH for variation of elevation, dL—the length of the segment, and L—total channel length from the midpoint of the segment where the index is calculated to the drainage divide.

6.4 Revelation of Neo-tectonism from Landform Distinctiveness in Conjunction with Drainage and Sedimentation—An Analysis

Tectonism creates and surficial processes modify earth's surface relief. The vertical component of plate-related movement is antecedent to topography, while erosion-deposition remoulds it. Exogenous sedimentary processes thus tend to obliterate topographic signature of tectonism. The extent of obliteration depends on the climate-related rate of erosion and how frequently tectonism interrupts the drift. Drainage and sedimentation are cogently affected. Tectonic signatures are, nevertheless, difficult to distinguish from effects of climate (Kober et al. 2013). The signature of neo-tectonism is, however, expected to be more readily obliterated in the chosen area because of wet climate. The huge data set generated in this study area will thus satisfy a long standing need. The study includes erection of digital elevation model for the study area, highlighting the different physical attributes of the said river course, determination of sinuosity of the latter, delineation of watershed basin, distinguishing drainage patterns and stream gradients and their corresponding stream lengths. Remote sensing helps reconstruct the multiphase histories of the said course belonging to the River Khari. However, only a few studies have focused on landscape development, conjunctively with the underlying relationship between landscape and structures. Facies analysis is taken recourse to reveal sedimentation dynamics. It is worth mentioning here that high-resolution facies analysis encompassing the testimony of architectural elements of genetic classification have been adopted in present study area and a detail

account of which has been represented in the following Sect. 6.4.2.1.

6.4.1 Landform Distinctiveness and Drainage

6.4.1.1 Changing Meander Geometry

Change in meander geometry indicates a distinct pattern of channel dynamism. For Kari river this change is remarkable which deserves a special treatment. Change in geometry has been portrayed through four basic variables (radius, amplitude, wavelength and channel length) and some ratio variables (Sinuosity index, radius-wavelength ratio, meander form index and meander shape index) discussed in the following sections.

Basic Variables

(a) **Radius of curvature (*r*)**

There is a direct relation between radius of curvature of a bend of meander and magnitude of volume of discharge and width of the channel. If wave length (λ) is constant, then smaller the radius of curvature, more intense is the meander (Das 2014). Average *r* for Khari river in 2017 (47.20 m) in comparison to 1972 (52.56 m) is decreased by 5.36 m. Radius of curvatures also found increased downstream (Fig. 6.4a, b). In 1972, average *r* for lower reach (122.23 m) was much higher than upper (39.74 m) and middle (61.56 m) reaches (Table 6.1). This is also a normal observation as channel width increases downstream and as per Leopold and Wolman (1960) there is nearly a constant ratio between *r* and λ and between *r* and *w*. The normal trend of downward increase of magnitude of radius of curvature was also recorded during 2017 also. During 2017, average *r* for upper reach was 36.16 m, for middle reach 48.62 m and for lower reach 127.38 m (Table 6.2).

(b) **Amplitude of meander (a_m)**

The vertical distance between crest and trough is called the peak-amplitude (A_m). River scientists often use A_m simply as amplitude. Physicists use the term 'amplitude' (a_m) to indicate half of the peak-amplitude which has been used in this paper. Amplitude used in this paper therefore is defined as the largest vertical distance of a bend apex along thalweg line from meander axis (m_{ax}). In this present study, average magnitude of amplitude of meander displayed a gradual increase from upper reach (79.99 m) via middle reach (138.24 m) to lower reach (223.13 m) in 1972 (Fig. 6.5a). The same trend was found in 2017 also (Fig. 6.5b). Average amplitude was 74.93 m at upper reach, 110.25 m at middle reach and 210.66 m at lower reach (Table 6.1). Spatial (upper, middle, lower reaches) variations in co-efficient of variation were not significantly different during 1972 (from 38.99 to 41.54). This fact appreciates the concept of 'scaled version' as channel width, the most stable variable of channel morphometry, increases downstream. But at present (in 2017), amplitude of meanders in middle reach with sub-surface fault and negative Bouguer's anomaly shows much more stability in magnitude (CV 51.99) in comparison to upper (CV 57.12) and lower (CV 50.38) reaches (Table 6.1).

(c) **Wave length (λ)**

Rivers are seldom straight through a distance greater than about ten channel widths (Leopold et al. 1992) and meandering is the obvious phenomenon of any natural river channels. Spatio-temporal changes in channel dynamics are well manifested through meander geometry and channel morphometry. Wavelength (λ) is one of the variables of meander geometry and is defined as crest to crest or trough to trough distance. A change in λ of a particular meander over time definitely indicates the dynamic nature of the

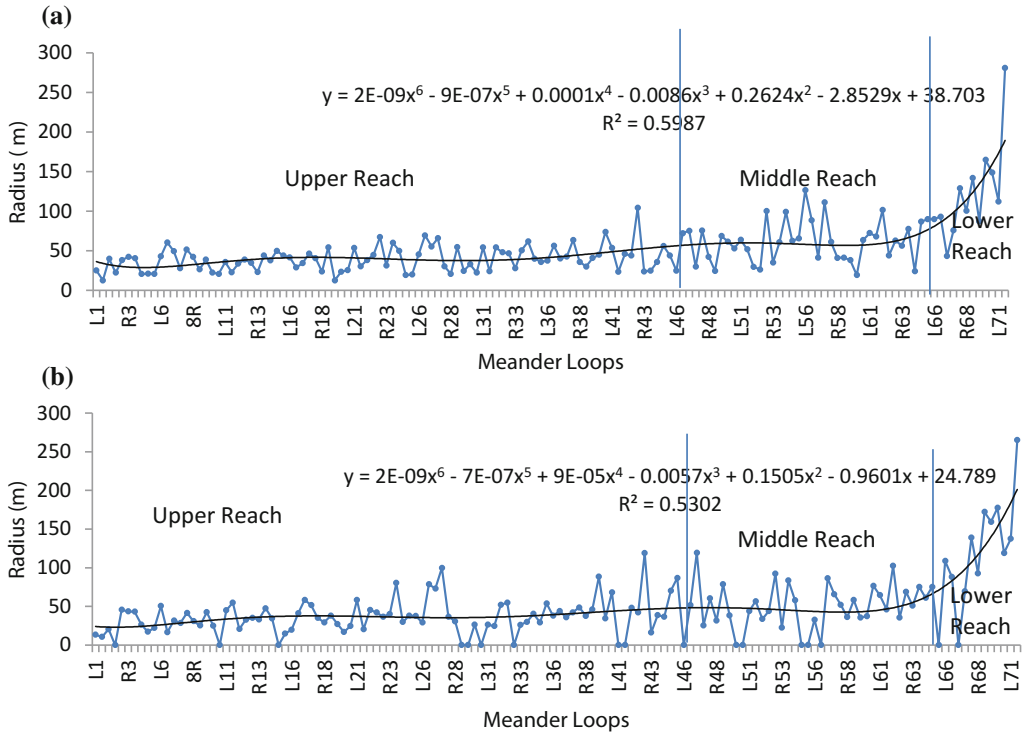

Fig. 6.4 **a** Spatio-temporal variation in radius (1972). **b** Spatio-temporal variation in radius (2017)

Table 6.1 Descriptive statistics of the basic variables

River reach	Descriptive statistics	Radius		Amplitude		Wave length		Channel length	
		1972	2017	1972	2017	1972	2017	1972	2017
Upper	Mean	39.74	36.16	79.99	74.93	184.18	155.49	376.85	380.63
	S.D	15.78	22.58	31.19	42.80	73.87	87.47	131.97	210.37
	C.V.	39.72	62.45	38.99	57.12	40.11	56.26	35.02	55.27
Middle	Mean	61.56	48.62	138.24	110.25	277.17	229.21	634.24	540.47
	S.D.	26.23	30.29	54.32	57.32	100.71	138.49	195.82	271.17
	C.V.	42.61	62.29	39.3	51.99	36.33	60.42	30.87	50.17
Lower	Mean	122.33	127.38	223.13	210.66	550.13	574.07	1179.97	1181.35
	S.D.	60.56	65.72	92.69	106.13	288.96	324.89	408.32	515.61
	C.V.	49.51	51.59	41.54	50.38	52.53	56.59	34.6	43.65

Computed from the topographical maps (1972) Google Earth images (2017). N.B: Mean and standard deviation (S.D.) in metre and coefficient of variation (C.V.) in %

channel. There is a general and obvious increase in wavelength of meander towards downstream due to gradual downstream increase in magnitude of other hydro-morphometric variables like width (w) and average depth (d) of the channel and discharge (Cotton 1952; Schumm 2005). This is because meander properties of different rivers are 'scaled version' of same set of

Table 6.2 Descriptive statistics of the ratio variables

River reach	Descriptive statistics	Sinuosity index		Radius-wave length ratio		Meander shape index		Meander form index	
		1972	2017	1972	2017	1972	2017	1972	2017
Upper	Mean	2.2	2.30	0.24	0.23	0.53	0.48	0.48	0.46
	S.D.	0.85	1.23	0.11	0.13	0.19	0.31	0.25	0.26
	C.V.	38.59	53.68	46.74	59.62	35.91	63.73	51.99	57.67
Middle	Mean	2.6	2.20	0.25	0.19	0.47	0.38	0.62	0.45
	S.D.	1.4	1.30	0.16	0.13	0.19	0.22	0.54	0.28
	C.V.	53.67	59.29	64.21	65.70	40.05	58.79	87.75	62.54
Lower	Mean	2.53	2.11	0.26	0.22	0.63	0.62	0.51	0.38
	S.D.	1.29	1.16	0.14	0.11	0.44	0.42	0.34	0.24
	C.V.	51.03	55.11	54.24	49.89	69.83	67.66	67.37	62.65

Computed from the topographical maps (1972) Google Earth images (2017). N.B: Mean and standard deviation (S.D.) in metre and coefficient of variation (C.V.) in %

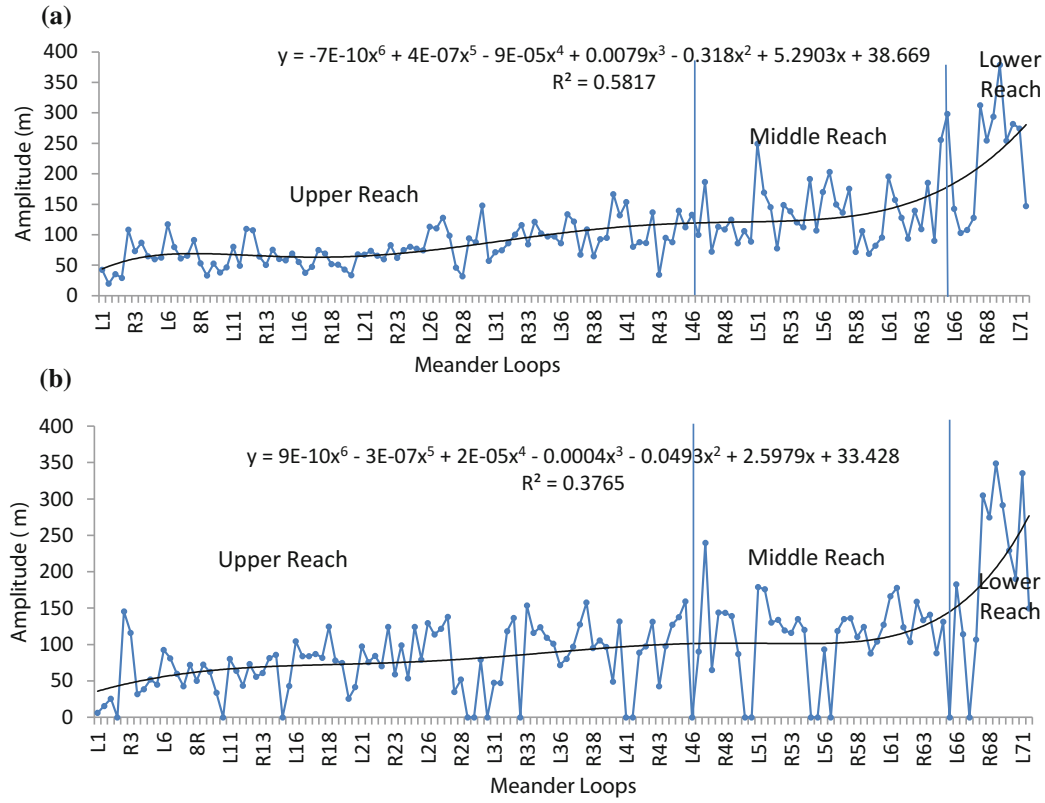

Fig. 6.5 **a** Spatio-temporal variation in amplitude (1972). **b** Spatio-temporal variation in amplitude (2017)

geometric variables (Leopold and Wolman 1960; Shahjahan 1970) and this is true for meanders of different reach of the same river.

Average magnitude of λ of meander showed a gradual increase (Fig. 6.6a) from upper reach (184.18 m) via middle reach (277.17 m) to lower

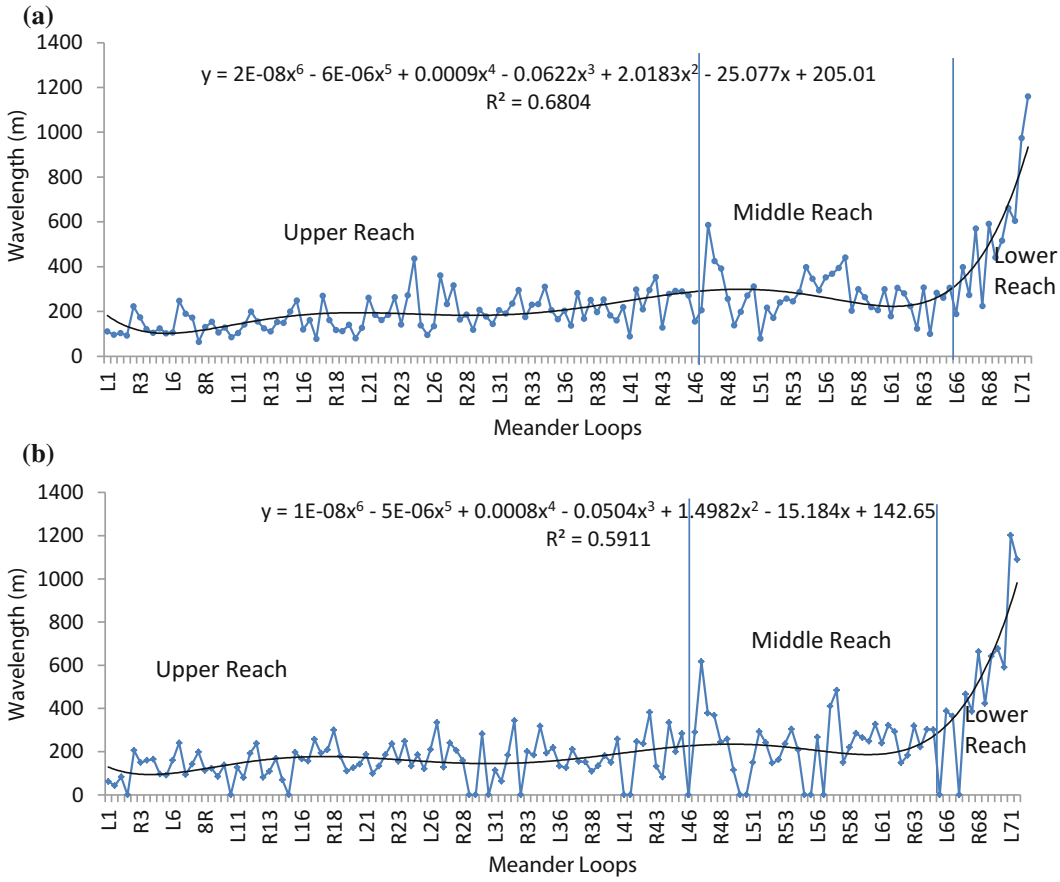

Fig. 6.6 **a** Spatio-temporal variation in wavelength (1972). **b** Spatio-temporal variation in wavelength (2017)

reach (550.13 m) in 1972 (Table 6.1). The same trend was found in 2017 also (Fig. 6.6b). Magnitudes were 155.49 m at upper reach, 229.21 m at middle reach and 574.07 m at lower reach. Spatio-temporal (upper, middle, lower reaches; in 1972 and 2017) variation in co-efficient of variation is the least for middle reach (36.33 in 1972 and 56.21 in 2017) (Table 6.1) which is most affected by sub-surface fault and displayed negative Bouguer's anomaly.

(d) Channel length per Loop (*l*)

Channel length or loop-wise channel length (*l*) is the length along thalweg line of the channel segment confined within a meander loop either to the left or to the right side of the meander axis. There was an increase in average length of channel per loop in 2017 in comparison to 1972 for all the three reaches (Fig. 6.7a, b). CV for length of channel per loop in 1972 was 30.87 (lowest) at middle reach and 35.02 (highest) at upper reach (Table 6.1). But in 2017, middle reach with tectonically significant substrate, became considerably unstable and CV increased to 50.17.

Ratio Measures

(a) Sinuosity index (SI)

Average sinuosity index in the year 1972 was 2.34 and in 2017 it was 2.26 (Table 6.2). Although some meander necks have been cut-off and detached from the river after 1972, yet the river again convoluted to SI of 2.26 at present (2017). This indicates the unrest, active and oscillating nature of the river. However, during

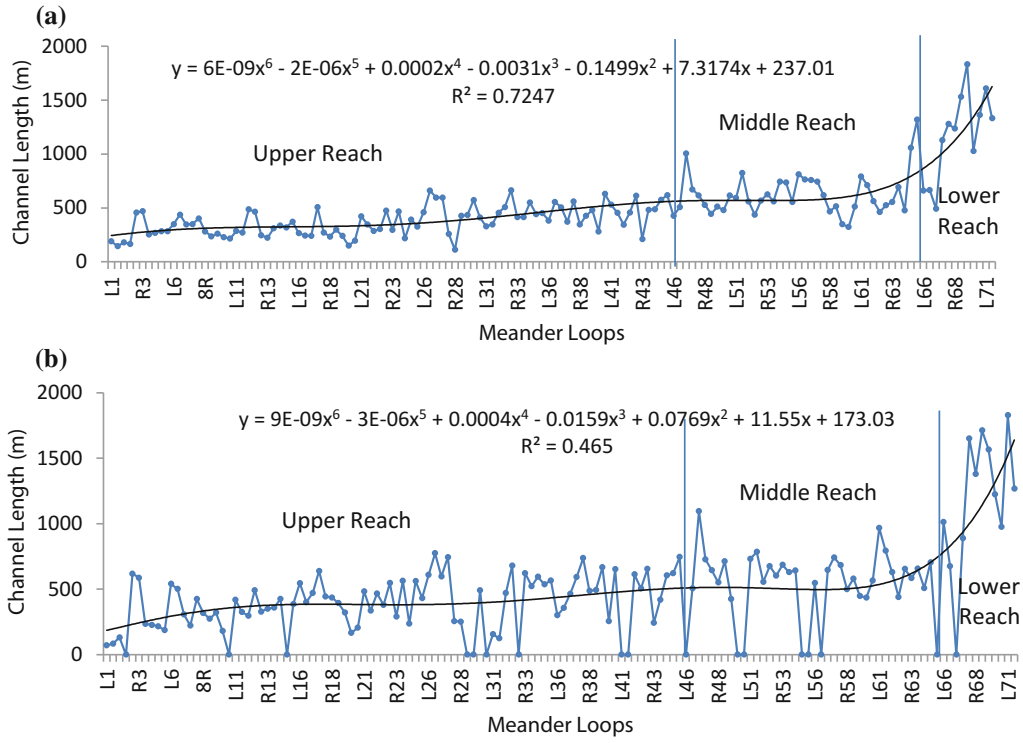

Fig. 6.7 **a** Spatio-temporal variation in channel length (1972) **b** Spatio-temporal variation in channel length (2017)

1972, SI was the maximum at middle reach (Fig. 6.8a), the reach most affected by negative Bouguer's anomaly and the presence of sub-surface faulting. But during 2017, SI at lower reach was reduced to 2.11 what was 2.53 during 1972 (Table 6.2). This indicates the phenomena of occurrence of cut-off of meander loops between these two periods. SI have been increased from 2.20 in 1972 to 2.30 in 2017 at upper reach and 2.60 in 1972 to 2.11 in 2017 at lower reach (Table 6.2). Even after neck cut-off of meanders, this increase in SI indicates active unrest nature of the channel.

(b) Radius-wavelength ratio (r/λ)

At upper reach of the Khari river, average ratio was decreased from 0.24 in 1972 to 0.23 in 2017. It indicates the phenomena of loop cut-off and it was found that during this time span, 10 cut-offs took place in this reach. During 1972, the average value of the ratio was near the value of a sine generated curve (0.25). For middle reach, average ratio was as like as perfect sine generated curve (0.25) in 1972 which was reduced to 0.19 in 2017 (Table 6.2). As S_mI of middle reach for the year was less than 0.5, it indicates the occurrence of loop apex and centre of curvature to the opposite sides of the m_{ax}. Therefore, reduced r/λ ratio in 2017 indicates relatively less intense meanders. In case of lower reach, r/λ ratio has been reduced from 0.26 in 1972 to 0.22 in 2017 but S_mI decreased from 0.63 to 0.62 (Table 6.2). These indicate the intense form of meander as well as very dynamic nature of the channel reach (Fig. 6.9).

(c) Meander shape index (S_mI)

Average S_mI for Khari river was 0.52 during 1972 and 0.46 during 2017 (Table 6.2). It indicates higher degree of convolution of meander (Fig. 6.10a, b). In 1972, averages of S_mI were 0.53 and 0.63 at upper reach and at lower reach

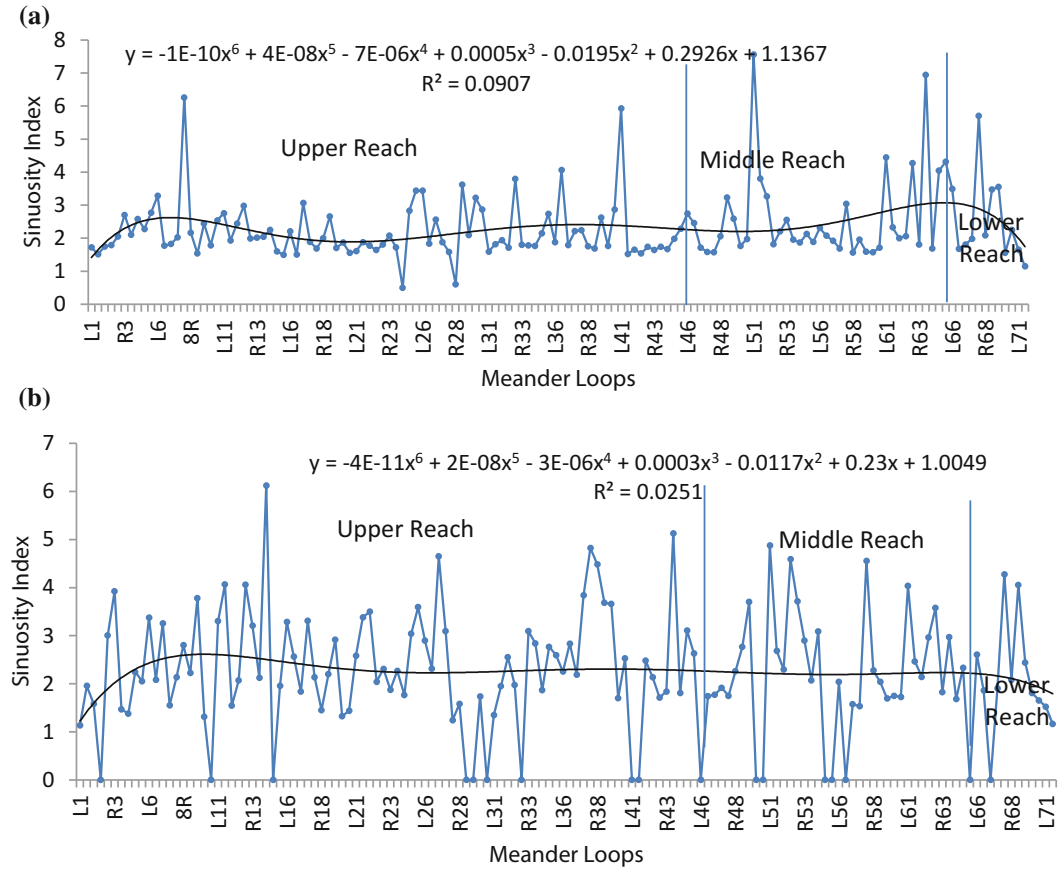

Fig. 6.8 **a** Spatio-temporal variation in sinuosity index (1972). **b** Spatio-temporal variation in sinuosity index (2017)

respectively (Table 6.2), which indicate intense nature of meander. At middle reach, the reach with −ve Bouguer's anomaly and sub-surface faulting, S_mI was 0.47 which indicates acute meanders. After 1972, meander necks were cut-off. Even then in 2017, S_mI at middle reach is reduced further to 0.38 indicating acute nature of meander (Table 6.2).

(d) Meander Form Index (F_mI)

Averages F_mI of Khari river in 1972 and 2017 were 0.52 and 0.45 respectively with a very little difference (0.07). In 1972, averages of F_mI at upper, middle and tail reaches were 0.48, 0.62 and 0.51 respectively indicating intense nature of meander curvature (Fig. 6.11a). In 2017, the values were 0.46, 0.45 and 0.38 (Table 6.2) respectively indicating relatively less intensity of meander curvature or experience of previous cut-off.

(e) Combined index of meander intensity (CIMI)

Meander intensity or degree of convolution of tortuous channel may be well snapped if several measures are blended together. Sinuosity index is the best measure for the degree of intensity or degree of convolution of meander. But whether the meander is approaching towards neck cut-off or how far from the ultimate fate is hardly configured in the index. That is why CIMI was formulated.

Higher CIMI for 2017 in comparison to 1972 indicates higher degree of intensity of meander

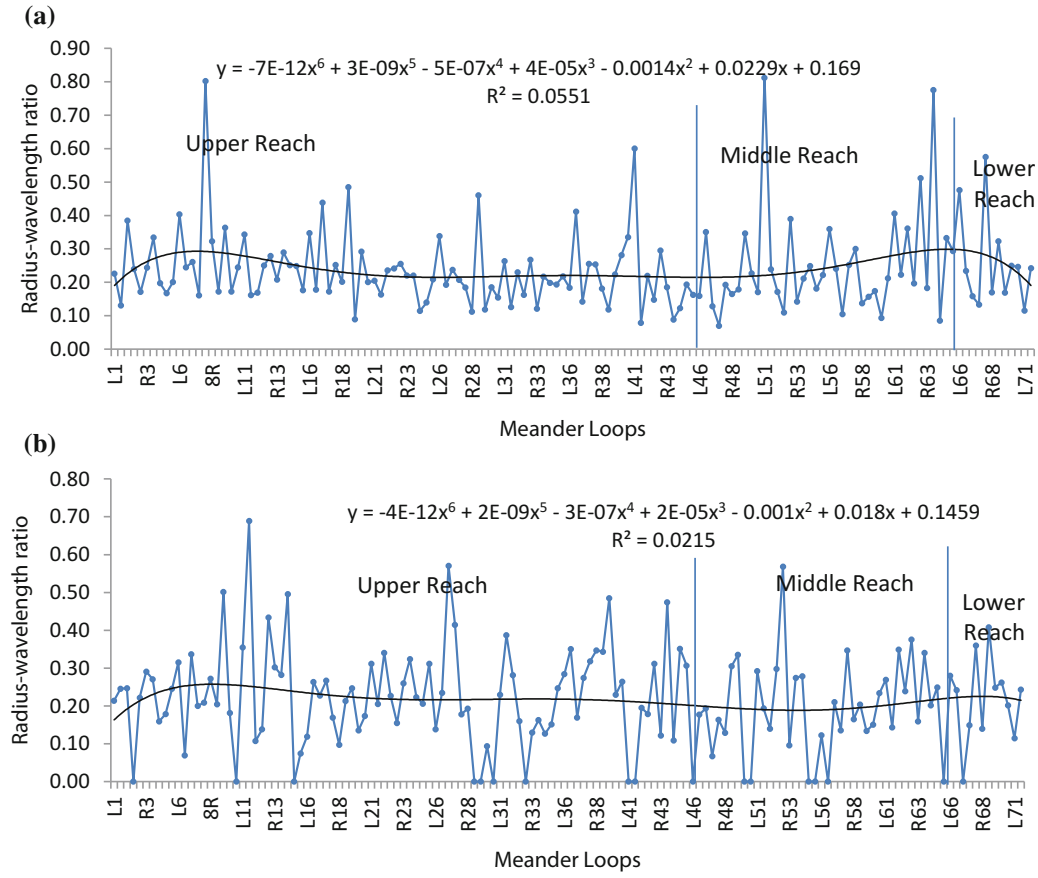

Fig. 6.9 **a** Spatio-temporal variation in radius-wavelength ratio (1972) **b** Spatio-temporal variation in radius-wavelength ratio (2017)

bends in 2017 (Table 6.3). Another interesting observation is that in both 1972 and 2017, CIMI is higher in middle reach which is set over the base with sub-surface fault and −ve Bouguer's anomaly. This observation indicates control of sub-surface geology over fluvial forms and processes.

6.4.1.2 Stream-Length Index or Stream Gradient Index

A more celebrated methodology to determine stream-length index (Hack 1973a, b) or stream gradient index (Seeber and Gornitz 1983; Burbank and Anderson 2001), however, takes measurements in successive equal contour intervals ignoring directional variability along the river course.

Rivers generally tend to acquire concave-up profile, especially in their downstream parts because of increasing contributions from tributaries. Against this background, convex-up geometry of the hypsometric curve of the Khari River studied herein, especially at their downstream ends points to possible influence of regional tectonics. The *H–L* (semi-logarithmic) plots or the Hack's profiles clearly document downstream fluctuations in channel-gradient along the present endeavour. The concavo–convex geometry of the Hack's profile manifests significant spatial change/s in pattern of disequilibrium with respect to the graded profile. This change without any lithologic correspondence can hardly be explained by climate which is a regional feature; a role of differential effect of

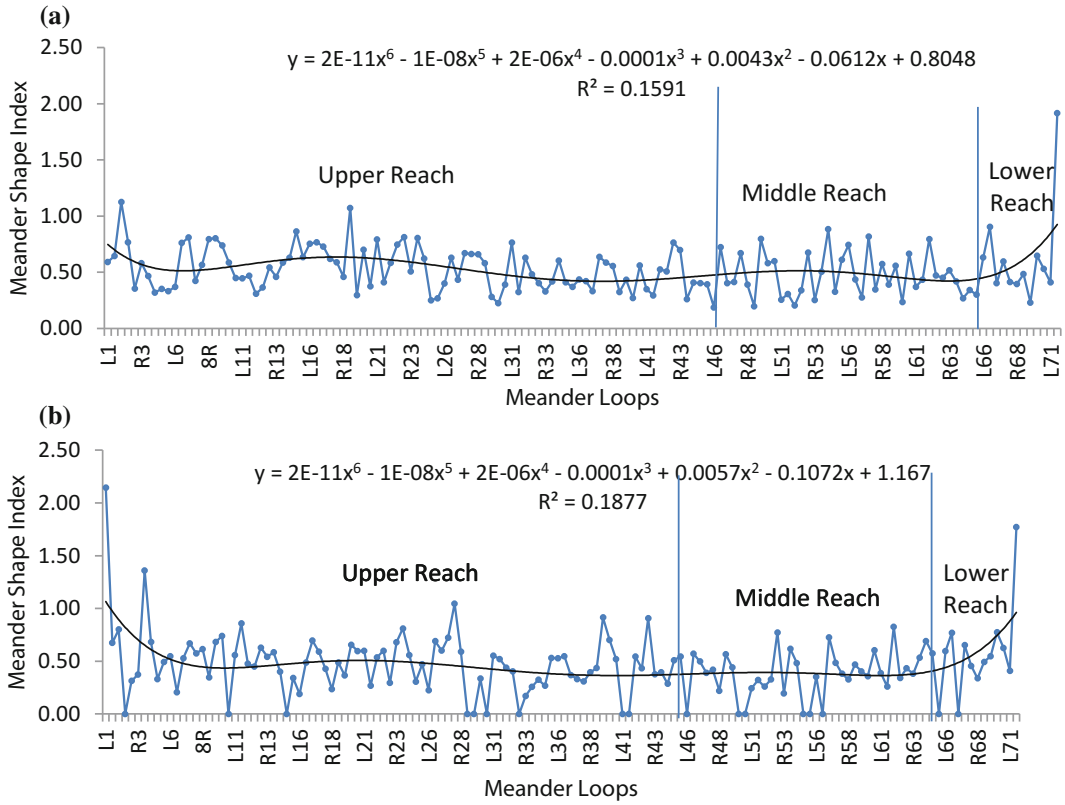

Fig. 6.10 **a** Spatio-temporal variation in meander shape index (1972). **b** Spatio-temporal variation in meander shape index (2017)

tectonics cannot be denied (Brookfield 1998). Apparently the basement uplift rate had been laterally differential; the marked part (*) was uplifted comparatively at a faster rate which has been evidently shown the relation with the adjacent Damodar fault (Fig. 6.12). Significantly this disequilibrium manifestation of graded profile can be explained with the association of different sub-surface faults represented by seismotectonic map encompassing Bouguer anomaly (Fig. 6.13).

Marked downstream steepening of Hack's profile across the faults is a common feature for the studied river and without correspondence to regional lithological change testifies the tectonic effect.

The SL profile, nevertheless, rises at basement for the river studied here without any regard to lithologic change and that unambiguously points to neo-tectonism.

6.4.1.3 Unpaired Terrace

The river channel in the present endeavour is no more aggradational, but deeply incisive. The river cuttings are now present as wind gaps and the active channel banks are sculpted by multi-generational terraces, predominantly unpaired (Fig. 6.14) which again is a distinct manifestation of neo-tectonism.

6.4.2 Sedimentological Aspects

6.4.2.1 Facies Analysis

Lithologically unconsolidated quaternary sediment constituting the studied herein is entirely

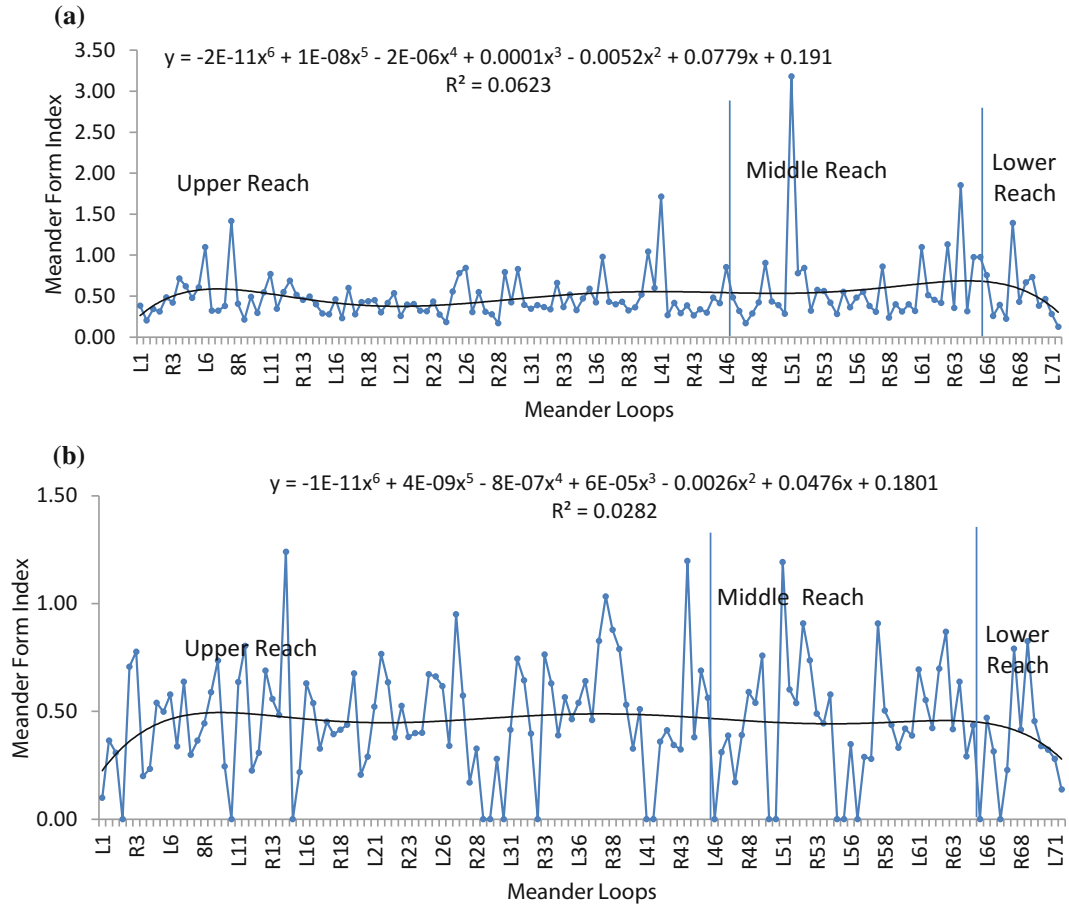

Fig. 6.11 **a** Spatio-temporal variation in meander form index (1972). **b** Spatio-temporal variation in meander form index (2017)

Table 6.3 Average CIMI of the meander loops

Reach	$\frac{la_m^2}{r\lambda^2}$	
	1972	2017
Upper	3.58	5.20
Middle	5.12	5.30
Lower	3.18	2.50

Source Computed from the topographical maps (1972) Google Earth images (2017)

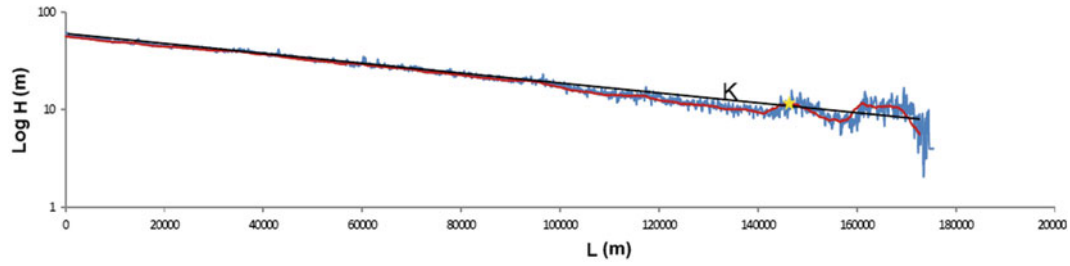

Fig. 6.12 Semilogarithmic plot of H (elevation) against *L* (stream length) variations along the said river. The graded profile is represented by the straight line and gradient index is marked by K studied herein. The fault is indicated by the star symbol. Computed from SRTM DEM

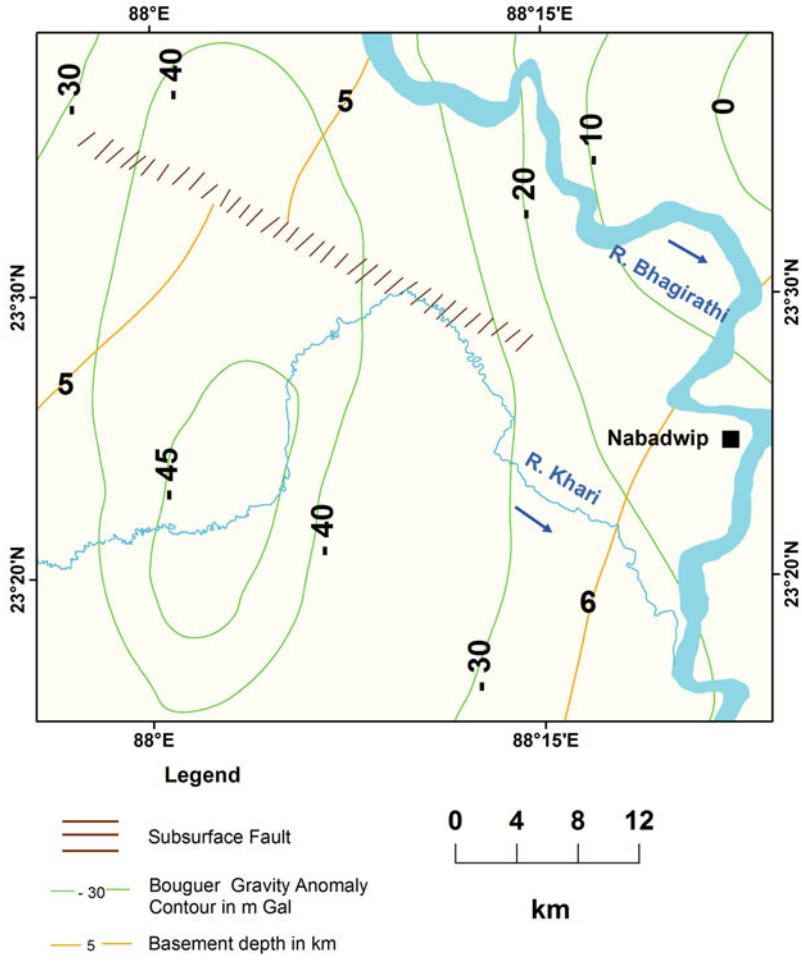

Fig. 6.13 Seismotectonic map of lower Khari river basin. *Source* GSI, 2001

siliciclastic, ranging from sand to mud. Altogether five distinctive facies have been recognized; the large spectral variation in their character reflects large variation in sedimentation dynamics through space and time. The facies designation adopted in this section following Miall (1985). All the facies are described and interpreted below

Facies designation	Facies name	Facies description	Facies interpretation
Sh	Planar laminated sand	Planar laminated sand with sheet-like or tabular geometry (Fig. 6.15c)	Sheet flow product, possibly generated by reworking of bar-top sediment during falling water stage
Sl	Planar laminated fine-grained sand periodically interrupted by silt stringes	This facies is of fine-grained sand internally characterized by stacked up sets of planar laminae separated from each other by low angle silt drapes (Fig. 6.15a)	This facies resemble levee deposits. The fine-grained nature of the sediment suggests deposition away from channel thalweg and on channel bank. The successive low angle silt laminae manifest periodic levee accretion
St	Trough cross-stratified Sand	This facies is trough cross-stratified in sand, completely or nearly pebble-free (Fig. 6.15e)	This facies is inferred as deposit within small channels. This facies presumably formed under relatively lower flow intensity than the facies Sl
Fl	Ripple laminated silt	This facies is made of silt internally characterized by small scale trough x-strata and appear to have sheet-like geometry within outcrop limit. At places root-moulds abound within this facies (Fig. 6.15d)	It is an obvious product of low energy domain, possibly in the overbank region. This contention is corroborated by its common association with overbank mud. Besides, local abundance of root-moulds further corroborates the scheme of deposition envisaged
Fr	Mud	This facies is characterized by mud bodies having tabular geometry; however, their surfaces may be knobby, They may bear fine planar laminae but more often than not look massive and bear many root casts. Rootlets often concentrate along the top surfaces of the beds. Multiple units of this facies may stack up vertically (Fig. 6.15b)	This is low energy product of overbank origin; the contention is further corroborated by the presence of rootcasts. Preferred concentration of rootlets along bed top surfaces suggests existence of omission surfaces, perhaps representing intervals between successive floods. The vertical stacking of this facies manifests subsidence

6.4.2.2 Soft Sediment Structures

Plenty of soft sediment deformation structures (Seth et al. 1990; Sarkar et al. 1995, 2002) are found scattered within the sediment piles constituting the studied herein. They are of varied kinds: fluid escape, single-lobated convolute, multi-lobated convolute, imbricated convolute, contorted laminae, sag and pseudonodule structures (Fig. 6.16a, b). Preferred concentration of these structures, nonetheless, along the contacts between successive episodic phases. Such concentrations of soft sediment deformation structures are most conspicuous (Fig. 6.16a, b) and having lateral extent of same stratigraphic level, encompassing the entire watershed basin. Such conspicuous concentration as well as wide lateral

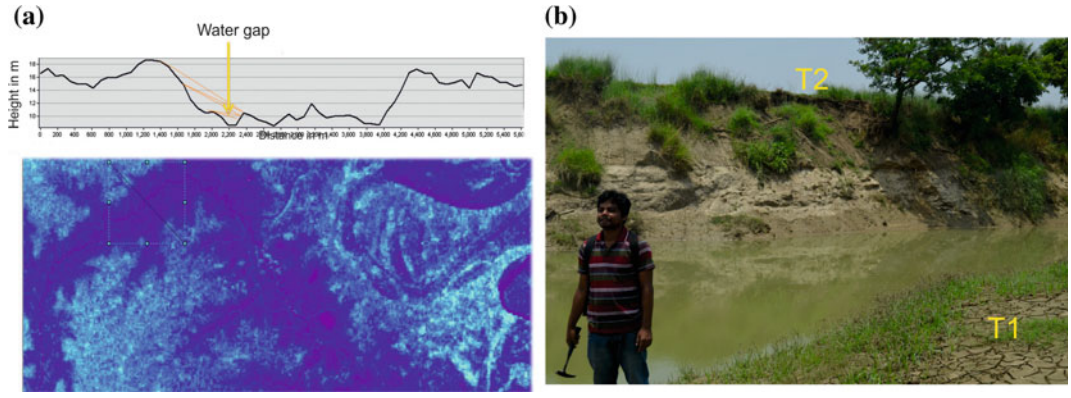

Fig. 6.14 **a** Transverse valley profile of the river Khari sculpted by unpaired terraces connected by dashed lines. Altitudes are shown in metres. **b** Field photograph of unpaired river terraces

Fig. 6.15 Field photographs of few distinctive facies with designations: **a** Planar laminated fine-grained sand with intermittent silt stringes (Sl) **b** Muddy with rootcasts (Fr) **c** Planar laminated sand (Sh) **d** Ripple laminated silt (Fl) **e** Trough cross-stratified sand (St)

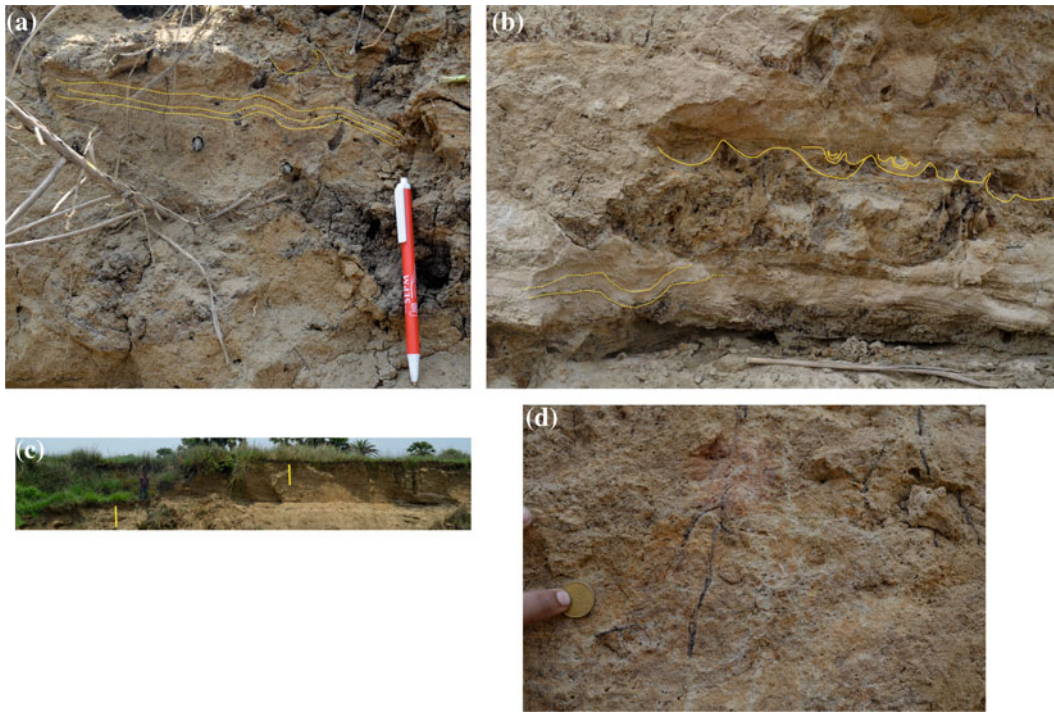

Fig. 6.16 Various types of Soft-deformational structures along the fan systems shown here as imprint of tectonic jerking: **a** Contorted laminae and fluid escape structure **b** Contorted laminae and multi-lobated convolute **c** Ferruginous crust marked by yellow head arrows **d** Rootlet

extent of soft sediment deformation structures in the said river section further corroborates the effect neo-tectonism.

6.5 Conclusion

Neo-tectonism is an ongoing process which has steadied the evolution of Khari river basin marked by its intensified growth of steam meandering. During 1972–2017, the average sinuosity has decreased with time due to ten cut-offs. This dictates a clear pattern of unstable and frequently changing river behaviour which has striated the channel to a certain extent. The reach-wise analysis of meander geometry depicts that the middle reach of this river is more unstable than its lower or upper counterpart due to the effect of structural control (negative Bouguer anomaly coupled with the presence of sub-surface fault). Variations in stream gradient indices along channels of the rivers, without correlatable lithologic changes, clearly testify dominant tectonic control on landform and drainage. Ferruginous crusts, scouring surfaces and rootlet concentrations at many stratigraphic levels is in accordance with generally discontinuous sedimentation on alluvial plains, but their lateral persistence over a distance of ~195 km stimulates the perception of regional hiatuses of probable tectonic implication. It has been further corroborated by the conspicuous concentration as well as wide lateral extent of soft sediment deformation structures in the said river section. Deep incisions made by the present-day river on the plains with unpaired terraces, nonetheless, imply recent change in condition favouring degradation instead of aggradation.

N. B. For special understanding on influence of faulting on the extra-channel geomorphology of the Ajay-Damodar interfluve readers may go

through Chap. 4 of this volume. Imprint of neo-tectonism and other geophysical control on channel pattern adjustment is well picturized in Chap. 5 of this volume.

References

Agarwal K, Singh I, Sharma M, Sharma S, Rajagopalan G (2002) Extensional tectonic activity in the cratonward parts (peripheral bulge) of the Ganga Plain Foreland Basin, India. Int J Earth Sci 91(5):897–905

AGI (2009) Glossary of geology. American Geological institute, Washington, D.C., online version. www.agiweb.org. Accessed Nov 2009

Akter J, Sarker MH, Popescu L, Roelvink D (2016) Evolution of the Bengal Delta and its prevailing processes. J Coast Res 321:1212–1226

Ashley GH (1931) Our youthful scenery. Geol Soc Am Bull 42:537–546

Bil M (2002) The identification of neotectonics based on changes of valley floor width. Landform Anal 3:77–85

Brice JC (1964) Channel patterns and terraces of the Loup rivers in Nebraska, U.S. Geological Survey, Prof. Paper 422D. In: Morisawa M (1968) Streams: their dynamics and morphology. McGraw Hill Book Co., New York, p 138

Brice JC (1984) Planform properties of meandering river. In: Elliott CM (ed) Proceedings of the conference of river meandering'83. American Society of Civil Engineers, New Orleans, Louisiana, pp 393–399

Brookfield ME (1998) The evolution of the great river systems of southern Asia during the Cenozoic India-Asia collision: rivers draining southwards. Geomorphology 22:285–312

Burbank DW, Anderson RS (2001) Tectonic geomorphology. Blackwell Scientific, Oxford, p 270

Cotton CA (1952) Geomorphology an introduction to the study of landforms. Wiley, New York, p 100

Cremon ÉH, Rossetti DD, Sawakuchi AD, Cohen MC (2016) The role of tectonics and climate in the late quaternary evolution of a Northern Amazonian River. Geomorphology 271(15), 22–39

Cunha PP et al (2005) Tectonic control of the Tejo river fluvial incision during the late Cenozoic, in Ródão—central Portugal (Atlantic Iberian border). Geomorphology 64:271–298

Das BC (2014) Two indices to measure the intensity of meander. In: Singh RB, Hassan MI (eds) Advances in geographical and environmental sciences, pp 233–246

Dar RA, Chandra R, Romshoo SA (2013) Morphotectonic and lithostratigraphic analysis of intermontane Karewa Basin of Kashmir Himalayas, India. J Mt Sci 10(1):1–15

Dey S (2014) Fluvial processes: meandering and braiding. In: Fluvial hydrodynamics. GeoPlanet: earth and planetary sciences. Springer, Berlin, Heidelberg

Ghosh S, Islam A (2016) Quaternary alluvial stratigraphy and palaeoclimatic reconstruction in the Damodar River Basin of West Bengal. In: Das B, Ghosh S, Islam A, Ismail M (eds) Neo-Thinking on Ganges-Brahmaputra Basin Geomorphology. Springer Geography. Springer, Cham

Goodbred SL Jr (2003) Response of the Ganges dispersal system to climate change: a source-to-sink view since the last interstade. Sed Geol 162(1–2):83–104

Goodbred JS, Kuhel SA (2000a) Enormous Ganges-Brahmaputra sediment load during strengthened early Holocene monsoon. Geology 28(12):1083–1086

Goodbred SL Jr, Kuhel SA (2000b) The significance of large sediment supply, active tectonism, eustasy on the margin sequence development: late quaternary stratigraphy and evolution of the Ganges-Brahmaputra Delta. Sed Geol 133(3–4):227–248

Goswami C (2011) Tectonic control on the drainage system in a piedmont region in tectonically active eastern Himalayas. Front Earth Sci. https://doi.org/10.1007/s11707-012-0297-z

Hack JT (1973a) Drainage adjustments in the Appalachians. In: Marisawa M (ed) Fluvial geomorphology. State University of New York, Binghamton, NY, pp 51–69

Hack JT (1973b) Stream profile analysis and stream-gradient index. J Res US Geol Sur 1(4): 421–429

Islam A, Guchhait SK (2017) Analysing the influence of Farakka Barrage Project on channel dynamics and meander geometry of Bhagirathi river of West Bengal, India. Arab J Geosci 10(11)

Kober F, Zeilinger G, Ivy-Ochs S, Dolati A, Smit J, Kubik PW (2013) Climatic and tectonic control on fluvial and alluvial fan sequence formation in the Central Makran Range, SE-Iran. Global Planet Change 111:133–149

Lahiri S (1996) Channel pattern as signature of neotectonic movements—A Case study from Brahmaputra Valley in Assam. J Indian Soc Remote Sens 24 (4):265–272

Latrubesse EM, Franzinelli E (2002) The Holocene alluvial plain of the middle Amazon River, Brazil. Geomorphology 44(3–4):241–257

Leopold LB, Langbein WB (1966) River meanders. Sci Am 214(6):60

Leopold LB, Wolman MG (1957) River channel patterns-braided, meandering and straight. U.S. Geological Survey, Prof. Paper 282B. In: Morisawa M (1968) Streams: their dynamics and morphology. McGraw Hill, New York, p 138

Leopold LB, Wolman MG (1960) River meanders. Bull Geol Soc Am 71:774. In: Julien PY (1985) Planform geometry of meandering alluvial channels. Civil Engineering Department, Engineering Research Center, Colorado State University, p 6

Leopold LB, Wolman MG, Miller JP (1964) Fluvial processes in geomorphology. W.H. Freeman and Company, San Francisco and London, p 281

Leopold LB, Wolman MG, Miller JP (1992) Fluvial processes in geomorphology. Dover Publications Inc., New York, p 281

Mats VD, Khlystov OM, Batist MD, Ceramicola S, Lomonosova TK, Klimansky A (2000) Evolution of the academician ridge accommodation zone in the central part of the baikal rift, from high-resolution reflection seismic profiling and geological field investigations. Int J Earth Sci 89(2):229–250

Miall AD (1985) Architectural element analysis: a new method of facies analysis applied to fluvial deposits. Earth Sci Rev 22:261–308

Perucca LP et al (2013). Morphotectonic and neotectonic control on river pattern in the Sierra de la Cantera piedmont, central Precordillera, province of San Juan, Argentina. Geomorphology. https://doi.org/10.1016/j.geomorph.2013.09.014

Radoane M et al (2003) Geomorphological evolution of longitudinal river profiles in the Carpathians. Geomorphology 50:293–306

Rosenau MR (2014) Tectonics of the Southern Andean intra-arc zone (38°–42°S). An unpublished PhD dissertation. Free University of Berlin, Department of Geosciences, Berlin

Rosgen DL (1994) A classification of natural rivers. Catena 22(3):169–199

Roy S, Sahu AS (2015) Quaternary tectonic control on channel morphology over sedimentary low land: a case study in the Ajay-Damodar interfluve of Eastern India 6(6):927–946

Sarkar S, Banerjee S, Chakraborty S (1995) Synsedimentary seismic signature in Mesoproterozoic Koldaha Shale, Kheinjua formation, central India. Indian J Earth Sci 22:158–164

Sarkar S, Chakraborty S, Banerjee S, Bose PK (2002) Facies sequence and cryptic imprint of sag tectonics in late Proterozoic Sirbu Shale, central India. In: Altermann W, Corcoran P (eds) Precambrian sedimentary environments: a modern approach to ancient depositional systems. Special publication of the International Association of Sedimentologists, No. 33. Blackwell Science, pp 369–382

Sarkar A, Sengupta S, McArthur JM, Ravenscroft P, Bera MK, Bhusan R et al (2009) Evolution of Ganges-Brahmaputra western Delta plain: clues from sedimentology. Quatern Sci Rev 28:2564–2581

Schumm SA (1963) Sinuosity of alluvial rivers of the great plains. Geol Soc Ma Bull 74:1089–1100. In: Morisawa M (1968) Streams: their dynamics and morphology. McGraw Hill Book Co., p 138

Schumm SA (2005) River variability and complexity. Cambridge University Press, Cambridge, p 65

Seeber L, Gornitz V (1983) River profiles along the Himalayan arc as indicators of active tectonics. Tectonophysics 92:335–367

Sen PK (1976) A study of the hydrological characteristics of the Banka Basin. Indian J Power Valley Develop, pp 353–358 (November, Calcutta)

Sen PK (1978) Evaluation of the hydrogeomorphological analysis of the Bhagirathi-Hooghly and Damadar interfluve: UGC research project. Department of Geography, The University of Burdwan

Seth A, Sarkar S, Bose PK (1990) Synsedimentary seismic activity in an immature passive margin basin, lower member of Katrol Formation, Upper Jurassic, Kutch, India. Sed Geol 68:279–291

Shahjahan M (1970) Factors controlling the geometry of fluvial meanders. Int Assoc Sci Hydrol B 15(3):13–24

Shukla UK, Bora DS, Singh CK (2009) Geomorphic positioning and depositional dynamics of river systems in lower Siwalik Basin, Kumaun Himalaya. J Geol Soc India 73:335

Silver CRP, Murphy MA, Taylor MH, Gosse J, Baltz T (2015) Neotectonics of the western Nepal fault system: implications for Himalayan strain partitioning. Tectonics 34(12):2494–2513

Sinha-Roy S (2001) Neotectonically controlled catchment capture: an example from the Banas and Chambal drainage basins, Rajasthan. Curr Sci 80(2):25

Sougnez N, Vanacker V (2011) The topographic signature of quaternary tectonic uplift in the Ardennes Massif (Western Europe). Hydrol Earth Syst Sci 15:1095–1107

Štěpančíková P et al (2008) Neotectonic development of drainage networks in the East Sudeten Mountains and monitoring of recent fault displacements (Czech Republic). Geomorphology 102:68–80

Stolum HH (2013) In: Richeson D (ed) The geometry of meandering rivers. Internet: www.divisbyzero.com-1490x718

Timar G (2003) Controls on channel sinuosity changes: a case study of the Tisza River, the Great Hungarian Plain. Quatern Sci Rev 22:2199–2207

Zámolyi et al (2010) Neotectonic control on river sinuosity at the western margin of the Little Hungarian Plain. Geomorphology 122:231–243

7 Historical Evidences in the Identification of Palaeochannels of Damodar River in Western Ganga-Brahmaputra Delta

Prasanta Kumar Ghosh and Narayan Chandra Jana

Abstract

To understand palaeo-climatic conditions and also tectonic activities of the past, it is necessary to identify the probable ancient tracks of a river. Among many approaches, at the primary level, the written evidences like old literatures may be used as basic tools for palaeochannel identification and mapping. India being rich in religious texts and literatures, offers a vast scope for the study of historical geography as well as palaeo-geography. Keeping in view the above concept, we have tried to identify and mapping the palaeochannels of Damodar fan delta of West Bengal with the help of medieval *Mangal-kavya*. In the poems of *Ketakadasa Kshemananda's Manasamangal-kavya* of seventeenth century, Damodar River took an important place and it is the main cause of our selection of it for our present study. In *Manasamangal-kavya*, many settlements have been mentioned which helps to identify the locations of palaeochannels. Result shows that below Barddhaman (West Bengal), the Damodar River or its deltaic distributaries was flowing east to meet the Bhagirathi River during seventeenth century. We also get positive result when we tried to calibrate the information with other old maps.

Keywords

Palaeochannel · Historical geography
Palaeo-geography · Damodar river · Damodar fan delta

7.1 Introduction

Geography is considered as the study of spatial organization expressed through processes and patterns of the earth surface. The spatial organization is multi-dimensional and time, the fourth dimension, plays a vital role in determining the characteristics of a region. A comprehensive study of a region may be complete only when facts behind facts have been systematically investigated and correlation properly established (Shukla 2013). In this context, for systematic investigation of spatial organization, the study of palaeo-geography is essential to reconstruct the geography of the past. Palaeochannels are the long remnant scars of rivers/streams which were

P. K. Ghosh (✉) · N. C. Jana
Department of Geography, The University of Burdwan, 713104 Burdwan, West Bengal, India
e-mail: gprasanta05@gmail.com

N. C. Jana
e-mail: jana.narayan@gmail.com

B. C. Das et al. (eds.), *Quaternary Geomorphology in India*,
Geography of the Physical Environment, https://doi.org/10.1007/978-3-319-90427-6_7

flowing either ephemeral or perennial during the geological past but presently these are either buried or lost or shifted due to internal (tectonic activity) and external (climatic, geomorphic and anthropogenic) activities, is an important component of palaeo-geography (Goudie ed. 2004; Charlton 2008; Nandini et al. 2013; Kumar 2011) because it represent the distribution of valley systems as these existed at a given geological time in the past (Bates and Jackson 1980). Its mapping and identification also has great importance in geology and climatology as palaeochannels has good groundwater potentiality and preserves sedimentary records useful to understand the palaeo-climatic conditions and also tectonic activities of past (Nandini et al. 2013).

There are certain approaches for palaeochannel identification. After Knighton (1984), the whole approaches can be classified as (i) Graphical sources, (ii) Sedimentary evidences, (iii) Written evidences, (iv) Direct measurement and (v) Dating techniques. Among those, at the primary level, written evidences like old literatures may be used as basic tools for palaeochannel identification and mapping. Keeping in view this concept, the present work aims to show the importance of historical evidences in the identification of palaeochannels in Damodar fan delta of West Bengal. With rich heritage of religious texts and literatures, India offers a vast scope for the study of historical geography as well as palaeo-geography. For example, two great epics of India *The Ramayana* and *The Mahabharata* highlight the physical and cultural landscapes of ancient India. The River *Saraswati* has been described in many hymns of Vedic literature. Thus old literatures like *Veda, Upanisads, Puranas, Epics* and many other *Sanskrit* writings like Kautilya's *Arthasastra* are authentic sources for attempting a comprehensive description of ancient Indian geographical knowledge, thoughts and concepts which are still awaiting to be unraveled by a team of interested and competent scholars (Tamaskar 1989).

7.2 Previous Works

Tamaskar (1989) in his book "*Geographical knowledge in Upanisads,*" has tried to explain the rich ore of geographical knowledge lying hidden in most of the known and published Upanisads. A*di-kavya* of Sanskrit literature *The Ramayana* also represents the physical and cultural scenario of ancient India (Shukla 2013). In Tamil literature "*Kalingathuparani*" there is description of River "Palar" which was flowing north of Kanchipuram city but the same river is now flowing south of it (Ramasamy 2005). With the help of medieval Bengali literature, Bandyopadhyay (1996) has tried to identify the palaeochannels of *Bhagirathi* or *Adi-Ganga* River in West Bengal. In the *Matsyapurana* (a sixth century BC tract) the present Damodar River is named *Mahagauri* and has been described as a rocky River (*Antasira*) and a river that is difficult to encounter (*Durgama*) (Ali 1966; Bhattacharyya 2011), which indicate the upstream bedrock-controlled courses of Damodar River. In *Vedic* literature, description of ancient *Saraswati* River of western India influence many researchers (Oldham 1886; Murthy 1980; Singhvi and Kar 1992; Valdiya 1996, 2013; Kalyanaraman 1997; Mukherjee 2001; Tripathi et al. 2004; Sinha et al. 2012) to work in this desert area of western part of India. Not only in the *Rigved*, but also in the *Purans* and in the epic *Mahabharata*, there was the description of this mighty River *Saraswati* (Valdiya 2017), which flowed for 1000 km parallel to the River Indus from the Himalaya to the Arabian Sea. Krishnan (1968) has observed that "The Saraswati has been described in Vedic literature (probably 5000 BC or earlier) as a great river—greater even than the Indus and Ganges." According to Vedic literature, more than 1200 settlements, including many prosperous towns of the Harappan culture (4600–4100 years Before Present—BP) and ashrams of *rishis* (sages) lay on the banks of this lifeline of the Vedic time (Valdiya 1996). In recent times, using satellite images and geo-electric resistivity evidence, researcher

has proved the existence of a large and long-lived palaeo-fluvial system in this region (Yashpal et al. 1980; Bhadra et al. 2009; Gupta et al. 2011; Sinha et al. 2012).

Taking clues from the above-mentioned literature, an integrated and basic approach of palaeochannels identification in the Damodar fan delta of West Bengal has been attempted.

7.3 Study Area

Damodar River is one of the important right-bank tributary of the River Hooghly (Ganges) in eastern India that drains a basin area of 23179.78 km^2 (22° 15′N–24° 32′N latitude and 84° 39′–88° 05′E longitude) (Fig. 7.1). Originate from Birjanga hill of Chotanagpur Plateau at

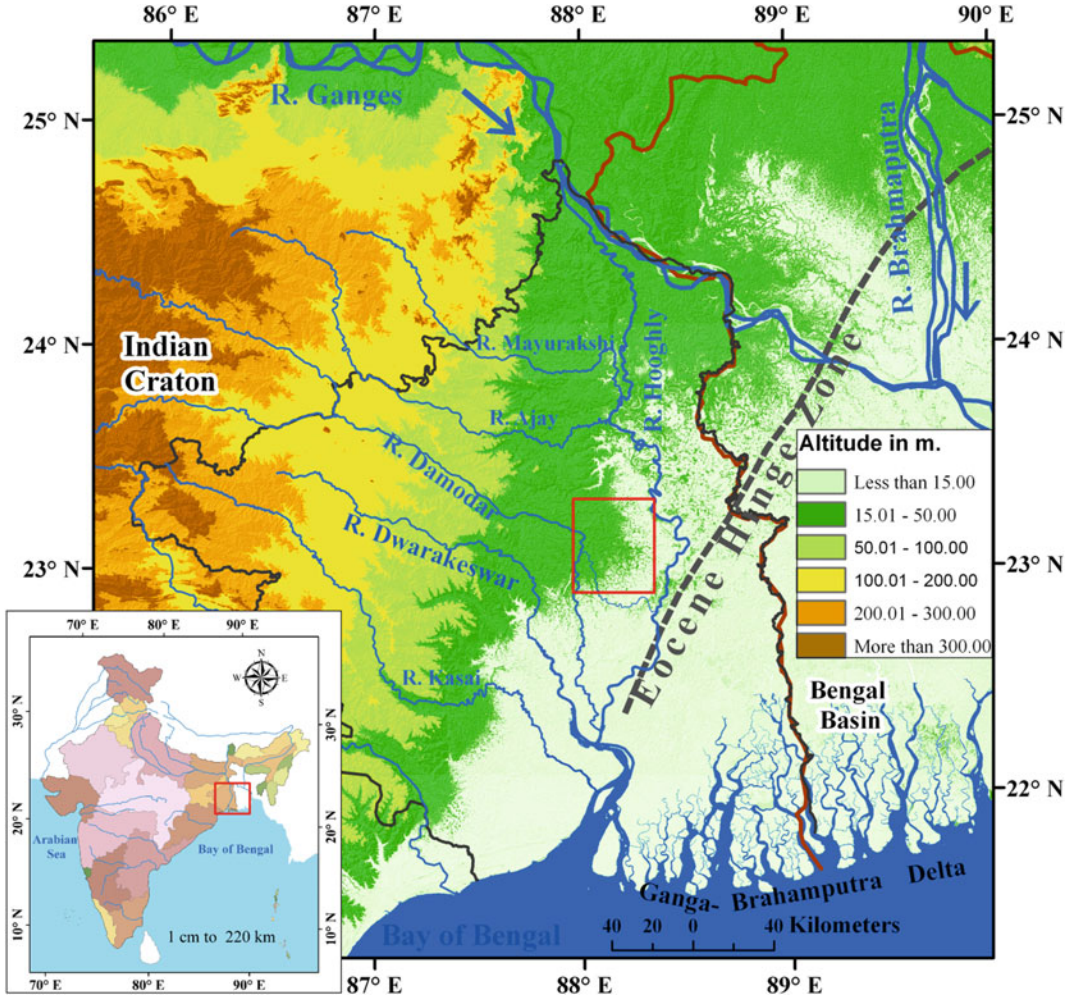

Fig. 7.1 Location map of the study area and surroundings. The black dashed line is the hinge zone indicating the transition between the Indian Craton and the thick sediments of the Bengal Basin. National boundaries are indicated by deep brown lines. Black polygon indicates the southern part of West Bengal. Red box indicates the location of Damodar fan delta

an elevation of 1000 m msl at 23° 38′ 53.45″N and 84° 39′ 35.18″E, the River flows total 577.81 km (295.07 km in Jharkhand state and 282.74 km in West Bengal state) before debouching into the Bhagirathi–Hooghly River. Below Barddhaman (West Bengal), it abruptly changes its course and then bifurcates into two channels viz. the Damodar channel (also known as Amta channel) and the Kanka-Mundeshwari channel. The main channel finally meets the Hooghly River; ultimately join with the Bay of Bengal. The regional slope of this basin is towards east to southeast. The master slope is however towards southeast (Roy and Banerjee 1990). The average annual rainfall of the catchment is 130.05 cm and about 82% of the annual rainfall occurs during the monsoon season, i.e., June to September (Pramanik and Rao 1952). It is a highly flood-prone river as it and its tributaries are fed by uncertain monsoonal rains, and tropical cyclonic storms embedded within the monsoon circulation. To realize the Damodar River as flood-prone (known as "Sorrow of Bengal") it is important to note that the floods of peak flow above 8496 cumec had been occurred 37 times between the years 1823 and 2007 (Bhattacharyya 2011). Flash Flood Magnitude Index (FFMI) reveals that Damodar River of India is generating superior value in FFMI (0.325) than World average (0.278) and other Indian Rivers (Kale 2003). Due to high magnitude of ancient flood with huge sediment discharge, the River had formed a fan delta (Fig. 7.1) between the Damodar River in the west and the Hooghly River in the east from Khari River in north to present location of confluence. This deltaic plain consists of two alluvial plains namely the Memari fan trending east and the Tarakeswar fan trending south (Fig. 7.2) (Mallick and Niyogi 1972; Deshmukh et al. 1973; Niyogi 1975), which are extends up to 70 and 40 km in the north–south and east–west directions (Singh et al. 1998), while SRTM satellite image (Jarvis et al. 2008) shows that the altitude of this area ranges from 10 to 30 m. (Figure 7.1). Morphologically the study area is divisible into the Kusumgram (marked by 1 in Fig. 7.2) and Kalna Plains (marked by 2A and 2B in Fig. 7.2) gradually come down in elevation in the east and southeast (Acharyya and Shah 2007). The whole deltaic plain is characterized by a network of palaeochannels with associated natural levees and swamps forming a dichotomous pattern (Howard 1967; Pal and Mukherjee 2010).

7.4 Methodology

Ancient writers described the physical facts they were writing about, in spiritual language, but the facts were there all the same. These spiritual interpretations of physical facts in the old classics are delightful studies. *Mangal-kavyas* are not exception in this regard. These are auspicious poems dedicated to rural deities and appear as a distinctive feature of medieval Bengali literature (Bhattacharyya 1975). Among these Mangal-kavyas, *Manasamangal-kavya* is rich in description of rivers of Bengal. Because, Manasa is the goddess of snakes in the Hindu pantheon and Bengal as a land swept by many rivers and abounding in bogs and marshes, is the natural habitat of a variety of species of snakes. The earliest composition of *Manasamangal* or *Padma-Purana* was penned by Bengali author Vijay Gupta of the fifteenth and sixteenth century (Gupta 1970). After that many writer wrote the songs of goddess *Manasa*, among those Ketakadasa Kshemananda's songs were most popular which was wrote during middle of seventeenth century (Bhattacharya 1987). Ketakadasa Kshemananda lived in Rarh Bengal (Bhattacharya 1987) and Damodar is the main river of Rarh Bengal. That is why, in his poems Damodar River took an important place and it is the main cause of our selection of Ketakadasa Kshemananda's Manasamangal-kavya for our study. Manasamangal-kavya mentioned settlement like Barddhaman, Gangpur, Baidyapur, Narkeldanga, Gaharpur, Tribeni, etc., which were located beside previous channels of Damodar River. These settlements are identified in SoI (Survey of India) Topographical maps (No. 73M/11, 73M/12, 73M/15, 73M/16, 79A/4, 79A/8, 79B/1 and 79B/5), then marked and saved as point vector in Google Earth Images. Saved kml File of

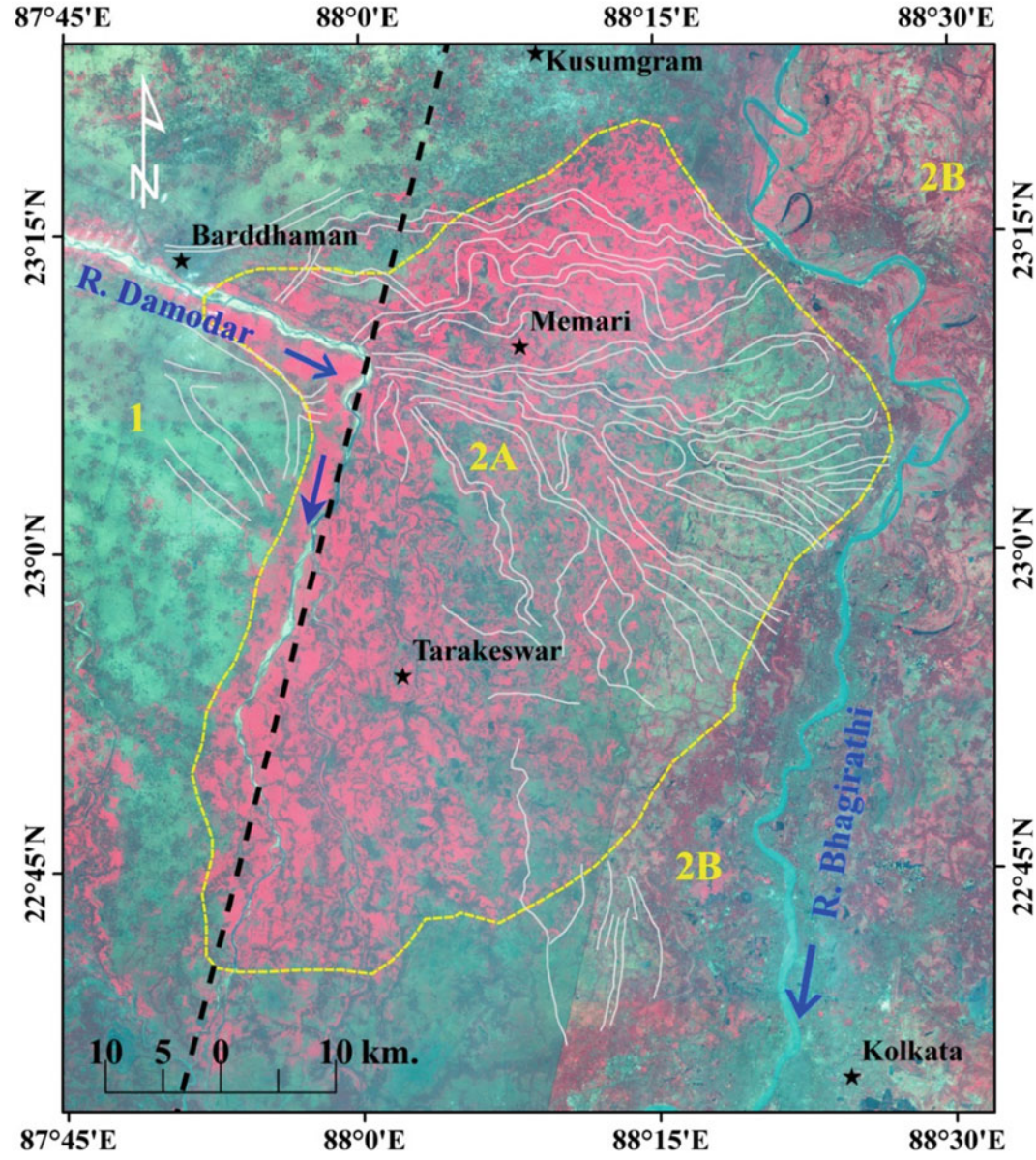

Fig. 7.2 LISS IV image (Dated 22nd December, 2013–20th January, 2014; Purchased from NRSC, ISRO) of the study area and surroundings. The yellow line is indicating the Damodar fan delta. White lines are palaeochannels which are identified by many tanks and low-lying agricultural plots. Black dashed line indicates the position of Damodar fault along the lower course of River Damodar. Morphostatigraphic units: 1—Kusumgram Plain (Older delta plain, Pleistocene–Holocene); 2—Kalna Plain (Younger delta plain, Holocene), 2A—Damodar fan delta plain, 2B Bhagirathi delta plain. *Source* Modified after Acharyya and Shah (2007) and Singh et al. (1998)

point vectors then we have opened in Arc-GIS v-9.3 platform and connect them, which form a 75.5 km liner pattern below Barddhaman up to Bhagirathi or Hooghly River. Thus we have identified the palaeochannel of Damodar River. In this area other palaeochannels also can be identified by many tanks and low-lying agricultural plots. With the help of SRTM, linear image

Fig. 7.3 Ruins and mounds claimed to be Lakshmindara-Behula's bridal chamber at Champaknagr/Kasba

self-scanning (LISS) IV and Google Earth image, maps have been prepared in ERDAS Imagine 9.0 and Arc-GIS 9.3 platforms.

7.5 Discussion

Kasba (23° 20′ 38.48″N and 87° 30′ 57.38″E), a village in Galsi police station; it also goes by the name of *Kasba-Champai*. Tradition says that *Champai*, the capital of the kingdom of *Chand Sadagar* of the *Manasamangal-kavya* was located here (Wikipedia). Two mounds (about 120 ft * 30 ft each) (Fig. 7.3) are shown as the ruins of the palace of *Chand Sadagar* and Santali hill associated with the name of *Lakshindar*, his son. Atop the mounds there are broken pieces of stones and bricks. There also a Siva temple here and the *lingam* is traditionally believed to have been established by *Chand Sadagar* (Fig. 7.4).

Manasamangal recounts that the deity *Manasa* forced *Chand Sadagar* to her worship to establish her place among the pantheon of Hindu gods and goddess. But the rich merchant *Chand Sadagar*, an ardent devotee of Shiva (The God of destruction in Hindu mythology), refuses to recognize *Manasa's* godhead. *Manasa* takes revenge by drowning *Chand's* seven ships at sea and killing his six sons. It has been mentioned in Ketakadasa Kshemananda's *Manasamangal* as (Bhattacharya 1987).

(a) *Champak nagar-e ghar Chand Sadagar Manasar sohit bad kore nirantor, Debir kopete tar choy putro more Tothacho debota boli na mane tahare* (1/4) (Meaning: Chand Sadagar who lives in Champak village, has a clash with *Manasa*. *Manasa* penalized him by killing his six sons, in spite of that Chand was not agreed to worship her).

Chand is determined to save his youngest seventh son Lakhhindar while Manasa has also vowed to wreck vengeance on the young boy. *Lakhhindar* is stung by *Kalnagini* (a poisonous snake) on his wedding night and his newly wed wife *Behula*, travels by a boat through Gangur, Banka and Damodar River with her husband's

Fig. 7.4 Siva temple at Kasba. Inset pictures of Bengali sentence are written in the wall of temple. Which means *Chmpaknagar* is another name of Kasba village (*Upper inset*) and the temple has been established by Chand Sadagar (*Lower Inset*)

corpse, hoping for the restoration of Lakhhindar's life. Name of these rivers are mentioned as

(b) *Behula bhasia jai Gangur-er jole* (37/16) (Meaning: Behula floating in the current of Gangur River), and
(c) *Bhasia bhasia pailo Banka Damodar* (40/6) (Meaning: After that Behula find the River Banka and Damodar)—Bhattacharya (1987, p. 59 and 62).

During her travel in the Damodar River, as described in Manasamangal, Behula found some villages, which are pointed out in Table 7.1 and Fig. 7.2.

It is also clearly cited in Manasamagal that the confluence of the mentioned river was near *Gaharpur* (22° 59′ 41.28″N and 88° 24′ 28.33″ E), which is described as

(d) *Gaharpur bhasia Gangar jole mili* (45/50) (Meaning: near Gaharpur, Behula's boat came into River Ganges or Bhagirathi)—Bhattacharya (1987, p. 74).

We also get another settlement named Kandorsona (23° 12′ 34.31″N and 87° 55′ 58.01″E), which is 10 km away from the town of Barddhaman, and 1.5 km from Gangpur Railway Station. Traditionally believe that the earrings of Behula dropped there.

If we connect all these settlement, we will get 75.5 km liner pattern or palaeochannel of Damodar River from Barddhaman town to Bhagirathi River (Fig. 7.5). Which indicate that below Barddhaman (West Bengal), the Damodar River or one of it's deltaic distributary was flowing east to meet the Bhagirathi River during seventeenth century (when the Manasamangal was written).

Table 7.1 Strandline villages of the palaeochannel of Damodar River as mentioned in Manasamangal-kavya

Localities (arranged in downstream order according to description)	Geographical location	In which part of Manasamangal, localities are mentioned
Nabakhanda	23° 18′ 37.41″N and 87° 33′ 33.76″E	40/4
Gobindapur	23° 15′ 19.11″N and 87° 34′ 50.79″E	40/7
Barddhaman	23° 13′ 13.61″N and 87° 51′ 3.75″E	40/7
Gangapur/Gangpur	23° 13′ 12.89″N and 87° 54′ 42.35″E	40/8
Amadpur	23° 12′ 22.79″N and 88° 5′ 23.76″E	40/48
Newadar ghat/Newapara	23° 9′ 44.83″N and 88° 16′ 18.66″E	40/32
Narkeldanga	23° 10′ 4.36″N and 88° 14′ 21.29″E	40/33
Baidyapur	23° 9′ 35.90″N and 88° 14′ 44.14″E	40/40

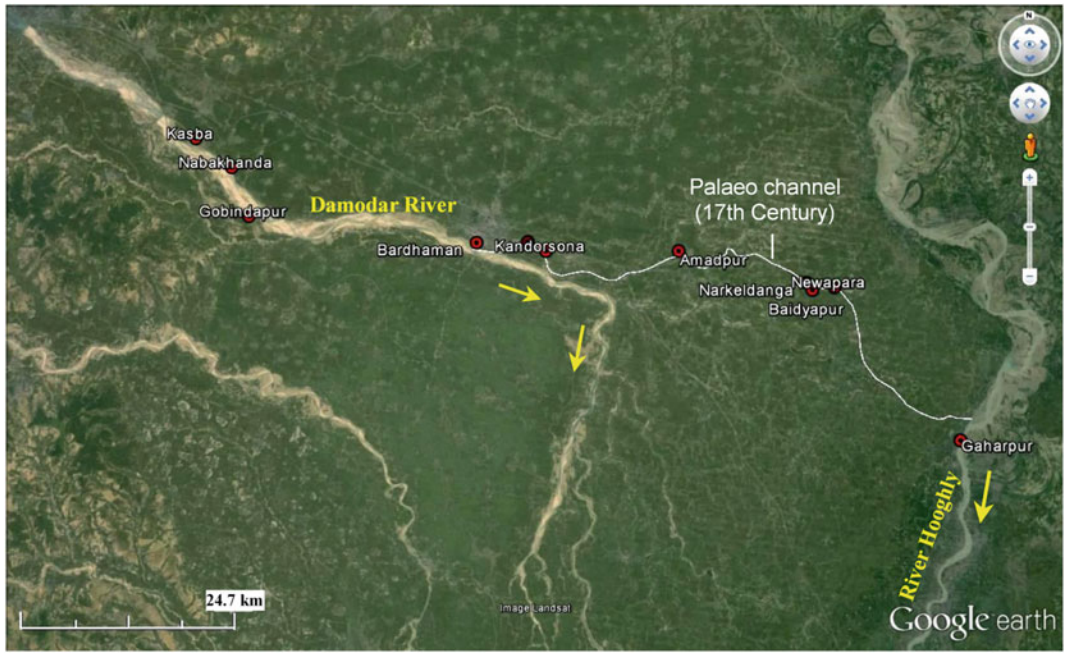

Fig. 7.5 Travel path of Behula's boat. Red circles are the settlements mentioned in *Manasamangal*

The map of Vanden Broucke of seventeenth century (1660) and palaeochannels map of Acharyya and Shah 2007 (Fig. 7.2) also supports the identified palaeo-path of River Damodar.

But later than below Barddhaman, either it has since fully rotated its course or due to close up of the distributaries, the river shifted its mouth 128 km to the south (Deshmukh 1973; Acharyya and Shah 2007), leaving behind numerous palaeochannels like Behula, Gangur, Ghea, Kunti, Kana Damodar, etc. (Ghosh and Mistri 2012) (Figs. 7.6 and 7.7).

According to Willcocks, "turning the Damodar was beyond the power of man like Bhagirath." To support this theory he also gave example of King Menes, who turned the Nile from extreme western limit of the valley to the eastern limit to protect the temples of Memphis from the eastern nomads about 6000 years ago (Willcocks 2001). In Damodar fan delta, there are number of

Fig. 7.6 Part of former courses of River Damodar at Konarpur near Barddhaman town (23° 15′ 23″N and 87° 46′ 6″E)

Fig. 7.7 Part of former courses of River Damodar at Boragari near Boinchi (23° 7′ 32″N and 88° 9′ 45″E). *Source* Majumder (2013)

palaeochannels which are called kana Rivers. He also considered these palaeochannels as excavated canals from Damodar. Because the word Kanwa is derived from *kan* an old Persian or Arabic word, meaning *to dig*. According to him, for irrigation purpose, seven canals or *kanas* were dug and between them they disposed the whole excess supply which passed Burdwan and constituted a new delta. Construction of embankment along the left bank of the river may cause delink of distributaries in Damodar fan delta and forces the river to confine within present channel. It is also considered by many scholars that tectonic events are the causes behind the bends of Damodar River. According to Singh et al. (1998), the lower course of the River Damodar is confined by Damodar fault (Fig. 7.2). But this research finding may also be criticized. Because in recent publication entitled "Seismotectonic Atlas of India and its Environs" (Dasgupta et al. 2000) of Geological Survey of India did not support the presence of any subsurface fault along the present lower Damodar channel (Fig. 7.8). Absence of Seismotectonic activity for long time and almost 6 km thick

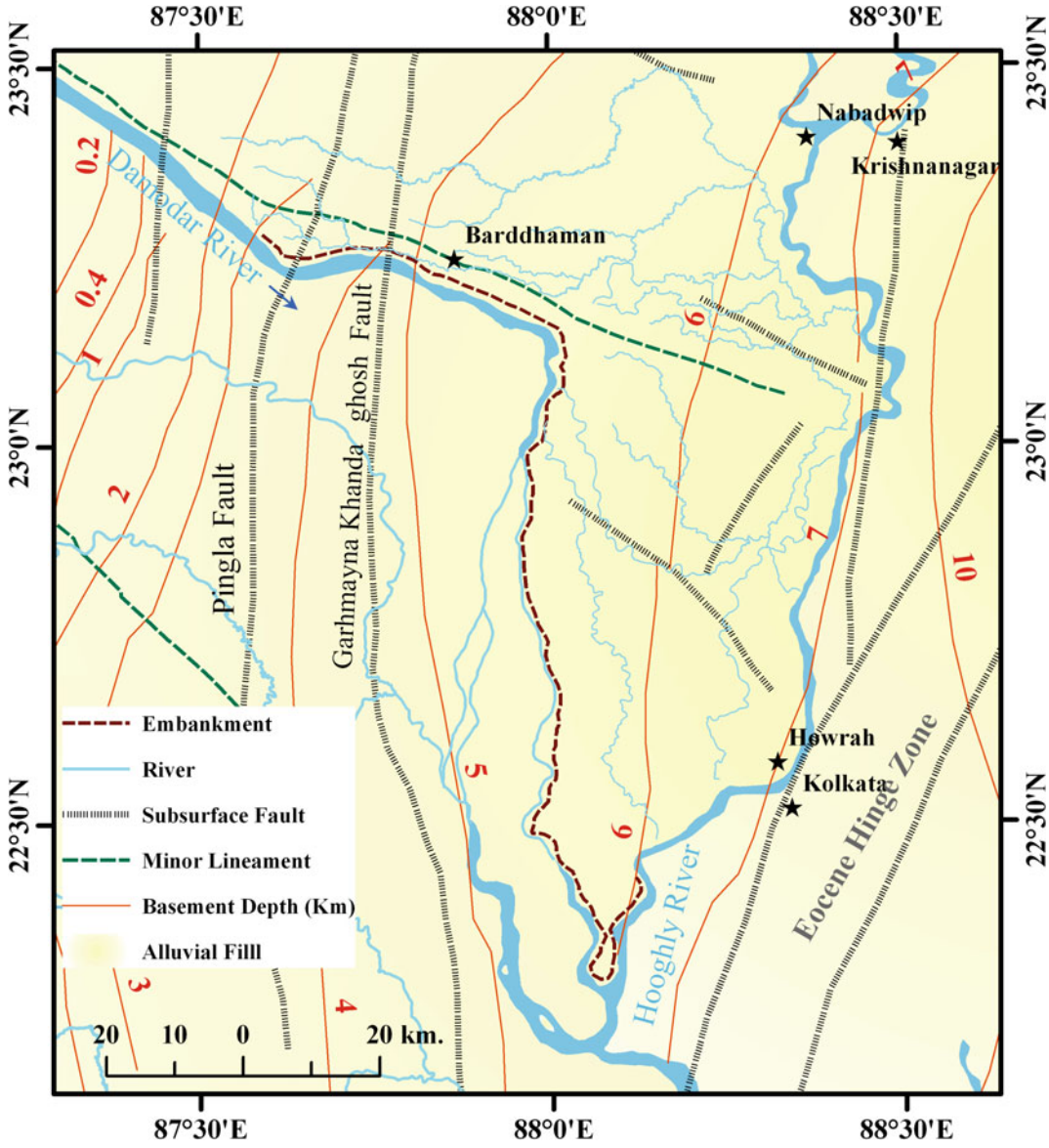

Fig. 7.8 Drainage and tectonic map of study area (Modified after Dasgupta et al 2000)

alluvium deposition on hard rock in this region also questioning the tectonic control of the channel. Keeping in view the above findings in backdrop, more interdisciplinary study and research are essential to reach at a scientific explanation of the bending of the Damodar River.

7.6 Conclusion

In view of the above observation, it can be surmised that primarily written evidences like old literatures may be used as basic tools for palaeochannels identification and mapping. This has been exemplified in case of Damodar River in West Bengal where it is observed that an old regional folk story plays an important role in the identification of its palaeochannels. It may be mentioned in this context that identified palaeochannels of Damodar River also coincide with old maps of seventeenth century. It indicates that with the help of available old literature researcher at primary level can identify the probable ancient tracks of a river to unfold a valuable history of river courses. Besides, with rich heritage of religious texts and literature, there is vast scope for the study of historical geography or palaeo-geography in India. However, it is to be noted that the poets of the Mangal kavyas were mostly of romantic nature as reflected in their description and many of them were poor in geographical knowledge.

Acknowledgements The authors are sincerely grateful to Central library and Department of Geography of The University of Burdwan, for providing the necessary supports to do this work. Thanks are accorded to Dr. Arijit Majumder and Sujay Bandyopadhyay for their continuous assistance and suggestion.

References

Acharyya SK, Shah BA (2007) Arsenic-contaminated groundwater from parts of Damodar fan-delta and west of Bhagirathi River, West Bengal, India: influence of fluvial geomorphology and quaternary morphostratigraphy. Environ Geol 52:489–501. https://doi.org/10.1007/s00254-006-0482-z

Ali SM (1966) The geography of the puranas. People's Publishing House, New Delhi

Bandyopadhyay S (1996) Location of the Adi Ganga palaeochannel, South 24 Parganas, West Bengal: a review. Geogr Rev India 58(2):93–109

Bates RL, Jackson JA (eds) (1980) Glossary of geology. American Geological Institute, Falls Church

Bhadra BK, Gupta AK, Sharma JR (2009) Saraswati Nadi in Haryana and its linkage with the Vedic Saraswati River – integrated study based on satellite images and ground based information. J Geol Soc India 73: 273–288

Bhattacharya B (ed) (1987) Manasa Mangal of Ketakadasa Kshemananda. Sahitya Akademi (Bengali), New Delhi

Bhattacharyya A (1975) History of the Bengali Mangalkavyas, 6th edn. A Mukherji and Co. Pvt. Ltd., Calcutta

Bhattacharyya K (2011) The lower Damodar River, India: understanding the human role in changing fluvial environment. Springer, New York

Charlton R (2008) Fundamentals of fluvial geomorphology. Routledge Publication, New York, p 136

Dasgupta S, Pande P, Ganguly D, Iqbal Z, Sanyal K, Venkatraman NV, Sural B, Harendranath L, Mazumdar K, Sanyal S, Roy A, Das LK, Misra PS, Gupta H (2000) Seismotectonic atlas of India and its environs. In: Narula PL, Acharyya SK, Banerjee J (eds) Geological Survey of India, Special Publication No. 59, Sheet 24: Chotonagpur Gneissic Terrain, Rajmahal Basin and Bengal Basin

Deshmukh DS (1973) Geology and groundwater resources of the alluvial area of West Bengal. Bull Geol Surv India 34B:451

Deshmukh DS, Prasad KN, Niyogi BN, Biswas AB, Guha SK, Seth NN, Sinha BPC, Rao GN (1973) Geology and groundwater resources of alluvial areas of West Bengal. Bull Geol Surv India Ser B 34:1–451

Ghosh S, Mistri B (2012) Reconstructing the phases of channel shifting through identification of palaeochannels and historical accounts of extreme floods of Damodar River in West Bengal. Indian J Geomorphol 17(2):65–80. ISSN: 0973-2411

Goudie AS (ed) (2004) Encyclopedia of geomorphology, vol 2. Routledge Publication, New York, pp 743–744

Gupta RK (ed) (1970) Padma Puran or Mansa Mangal of Bijoy Gupta. Rajendra Library, Calcutta

Gupta AK, Sharma JR, Sreenivasan G (2011) Using satellite imagery to reveal the course of an extinct river below the Thar Desert in the Indo-Pak region. Int J Remote Sens 32(18):5197–5216. https://doi.org/10.1080/01431161.2010.495093

Howard AD (1967) Drainage analysis in geologic interpretation: a summation. Am Assoc Petrol Geol Bull 51:2246–2259

Jarvis A, Reuter HI, Nelson A, Guevara E (2008) Hole-filled seamless SRTM data V4, International Centre for Tropical Agriculture (CIAT)

Kale VS (2003) Geomorphic effects of monsoon floods on Indian rivers. Nat Hazards 28:65–84

Kalyanaraman S (1997) Sarasvati River (circa 3000–1500 B.C.). Sarasvati Sindhu Research Centre, 19 Temple Avenue, Chennai 600015. Available in http://www.hindunet.org/hindu_history/sarasvati/sartxt.PDF

Knighton D (1984) Fluvial forms and processes. Edward Arnold (Publisher) Ltd. London. ISBN 0-7131-6405-0

Krishnan MS (1968) Geology of India and Burma, 5th edn. Higginbothems Publication

Kumar V (2011) Palaeo-Channel. Encyclopedia of Snow, Ice and Glacier. In: Singh VP, Singh P & Haritashya UK (eds) Springer, Dordrecht: The Netherlands, p. 803, ISBN: 978-90-481-2641-5

Majumder A (2013) Ground water budgeting and its management in Pundua block of Hugli district, West Bengal, unpublished Ph.D. thesis. Department of Geography, The University of Burdwan

Mallick S, Niyogi D (1972) Application of geomorphology in groundwater prospecting in the alluvial plains around Burdwan, West Bengal. Indian Geohydrol 8:86–98

Mukherjee A (2001) Rigvedic Sarasvati: myth and reality. Breakthrough 9, No. 1

Murthy SRN (1980) The Vedic River Saraswati, a myth or fact – a geological approach. Indian J Hist Sci 15 (2):189–192

Nandini CV, Sanjeevi S, Bhaskar AS (2013) An integrated approach to map certain palaeochannels of South India using remote sensing, geophysics, and sedimentological techniques. Int J Remote Sens 34 (19):6507–6528

Niyogi D (1975) Quaternary geology of the coastal plain in West Bengal. Indian J Earth Sci 2:51–61

Oldham RD (1886) On probable changes in the geography of the Punjab and its rivers. Asiatic Soc Bengal. 55:322–343

Pal T, Mukherjee PK (2010) Search for groundwater arsenic in Pleistocene sequence of the Damodar River flood plain, West Bengal. Indian J Geosci 64 (1–4):109–112

Pramanik SK, Rao KN (1952) Hydrometeorology of the Damodar catchment, Ind Met Dep Mem. 29(4): 429–431

Ramasamy SM (2005) Remote sensing of river migration in Tamilnadu. In: Ramasamy SM (ed) Remote sensing in geomorphology. Published by New India Publishing Agency, New Delhi. ISBN 81-89422-05-7

Roy BC, Banerjee K (1990) Quaternary geological and geomorphological mapping in parts of Bardhaman and Bankura districts and preliminary assessment of sand deposits suitable for construction and other allied purposes. Progress report for the field season 1988–89. Geological survey of India

Shukla RK (2013) Ramayana: a study in ancient Indian geography. An unpublished Ph.D. thesis submitted to Bundelkhand University, Jhansi, India

Singh LP, Parkash B, Singhvi AK (1998) Evolution of the lower Gangetic plain landforms and soils in West Bengal, India. Catena 33:75–104

Singhvi AK, Kar A (1992) Thar Desert in Rajasthan. Geological Society of India, Bangalore, p 191

Sinha R, Yadav GS, Gupta S, Singh A, Lahiri SK (2012) Geo-electric resistivity evidence for subsurface palaeochannel systems adjacent to Harappan sites in northwest India; Quaternary International, http://dx.doi.org/10.1016/j.quaint.2012.08.002

Tamaskar BG (1989) Geographical knowledge in Upanisads. Indus Publishing Company, New Delhi. ISBN 81-85182-29-9

Tripathi JK, Bock B, Rajamani V, Eisenhauer A (2004) Is River Ghaggar, Saraswati? Geochemical constraints. Curr Sci 87(8):1141–1145

Valdiya KS (1996) River piracy: Saraswati that disappeared. Resonance 19–28

Valdiya KS (2013) The River Saraswati was a Himalayan-born river. Curr Sci 104(1):42–54

Valdiya KS (2017) Prehistoric River Saraswati, Western India: geological appraisal and social aspects, Society of Earth Scientists series. Springer International Publishing AG, Switzerland. ISBN 978-3-319-44223-5, ISBN 978-3-319-44224-2 (eBook)

Willcocks W (2001) Ancient system of irrigation in Bengal in 'Rivers of Bengal', vol 1

Yashpal, Sahai B, Sood RK, Agrawal DP (1980) Remote sensing of the 'lost' Saraswati' River. Proc Indian Acad Sci (Earth Planet Sci) 89:317–331

8 Application of Remote Sensing and GIS in Understanding Channel Confluence Morphology of Barakar River in Western Most Fringe of Lower Ganga Basin

Sumantra Sarathi Biswas, Raghunath Pal and Padmini Pani

Abstract

The channel confluences are the sensitive junctions that face significant hydraulic and morphological changes within the river system. Five major confluences of the Barakar River have been considered for the geomorphic investigation. The various data products, i.e. Topographical maps (1955), IRS LISS III Satellite Images (2011), Digital Elevation Data (ASTER DEM) (2011), and the Google Earth Map (2009–2015) have been used in this study. The study concerns the morphology of the confluences and the impacts of confluence angle, tributary length, tributary basin area and lithological controls on the confluences especially in the Quaternary period. There is no definite cause–effect relationship of confluence angle to scour depth and w/d ratio but has a positive relationship between w/d ratio of the post-confluence stream and the area of the tributary basin. The studied confluences are significantly controlled by the lithological influences and it almost defies other effective factors i.e. confluence angle, tributary length, etc.

Keywords

Confluence angle · Scour depth · W/d ratio
Channel bathymetry · Lithology

8.1 Introduction

The tributaries of a river system are the primary sources of water and sediment to the trunk stream along with the trunk segment itself. The interactions between tributaries and the main stream at a different location on the main stream segment play the important roles in all aspects such as on the river system morphology, sedimentology, hydrology and ecological habitats at the reaches of the confluence zones (Kennedy 1984; Roy and Sinha 2007). The channel confluences are the critical interfaces where two streams with distinct characteristics meet together and it is really difficult to investigate the complexity and the changes of the both local and downstream characteristics of river channel confluences scientifically (Roy 2008a, b). The tributaries have rich scale impacts on the main stem

S. S. Biswas (✉) · R. Pal · P. Pani
Centre for the Study of Regional Development, Jawaharlal Nehru University, New Delhi 110067, India
e-mail: sumantra.geo5@gmail.com

S. S. Biswas
Department of Geography, Sukumar Sengupta Mahavidyalaya, Keshpur 721150, West Bengal, India

B. C. Das et al. (eds.), *Quaternary Geomorphology in India*,
Geography of the Physical Environment, https://doi.org/10.1007/978-3-319-90427-6_8

characteristics and the type and extent of geomorphological changes of the main stem are related to the characteristics of the tributaries (Ferguson and Hoey 2008). Flow separation, flow convergence/divergence, and secondary circulation, etc. give impact to the immediate downstream of the confluence (Rhoads and Kentworthy 1995, 1998). The changes of channel gradient at the confluence point effect on longitudinal variations in sediment transport rate that can reduce the substrate size and increase the floodplains width in the upstream of the confluences. It impacts the down segment confluences including coarser substrates, increased channel width, pool depth and the occurrence of bars (Rice 1998; Benda et al. 2004).

The research works on confluence science have been neglected by the earth scientists for many years (Stevens et al. 1875). Although, in the last two decades of the twentieth century, the research on confluence science emerged prolifically with the advancement in instrumentation, the development of experimental design and numerical model, field studies and the uses of satellite images and digital elevation data. Some notable works have been carried out on the flow separation and hydraulic geometry, hydrodynamic features (Best and Reid 1984; Best 1986), in the patterns of flow separation, flow convergence/divergence and secondary circulation immediately downstream from the confluence (Rhoads and Kentworthy 1995). But, it was in 1976, when the seminal work of Mosley on channel confluences was published, a laboratory experiment that paved the way for the identification and analysis of flow structure and channel bed characteristics of segment confluence (Mosley 1976; Roy 2008a, b). In the last decade of the twentieth century, several research works on the confluence geomorphology have been published by S. P. Rice, A. G. Roy and B. L. Rhoads and a book entitled 'River Confluences, Tributaries and the Fluvial Network' edited by them was published in 2008. These are the tremendous works still to date, concocted many ways to investigate the confluence morphology and to identify influencing factors intricately. These studies may enhance and enrich the future research works on the confluence morphology intensively. But the reality is that the study of the river confluences has received a very little attention by fluvial geomorphologists. Surprisingly, in India, very few research on confluence study has been worked until today as far as the availability of literature is concerned. There may be the confluence of two streams of the same order, but in this study, the junctions of the main stem with its tributaries have been considered. The Barakar River is the principal tributary of the Damodar River of the Ganga river system in the eastern India. It is a non-perennial and sinuous sand–gravel mixed bedrock channel (Biswas and Pani 2016) with high sand discharge (Khan 1987) and moderate to high soil loss throughout the catchment area (Biswas and Pani 2015). The Barakar River passes through the Chotanagpur Plateau region to some extent to the north. Several tributaries have met with the mainstream of Barakar River from the different parts of Chotanagpur Plateau in a different asymmetrical angle that has a notable impact on the confluence, and downstream channel morphology as previous literature on confluence science reflects. Lithological influences on the confluence zone have developed the stable confluence points rather than the dynamic as observed in the alluvial channel. In this chapter, five major confluences (Keso confluence at Parsabad, Barsoti confluence at Barwadih, Irga confluence at Narangi, Usri confluence near Maheshpur and Khudia confluence at Baidyanathpur) of the Barakar River have been considered for geomorphic analysis (Fig. 8.1). These tributaries have the significant impacts on the main river as these have the ample amount of discharge during the monsoonal period to form a distinct main stem channel morphology.

The present study is an attempt to understand the geomorphic characteristics of the confluences, to investigate the influence of the confluence angle to the morphology of different confluences and to inspect the impacts of the length and the basin area of the tributaries on the confluence geometry. Moreover, it is an attempt to understand the structure and dynamic nature of the confluences of a plateau river as most of the

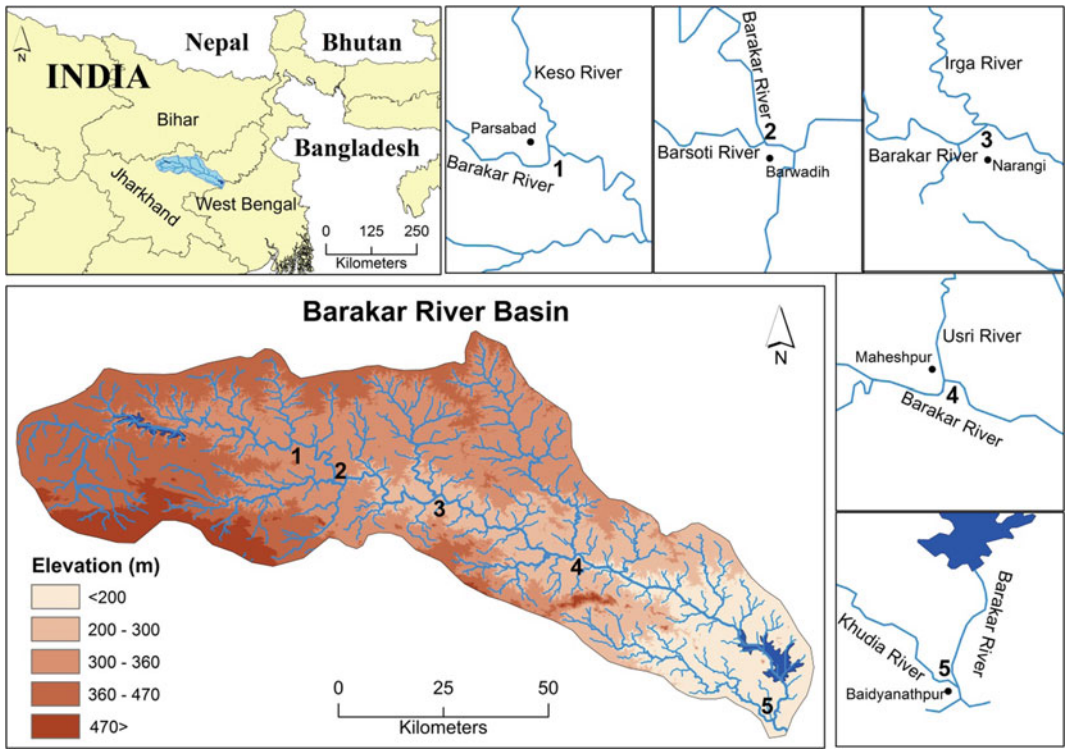

Fig. 8.1 Location of the studied five major confluences of the Barakar River, 1—Keso, 2—Barsoti, 3—Irga, 4—Usri, 5—Khudia confluences

previous works have been done on confluence dynamics of alluvial channels. Thus, the authors have selected the Barakar River, which is wholly confined in Chotanagpur plateau and sand–gravel–bedrock mixed in nature. It is important as the confluence zones have the impacts on channel morphology rather than the channel planform through the Cretaceous to the Quaternary Period.

8.2 Regional Setting

The Barakar River, originating near Padma in Hazaribagh district of Jharkhand, flows for 256 km across the northern part of the Chotanagpur Plateau, along the broad valley of Parashnath-Tundi Ridge (Mahadevan 2002), mostly in a west to east direction before joining the Damodar near Dishergarh in Bardhhaman district of West Bengal. It has a catchment area of $\sim$6160 km^2 (Biswas and Pani 2016). The main tributaries, which have been considered in this study, of the Barakar River, are Keso, Irga, Usri (left bank of the Barakar River) and Barsoti, Khudia (right bank of the Barakar River) that flows from the north and south to the main stream respectively (Fig. 8.1). These rivers flow on at different altitude that has varying lithology and most of the rivers having water parties, waterfalls, scarp, rugged topography and moderately sinuous (P = 1.39) in nature (Prasad 1982; Khan 1987). The rivers are most effective in rainy or flood season or on a steep slope and equilibrium of rivers have to be adjusted with seasonal discharge variability (Mahadevan 2002). The river basin is moderately dissected as the density of the confluences of the basin is low to moderate and cover approx. 76% of density zone where the no. of confluences per sq. km. is 3–40 and rest portion of the basin (24%) have no confluence or high density (number of

confluence is 16–50) (Prasad 1979). As it is mentioned in the introduction that the trunk channel is sinuous sand–gravel bedrock type and probably the channels of the river basin are not entirely controlled by faults, joints and adjusted to the local lithology but also controlled by sediment deposition that fits moderately resistant channel network, as it is found that the greater percentage of the basin confluence density is low to moderate. Probably, that is why, the number of major confluences is not very high as we have found only the five major confluences (Biswas 2014). Paleochannel study reveals that the width of the Barakar River was 235–415 m and 3.7–5.5 m deep and flowed on a slope of 0.00035 (Khan 1987). The Barakar River Basin is characterised by the monsoon climatic characters of dry winter and wet summer with hot weather from March to May and cold weather from November to February. Maximum rainfall takes place during July to September that accounts for more than 90% of the total rainfall in the basin. The lower section of the catchment area has experienced more rain in the monsoonal season (Biswas 2014). The downstream areas, especially after the Maithon dam, have a considerable impact on the channel confluence geometry. Moreover, the sand and gravel mining from the river bed year after year has a significant role in the river bed morphology as well as the structure of the confluences (Biswas 2014).

8.3 Materials and Methods

The data for the present study are collected from various sources. Some data like channel width and spot height, etc. are also obtained from the field survey in the Barakar River Basin. The sources that provide the different types of data are given in Table 8.1.

The aim of this chapter is to explore the geometry of five major confluences of the studied river considering the influences of confluence angle and basin characteristics of the tributaries. Water flow in the non-perennial tributaries is not solely responsible for the changes in the confluence geometry. Therefore, confluence angle, depth, width, surface area; w/d ratio (Width/depth ratio) of the main stem (upstream and downstream of the confluences) and tributaries; length and basin area of the tributaries etc. have been taken into consideration and analysed. In this chapter, historical influence means the changing confluence sites or confluence dynamics and characteristics over a long time have not been considered because of unavailability of data sources, but another important cause is geologic setting of the Barakar River basin (rocky and non-alluvial channel character of the basin enforces the channel and its confluences to be less dynamic). The morphological characteristics of the confluences have been investigated by analysing all the above-mentioned data sources.

Table 8.1 Data types used for the study

Data types	Data sources
Satellite images	IRS P6 (RESOURCESAT-1)—LISS III (2011)
Digital Elevation Data (DEM)	ASTER DEM (2011)
Topographical maps	Survey of India (72H/7, 72H/8, 72H/11, 72H/12, 72H/15, 72H/16, 72L/4, 72L/8, 73I/9, 73I/13, 73I/14) (1:50,000); National Atlas and Thematic Mapping Organization (NATMO)
Others	Google Earth Map (2009–2015) and field survey

In order to show the overview of the morphology of the confluences IRS P6 LISS III (spatial resolution 23.5 m) (2011) and Google Earth map (2009–2015) have been used and to reach to the accuracy as far as possible Google Earth Map and tools and field survey data have been used. There was a problem to measure accurately the geometric properties like width, depth, etc. of the studied section because the spatial resolution of ASTER DEM (2011) is 30 m. In order to measure the width and depth of the channel, laser distance metre and dumpy level instrument have been used. To ensure whether ASTER DEM data and Google Earth give correct information or not, spot height values had been taken from the topographic sheet and field survey data. Then the values had been plotted against the DEM values and the result is satisfactory. The field survey had been done during the winter season and the channel was almost dry and with a little flow of water.

In order to measure the predicted angle of a confluence, several equations have been used mainly by civil engineers, e.g. Horton's equation (1945), Lubowe's equation (1964) based on Horton's momentum equation. Howard's equation (1971), an extension and modification of Horton's momentum and energy equation, etc. Horton suggested that confluence angle between the main stream and a tributary as,

$$\cos\theta = \tan s_c / \tan s_g \tag{8.1}$$

where, s_c is the channel slope of the main stream and s_g is the slope of the tributary. Horton's equation (Eq. 8.1) stated that streams of equal gradient cannot meet and modification for this two, the equations (Eqs. 8.1 and 8.2) were suggested by Howard that for both the channels, tributary and upstream of a confluence

$$\cos\theta_1 = s_3/s_1 \tag{8.2}$$

$$\cos\theta_2 = s_3/s_2 \tag{8.3}$$

where, θ_1 and θ_2 are the angles of confluence with respect to the main upstream and tributary for a single confluence respectively, and s_1, s_2 and s_3 are the slopes of main upstream, tributary and main downstream or continuing stream respectively (Mosley 1976). Further, Howard modified (Eqs. 8.4 and 8.5) the Eqs. 8.2 and 8.3 into

$$\cos\theta_1 = \left[\frac{Q_1 + Q_2}{Q_1}\right]^u \tag{8.4}$$

$$\cos\theta_2 = \left[\frac{Q_1 + Q_2}{Q_2}\right]^u \tag{8.5}$$

where, Q_1 and Q_2 are the discharge of tributary and the main upstream respectively, u represents a coefficient. Based on Howard Eqs. 8.4 and 8.5 and momentum equation Mosley (1976) developed an equation (Eq. 8.6) for the predicted angle of a confluence i.e.

$$M_1 \sin\theta_1 = M_2 \sin(\theta - \theta_1) \tag{8.6}$$

where, M_1 and M_2 are the momentum of the tributary and the main upstream, θ_1 and $\theta - \theta_1$ are the confluence angles ($\theta = \theta_1 + \theta_2$). To find out the actual angle (θ) between the main stem and tributaries at the confluences, we have used a graphical technique adopted and slightly modified from Mosley's momentum equation (Fig. 8.2) with the help of IRS LISS III satellite images (2011) and Google Earth Maps (2009–2015). In this study, the Eqs. 8.2 and 8.3 have been taken into consideration because there is a small difference of the values of confluence angle for the two different methods (Horton's method and graphical method). The confluence angles for the Horton's method are 95° (Keso), 72° (Barsoti), 53° (Irga), 88° (Usri) and 80° (Khudia) whereas the confluence angles for the graphical method are 89°, 64°, 45°, 79° and 71° respectively. In case of Horton's method, the slope of main upstream (s_1), tributary (s_2) and main downstream (s_3) have been calculated from constructed longitudinal profiles from ASTER DEM (2011) considering a distance of 5 km from the confluence. The problem in the use of the Eqs. 8.4 and 8.5 is the unavailability of discharge data. In case of the Eq. 8.6, the limitation is to calculate the values of momentum for each

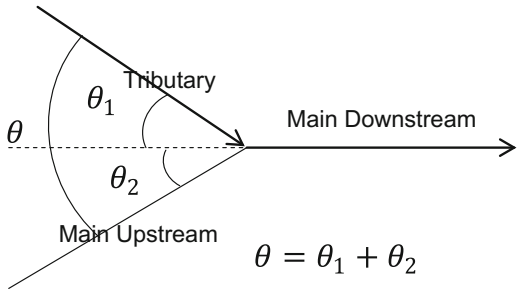

Fig. 8.2 Sketch for confluence angle measurement (After Mosley 1976)

confluence. Because, momentum is a function of the density of water (q), water discharge (Q) and mean velocity (v) and again it is a problem of data unavailability. Although the density of water is known to us, other two variables are depended on instrumental measurement that could not be done. Thus, the Eq. 8.6 has been simplified means momentum has been removed and used a graphical technique for the measurement of confluence angle which has given. The technique for angle measurement of each confluence is, a straight line has been drawn from each confluence between tributary and main upstream which is parallel to main downstream towards the reverse of the flow direction, considering an acute angle with respect to the main downstream (Fig. 8.2). The method gives acceptable values of the confluence angles which are comparable with the values calculated after Horton's method.

In order to detect the relation of tributary length and basin area with the confluence morphology, all the tributaries length and the area of the basin have been measured in ArcGIS 10 by using IRS P6 LISS III (2011). The help of topographical maps (1:50000) has also been considered for the accuracy. The cross sections have been generated from ASTER DEM data using 3D Analyst tools in ArcGIS platform (Sanyal et al. 2014). The verification of DEM data has been done with the help of spot height values that have been picked up from the SOI toposheets and GPS (GARMIN GPS Map 76, accuracy ~4.5 m) when the field survey was being done. There is a considerable positive linear relationship ($R^2 = 0.99$) between DEM elevation and toposheet spot height (Fig. 8.3a). The error of ASTER DEM has been analysed using the differences between ASTER DEM and spot height values from the SOI toposheets and GPS data (Sanyal et al. 2013) (Fig. 8.3b). In this chapter, it has been tried to put and explain some relations of variables related to the confluence geometry and its controlling factors i.e. the relationship between w/w/d ratio of downstream with upstream and the tributary, the relation of confluence angle and tributary basin area with the scour depth of the confluences etc. (Best and Ashworth 1997; Best

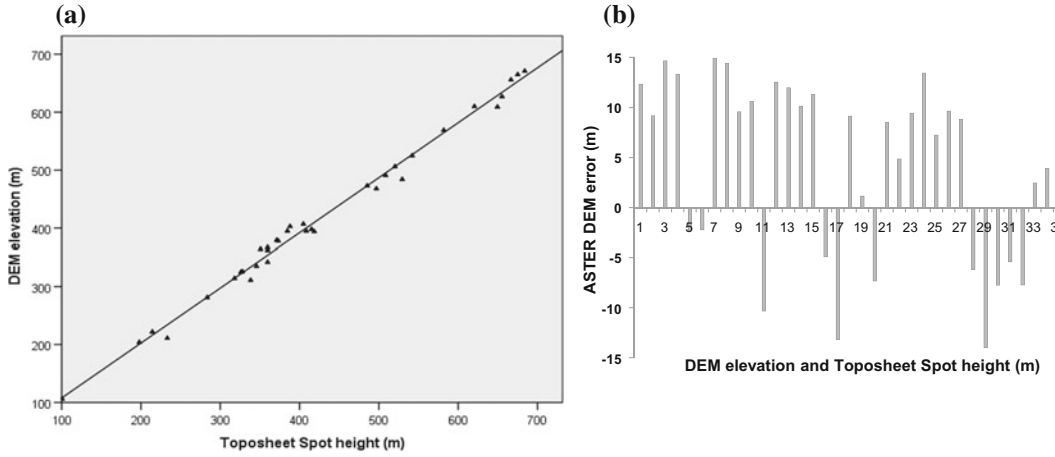

Fig. 8.3 Authentication of ASTER DEM data of the study area. **a** Plotting of Toposheet Spot height against DEM elevation value. **b** Error of ASTER DEM has been calculated using difference between DEM elevation and Toposheet Spot height. Positive and Negative values indicate Toposheet Spot height is higher than ASTER DEM and Toposheet Spot height is lower than ASTER DEM respectively

et al. 2007). For the analysis of confluence geometry, thalweg depth has been considered instead of each point depth along the perimeter of a cross section. For this, a bias due to non-consideration of the channel depth for the area calculation exists. To show the channel surface roughness at the confluences, bathymetric analysis has been done using the contour (Best et al. 2007) of 5 m (for the Khudia river confluence) and 2 m (for rest of the confluences) interval. A correlation matrix has been prepared considering three variables viz. confluence angle, scour depth and width-depth for the five confluences to reflect the relationship between the several parameters of the studied confluences.

8.4 Results and Discussions

8.4.1 Morphology of the Confluences

8.4.1.1 Changes in the Form Ratio (w/d)

The variation of the confluence morphology is associated with the variations in the width and depth of upstream and downstream section of the main stem (Roy and Woldenberg 1986). The downstream reach has the greater width and depth at a cross section in general (Rhoads et al. 2009). In this study, the relationship between width and depth is strongly positive ($R^2 = 0.85$) in the downstream, where the upstream reflects stagnancy on change ($R^2 = 0.10$) which explicitly represents the influence of tributary channels more specifically interface angle, water discharge and sediment load (Fig. 8.7a). The relationship is distinct near to the mouth of the Barakar River. The downstream sections have more water discharge as it is the combined flow of the main stem and the tributary. The w/d ratio has been calculated at three cross sections (Fig. 8.4) constructed for up streams, down streams and tributaries from each studied confluence considering one kilometre distance respectively. Both the Fig. 8.7b and 4 depict the greater w/d ratio in the down streams from each confluence of the Barakar River. Another significant finding is a gradual increase in the variation of the w/d ratio towards Khudia from Barsoti except in the case of Keso confluence which indicates the eternity

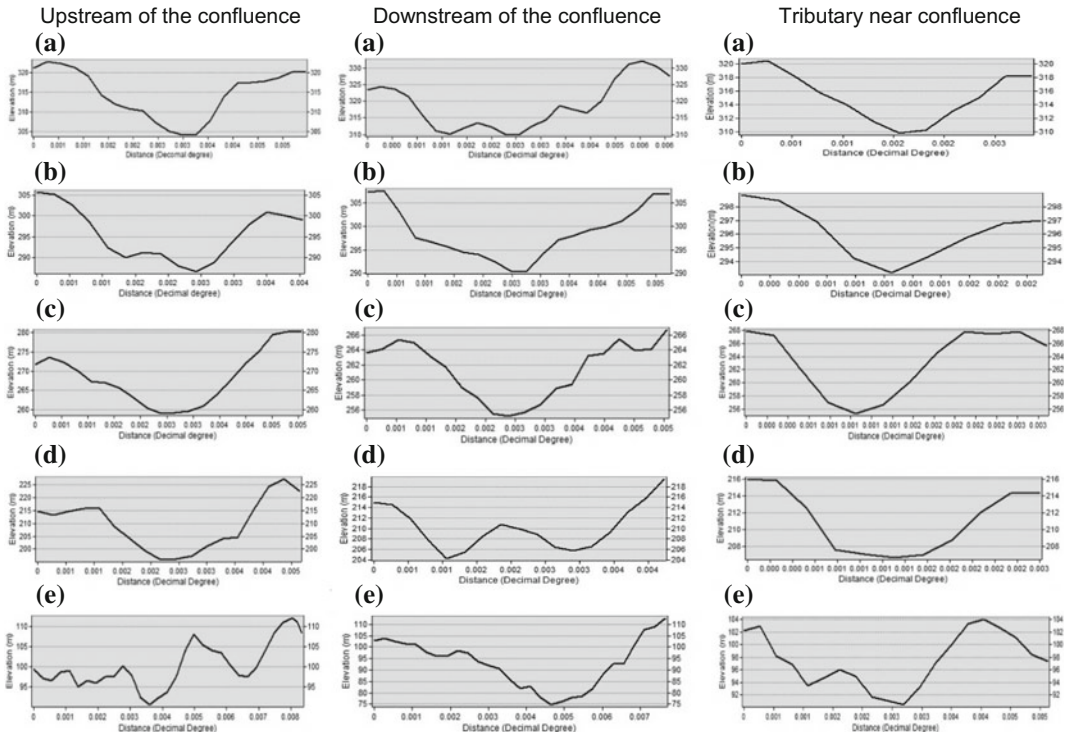

Fig. 8.4 Cross-sections at confluence zones, A—Keso, B—Barsoti, C—Irga, D—Usri, E—Khudia confluences

of general channel geometric rule, i.e. increasing channel volume towards the downstream. Only one exception, i.e. Keso, probably because of local flatland existence and slope declination with less water discharge. Furthermore, it has also been investigated that, all the confluences are associated with the high w/d ratio in the downstream of the confluences (except the confluence of Khudia) and a low w/d ratio of the tributary except the Barsoti (Fig. 8.7b). Lithological control (occurrences of sandstone) on the river bank prevents the dynamics of the w/d ratio at the studied confluence zone. The non-perennial nature of the tributary put little impacts on the river channel geometry.

8.4.1.2 Occurrences of Scour Depth at the Downstream

The scour that occurs at the confluence of two channels is called confluence scour (Klassen and Vermeer 1988). Confluence scour has the geomorphological importance as it is the node in the channel network that controls the distribution of sediment in the downstream, bar construction and channel migration (Ashmore and Parker 1983). The scour depth can be estimated with the help of average depth of the upstream tributaries and the confluence angle (Rezaur et al. 1999). At the confluences of the Barakar River, the scour depth ranges from 6 to 15 m (Fig. 8.5). The scour depth for the studied confluences is ~6.1 m for Keso, ~8.3 m for Barsoti, ~6.4 m for Irga, ~7.1 m for Usri, and ~14.5 m for Khudia. The location of scour at the confluence varies for the studied five confluences and the causes of variation are confluence lithology, continuous flow way, but the interface angle has not considerable impact although here a little negative relation has been found between scour depth and interface angle (Figs. 8.6 and 8.7c). The shape and size are also varied in the different confluences that come into existence of uniqueness of each confluence identity (Fig. 8.5). It would be generalised if geological controls and

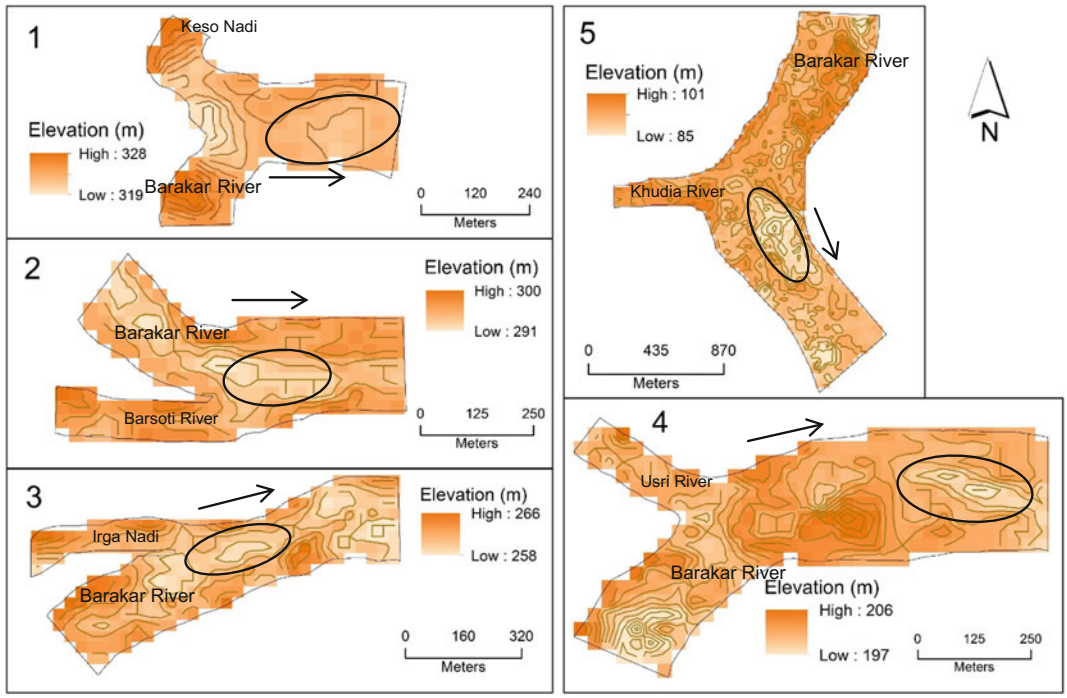

Fig. 8.5 Bathymetric images of major five confluences, 1—Keso, 2—Barsoti, 3—Irga, 4—Usri, 5—Khudia confluences, inner curve lines showing contour with 2 m interval for 1st, 2nd, 3rd and 4th confluences and 5 m interval for 5th confluence. The circles represent the scour depth at the confluence zones

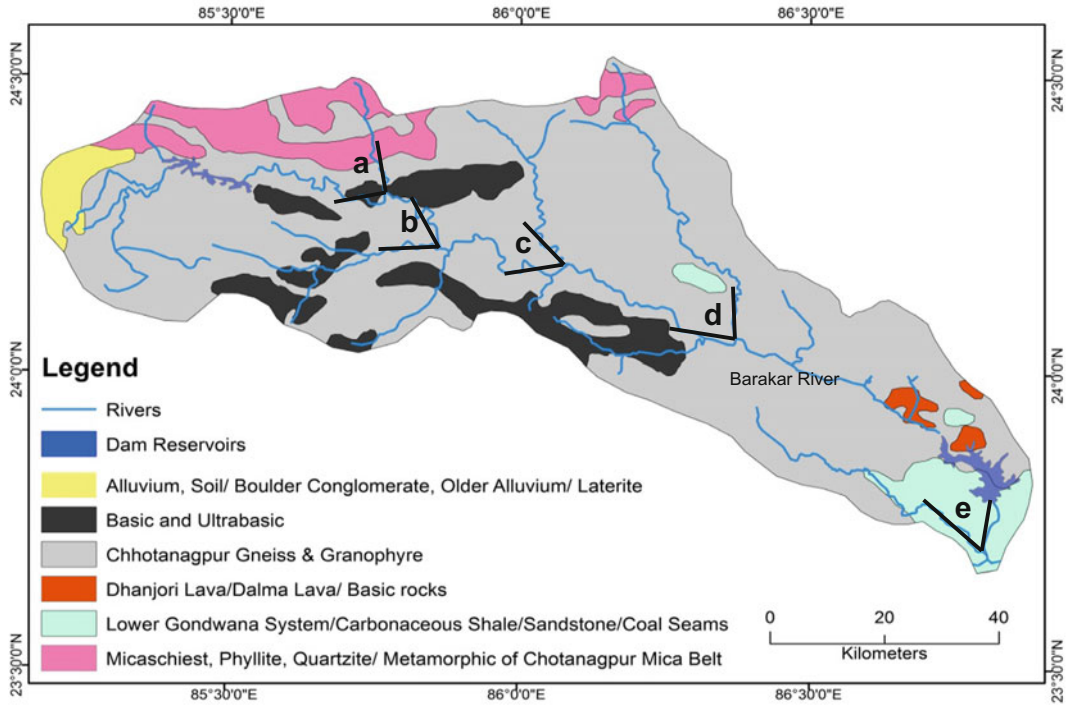

Fig. 8.6 Underlying lithology of the Confluence zones of the Barakar River basin and observed confluence angle at different confluences i.e. a—Keso (89°), b—Barsoti (64°), c—Irga (45°), d—Usri (79°) and e—Khudia (71°)

confluence angle are considered as the reasons because there may be channel system power and energy exerted by turbulence pattern, secondary flow, channel bed shear stress, sediment load and sediment particle properties, etc. Another geometric characteristic of the channel morphology is that low inter-contour spacing indicates the steepness of slope. It is gentle where spacing is greater, of course, for the scour and channel bar, the inter-contour spacing is less as visible in Fig. 8.5.

8.4.2 Confluence Angle and Its Impacts on Confluence Geometry

The channel configuration at the confluences is the reflection of the meeting angle between the main stem and the tributary. Confluence angle determines the downstream turbulence, scour depth, stagnation zone, flow separation zone, maximum velocity zone, w/d ratio of the confluence and other channel geometrical aspects. Rezaur et al. (1999) have estimated that the angle of incidence 15°–75° has been associated with the rapid increase of the scour depth and it occurs slowly up to 120°. From the Fig. 8.7c, an increase in confluence angle with the increase of scour depth has been observed at the studied confluences. Figure 8.5 indicates dark coloured portions are associated with the low contour spacing that indicates the presence of pool as a result of confluence scour. The scour depth is the consequence of the mixed hydraulic shear stress of tributary and mainsteam channel flow. In these reaches, the vertical incision is distinct rather than lateral accretion as the later has been obstructed due to hard land masses and bedrock channel bank. In these studied sections, the impacts of confluence angle to the w/d ratio and the scour depth just below the downstream of the confluence have been investigated. The scour depth has been observed at most of the

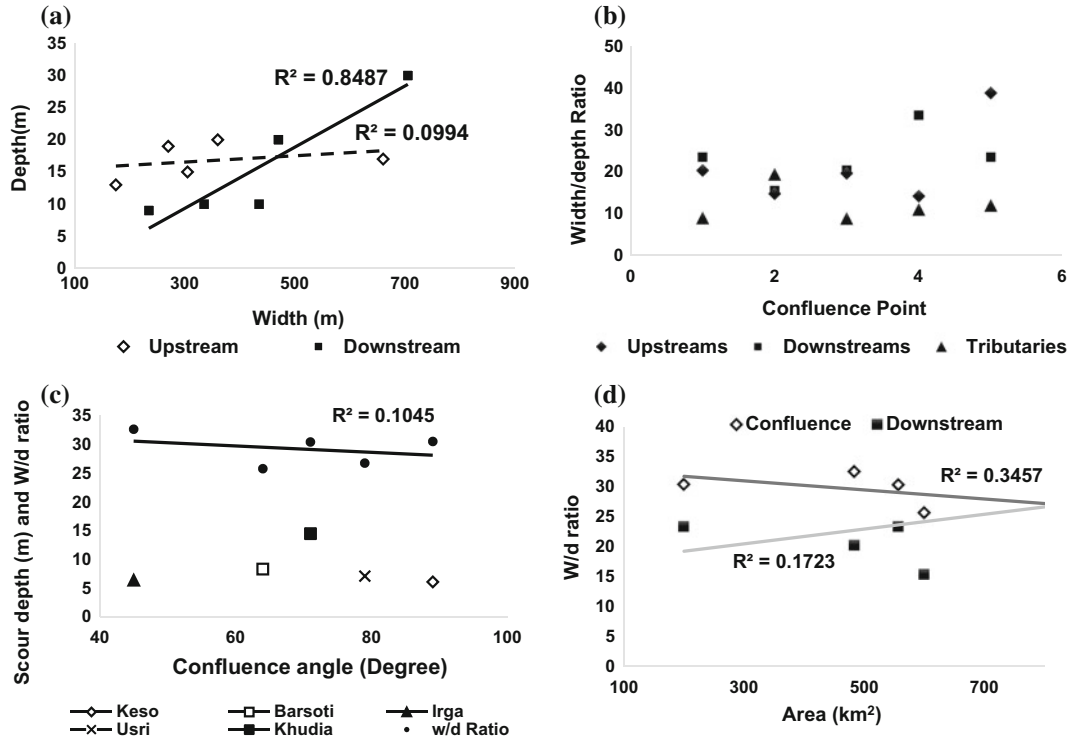

Fig. 8.7 **a** Width-depth relationship at the confluence zones. **b** Width-depth ratio at the different section of the confluence zones. The downstream and upstream of the main stem have been considered. **c** Scour depth and W/d ratio in relation to the confluence angle at the major five confluences. **d** Relation between W/d ratio at the confluences and at the downstream of the main stem with the tributary area

confluences and the result is a positive increase in scour depth with the increase of confluence angle for Irga, Barsoti and Khudia. In the case of Khudia, the scour depth is exceptionally high (∼14.5 m) compared to the other confluences, where, confluence angle is 71°. The high values (∼14.5, ∼8.3, ∼7.1 m) of confluence scour have been found at the angle of 71°, 64° and 79° respectively (Fig. 8.7c), which is surprisingly matched with that of the Rezaur's observation (Rezaur et al. 1999). On the other hand, scour depth is very low for Keso and Usri confluences and does not follow the trend which is being maintained by other three confluences. Eventually, the graph (Fig. 8.7c) is showing a discrete distribution of scour depth at different confluence angle. It is Irga, where, scour depth and confluence angle both are very low (∼6.4 m and 45° respectively), again represents the Rezaur's observation as correct. This study has been done considering the confluences of non-perennial gravel mixed sinuous bedrock channel and we found that the relation between scour depth and confluence angle maintain the statement of Rezaur's observation. It means it is probable that the Rezaur's observation may fit with the confluences of other gravel mixed sinuous bedrock channels. There are some exceptions in the relation between these two; one is no linear relationship between scour depth and confluence angle and the rate of change in scour depth also does not maintain continuity with the change in confluence angle. The w/d ratio of the confluences has slightly negative relation ($R^2 = 0.1045$) with the angle but not very significant. The high w/d ratio of Irga (32.64) has enjoyed with the low confluence angle of 45°. For w/d ratio, the exception also exists in the changing rate like scour depth in relation to confluence angle. An interesting fact about the

Table 8.2 Correlation matrix among the confluence parameters (confluence angles, w/d ratio, scour depth)

	Confluence angles	Scour depths	W/d ratio
Confluence angles	1	0.004	−0.318
Scour depths	0.004	1	0.022
W/d ratio	−0.318	0.022	1

high scour at Khudia confluence may be the effects of Maithon Dam also as the dam is located just 11 km upstream of the confluence. The sudden release of water having a high stream power can act as scouring agent. Above discussion shows the drastic anomaly concerning various aspects of confluence geometry with confluence angle, which clearly indicates the dominant regional lithologic influences, the highly dissected surface of the basin and plateaux location of the basin and seasonality in channel flow (all are independent factors).

The findings of the correlation matrix (Table 8.2) (considering three variables viz. confluence angle, scour depth and width-depth at the five confluences) are insignificant but positive for the relation between confluence angles and scour depths (0.004) and moderately significant, but negative between confluence angle and the w/d ratio (−0.318). One more relation that is also insignificant but positive (0.022) between scour depth and the w/d ratio, has been found which indicates an increase in scour depth proceeds to an increase in the w/d ratio. Although the value of the correlation between confluence angles and scour depths is very low because of the abnormality in confluence structure. The influence of the angles in the case of some confluences is very significant that has already been discussed above.

8.4.3 Impacts of Tributary Length and Area on the Confluence Morphology

Tributary length and area contribute to the heterogeneity of the recipient main and the confluence downstream morphology (Rice et al. 2006). But, in this study, the length and the area of the tributaries (Keso, Barsoti, Irga, Usri and Khudia) have a little contribution to the change in the formation of the morphology of the confluences. There exists slightly negative relation between the length (R^2 = 0.1269) and area (R^2 = 0.3457) of the tributaries to the confluence w/d ratio (Fig. 8.7d).

But it is surprising that the relation between the area of the tributaries and the downstream of the confluences, w/d ratio is positive (R^2 = 0.1723). The higher the length and the area of the tributaries, greater will be the impact on the mainstream channel geometry. From the statistical relation, it is hardly possible to say that the effect of tributaries is more prominent in the downstream of the confluence rather than the confluence zone because generally, the impact of the tributaries on the confluences should be more influential along with the downstreams which is not appear in this study. The probable cause of the anomaly in the statistical relation somewhere indicates the lithological influences. The ternary diagram shows relatively a little impact of tributary length and area on the confluence w/d ratio for Keso, where, other four confluences shows more or less equal importance of the two independent variables (tributary length and area) (Fig. 8.8).

8.4.4 Quaternary Influences on Confluence Morphology

The Barakar River basin is a part of the Chotanagpur Plateau, which is very complex in structure and lithospheric adjustment (Sen and Prasad 2002). The Barakar River basin formation is related to the Vindhyan and Gondwana Super Group of the Palaeozoic era and Chotanagpur gneiss and granophyre with the capping of

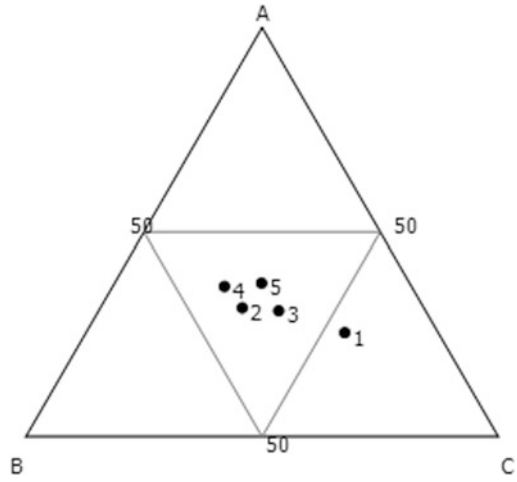

Fig. 8.8 The ternary diagram shows the relation among three variables, A—Tributary length, B—Tributary basin area, C—Confluence w/d ratio. The points are different confluences, 1—Keso, 2—Barsoti, 3—Irga, 4—Usri and 5—Khudia

laterite at some places. Over an extended period, irregular erosional forces evolved gneissic-granitic Pre-Cambrian land surfaces. Then an ice age in the Upper Carboniferous and a fault trough formation during the Permian Period moulded the structure of the basin. A desert type environment during the Triassic and Jurassic period remoulded the basin massively and all these have their footprints in the landscapes and rocks (Kirk 1950). An interesting fact is that exposed new sedimentary deposits and old Gondwana Formation both have been restructured by the force of tropical weathering and channel incision from the Cretaceous Period to the Holocene through the Tertiary and Quaternary, means in the basin, youth and maturity both move forward simultaneously. The Barakar Formation has been derived from the name of the Barakar River, drained a broad undulating lower surface with the mixed-paired terraces formation. It is made up of coarse, soft white to fawn coloured massive cross-bedded sandstone, shale with coal seams (Wadia 1975; Mahadevan 2002) and grit with conglomerate and a bed of shale. In the upstream section, there are several patches of Basic and Ultrabasic and in the downstream section, there are few patches of Dhanjori Lava/Dalma Lava/Basic rocks (Fig. 8.6). The crystalline metamorphic granitic gneiss of Achaean age forms the basement of the drainage basin and these are overlain by Gondwana sedimentaries. The sedimentaries are deposited in the faulted trough or drainage basins. The Gondwana Super Group consists of several formations, such as Kaharbari, Barakar, Barren Measures and Raniganj formations. Since this region is a part of the Singhbhum Craton (Meert et al. 2010), frequent neotectonic activities are not very significant (Singh, 1971). But, an indication of youthful topography signifies some incision and rejuvenation processes in the Quaternary period.

In the upper regime of the Barakar River, between the confluences of its tributaries Keso and Barsoti, channel incision (depth from ~10 to 15 m) is significant (Biswas and Pani 2016). The incised channel are the result of tectonically driven rejuvenation in Triassic to Quaternary period. Moreover, the longitudinal profile of the river is interrupted by some knickpoints. The river runs along the banded gneiss and down-cutting incision through the rejuvenation in the Quaternary period are the main reason for knickpoint developments (Biswas and Pani 2016). Furthermore, the lower and middle sections of the basin, proximity to the Bengal basin, exhibit the deposition of Quaternary young alluvial sediments over the Precambrian and Gondwana deposition in the plateau fringe and Rarh region. Moreover, during Quaternary period, a significant ash bed of 1.83 m thick occurs at the Barakar River section, opposite of Barakar town, near the confluence zone with the Khudia River (Mahadevan 2002). The changes in the Form Ratio at the confluences are the result of long-term sedimentation and denudation in the Quaternary period along with several hydraulic behaviours. Sandstone contains decomposed feldspar and its uneven hardness and weathering (Krishnan 1982) with a rough surface produce potholes of more than one metre in diameter in the stream bed through the Quaternary period. And it is the general channel bed geomorphic structure of the Barakar River including all the studied confluences (Fig. 8.9b). In the downstream section, the significant abrasion process

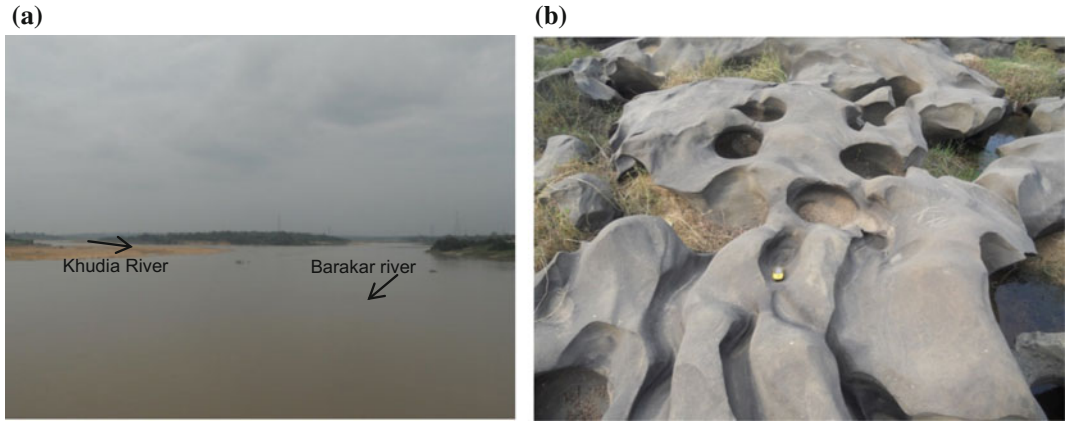

Fig. 8.9 **a** The confluence of Khudia River and Barakar River in monsoon season, **b**. Pothole development of Gondwana sandstone at the downstream section of Khudia River confluence near Dishergarh

with high flow discharge (Fig. 8.9a), velocity and shear stress in a confined channel produce discernible potholes. Several grooves with varying sizes are also prominent in the inner channel beds that hardly get any types of flow except in the rainy season. The lithological structures produce the stable confluence zones. The confluences are lying on the Granitic Gneiss and Gondwana sediment (Fig. 8.6). Thus, the geological structure intensifies the little effects of the tributaries on the scour depth and w/d ratio at the confluence zone and the river banks are characterised with the hard sandstones that favour the stable confluence zone. However, these underlying structural controls have put an impact on the angle of the tributaries, confluence geometry, an anomaly in the relation between two, and downstream morphology. For all the confluences, the Quaternary as well as the pre-Quaternary tectonic and lithospheric controls are probably the major independent factors which characterise the confluences in all aspects than other some active independent factors viz. channel flow, discharge volume, etc.

8.5 Conclusion

Channel confluences are the key geomorphic nodes in the fluvial systems, but different in character for different fluvial environment viz. alluvial, bedrock, etc. The present study is focused on bedrock channel confluences and the major findings reflect drastic anomaly of the morphology of the confluences in all aspects controlled by underlying structure, where, for the alluvial channel, it is rarely controlled by lithology what have been mentioned in previous studies. The presence of bedrock at the bank and channel bedrock outcrop put an insignificant relationship among the several confluence parameters. So, lateral oscillation of the river channel and the confluences is negligible. The stagnant confluences are related to the absence of major neotectonic activities in the cratonic part of Indian peninsula. Changes in width and depth in the downstream regime are significant and the cross-sectional area is larger in this regime. The junctions under the study have been experienced with confluence scour due to the high energy and the flow of water. It can be demonstrated that the fluvial processes at these junctions have developed only in case of some specific properties viz. a mix alluvial and gravel river bed channel. The hard landmass retards the riverine processes to develop the dynamicity of the confluences fully as it is seen in alluvial channels. Moreover, the study is based on remote sensing and other geospatial techniques and a little information had been collected from field survey, where, flow velocity, discharge volume, etc. could not be measured. The studied confluences convey

plateau characteristics, less diverse but distinct from other tropical origin confluences. Therefore, to address the precise explanation of confluence nature laboratory experimentation, accurate field measurement and model building, etc. are required.

References

Ashmore P, Parker G (1983) Confluence scour in coarse braided streams. Water Resour Res 19(2):392–402. https://doi.org/10.1029/WR019i002p00392

Benda L, Andras K, Miller D, Bigelow P (2004) Confluence effects in rivers: interactions of basin scale, network geometry, and disturbance regimes. Water Resour Res 40:1–15. https://doi.org/10.1029/2003WR002583

Best JL (1986) The morphology of river channel confluences. Prog Phys Geogr 10(2):157–174. https://doi.org/10.1177/030913338601000201

Best JL, Reid I (1984) Separation zone at open-channel junctions. J Hydraul Eng 110(11):1588–1594

Best JL, Ashworth PL (1997) Scour in large braided rivers and the recognition of sequence stratigraphic boundaries. Nature 387:275–277. https://doi.org/10.1038/387275a0

Best JL, Ashworth PJ, Sarker MH, Roden JE (2007) The Brahmaputra-Jamuna River, Bangladesh. In: Gupta A (ed) Large river: geomorphology and management. Wiley, Chichester, pp 395–430

Biswas SS (2014). Role of human induced factors, soil erosion and climatic variability in changing the fluvial system: a case study of the Barakar River Basin, India. Unpublished M. Phil. dissertation, Jawaharlal Nehru University, New Delhi

Biswas SS, Pani P (2015) Estimation of soil erosion using RUSLE and GIS techniques: a case study of Barakar River basin, Jharkhand India. Model Earth Syst Environ 1(4):1–13. https://doi.org/10.1007/s40808-015-0040-3

Biswas SS, Pani P (2016) Characteristics of a mixed bedrock-alluvial channel in a plateau and plateau fringe region: a study on the Barakar river of the Chotanagpur Plateau India. Environ Process 3(4):981–999. https://doi.org/10.1007/s40710-016-0190-y

Ferguson R, Hoey T (2008) Effects of tributaries on main-channel geomorphology. In: Rice SP, Roy AG, Rhoads BL (eds) River confluences, tributaries and the fluvial network. Wiley, West Sussex, England, pp 183–206

Kennedy BA (1984) On Playfair's law of accordant junctions. Earth Surf Proc Land 9:153–173. https://doi.org/10.1002/esp.3290090207

Khan ZA (1987) Paleodrainage and paleochannel morphology of a Barakar river (Early Permian) in the Rajmahal Gondwana basin, Bihar, India. Palaeogeogr Palaeoclimatol Palaeoecol 58(3–4):235–247. https://doi.org/10.1016/0031-0182(87)90063-0

Kirk W (1950) The Damodar valley. "Valles Opima". Geogr Rev 40(3):415–443

Klassen GJ, Vermeer K (1988) Confluence scour in large braided rivers with fine bed material. Budapest. In: International conference on fluvial hydraulics

Krishnan MS (1982) Geology of India and Burma, 6th edn. CBS Publishers and Distributors Pvt. Ltd., New Delhi

Mahadevan TM (2002) Geology of Bihar and Jharkhand. Geological Society of India, Bangalore

Meert JG, Pandit MK, Pradhan VR, Banks J, Sirianni R, Stroud M, Brittany N, Gifford J (2010) Precambrian crustal evolution of Peninsular India: A 3.0 billion year odyssey. J Asian Earth Sci 39(6):483–515. https://doi.org/10.1016/j.jseaes.2010.04.026

Mosley MP (1976) An experimental study on channel confluences. J Geol 84(5):535–562

Prasad N (1979) Hydrographic network and drainage basin analysis: a case study of the Barakar basin. Geogr Rev India 41(4):299–303

Prasad N (1982). Some aspects of meandering streams of the Barakar basin and their sinuosity indexes. In: Sharma HS (ed) Perspectives in geomorphology vol 4: essay on Indian geomorphology, Concept Publishing Company, New Delhi, pp. 93–102

Rezaur RB, Jayawardena AW, Hossain MM (1999) Factors affecting confluence scour. In: Jayawardena AW, Lee JHW, Wang ZY (eds) River sedimentation. Balkema, Rotterdam, pp 187–192

Rhoads BL, Kentworthy ST (1995) Flow structure at an asymmetrical stream confluence. Geomorphology 11:273–293. https://doi.org/10.1016/0169-555X(94)00069-4

Rhoads BL, Kentworthy ST (1998) Time-averaged flow structure in the central region of a stream confluence. Earth Surf Proc Land 23:171–191. 10.1002/(SICI)1096-9837(199904)24:4<361::AID-ESP982>3.0.CO;2-5

Rhoads BL, Riley JD, Mayer DR (2009) Response of bed morphology and bed material texture to hydrological conditions at an asymmetrical stream confluence. Geomorphology 109:161–173. https://doi.org/10.1016/j.geomorph.2009.02.029

Rice S (1998) Which tributaries disrupt downstream fining along gravel-bed rivers? Geomorphology 22:39–56. https://doi.org/10.1016/S0169-555X(97)00052-4

Rice SP, Ferguson RI, Hoey TB (2006) Tributary control of physical heterogeneity and biological diversity at river confluences. Can J Fish Aquat Sci 63(11):2553–2566

Roy AG (2008a) Introduction to part I: river channel confluences. In: Rice SP, Roy AG, Rhoads BL (eds) River confluences, tributaries and the fluvial networks. Willy, Chichester, pp 13–15

Roy AG (2008b) River channel confluences. In: Rice SP, Roy AG, Rhoads BL (eds) River confluences, tributaries and the fluvial network. Wiley, West Sussex, England, pp 13–16

Roy AG, Woldenberg MJ (1986) A model for changes in channel form at a river confluence. J Geol 94(3): 402–411

Roy N, Sinha R (2007) Understanding confluence dynamics in the alluvial Ganga-Ramganga valley, India: an integrated approach using geomorphology and hydrology. Geomorphology 92:182–197. https://doi.org/10.1016/j.geomorph.2006.07.039

Sanyal J, Carbonneau P, Densmore AL (2013) Hydraulic routing of extreme floods in a large ungauged river and the estimation of associated uncertainties: a case study of the Damodar River India. Nat Hazards 66 (2):1153–1177. https://doi.org/10.1007/s11069-012-0540-7

Sanyal J, Carbonneau P, Densmore AL (2014) Low-cost inundation modelling at the reach scale with sparse data in the Lower Damodar River basin India. Hydrol Sci J 59(12):2086–2102. https://doi.org/10.1080/02626667.2014.884718

Sen PK, Prasad N (2002) An introduction to the geomorphology of India. Allied Publishers Pvt. Ltd., New Delhi

Singh RL (1971) India: a regional geography. National Geographical Society of India, Varanasi

Stevens MA, Simons DB, Richardson EV (1875) Nonequilibrium river form. Hydraul Div, A. S. C. E 101(HY 5):557–565

Wadia DN (1975) Geology of India, 4th edn. Tata McGraw-Hill Publishing Company Limited, New Delhi

9 Morphological Aspects of the Bakreshwar River Corridor in Western Fringe of Lower Ganga Basin

Debika Banerji and Priyank Pravin Patel

Abstract

The Bakreshwar River flows across south-central Birbhum District in West Bengal from west to east. Along its course, it traverses through varying lithological and physiographic units that influence and alter the morphological character of the river channel, its floodplain aspects as well as the human occupancy and use of adjacent riparian tracts. This study uses computed hydraulic parameters of the river along with planform channel images and land use maps to demarcate the river corridor. Within this demarcated river corridor, several terrain and channel attributes are investigated and their interlinkages are highlighted. Stream reach classification after the Rosgen method is done to demarcate morphologically distinct channel stretches and identify those of a similar character.

Keywords

Bakreshwar · Channel morphology
River corridor · Rosgen

9.1 Introduction

Rivers and river systems may be considered as the most important geomorphic agent operating over the Earth's surface (Morisawa 1968). River channel behaviour determines channel patterns (Kleinhans 2010), which in turn represents channel form adjustment with the underlying topographic base (Ouimet et al. 2009), often conditioned by human use of these environments, particularly in inhabited stream corridors adjacent to the main channel (Stanford and Ward 1993). Riverine plains, either erosional or depositional, are responsible for and, in turn, affected by the geomorphic and anthropogenic developments in an entire region. Changes in channel characteristics cause changes in the surrounding landscape and vice versa (Allan 2004). By studying existent channel characteristics, the behavioural patterns of the river can be judged in different reaches (Sayre and Kennedy 1973) and also be used to highlight a cause–effect relationship with the underlying structure and associated anthropogenic interferences. Universal physical laws govern streams, yet every stream passes in a unique way through its landscape. Gravity and

D. Banerji
Department of Geography, Visva-Bharati University, Santiniketan, West Bengal, India
e-mail: debika.banerji@gmail.com

P. P. Patel (✉)
Department of Geography, Presidency University, Kolkata, India
e-mail: priyank999@hotmail.com

B. C. Das et al. (eds.), *Quaternary Geomorphology in India*,
Geography of the Physical Environment, https://doi.org/10.1007/978-3-319-90427-6_9

water are constants, so all streams tend towards a single ideal form; however, differences in location and physical conditions create the range of forms seen. Each stream futher balances erosion, transport and deposition in the context of its climate and landscape (Harrelson et al. 1994).

A river corridor may be broadly defined as the land immediately adjoining the river (Alexander 2005). It includes the width of the channel in which the water flows and is typically expanded to account for the extensive influence of the watercourse in the surrounding landscape (US EPA 1992). The width of a corridor is defined by the lateral extent of the meanders, termed as the width of the meander belt and is governed by the site and situation of the valley landforms, surface geology and length and slope parameters of the river channel (Vermont Agency of Natural Resources 2005). Delimiting such corridors depends upon a number of factors, including the condition and character of the channel itself and human use of the land around. Thus, they can be demarcated according to a specified distance from the river, or on the basis of physiographic features or through inclusion of land cover and land use unit boundaries (Hawes and Smith 2005). Corridors, acting as riparian buffers, also help in preserving the various aspects of a channel (Wenger 1999) which make them fit as a wildlife habitat, be a source of water supply for domestic and other uses, apart from stabilizing the channel itself (Naiman et al. 1993), thus controlling to some extent the detrimental effects of flooding and bank erosion. Therefore, geomorphic analysis of a channel along with its corridor is essential in order to constitute a knowledge base which is likely to help in stabilizing the channel and minimizing its hazardous impacts on the region while conserving its ecological functions (Mondal and Patel 2018).

Channel geometry is a three-dimensional, cross-sectional, planform and long profile property constituting the complete morphology of a river (Richards 1982), while the channel pattern is the configuration of a river as it appears in its planform and reflects the hydrodynamics of flow within the channel and associated processes of sediment transfer and energy dissipation (Richards 1982). Alluvial channels are of different types and these exist along an energy gradient, ranging from high energy braided and straight channels to low energy anastomosing channels (Charlton 2008). The pattern and form of the alluvial river gives an idea about the energy with which it is sculpting the landscape. Research on meandering channels (Langbein and Leopold 1966; Hey 1976; Julien 1985; Williams 1986; Hudson and Kesel 2000) have traditionally been based primarily on examining meander morphology and channel geometry (Hickin 1974) and their relationship with primary control factors (Schumm 1960). Channel shifting, so typical of meandering alluvial channels in their lower courses, arises from meander migration due to bank erosion coupled with allied changes in channel morphology and hydraulics (Thomas and Sharma 1998; Gagoi and Goswami 2014; Pati et al. 2008). A clear description of the shape of a river's long profile is evident from its slope or gradient which can be expressed as a graphic representation of the ratio of the fall of the channel to its length over a given reach. Thus, it is the representation of the channel bed in longitudinal view (Knighton 1998). The long profiles of most rivers have been studied to identify areas where slow tectonic adjustments have been taking place (Begin 1975; Seeber and Gornitz 1983).

Definitions and constituting elements of river corridors have been discussed by Tockner et al. (2003). The methodology for the studying of reference reaches along a channel for characterizing it has also been succinctly explained by Harrelson et al. (1994) and Rosgen (1998). Further studies examining the geomorphology of channel reaches and channel pattern classifications have been done by Rosgen (1994, 2001a) and Hey et al. (1994), among others. Riparian Buffers (Wegner and Fowler 2000) constitute an important element of watersheds since they protect the river corridors from impacts related to human land use and their maintenance has been identified as the most effective means for protecting channel resources (Hawes and Smith 2005). Efficient buffering projects have been extended both for bank stabilization as well as for wildlife habitat restoration in many rivers of the

United States, where their widths range from 100 ft for bank erosion protection to over 300 ft for habitat conservation along the corridor (Verry et al. 2000). Such buffer zones have also been constructed for free expansions of meanders in some rivers where the width of the buffer has been determined by the lateral extent of the meanders, termed as the meander belt width, which is governed by valley side landforms, surface geology and channel slope (Vermont Department of Environmental Conservation 2013). A shift in approaches to stream restoration has been observed in recent times from traditional ones, which had sought to directly alter the channel itself, towards a geomorphologically more sound approach that provides restoration in the surrounding floodplain or the riparian zone (Doppelt et al. 1993). Application of such projects is seen in the Rosgen Channel Reach Classification System (1994), where emphasis has been given to the measured morphological relations associated with bankfull flow, geomorphic valley types and geomorphic stream types. Towards this, a number of master plans have been designed by independent researchers and landscape designers (van den Berg 1995), individual states (Toms River Corridor Task Force 2004) as well as national water resources monitoring agencies (FISRWG 2001). The demarcation and analysis of river corridors and subsequent channel training and river restoration has also been promulgated as an effective mitigation measure against channel erosion and flood hazards (Piegay et al. 2005), providing a low-cost, eco-friendly approach that is likely to find resonance in developing countries having sparse resources.

However, river reach classification and stream corridor demarcation has rarely been done in India and such literature is very sparse (for a brief review of such studies, see Mondal and Patel 2018). Keeping in mind the views expressed by the proponents of this method for riparian area rejuvenation and restoration for ecological and economic benefits, the authors feel that its greater awareness and application can give suitable benefits in river management. A case study towards this methodological development has, therefore, been done on the Bakreshwar River for its channel corridor demarcation, which is the primary step towards reach classification and possible pursuance of any ensuing management policies.

9.2 Objectives

The objectives of the present study are therefore as follows:

- Description of the Bakreshwar River's course, along with allied geological and physiographic attributes.
- Analysis of channel cross-sectional and longitudinal attributes, sinuosity and channel patterns in different reaches, bedform and grain-size aspects of channel bed material for computation of channel hydraulic and hydrological parameters.
- Channel reach classification according to the Rosgen (1994) Method for the Bakreshwar River.
- Demarcation of the Bakreshwar River Corridor along with description of land use and land cover (LULC) and channel morphology aspects for select corridor windows.

9.3 The Study Area

The Bakreshwar River (Fig. 9.1) rises from the south of Rajnagar village (23° 56′N; 87° 19′E) near the West Bengal—Jharkhand state border, where rolling plains and small streams trickle down the wasteland—a short distance northwest of the hot springs of the same name at Bakreshwar Town (87° 22′ 30″E, 23° 52′ 50″N) some 16 km west of Suri (the Headquarters of Birbhum District). After following a zigzag course eastwards and receiving one by one the waters of almost all the rivulets of south Birbhum, it joins the Kopai River after flowing for nearly 100 km at 23° 47′N and 87° 47′E at an elevation of 28 m, just below Labhpur, to form the Koiya Nala, which flows further towards northeast to debouch into the Mayurakshi River, just beyond the eastern boundary of Birbhum District (O'Malley

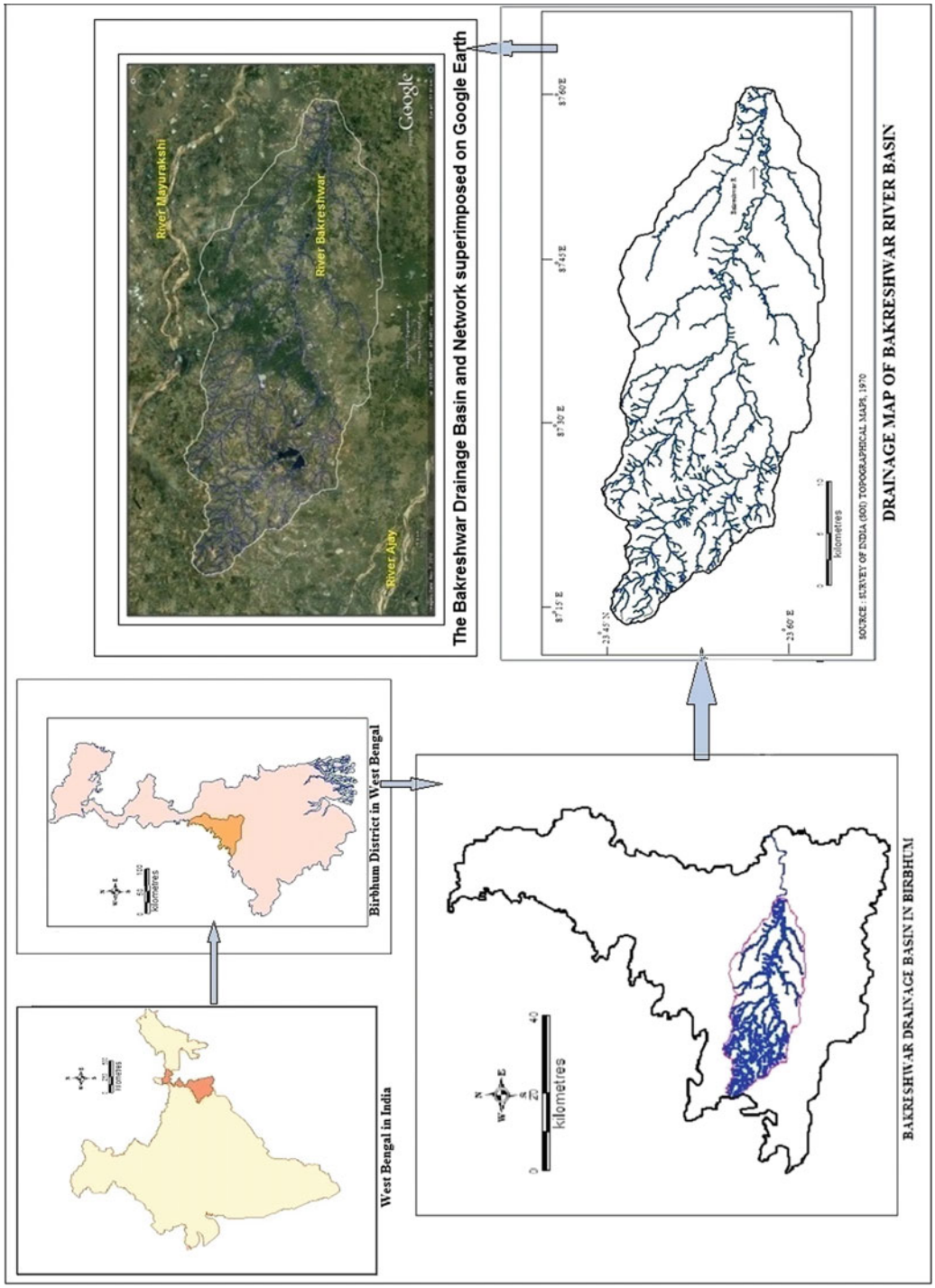

Fig. 9.1 Location map of the study area

1910). For the most part, the river flows over agricultural fields (often mono-cropped land) and in some places, there are vegetated, tree-lined banks or even thick groves. Sand deposits and bars within the channel are rarely seen in the upper reaches and only small meandering bends are prevalent, incised into the young alluvium. Further downstream, near Gaisara (23° 54′N; 87° 19′E), the river loops around sandbanks and vegetation and the natural vegetation cover seems to have been preserved along the river corridor in these stretches. Some point bar formation after Muktipur village (23° 53′N; 87° 20′E) is more evident. Near Bakreshwar town (23° 52′N; 87° 22′E), the river seems to be polluted with traces of eutrophication. Some rocky exposures on the bed of the river are seen here. In most places downstream of this point, the vegetation has been cleared to make way for agricultural fields. Some sandbars are noticed in the channel near Matijapur (23° 52′N; 87° 23′E). Euthrophication is noticed near Padampur village (23° 51′ N; 87°23′E) and Shimultari (23° 51′N; 87° 24′E), which increases moving further downstream towards the Neel Nirjan dam, where a considerable area has been submerged and the Bakreshwar Thermal Power Plant and Township are located. Further downstream, the river flows over barren land and the channel is usually dry or devoid of much flow. The topsoil here is quite useless for cultivation, consisting mostly of hard laterite but small patches of woods exist, part of localized afforestation programmes. Some forested lateritic tracts are seen near Bodakuri village (23° 47′N; 87° 25′E), where rocky exposures are also seen on the bed of the river. At Bishalpur (23° 47′N; 87° 27′E), extensive sandbars are present that grade into mud banks along some stretches. Bar deposits become abundant further downstream with shoals and point bars seen at many places. A meander loop is seen near Muradpur village (23° 49′N; 87° 32′E), with well-developed sandbars. Plantations are seen near Hatikra village (23° 49′N; 87° 35′E), along with well-developed meanders beyond the it. Meander cut-offs are seen near Jinaipur (23° 49′ N; 87° 37′E) and the river starts anastomosing further downstream. Abandoned oxbow lakes are seen along and adjacent to a number of channel reaches thereon. The scars left are visible, particularly from satellite images and these are often used for cultivation, being depressions where the soil moisture is retained even in the drier months. Near its mouth, the channel has deeply incised into its floodplain and follows a quite tortuous course. The river is affected by periodic high flows in the monsoon months and usually floods its adjacent lands but goes almost completely dry for the rest of the year. Such periodic alterations in the river regime and flow pattern accounts for the hydrological changes in the channel and impacts on its morphology and pattern.

9.4 Methodology

The step-wise methods adopted for the study (Fig. 9.2) are as follows:

- Digitization and mapping of the Bakreshwar River Channel from Survey of India (SoI) topographical maps of 1:50,000 scale—Map Nos. 73M/5, 73M/9 and 73M/13 and from higher resolution Google Earth image tiles for planform descriptions, measurements of channel pattern, sinuosity, meander curvatures and wavelengths and identification and demarcation of palaeo-channels.
- Preparing an elevation database for the channel from SOI maps and ASTER GDEM v2 tiles (resolution 30 m) for longitudinal profile extraction of the Bakreshwar River.
- Overlaying of the extracted long profile of the Bakreshwar River on geological and physiographic maps obtained from the Geological Survey of India (GSI)—District Resource Map of Birbhum and District Planning Map Series for Birbhum District (from the National Atlas and Thematic Mapping Organisation (NATMO) database) for demarcation of lithological and terrain units along and adjacent to the Bakreshwar River channel.
- Extensive field surveys at regular intervals (fifteen sites) along the Bakreshwar River from its source to mouth for measurement of channel cross-sectional and hydraulic parameters. Plotting of these measured parameters to obtain bank profiles and depositional bed form attitudes and their use in hydraulic equations

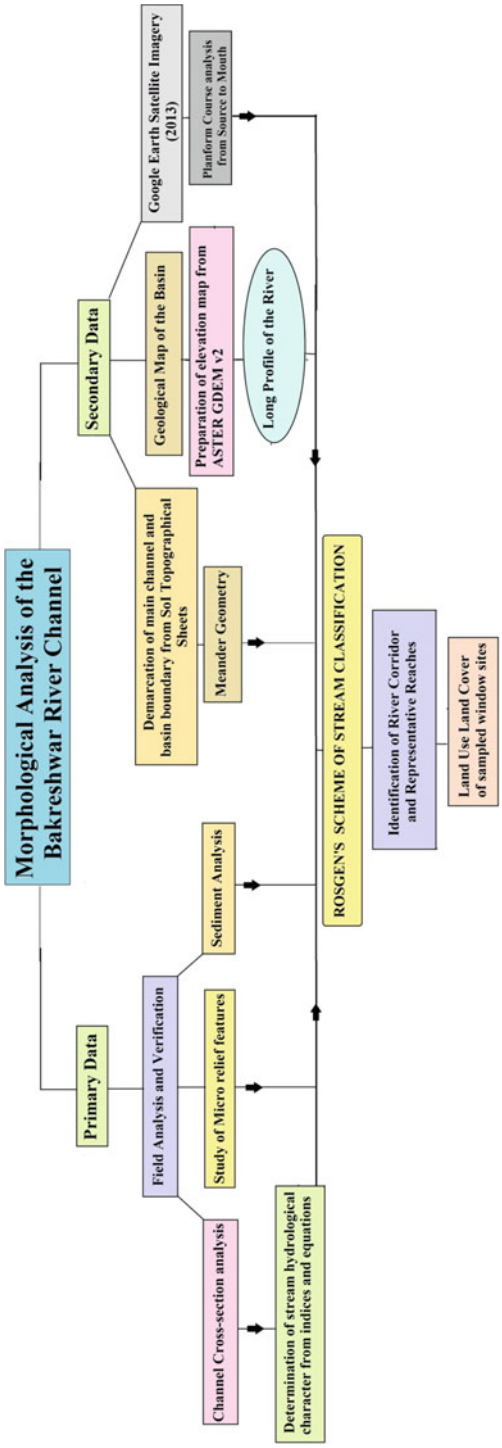

Fig. 9.2 Schematic representation of the adopted methodology

for deriving computed flow velocities and stream power at the measured sites.

- Bed and bank material sample collection from a number of sites along the channel for grain-size analysis, for determining bed and bank material parameter input into the ensuing Rosgen classification scheme (1994).
- Channel hydraulic parameters, planform attributes, sediment characteristics, associated LULC aspects and channel pattern properties have been used to classify the Bakreshwar River into Rosgen (1994) Stream Reaches for a more succinct codification, demarcating the typical assemblage of physiographic, hydrological and anthropogenic factors governing each stretch. The parameters evaluated under the principal criteria required for understanding the river hydrology and for achieving a stream reach classification are explained as follows:

(i) Planform attributes: Channel Planform or Meander Geometry helps in quantifying the development of meanders on the floodplain (Gurnell et al. 1994; Gilvear et al 2000). They depict the nature of the river in relation to the processes operative, equilibrium conditions existent as well as the channel adjustment to other factors such as geology and climate (Winterbottom 2000; Downs and Kondolf 2002; Clark et al. 2003). Channel planform parameters such as meander wavelength, amplitude, radius of curvature and channel width were measured at different stretches after digitization from Google Earth imagery. Sinuosity measures were carried out to understand the degree of deviation the river attains from its mean centre. Channel flow along the mean centre can be said to be a hypothetical entity (Leopold and Langbein 1966) but nonetheless it is useful in quantifying and demarcating reaches along the river. The Sinuosity Index (SI) was calculated using the following formula:

$$\text{SI} = \text{Channel (Thalweg) distance}/\text{Down valley distance (Leopold et al. 1964)}, \quad (9.1)$$

where SI = 1 indicates a straight channel; 1 < SI < 1.5 indicates a sinuous pattern; SI > 1.5 indicates a meandering pattern.

(ii) Channel hydraulic attributes: Channel hydraulics helps in the understanding of river behaviour and aids deciphering of how the different fluviometric and fluviological parameters shape the landscape. Stream power is the rate at which the energy of flowing water is expended on the bed and banks of a channel and provides the potential for the stream to perform geomorphic work. The spatial distribution of stream power along a channel has been linked to things like river form and flood-response behaviour in many studies (Bagnold 1966; Graf 1971; Knighton 1998). While theory predicts that stream power values along a channel long profile should peak in the mid-basin reaches (Knighton 1998), local variations in channel slope (and tributary effects on discharge) can cause significant deviations from this. Slope exerts an especially strong control on stream power and since many factors can affect the local slope of a channel, stream power can vary substantially at the reach scale, with variability from one reach to another being the rule. The different equations that have been used to calculate channel hydraulics are as follows:

$$\text{Hydraulic Radius}\,(R) = A/P \quad \text{(Leopold and Maddock 1953)} \quad (9.2)$$

$$\text{Manning } n \text{ equation}\,(\eta) = \left(R^{2/3}S^{1/2}\right)/v \quad \text{(Manning 1890)} \quad (9.3)$$

$$\text{Froude Number}\,(F_r) = u/(gd)^{0.5} \quad \text{(Froude 1868)} \quad (9.4)$$

$$\text{Total Stream Power per unit length}\,(\Omega) = \rho g R S v \quad \text{(Yang and Stall 1974)} \quad (9.5)$$

$$\text{Specific Energy}(E) = v^2(1/(2g+d)) \quad \text{(Yang 1972)}, \quad (9.6)$$

where A = cross-sectional area of the channel (m^2); P = wetted perimeter (m); R = hydraulic Radius (m); S = channel slope (m/m); η = Manning's roughness coefficient; u/v = channel flow velocity (m/s); g = acceleration due to gravity (9.8 m/s^2); d = depth (m); ρ = density of water (1000 kg/m^3).

(iii) The shape of a particle's form is an important aspect of study since it helps determine the processes operative, their magnitude as well as the particle's resistance capacity (Garcia and Parker 1991). Cailleux (1952) devised an index to measure the shape of a sediment particle with the help of the following formula:

$$R = 1000\,(2r/a) \quad \text{(Cailleux 1952)}, \quad (9.7)$$

where R = Cailleux Index of roundness; r = least radius of curvature in the principal scale; a = length of the long axis.

The R values range from 100 to 1000 with values tending towards 100 being rounder than the values that lie further away.

- Demarcation of the Bakreshwar River Corridor on basis of above the channel reach classification and subsequent examination of the attributes of select windows within the corridor from river source to mouth, in respect of channel pattern and alignment, LULC aspects and human use of the riverine environment.

9.5 Results and Discussion

9.5.1 Lithological–Physiographic Relationships and Channel Longitudinal Profile

Clearly, two broad physiographic units may be identified along the river's course, though the terrain is always characterized by a general southwards–southeastwards slope—the rocky igneous Archaean granitic surface (predominant in the upper one-third of the entire channel length) and the alluvium veneered floodplains (occupying the lower two-thirds). The floodplains may be further subdivided into flat low lying alluvial tracts and the higher undulating, at times, lateritic zones.

The granitic–gneissic zone is well defined and easily identifiable in the upper reaches of the river (Fig. 9.3). In some places, like Rajnagar (23° 56′N; 87° 19′E), rock outcrops jut out from the river bed and have weathered, forming feldspathic clays and angular quartz particles. These Archaeans are the oldest rock formations, comprising of granitoid and schistose rocks which crystallized at least 900 million years ago (NATMO 2000). The sulphurous hot springs of Bakreshwar (32° 52′N; 87° 02′E), probably lying along a fissure zone in the granite-gneiss, are also thought to have formed due to deformations within the Archaean—Gondwana complex of the area (O'Malley 1910). Emergence of hot water and gases is noticed here at seven different spots aligned northeast–southwest, which probably is a granite-gneiss fissure.

Further downstream, alluvial plains predominate, with the older, more compacted alluvium occupying the relatively higher reaches as compared to the lower-lying, softer, more unconsolidated younger alluvium. Their attitudes are more or less flat, unlike that of the rolling granitic topography (GSI 2001). The Older Alluvium (Bhangar) is coarse and generally of reddish colour, containing abundant disseminations of calcareous and limonitic concretions. This alluvium is probably of Middle Pleistocene age. The Newer Alluvium or Khadar, of recent to subrecent age, is mostly confined to the present day channels and contains less calcareous matter (GSI 2001).

Some isolated lateritic tracts are present, slightly elevated than the surrounding alluvial plains. Their ferralitic contents suggest a long and probably continuous exposure to subaerial conditions. Maybe these are residual weathering products of the nearly peneplained Archaean massif, carried by rivers into shallow coastal seas. Due to the recession of the sea, the estuaries of the streams draining the ferralitic–lateritic lands were prograded and the landscape of Birbhum derived its dissected features (Ghosh and Guchhait 2015). Usually, these mounds are unfertile and hence abandoned and bare, bereft of cultivation, though some tracts have been afforested. Laterite blocks (locally referred to as *moram*) are used for making bricks or paving roads. Gulling on these lateritic tracts has produced small badlands in many a place. The Kopai and Bakreshwar rivers' confluence exhibits some calcitic outcrops.

The extracted longitudinal profile of the main channel shows the topographic and lithological influences (Fig. 9.4). The Archaean complex forms the most resistant and thus steeper portion of the landscape, down which the river cascades, at times in puny rapids. Channel breaks are more evident in this section of the long profile than in other sections downstream. Over the Quaternary sediments, the profile assumes a much more relaxed posture, and deviations from a smooth parabolic concave upwards curve are less marked

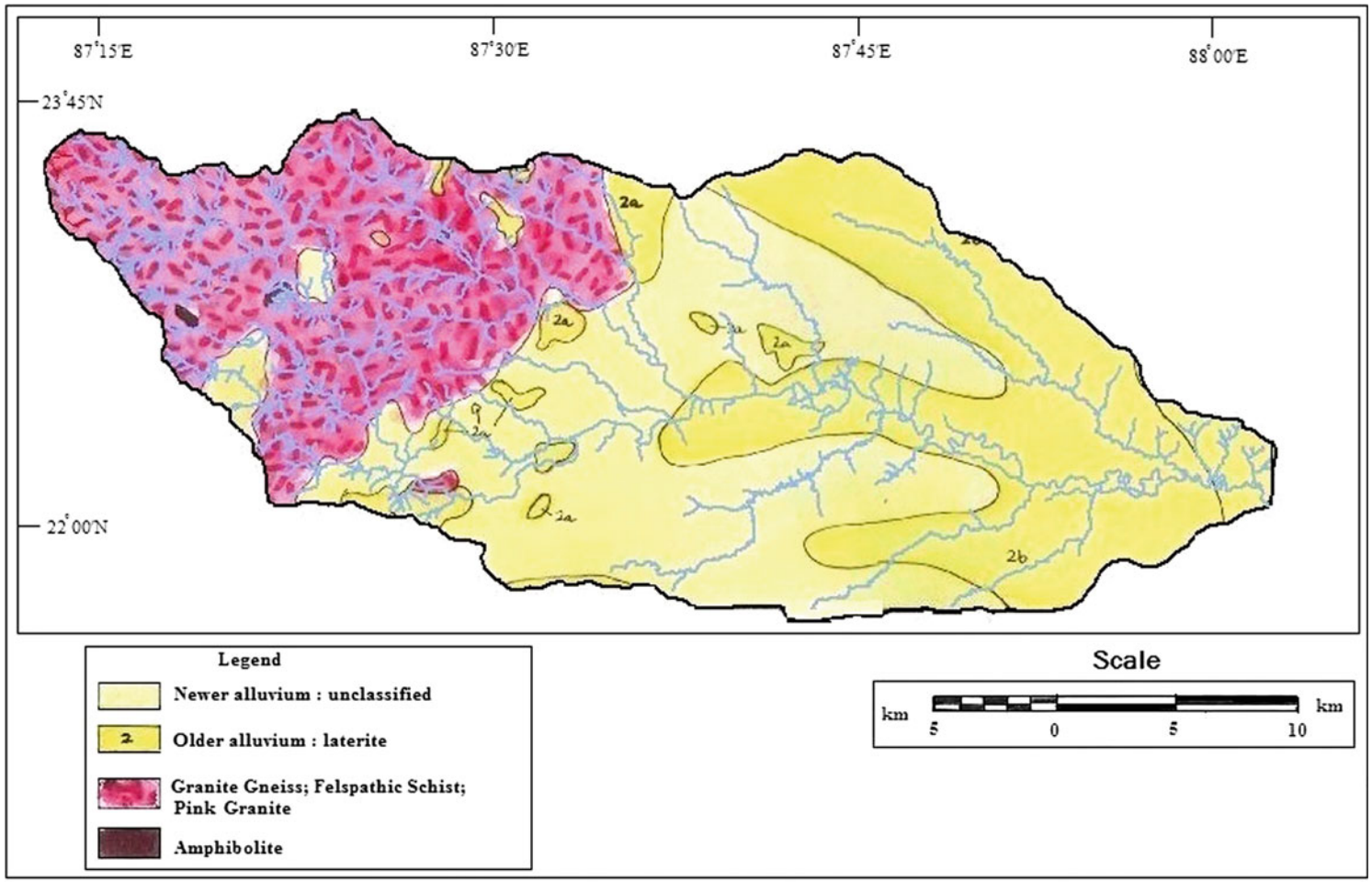

Source : District Resource Map, Birbhum, West Bengal, Geological Survey of India (GSI)

Fig. 9.3 Lithological cover of the Bakreshwar River Basin

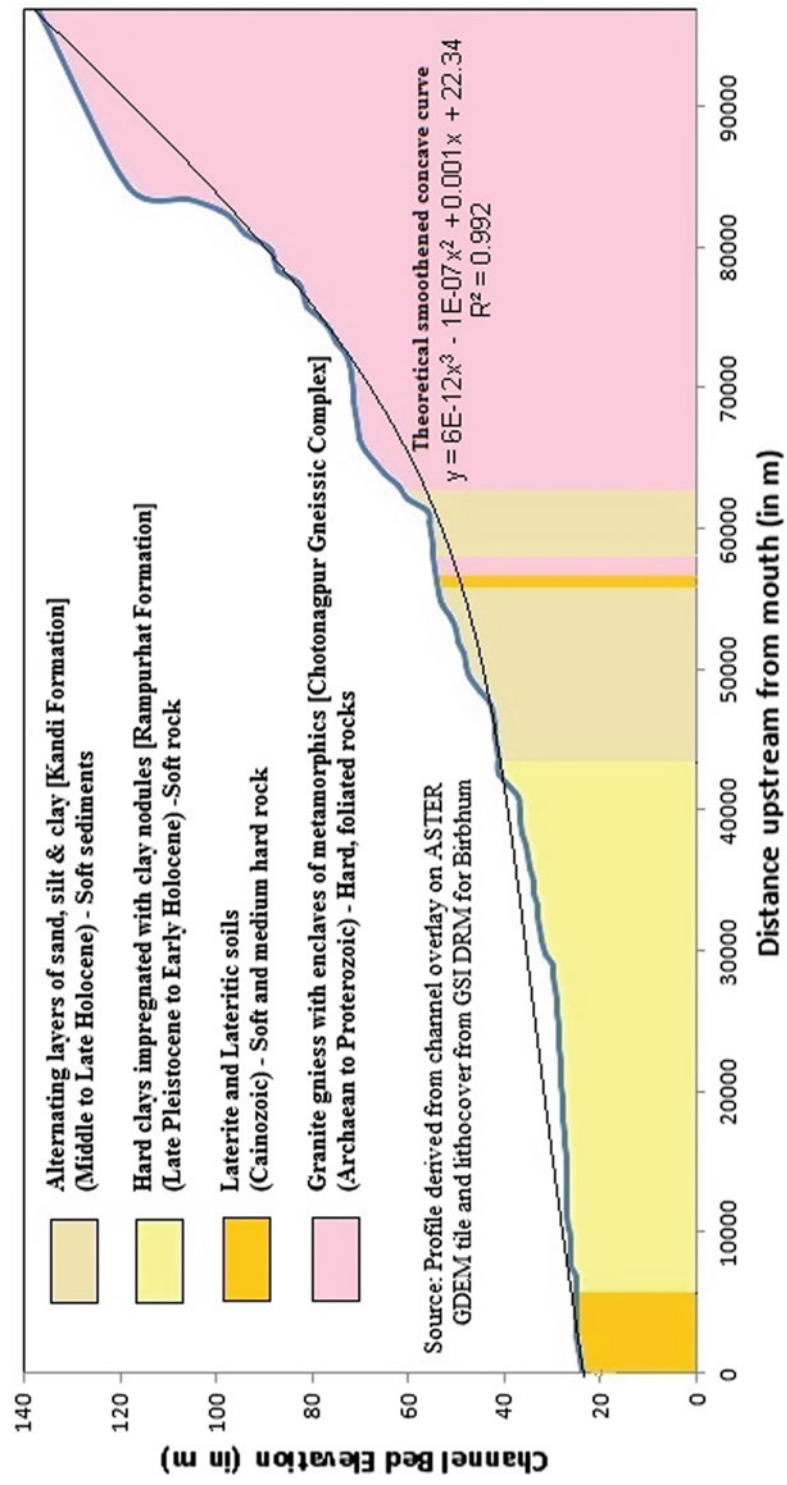

Fig. 9.4 Relating substratum and channel slope through long profile and lithological linkages

in this stretch. Thus for about two-thirds of its course, the Bakreshwar flows over gentle terrain and as seen subsequently, these are the tracts where it principally forms its floodplain with marked lateral meander sweeps, indicating the gradual and barely perceptible changes in relative elevation and channel slope.

9.5.2 Channel Cross-Sections

The cross-section of a river is an expression of the different hydraulic parameters which demonstrate how the river behaves and fashions the landscape (Charlston 1969; Holbrook et al. 2006). The reach of a channel is an adjustment between the amount and intensity of water flow, sediment-borne and the nature of the bank material (Park 1977; Gleason 2015). At a given reach, the mean velocity, mean depth and width of flowing water reflects the characteristics of the channel cross-section (Leopold et al. 1964; Lee and Julien 2006). A stream channel that changes from being relatively deep and narrow to being shallower and wider (i.e. increase in width/depth ratio) may experience a concurrent loss of pools which often provide important in-stream habitats for fish (Jowett 1998) and riparian habitats and landscapes can be effectively judged by using the hydraulic geometry and channel planform as surrogate variables (Brierley et al 2013; Cullum et al. 2016), albeit keeping in mind the limitations of using only this approach (Wohl 2004). Because bed shear stress would be increased in a wide, shallow cross-section, such channels would have a relatively higher potential for bedload transport and bank erosion and would generally be characterized as unstable.

Cross profiles across the Bakreshwar River channel were measured at fifteen sites (Table 9.1; Figs. 9.5 and 9.6). Both the channel width and depth increased downstream. At Rajnagar the channel width was very narrow—less than 4 m. At Abadnagar the channel width increased slightly with not much change in depth. Here, the channel banks were densely vegetated with inflowing small tributaries, called '*kando*' by the local people. Near Bakreshwar Town, the Bakreshwar River becomes properly defined and named. Here, two cross-sections were taken, one near the Bridge leading to the Town and the other near a cremation site. Granite

Table 9.1 Surveyed sites along the River Bakreshwar

Sl. No.	Surveyed sites	Latitude	Longitude	Remarks
1	Rajnagar	23° 56′N	87° 19′E	Upper course reaches
2	Abadnagar	23° 53′N	87° 17′E	
3	Muktipur	23° 53′N	87° 20′E	
4	Bakreshwar (Bridge)	23° 52′N	87° 22′E	
5	Bakreshwar (Town)	23° 52′N	87° 21′E	
6	Sagar	23° 48′N	87° 25′E	
7	Jostabad	23° 48′N	87° 30′E	Middle course reaches
8	Srikanthapur	23° 49′N	87° 34′E	
9	Hat Ikra (Bar)	23° 49′N	87° 34′E	
10	Hat Ikra	23° 49′N	87° 35′E	
11	Mohhamadnagar	23° 48′N	87° 29′E	
12	Tekedda	23° 48′N	87° 41′E	Lower course reaches
13	Kalikapur	23° 48′N	87° 47′E	
14	Labhpur	23° 47′N	87° 46′E	
15	Mouth	23° 47′N	87° 47′E	

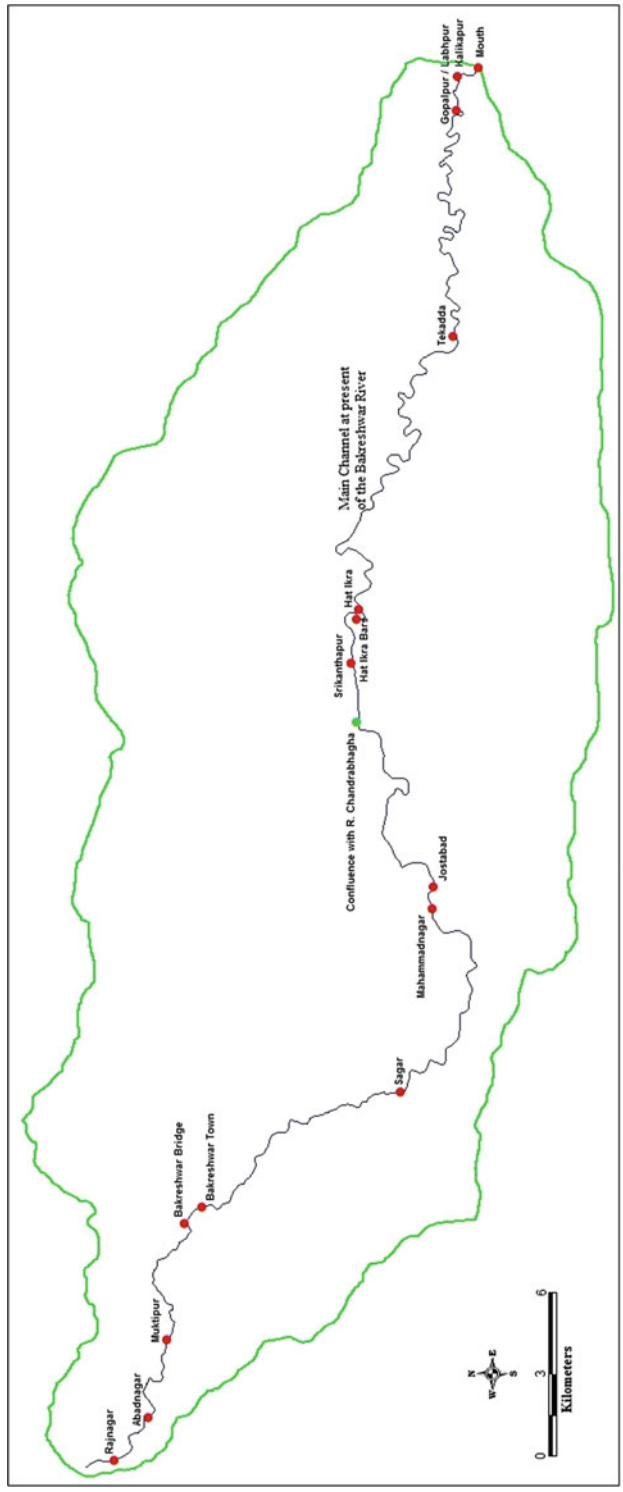

Fig. 9.5 Channel cross-section and sediment collection sites

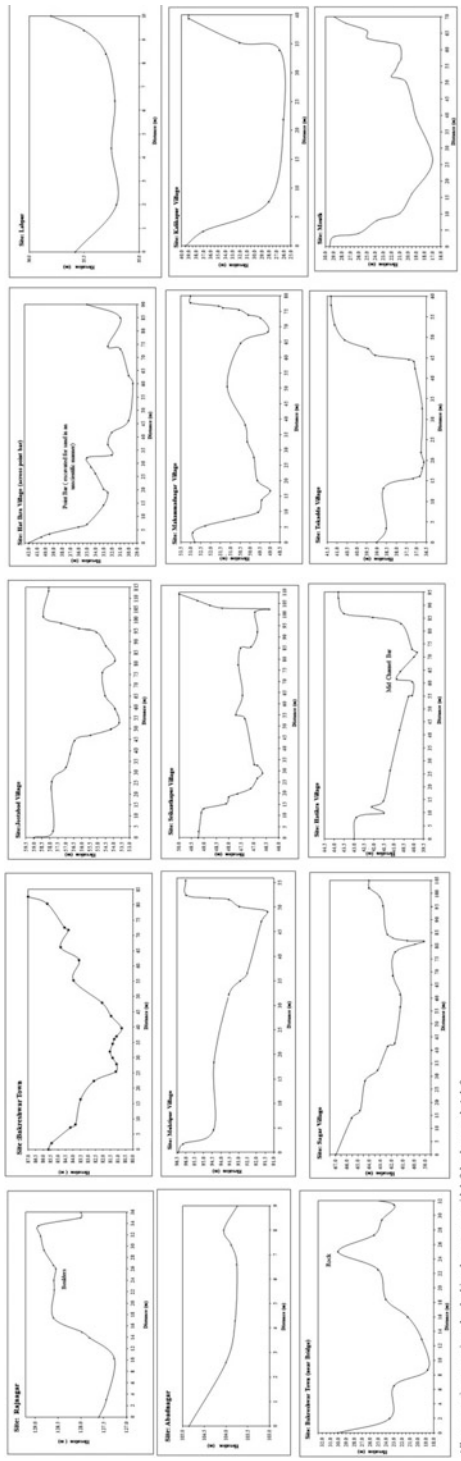

Fig. 9.6 Collaged cross-sections across the Barkeshwar River

boulder-strewn surfaces and bedrock exposures were seen near the bridge. However, by the cremation site, the river flows over flat lands with steep-sided banks and the river width increases considerably with an allied increase in depth. Near Muktipur and Sagar, the river flows over older alluvium and the channel is mildly entrenched. The right bank of the river is steeper than the left.

From the middle section onwards, the Bakreshwar starts following a sinuous course and forming wide meanders, most prominently at Hat Ikra. Here, a sudden increase in the river width allows small mid-channel bar deposits to form along with point bars. Two cross-sectional profiles were taken here—upstream and downstream of the bridge. The profile upstream passed over a hollowed point bar (due to sand quarrying) as indicated by the deep dug out pits in the profile. Hat Ikra's accessibility, well connected by a metalled road, facilitates sand quarrying here. Downstream, the profile exhibits steep incised banks on either flank and a small exposed mid-channel bar. At Jostabad, two similar thalweg channels may be identified with the central elevated zone indicative of a mid-channel bar. Similarly, near Srikanthapur, the cross-section across the channel indicates point and mid-channel bar developments.

The lower course of the River displays an anastomosing pattern of channel development and near the mouth, a well-developed meandering pattern. The cross-section taken at Tekedda shows a very steep right bank compared to the left, with the river width increasing dramatically. At Kalikapur, the channel becomes very wide with steep banks indicating moderate channel entrenchment. At Labhpur, a well-developed meandering channel of considerable width and depth is profiled with a steep right bank (cliff face) and point bar abutting left bank (slip-off face). The flooding limits can easily be identified by observing the steep, indented right bank face, marked each time the water level rises. The river here is wide and sluggish, continuing thus up to its confluence. This lower reach is quite prone to flooding.

9.5.3 Channel Sinuosity and Planform Meander Geometry

While the channel wavelength and amplitude increases steadily downstream, with especially the radius of curvature rising sharply in the lower reaches, channel width does not exhibit a corresponding increase. However, there is a slight increase in width in the lower stretches of the river course. From computed channel sinuosity index (SI) values (Fig. 9.7), the upper reach of the river, as a whole, is deemed to exhibit an irregular—sinuous pattern (SI—1.15), the central reaches show a meandering pattern (SI—2.2), while the lower reaches comprise of a highly developed and broadened meander belt with marked tortuosity in channel course (SI—3.1), with oxbow lakes and meander cut-offs adjacent to the tortuous, active channel. In the middle and especially the lower reaches, extensive floodplain development has taken place, as compared to just the sliver that is present in the upper course, within which the river course oscillates as it weaves its way across and over the floodplains.

9.5.4 Channel Hydraulic Parameters

A positive correlation between the stream power and the computed velocity shows the existence of close relationships between the two (Table 9.2; Fig. 9.8). Thus, an increase in the stream power can be attributed to an increase in the velocity of the flow in the channel (Stewardson 2005). The Specific energy of the river decreases downstream along with a decrease in the Froude's number and a number of exponents for each reach is derived through the regression plots, reflective of the typical downstream hydraulic geometry of most rivers (Dingman 2007; De Rose et al. 2008). Thus, there is a change in the flow dynamics of the channel, from a high energy channel in the upper reaches to a low energy, tranquil channel in the lower reaches, which could well be the effect of the dam put across the river, as the values differ sharply at the stations surveyed upstream and downstream of this structure, reflecting the use of this parameter to gauge stream erosion or deposition (Bizzi and Lerner 2015). Thus, the observed and computed parameters may not represent the true natural state of the channel, but rather that of a stream harnessed and with regulated flows. The narrow thalweg presently coursing through a wider and deeper bed in the lower course of the river (which is likely to have been sculpted during the pre-dam phase of the channel), is another probable testament to the above statement, as is the drop-off in the computed flow velocity progressively downstream.

9.5.5 Bed and Bank Material and Sediment Analysis at Different Reaches

9.5.5.1 Boulders and Pebbles

A boulder-strewn terrain, at times choking the main channel, is present near Rajnagar (Fig. 9.9). A correlation between the boulder lengths and widths reveals that there exists a negative yet weak correlation between the two, indicating that the boulders are more angular than round. Cailleux Index of Roundness (1952) values greater than 400 for the boulder samples further indicates that they are subangular to angular in shape. This may be because the fluvial forces have not yet fully modified them, in the generally shallow and often dry upper reaches, resulting in them being less rounded in shape.

At Hat Ikra, the Bakreshwar flows over alluvium terrain, actively eroding and excavating its course. Pebble deposits here (Fig. 9.9) reveal remnants of weathered granite–quartz, feldspar and iron concretions. These three minerals, due to their differing resistance to erosion, exhibit differing angular dimensions, with the predominantly quartz and feldspar pebbles having a longer x axis (length) than those formed of iron concretions, which are already quite rounded before being further modified by the river, at times into perfect globules. The Cailleux Index of Roundness for iron concretions have the greatest values on the scale as they are perfectly rounded, followed by those for feldspar pebbles and finally for the quartz pebbles. This may be

Table 9.2 Calculated hydraulic parameters of the Bakreshwar River for the fifteen surveyed sites

Sl. No.	Stations	Wetted perimeter (in m)	Area (in m^2)	Depth (in m)	Hydraulic radius (R) (in m)	Computed velocity using Manning's coefficient of roughness (v) (in m/s)	Specific energy (in MJ/kg)	Froude's number	Stream power (Ω/m)
1	RAJNAGAR	4.13	0.49	0.25	0.12	3.79	0.72	2.42	2203.34
2	ABADNAGAR	5.31	0.44	0.02	0.08	1.92	0.19	4.34	779.57
3	MUKTIPUR	19.11	22.65	1.5	1.19	26.39	33	6.88	153265.00
4	BAKRESHWAR (BRIDGE)	24.29	42.57	4	1.75	22.89	22.2	3.66	196570.35
5	BAKRESHWAR (TOWN)	29.97	33.62	1.75	1.12	25.45	30.34	6.15	139892.63
6	SAGAR	12.83	8.85	3	0.69	6.17	1.68	1.14	4170.88
7	JOSTABAD	53.83	98.99	0.5	1.84	11.96	7.12	5.4	21553.82
8	SRIKANTHAPUR	52.06	21.03	0.5	0.40	4.32	0.93	1.95	1710.19
9	HAT IKRA (BAR)	23.45	57.89	2	2.47	14.44	9.65	3.26	34934.45
10	HAT IKRA	7.43	1.37	0.5	0.18	2.56	0.33	1.16	462.59
11	MOHAMMADNAGAR	10.55	2.83	0.5	0.27	1.8	0.16	0.81	47.32
12	TEKEDDA	7.51	0.87	2.5	0.12	1.03	0.05	0.21	11.69
13	KALIKAPUR	28.83	46.7	4	1.62	5.97	1.51	0.95	947.70
14	LABHPUR	8.33	1.37	0.25	0.16	1.3	0.09	0.83	20.95
15	MOUTH	24.39	33.16	4	1.36	5.31	1.19	0.85	707.49

Source Field Survey based computations

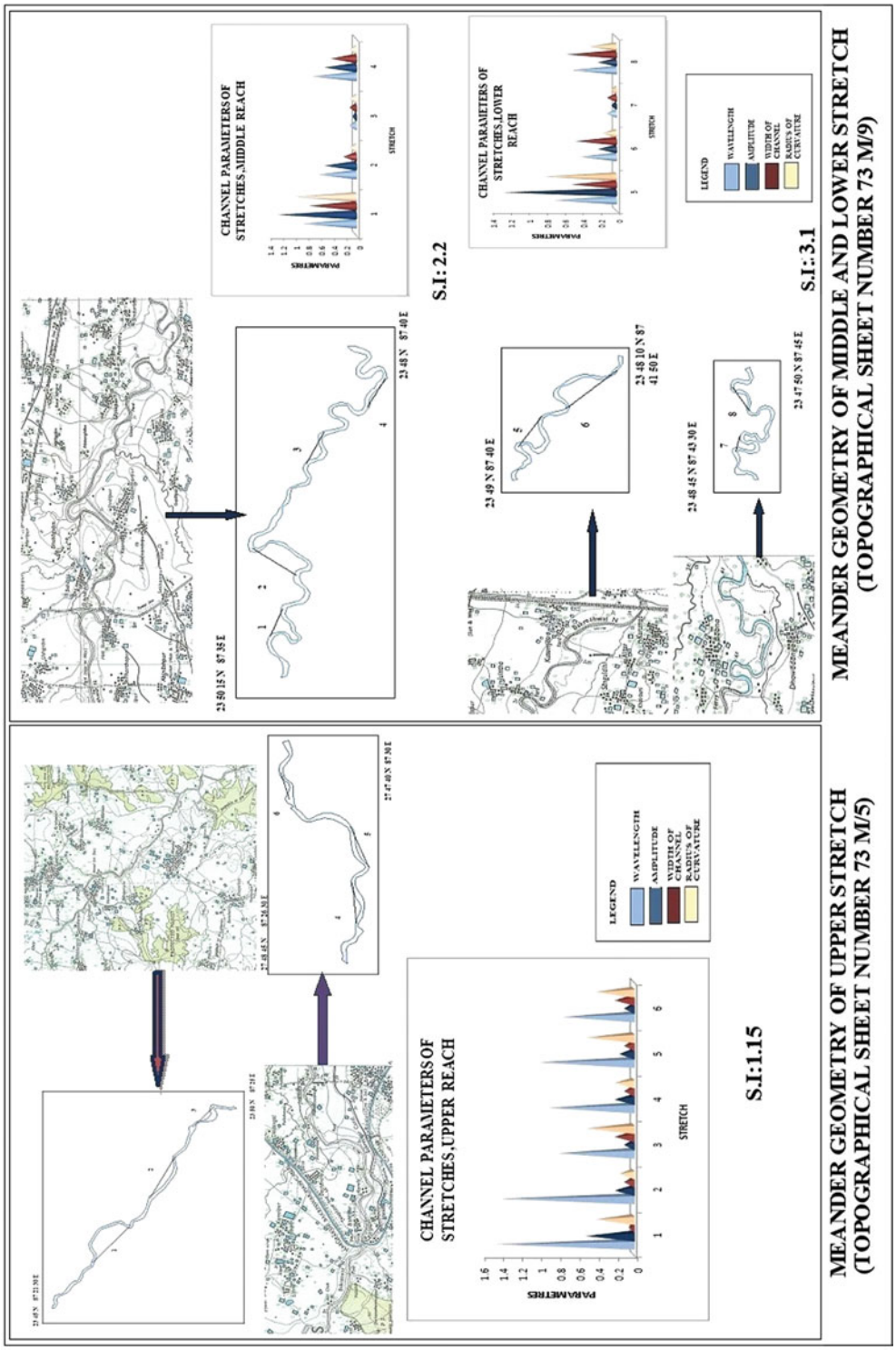

Fig. 9.7 Channel sinuosity measures at different reaches

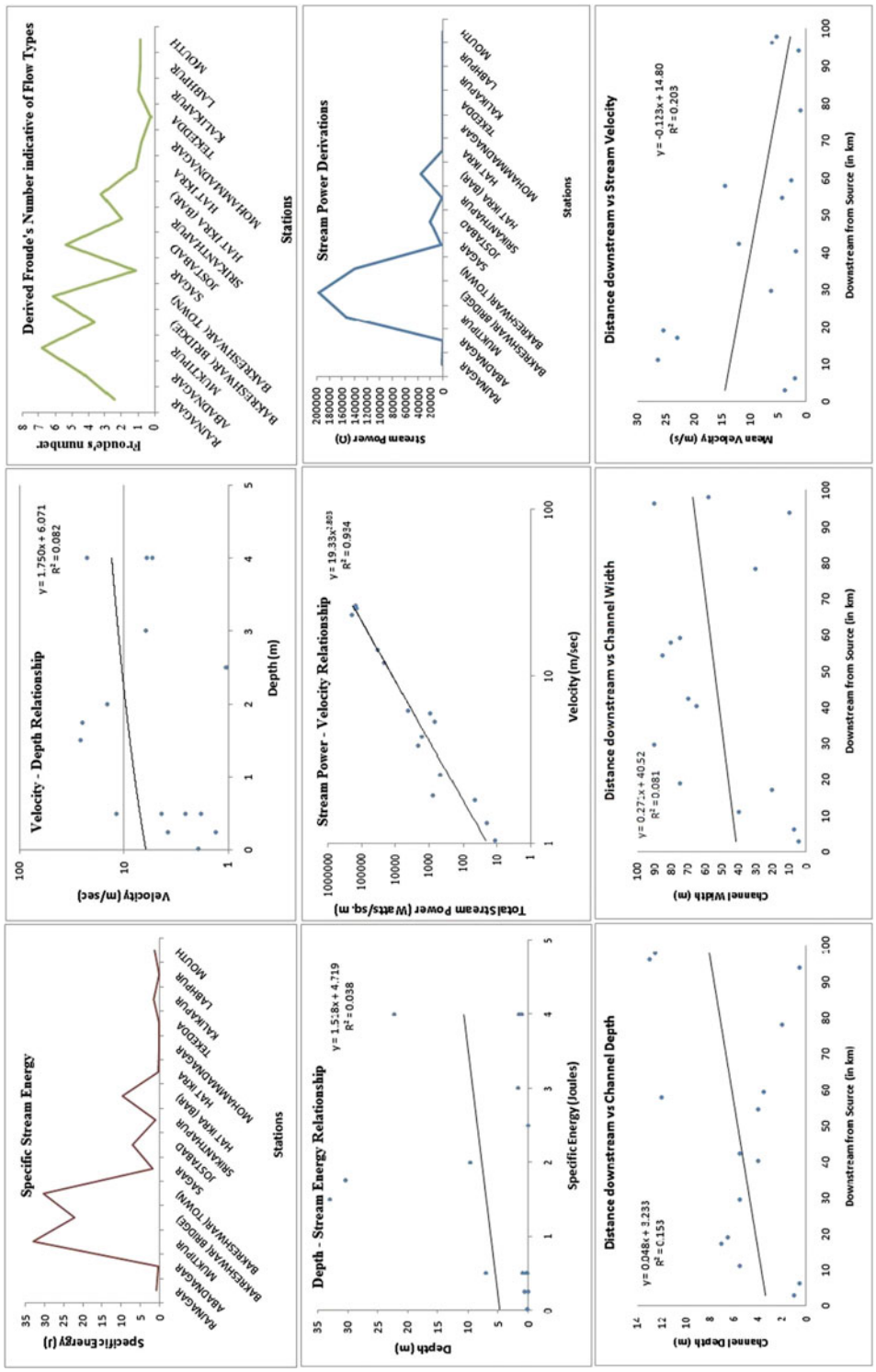

Fig. 9.8 Computed stream hydraulic parameters and inter–relationships

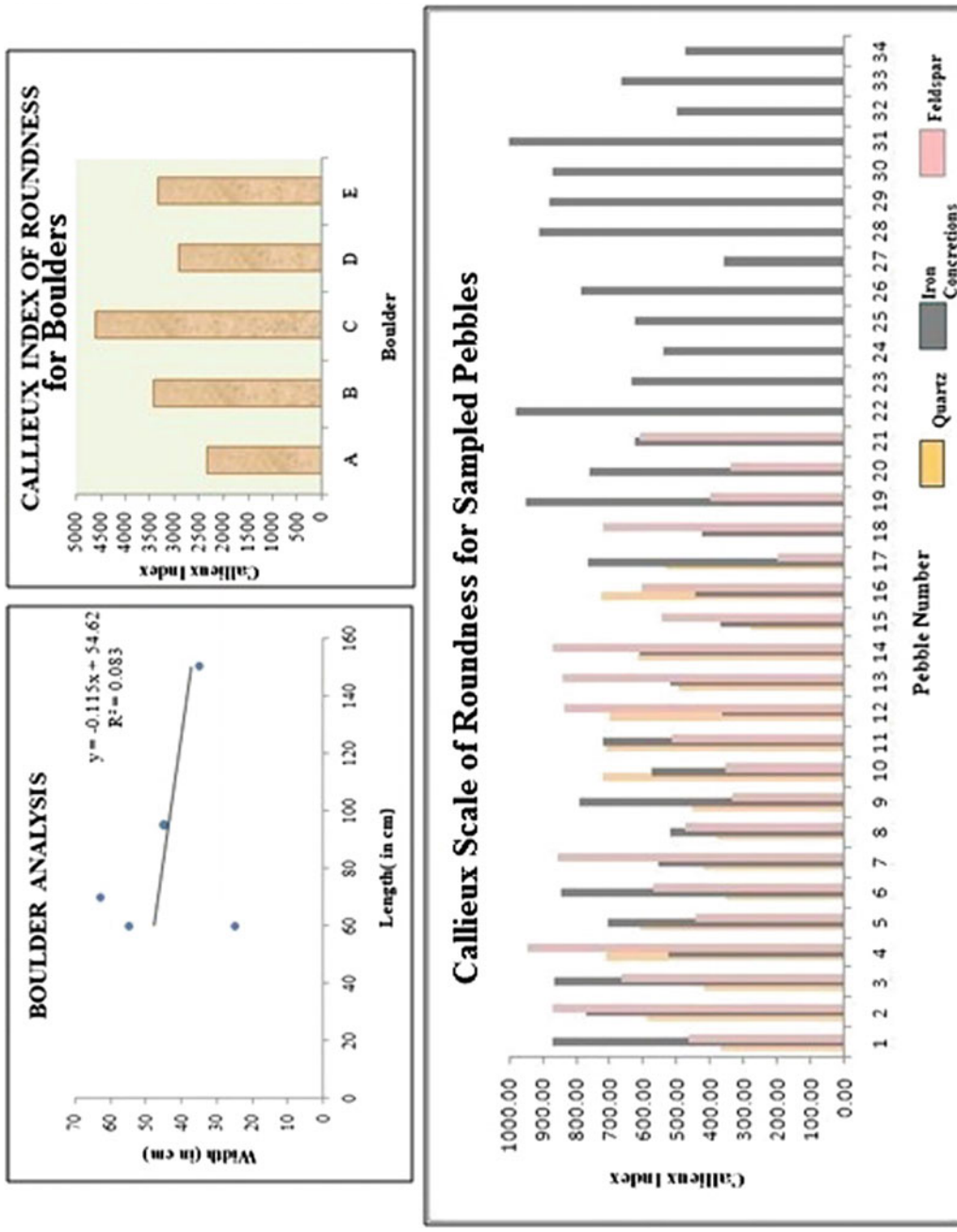

Fig. 9.9 Analysing coarse sediments—boulders and pebbles

because quartz is more resistant to erosion than feldspar and hence it is more angular and sub–angular in shape than feldspar, which tends to be more sub–rounded and sub–angular.

9.5.5.2 Finer Sediments

Alluvial channels, set in unconsolidated sediment, adjust their shape by entraining and redepositing bed material, reaching a steady state configuration or grade, when the flow can transport all sediment supplied from upstream without net deposition or erosion (Parker 1976; Nelson et al. 2003). Sediment samples from different sites were sieved, weighed and their percentages calculated according to the grain dimensions (Fig. 9.10). At Rajnagar, the sample consisted predominantly of coarse gravel, with some sand but very low fractions of silt and clay. Samples were collected from Abadnagar at two sites with both showing a very high percentage of very fine sand and an equal proportion of the other categories, except coarse pebbles, which are absent here. At the confluence of the Bakreshwar and the Chandrabhaga Rivers, sediment samples were collected from the banks, mid-channel bar and river bed. Sand category was found to be high in all the four samples. The mid-channel bar is composed of coarse, fine and very fine sands. The river bed shows similar characteristics with an additional slight presence of fine gravel, probably borne down by the streams from the upper reaches. The banks show the presence of all the sand categories, fine gravel and also a small percentage of coarse gravel. Near Hat Ikra, sediment samples were collected from both the banks and the bed, which are all predominated by fine sands. Additionally, silt and clay, coarse and fine sands and gravels are also noted on the banks, while all three categories of sand were recorded in the channel bed sample. At Labhpur, in the lower course, three samples were again collected from both banks and the bed with fine sand predominant in each. However, the right bank also had some very fine sand and silts and clays while the left bank showed the presence of some coarse gravels. The channel bed sample simply had the fine and very fine sands only. The sediment analysis reveals, as expected, the downstream fining of the grains from source to mouth.

9.5.6 Channel Bed Forms

Jackson (1975) specifically identified channel bars as sedimentary macroforms, in contrast to ripple and dune-like features, which he characterized as microforms and mesoforms, based on their scale. While the origin of the smaller sedimentary features may be sought in flow hydraulics, specifically in the way in which turbulent flow deforms the mobile stream bed, sedimentary macroforms owe their origin to the overall flow and sediment regime of the river and to geological controls on the river morphology (Ashmore 1991; Gordon et al. 2004; Church and Rice 2009).

Ripples Ripples were observed on the channel bed near Hat Ikra (Fig. 9.11). Their amplitude and wavelength measurements showed a positive correlation. Their depth was approximately 2–3 cm, implying their micro-relief nature, unstable character and genesis in a mild fluvial environment.

Point Bars River bars [persistent depositions of bed material (sediment)], essentially define the morphology of unconfined alluvial rivers, though they may also be present in bedrock channels and are also important in deciphering their flow regimes. The planform of a measured point bar (Fig. 9.11) at Hat Ikra revealed that the bar surface rose gradually from the bank base, was at a maximum in the centre due to pronounced deposition and then sloped downwards steeply to the water's edge.

9.5.7 Implementing the Rosgen Scheme (1994) for Channel Reach Classification of the Bakreshwar River

A quantitative model is necessary to understand the nature of the river in its various reaches

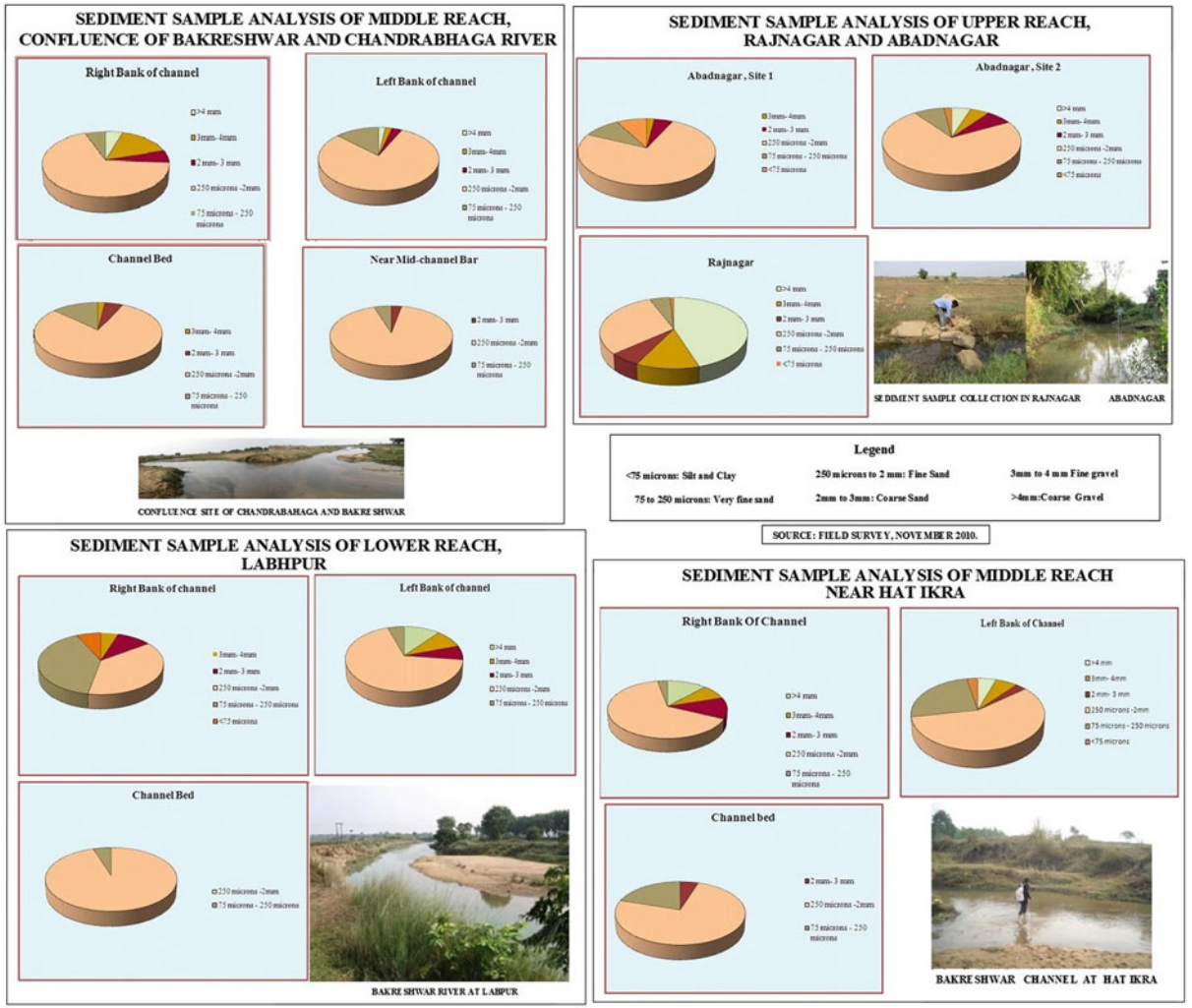

Fig. 9.10 Analysis of the finer sediments

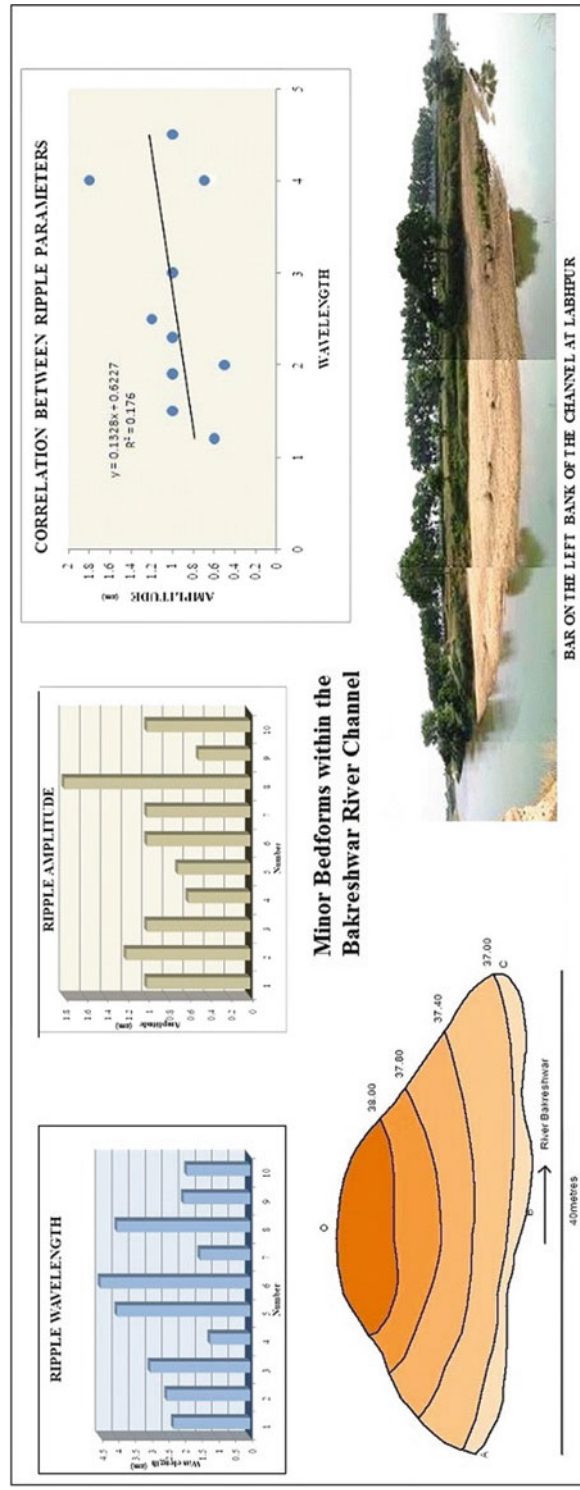

Fig. 9.11 Minor Bedforms—Point Bars and Ripples

(Bisson et al. 2006), and to classify its geomorphic diversity systematically (Cupp 1989; Carlson 2009). The main objectives of a quantitative model are to predict a river's behaviour from its appearance and to develop specific hydraulic and sediment relations for a given morphological channel type (Rosgen 1994), on the basis of cross-sectional parameters, channel slope and sinuosity values and type of bank and bed material (Galay et al. 1973). This is necessary since the entire river, while being a continuum for water, sediment and biota movement, actually functions in separate distinct reaches linked by transition zones and a distinctive characterisation and demarcation of such zones would not only create a river inventory for planning purposes but also enable more pertinent assessments of stream bank stability (Pfankuch 1975; Rosgen 2001c), riverside erodibility (Rosgen 2001b), sediment generation (Rosgen 2001a) and required restoration measures to achieve natural channel conditions (Rosgen 2006, 2007, 2011). By following Rosgen's general scheme of classification (Table 9.3), an attempt has been made to classify the Bakreshwar River accordingly in its various reaches. Primary importance was given to planform and cross-section parameters, augmented by field observations (Table 9.4). Rosgen's criteria of channel parameters (slope, depth, sinuosity and so on) did not entirely match with the actual observations.

River reaches categorized on basis of the above-tabulated scheme and values were thus identified and demarcated (Table 9.5; Fig. 9.12). The river is entrenched into the older alluvium throughout its course. Hence, the entrenchment values are <1.4 at most of the reaches. Sinuosity values more or less correspond to the expected classification values. Marked deviations from the Rosgen tabulated values are seen in case of the measured channel slope values, which are higher. This seemingly implies that similar geomorphic features may develop in higher slope regions as well and factors other than the slope can play an equally important role in determining the geomorphology of a river reach. Width–depth ratio is also extremely high in most of the stretches, with it being particularly high in the middle eaches of the river's course.

9.5.8 River Corridor Demarcation and Land Use–Land Cover Attributes of Select Windows

The river corridor has been demarcated systematically through selective analysis and visual interpretation. To aid in this, initially, a number of Google Earth screenshots (Fig. 9.13) have been used to examine the morphological character and associated vegetation relationships along the riparian tract, backed up by field observations in these same areas. Parameters ascertained include the variables used earlier in the Rosgen Channel Reach Classification along with the state of the existent natural vegetation and the distance of any palaeo-features from the current principal channel. The variable-width method has been preferred and used to delineate the probable river corridor extents—this being favoured over the fixed-width method where the entire corridor is marked at a set distance from the channel. The variable width occurs due to a differing sinuosity of the channel in its various reaches (as documented using the Rosgen Stream Reach Classification mechanism above), extent and degree of adjacency of natural vegetation along the banks and the limit to which the palaeo-channel features and meander cut-offs and oxbow lakes could be discerned from the presently active channel. Though harder to demarcate, the incorporation of these three variables provides a more flexible and geomorphologically resonative criteria for the river corridor demarcation. On the above basis, distances from the channel have been determined (Fig. 9.14) for each type of Rosgen Reach as well as making further adjustments as to this buffer width, where the same type of channel (e.g. types DA and E) occur more than once along the Bakreshwar's course, but in different settings. The demarcation of such a corridor basically provides an idea, foremost, as to where and how much the main

Table 9.3 Description of the Channel Morphological Parameters used to characterize and code the Bakreshwar River Reaches

Stream type	General description	Entrenchment ratio	Width-to-depth ratio	Channel sinuosity	Channel slope	Landform/Soil/Morphological features
Aa+	Very steep, deeply entrenched, debris transport, torrent streams	<1.4	<12	1.0–1.1	>0.10	Very high relief. Erosional, bedrock, or depositional features; debris flow potential. Deeply entrenched streams. Vertical steps with deep scour pools; waterfalls
A	Steep, entrenched, cascading, step-pool streams. High energy/debris transport associated with depositional soils. Very stable if bedrock or boulder-dominated channel	<1.4	<12	1.0–1.2	0.04–0.10	High relief. Erosional or depositional and bedrock forms. Entrenched and confined streams with cascading reaches. Frequently spaced, deep pools in associated step-pool bed morphology
B	Moderately entrenched, moderate gradient, riffle dominated channel with infrequently spaced pools. Very stable plan and profile. Stable banks	1.4–2.2	>12	>1.2	0.02–0.039	Moderate relief, colluvial deposition and/or structural. Moderate entrenchment and width-to-depth ratio. Narrow, gently sloping valleys. Rapids predominate with scour pools
C	Low gradient, meandering, point bar, riffle/pool, alluvial channels with broad, well-defined floodplains	>2.2	>12	>1.2	<0.02	Broad valleys with terraces, in association with floodplains, alluvial soils. Slightly entrenched with well-defined meandering channels. Riffle/pool bed morphology
D	Braided channel with longitudinal and transverse bars. Very wide channel with eroding banks	NA	>40	NA	<0.04	Broad valleys with alluvium, steeper fans. Glacial debris and depositional features. Active lateral adjustment with abundance of sediment supply. Convergence/divergence bed features, aggradational processes, high bed load and bank erosion
DA	Anastomizing (multiple channels) narrow and deep with extensive, well-vegetated floodplains and associated wetlands. Very gentle relief with highly variable sinuosities and width-to-depth ratios. Very stable stream banks	>2.2	Highly variable	Highly variable	<0.005	Broad, low-gradient valleys with fine alluvium and/or lacustrine soils. Anastomized (multiple channel) geologic control creating fine deposition with well-vegetated bars that are laterally stable with broad wetland floodplains. Very low bedload, high wash load sediment
E	Low gradient, meandering riffle/pool stream with low width-to-depth ratio and little deposition. Very efficient and stable. High meander width ratio	>2.2	<12	>1.5	<0.02	Broad valley/meadows. Alluvial materials with floodplains. Highly sinuous with stable, well-vegetated banks. Riffle/pool morphology with very low width-to-depth ratios

(continued)

Table 9.3 (continued)

Stream type	General description	Entrenchment ratio	Width-to-depth ratio	Channel sinuosity	Channel slope	Landform/Soil/Morphological features
F	Entrenched meandering riffle/pool channel on low gradients with high width-to-depth ratio	<1.4	>12	>1.2	<0.02	Entrenched in highly weathered material. Gentle gradients with a high width-to-depth ratio. Meandering, laterally unstable with high bank erosion rates. Riffle/pool morphology
G	Entrenched gully step-pool and low width-to-depth ratio on moderate gradients	<1.4	<12	>1.2	0.02–0.039	Gullies, step-pool morphology with moderate slopes and low width-to-depth ratio. Narrow valleys, or deeply incised in alluvial or colluvial materials (fans or deltas). Unstable, with grade control problems and high bank erosion rates

Modified from Rosgen (1994)

channel is likely to meander, shift or avulse, and thus possibly lay claim to land and livelihood. Such a buffer can also be used for stream restoration purposes, where riparian tracts are left untouched or afforested along the channel within the demarcated zones, in order to better or preserve river health, replenish flows and sustain the entire biotic environment dependent on it. Such buffers are sorely required along river courses like the Bakreshwar, due to the extent and intensity with which its floodplain is cultivated or otherwise used. They allow the channel to 'breathe' and rejuvenate ecologically.

To further emphasize the changing nature of the Bakreshwar and its adjacent riparian tract, a number of windows have been taken within the demarcated stream corridor (Fig. 9.15). Each window has been selected along the River Corridor to highlight and be representative of the land use and land cover and hydrologic relationships existing in each demarcated stretch of the river. The first window (LULC Window—1) illustrates the Bakreshwar river near its initiation as an established channel across its narrow floodplain. Most of the adjacent land to the corridor is left fallow. Patches of forests and a small settlement close to the main channel and some cultivated land in the corridor zone is evident. The river flows over some patches of barren ground, most probably evidences of infertile lateritic tracts. The second window depicts how human intervention has led to a change in the channel configuration and modification of the river corridor (LULC Window—2). The Neel Nirjan Dam has been constructed across the Bakreshwar River, arresting its normal flow. This has led to the formation of the reservoir, submerging large tracts of land adjoining the river. This change in the river channel and the adjacent riparian tract becomes more evident when the pre-dam construction era topographical map of the same location is compared with its present Google Earth image (Fig. 9.16). Most of the reservoir has been choked by eutrophication and the immediate vicinity of the barrage has been left barren. Thus, such river corridor mapping pre and post-dam construction or upstream and downstream of dam reaches can aid decipher the

Table 9.4 Computed parameters reach-wise for channel segment classification of the Bakreshwar River

Sl. No.	Stations	Channel slope (in m/m)	Flood prone width (in m)	Average depth (in m)	Maximum depth (in m)	Sinuosity	Bankfull width (in m)	Width–depth ratio	Entrenchment ratio
1	RAJNAGAR	0.5	0.5	0.25	1.0	1.58	4.13	16.52	0.12
2	ABADNAGAR	0.4	0.04	0.02	0.5	1.5	7.2	360.00	0.01
3	MUKTIPUR	0.35	3	1.5	5.5	1.6	40	26.67	0.08
4	BAKRESHWAR (BRIDGE)	0.5	8	4	7.0	1.52	20	5.00	0.40
5	BAKRESHWAR (TOWN)	0.51	3.5	1.75	6.5	1.49	75	42.86	0.05
6	SAGAR	0.1	6	3	5.5	2.2	90	30.00	0.07
7	JOSTABAD	0.25	1	0.5	5.5	2.25	70	140.00	0.01
8	SRIKANTHAPUR	0.2	1	0.5	4.0	2.35	85	170.00	0.01
9	HAT IKRA (BAR)	0.1	4	2	12.0	2.2	80	40.00	0.05
10	HAT IKRA	0.15	1	0.5	3.5	2.25	75	150.00	0.01
11	MOHAMMADNAGAR	0.03	1	0.5	4.0	2.5	65	130.00	0.02
12	TEKEDDA	0.03	5	2.5	2.0	2.5	30	12.00	0.17
13	KALIKAPUR	0.02	8	4	13.0	3	90	22.50	0.09
14	LABHPUR	0.01	0.5	0.25	0.5	3.09	10	40.00	0.05
15	MOUTH	0.01	8	4	12.5	3.12	58	14.50	0.14

Table 9.5 Classified and coded channel reaches of the Bakreshwar River

Sl. No.	Stations	Rosgen's stream classification code	Characteristic channel attribute
1	RAJNAGAR	A	Steep and entrenched channel, mainly boulders and large pebbles
2	ABADNAGAR	A	
3	MUKTIPUR	B	Moderately entrenched channel, gravel
4	BAKRESHWAR (BRIDGE)	B	
5	BAKRESHWAR (TOWN)	B	
6	SAGAR	C	Moderately meandering channel, smaller gravels and coarse sands
7	JOSTABAD	C	
8	SRIKANTHAPUR	C	
9	HAT IKRA (BAR)	C	Slightly meandering, medium to fine sands
10	HAT IKRA	C	
11	MOHAMMADNAGAR	E	Meandering Channel, coarse sands
12	TEKEDDA	DA	Anastomosing Channel, cut-offs, fins sands and clay
13	KALIKAPUR	DA	
14	LABHPUR	E	Meandering Channel, cut-offs, fine sands and clay
15	MOUTH	E	

Note Refer to Table 9.3 for fuller descriptions of the different stream reaches classified here

impacts that these structures have had on the channel (Friedman et al. 1998). Some afforested vegetation tracts in and around the river reveal attempts at restoration and habitat preservation. Some forests in the corridor have also survived. The third window has been selected just beyond the dam, where a dry channel bed has formed (LULC Window—3). However, the evidence of a meander scar denotes that the river probably did exhibit relatively more natural flow dynamics in the past. The fourth window shows the confluence of the Chandrabhaga River with the Bakreshwar River (LULC Window—4). Prominent point bars have developed on both sides of banks. The land is mostly cultivated with some natural vegetation clusters surviving. These are either the sacred groves or higher grounds that are deemed unsuitable for cultivation. Settlements in the Corridor become prominent. The fifth window is a depiction of the change of the river pattern as prominent meanders develop (LULC Window—5). Point bar development is quite marked and the natural vegetation has been preserved in the immediate vicinity of the river channel. However, beyond this, most of the land has been cultivated. The last window shows how there is a change in the river pattern from meandering to anastomosing, depicting a change in the hydrology of the river as it slowly winds along its course to meet the Kopai River (LULC Window—6). A number of paleochannels mark the previous courses of the river, where it had migrated across its floodplain. The principal land use here is cultivation and there are some forest patches in the close vicinity of the main channel. For each of the windows, the extents of the possible Riparian Buffers that may be created to conserve the stream ecology have also been demarcated. Only in one reference reach (LULC Window—5), is the channel thickly guarded by forests and there exists a greater need for more such stretches along the Barkeshwar's course in order to retard channel migration and allow riverbed stabilization.

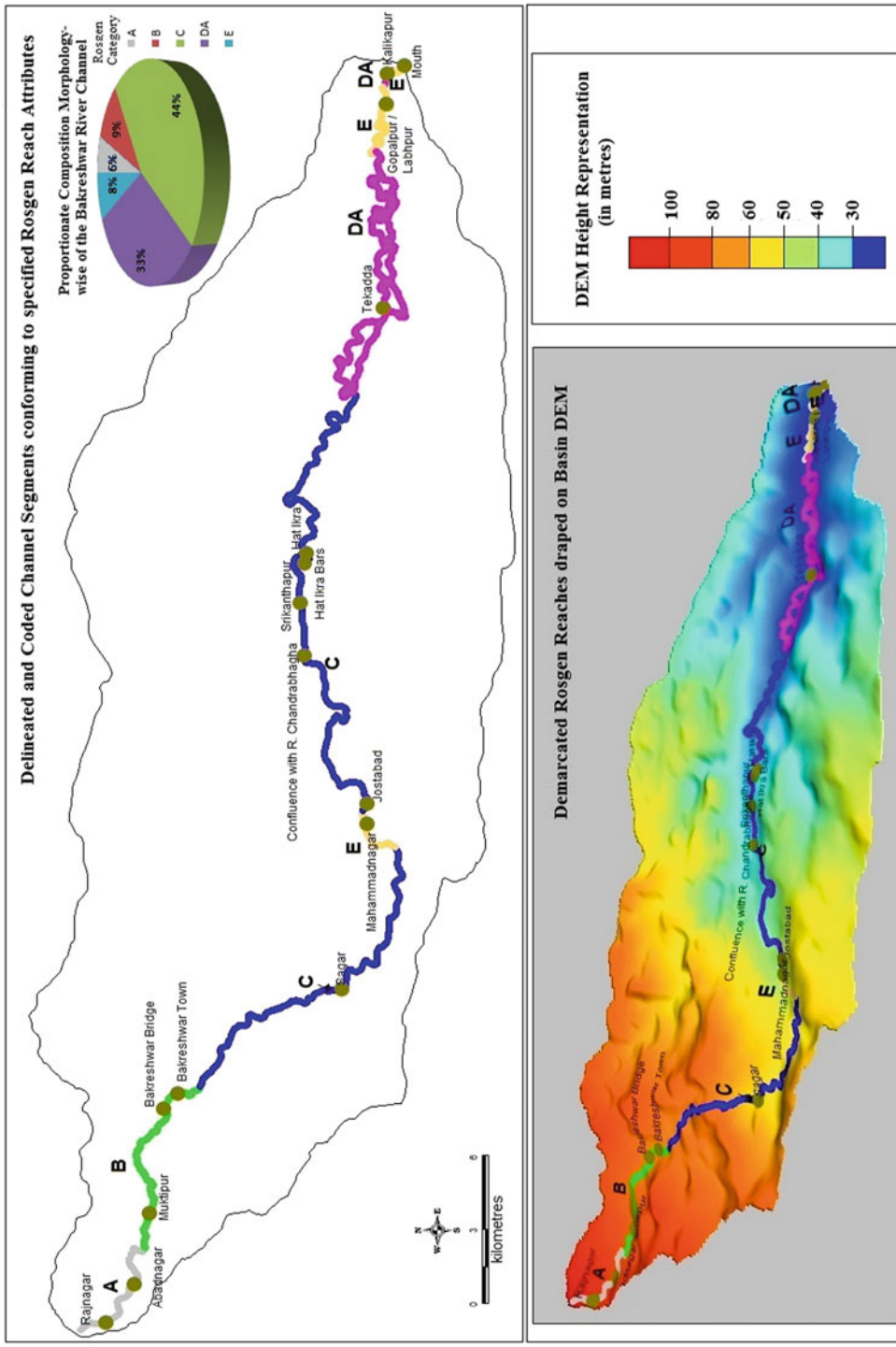

Fig. 9.12 Demarcated Rosgen reaches for the Bakreshwar River

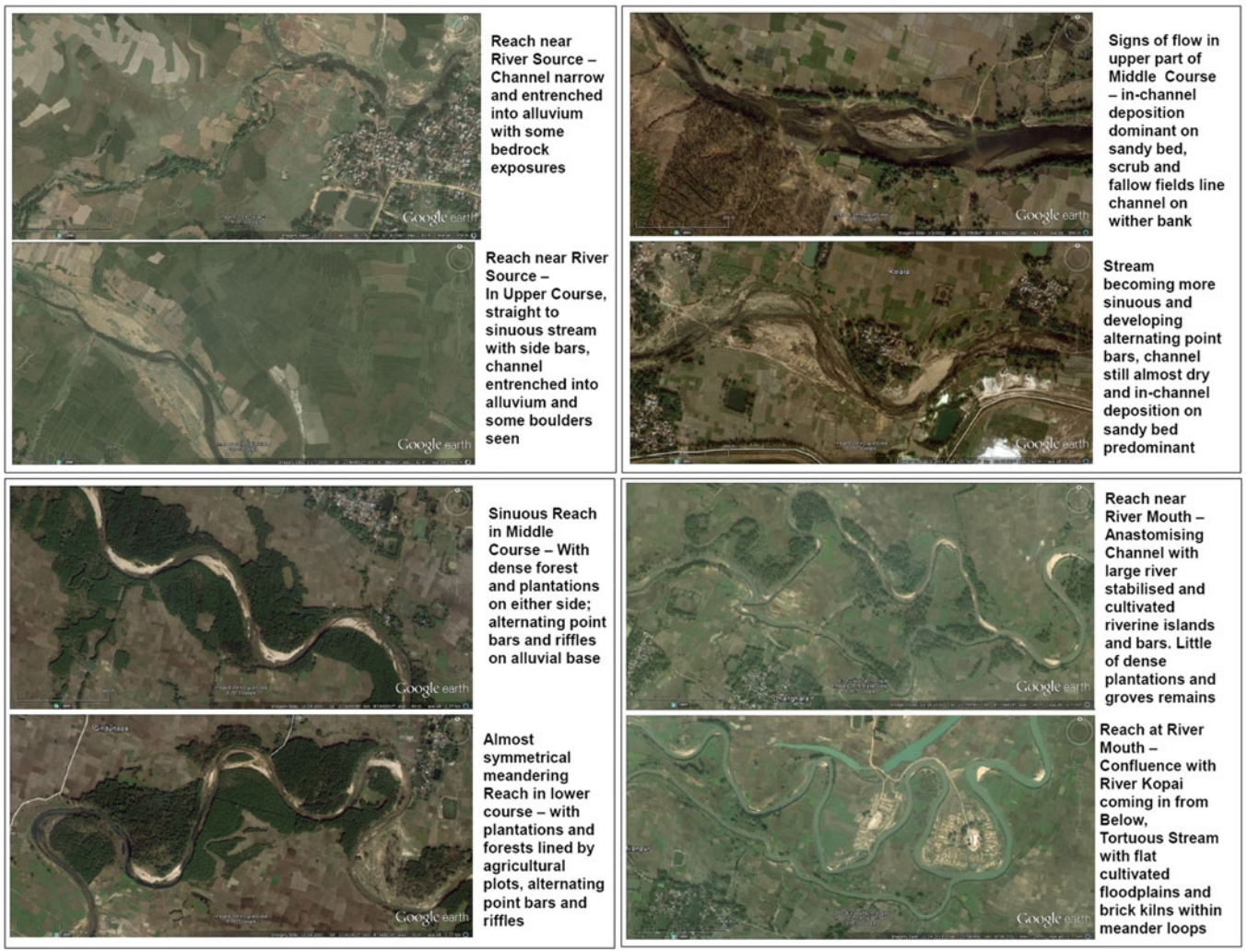

Fig. 9.13 Google Earth windows for aiding river corridor demarcation

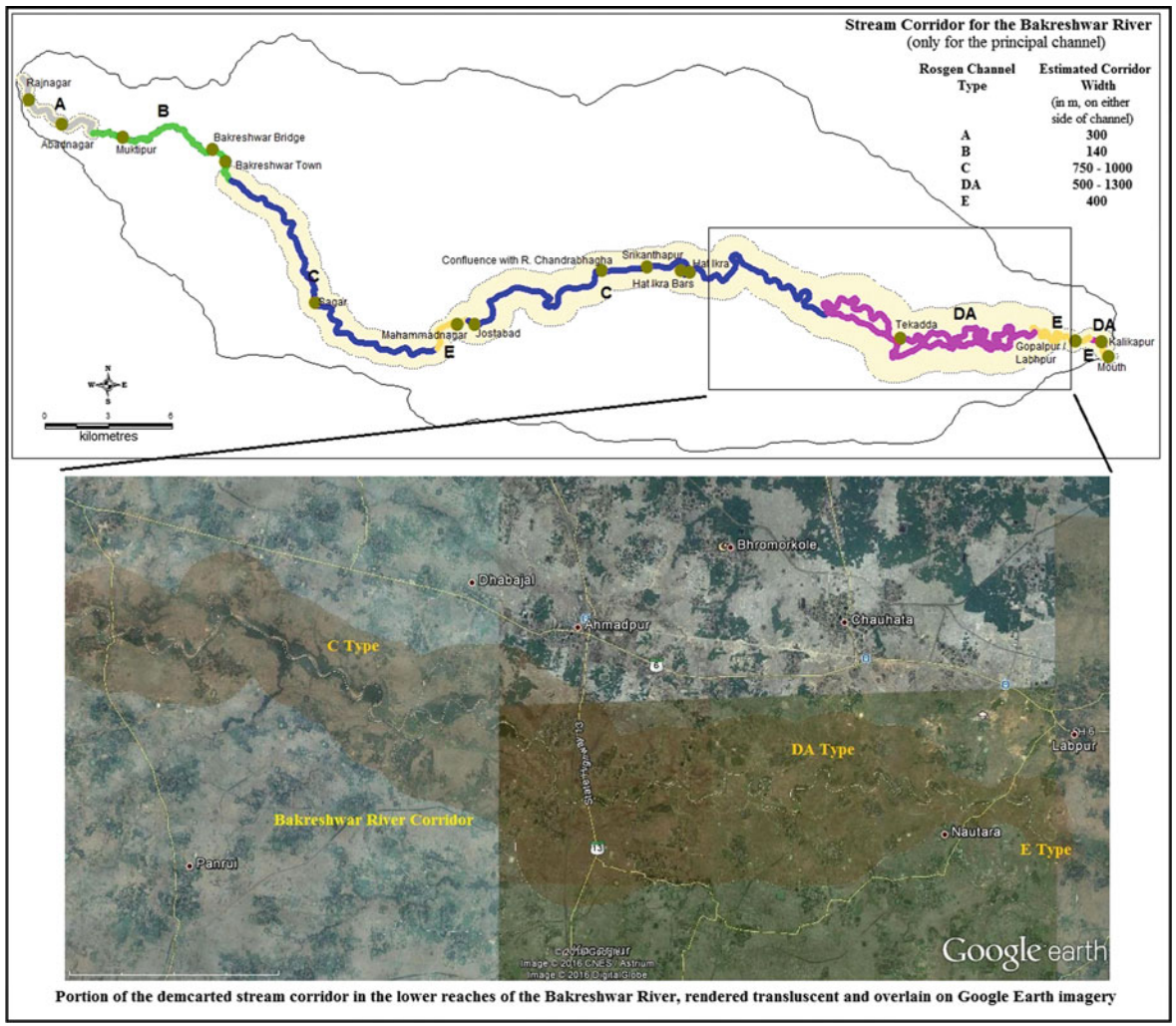

Fig. 9.14 Stream corridor demarcation for the Bakreshwar River

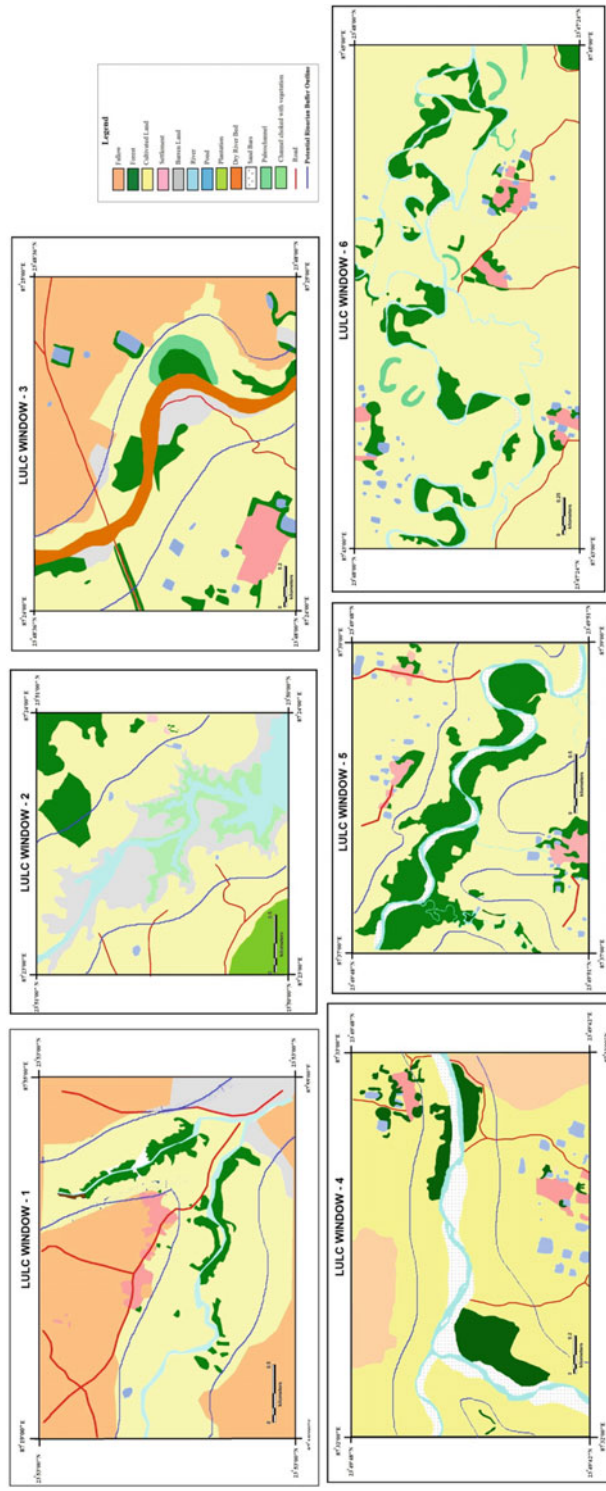

Fig. 9.15 Landuse and land cover of the sampled windows along the Bakreshwar River corridor

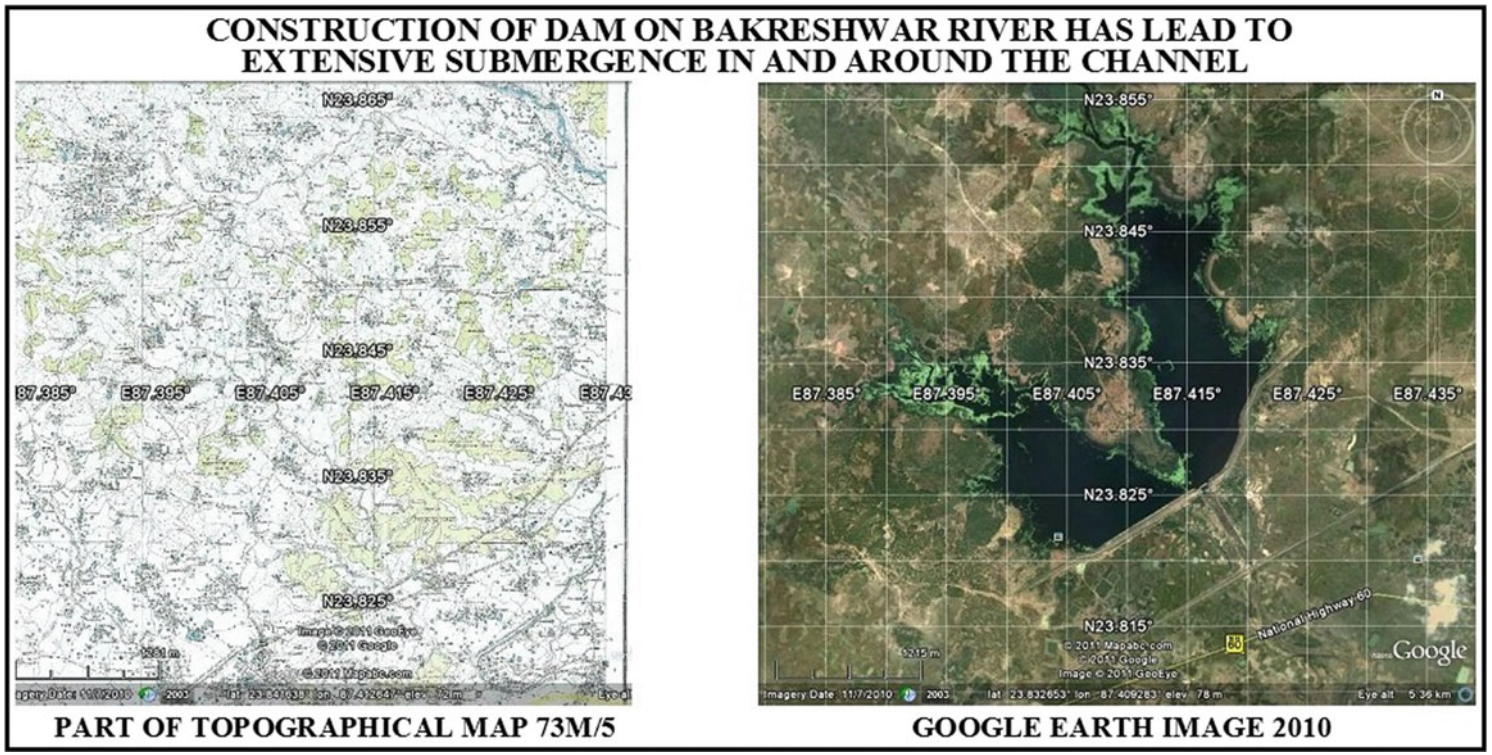

Fig. 9.16 Dam-induced changes in the stream corridor

9.6 Conclusion

Rivers change in morphology and behaviour markedly from their source to their mouth. Therefore, reach-wise demarcation of channel attributes is paramount towards garnering a holistic understanding of the entire river, while also accruing site-specific knowledge on hydraulic and hydrological parameters. Such understanding of the interplay between the hydraulic geometry, flow characteristics and sediment transportation can give reach-level insights into floodplain development (Bridge 1993) and also facilitate computational modelling of such landscapes (Howard 1996). Plans for channel modification for human use or natural hazard mitigation can feasibly be most effectively implemented within such a framework. The study has attempted to divide the Bakreshwar River following the Rosgen formulated procedure for the same though an amalgamation of numerous field-derived attributes, while also augmenting it with much reference satellite imageries for succinct codification. The end result lays bare the differential channel behaviour in different stretches while also highlighting the need for the development of riparian buffers to allow ecologically sustainable relationships between the physical channel aspects, the aquatic communities dependent on them and the human settlements populating its banks. The promulgation of further such studies and reach demarcation on other channels and indeed, on each tributary of an entire basin (Reid et al. 2008), using this or other similar methodologies (i.e., Brierley and Fryirs 2005; Buffington and Montgomery 2013) can serve to build a hydrological, morphological and ecological 'census' of streams, which would then provide the baseline information needed for soil erosion, flood and channel shifting mitigation frameworks and other such investigations.

References

Alexander C (2005) Riparian buffers and corridors. Technical papers. Vermont Agency of Natural Resource, Waterbury

Allan JD (2004) Landscapes and riverscapes: the influence of land use on stream ecosystems. Annu Rev Ecol Evol Syst 35:257–284

Ashmore PE (1991) How do gravel-bed rivers braid? Can J Earth Sci 28(3):326–341

Bagnold RA (1966) An approach to the sediment transport problem from general physics. USDI Geological Survey, Professional Paper 4221

Begin ZB (1975) Structural and lithological constraints on stream profiles in the Dead Sea Region, Israel. J Geol 83(1):97–111

Bisson PA, Buffington JM, Montgomery DR (2006) Valley segments, stream reaches and channel units. In: Hauer FR, Lamberti GA (eds) Methods in stream ecology. Academic Press, Elsevier, San Deigo, pp 23–49

Bizzi S, Lerner DN (2015) The use of stream power as an indicator of channel sensitivity to erosion and deposition processes. River Res Appl 31:16–27

Bridge JS (1993) The interaction between channel geometry, water flow, sediment transport and deposition in braided rivers. Geol Soc, Lond, Spec Publ: Lyell Collect 75:13–71

Brierley GJ, Fryirs KA (2005) Geomorphology and river management: applications of the river styles framework. Blackwell Publishing, Oxford

Brierley GJ, Fryirs KA, Cullum C, Tadaki M, Huang HQ, Blue B (2013) Reading the landscape: integrating the theory and practice of geomorphology to develop place-based understandings of river systems. Prog Phys Geogr 37(5):601–621

Buffington JM, Montgomery DR (2013) Geomorphic classification of rivers. Treatise Geomorphol 9:730–767

Cailleux A (1952) Morphoskopischeanalyse der geschiebe und sandkorner und ihrebedeutung fur die palaoklimatologie. GeologischeRundschau 40(1):11–19

Carlson EA (2009) Fluvial riparian classification for national forests in the western United States. Thesis, University of Colorado, Fort Collins

Carlston CW (1969) Downstream variations in the hydraulic geometry of streams: special emphasis on mean velocity. Am J Sci 267(4):499–509

Charlton R (2008) Fundamentals of fluvial geomorphology. Routledge, New York

Church M, Rice SP (2009) Form and growth of bars in a wandering gravel-bed river. Earth Surf Proc Land 34 (10):1422–1432

Clarke SJ, Bruce-Burgess L, Wharton G (2003) Linking form and function: towards and eco-hydromorphic approach to sustainable river restoration. Aquat Conserv: Mar Freshw Ecosyst 13(5):439–450

Cullum C, Rogers KH, Brierley G, Witkowski ETF (2016) Ecological classification and mapping for landscape management and science: foundations for the descriptions of patterns and processes. Prog Phys Geogr 40(1):38–65

Cupp CE (1989) Stream corridor classification for forested lands of Washington. Washington Forest Protection Association, Olympia, Washington, USA

De Rose R, Stewardson MJ, Harman C (2008) Downstream hydraulic geometry of rivers in Victoria, Australia. J Hydrol 99(1–4):302–316

Dingman SL (2007) Analytical derivation of at-a-station hydraulic geometry relations. J Hydrol 334(1&2): 17–27

Doppelt R, Scurlock M, Frissell C, Kar JR (1993) Entering the watershed: a new approach to save America's River Watersheds. Electron Green J 1 (4):462

Downs PW, Kondolf GM (2002) Post-project appraisal in adaptive management of river channel restoration. Environ Manage 29(4):477–496

FISRWG (2001) Stream corridor restoration: principles, processes, and practices. The Federal Interagency Stream Restoration Working group (FISRWG) (15 Federal agencies of the US Govt.). GPO Item 0120-A. SubDocs A 57.6/2: EN3/PT.653

Friedman JM, Osterkamp WR, Scott ML, Auble GT (1998) Downstream effects of dams on channel geometry and bottomland vegetation: regional patterns in the great plains. Wetlands 18(4):619–633

Froude W (1868) Law of comparison. Principles of Naval Architecture, London

Gagoi C, Goswami DC (2014) A study on channel migration of the Subansiri river in Assam using remote sensing and GIS technology. Curr Sci 106 (8):1113–1120

Galay VJ, Kellerhals R, Bray DI (1973) Diversity of river types in Canada. In: Fluvial processes and sedimentation—proceedings of hydrology symposium No. 9. National Research Council of Canada, Ottawa, pp 217–250

Garcia M, Parker G (1991) Entrainment of bed sediment into suspension. J Hydraulic Eng 117(4):414–435

Ghosh S, Guchhait S (2015) Characterization and evolution of primary and secondary laterites in northwestern Bengal Basin, West Bengal, India. J Palaeogeogr 4 (2):203–230

Gilvear D, Winterbottom S, Sichingabula H (2000) Character of channel planform change and meander development: Luangwa River, Zambia. Earth Surf Process Land 25(4):421–436

Gleason CJ (2015) Hydraulic geometry of natural rivers: a review and future directions. Prog Phys Geogr 39 (3):337–360

Gordon ND, McMahon TA, Finlayson BL, Gippel CJ, Nathan RJ (2004) Stream hydrology: an introduction for ecologists. Wiley, Chichester

Graf WH (1971) Hydraulics of sediment transport. McGraw-Hill Book Co., Inc., New York

GSI (2001) District resource map—Birbhum. Geological Survey of India, Kolkata

Gurnell AM, Downward SR, Jones R (1994) Channel planform change on the River Dee meanders. Regulated Rivers: Res Manage 9(4):187–204

Harrelson CC, Rawlins CL, Potyondy JP (1994) Stream channel reference sites: an illustrated guide to field technique. Gen. Tech. Rep. RM-245. Fort Collins, Colorado

Hawes E, Smith M (2005) Riparian buffer zones: functions and recommended widths. Yale School of Forestry and Environmental Studies for the Eight Mile River, Wild and Scenic Study Committee, Connecticut

Hey RD (1976) Geometry of river meanders. Nature 262:482–484

Hey RD, Heritage GL, Patteson M (1994) Impact of flood alleviation schemes on macrophytes. Regulated Rivers: River Res Appl 9(2):103–119

Hickin EJ (1974) The development of meanders in natural channels. Am J Sci 247:414–442

Holbrook J, Scott RW, Oboh-Ikuenobe FE (2006) Base-level buffers and buttresses: a model for upstream versus downstream control on fluvial geometry and architecture within sequences. J Sediment Res 76(1):162–174

Howard A (1996) Modelling channel evolution and floodplain morphology. In: Anderson MG, Walling DE, Bates PD (eds) Floodplain processes. Wiley, Chichester

Hudson PF, Kesel RH (2000) Channel migration and meander-bend curvature in the lower Mississippi River prior to major human modification. Geology 28(6):531–534

Jackson RG II (1975) Hierarchical attributes and a unifying model of bed forms composed of cohesionless material and produced by shearing flow. Geol Soc Am Bull 86:1523–1533

Jowett IG (1998) Hydraulic geometry of New Zealand rivers and its use as a preliminary method of habitat assessment. Regulated Rivers: Res Manage 14:451–466

Julien PY (1985) Planform geometry of meandering alluvial channels. Report CER84-85PYJ5, Civil Engineering Department, Engineering Research Center, Colorado State University, Fort Collins, Colorado

Kleinhans MG (2010) Sorting out river channel patterns. Prog Phys Geogr 34(3):287–326

Knighton AD (1998) Fluvial forms and processes: a new perspective. Edward Arnold, New York

Langbein WB, Leopold, LB (1966) River meanders—theory of minimum variance. United States Geological Survey Professional Paper 422-H, Washington

Lee J, Julien P (2006) Downstream hydraulic geometry of alluvial channels. J Hydraulic Eng 132(12):1347–1352

Leopold LB, Langbein WB (1966) River meanders. Sci Am 214(6):60

Leopold LB, Maddock T (1953) The hydraulic geometry of stream channels and some physiographic

implications. United States Geological Survey Professional Paper 252, Washington
Leopold LB, Wolman MG, Miller JP (1964) Fluvial processes in geomorphology. Freeman and Co., San Francisco
Manning R (1890) On the flow of water in open channels and pipes. Trans Inst Civil Eng Ireland 20:161–207
Morisawa M (1968) Streams—their dynamics and morphology. McGraw-Hill Co., New York
Mondal S, Patel PP (2018) Examining the utility of river restoration approaches for flood mitigation and channel stability enhancement: a recent review. Environ Earth Sci 77(5):195
Naiman RJ, Decamps H, Pollock M (1993) The role of riparian corridors in maintaining regional biodiversity. Ecol Appl 3(2):209–212
NATMO (2000) District planning map series—Birbhum. National Atlas and Thematic Mapping Organisation, Kolkata
Nelson JM, Bennett JP, Wiele SM (2003) Flow and sediment-transport modeling. In: Kondolf GM, Piegay H (eds) Tools in fluvial geomorphology. Wiley, Chichester
O'Malley LSS (1910) Bengal district gazetteers—Birbhum: geography, travels and description. The Bengal Secretariat Book Depot, Kolkata
Ouimet WB, Whipple KX, Granger DE (2009) Beyond threshold hillslopes: channel adjustment to base level fall in tectonically active mountain ranges. Geology 37 (7):579–582
Park CC (1977) World-wide variations in hydraulic geometry exponents of stream channels: an analysis and some observations. J Hydrol 33(1&2):133–146
Parker G (1976) On the cause and characteristic scales of meandering and braiding in rivers. J Fluid Mech 76:457–483
Pati JK, Lal J, Prakash K, Bhusan R (2008) Spatio-temporal shift of the western bank of the Ganga River, Allahabad city and its implications. J Indian Soc Remote Sens 36:289–297
Pfankuch DJ (1975) Stream reach inventory and channel stability evaluation. United States Department of Agriculture Forest Service No. R1-75-002, GPO No. 696-260/200. Washington D.C
Piegay H, Darby SE, Mosselman E, Surian N (2005) A review of techniques for delimiting the erodible river corridor: a sustainable approach to managing bank erosion. River Res Appl 21:773–789
Reid HE, Gregory CE, Brierley GJ (2008) Measures of physical heterogeneity in appraisal of geomorphic river condition for urban streams: Twin Streams Catchment, Auckland, New Zealand. Phys Geogr 29 (3):247–274
Richards K (1982) Rivers: forms and processes in alluvial channels. Methuen, London and New York
Rosgen DL (1994) A classification of natural rivers. CATENA 22:169–199
Rosgen DL (1998) Stream classification field guide. Wildland Hydrology, Pagosa Springs, Colorado
Rosgen DL (2001a) A hierarchical river stability/watershed-based sediment assessment methodology. In: Proceedings of the seventh federal interagency sedimentation conference, vol 1. Subcommittee on Sedimentation, Reno, pp II-97–II-106
Rosgen DL (2001b) A practical method of computing streambank erosion rate. In: Proceedings of the seventh federal interagency sedimentation conference, vol 1. Subcommittee on Sedimentation, Reno, pp II-9–II-15
Rosgen DL (2001c) A stream channel stability assessment methodology. In: Proceedings of the seventh federal interagency sedimentation conference, vol 1. Subcommittee on Sedimentation, Reno, pp II-18–II-26
Rosgen DL (2006) Watershed assessment of river stability and sediment supply (WARSSS). Wildland Hydrology Books, Fort Collins
Rosgen DL (2007) Rosgen geomorphic channel design. In: Bernard J, Fripp JF, Robinson KR (eds) Part 654 stream restoration design national engineering handbook (201-VI-NEH). United States Department of Agriculture Natural Resources Conservation Service, Washington D.C.
Rosgen DL (2011) Natural channel design: fundamental concepts, assumptions and methods. In: Simon A, Bennett SJ, Castro JM (eds) Stream restoration in dynamic fluvial systems: scientific approaches, analyses and tools. Geophysical monograph series, vol 194. American Geophysical Union, Washington D.C., pp 69–93
Schumm SA (1960) The shape of alluvial channels in relation to sediment type. U S Geol Sur Prof Pap B 352:17–30
Seeber L, Gornitz V (1983) River profiles along the Himalayan arc as indicators of active tectonics. Tectonophysics 92:335–367
Sayre WW, Kennedy JF (eds) (1973) Degradation and aggradation of the Missouri river. In: Proceedings of a workshop held in Omaha, Nebraska for Iowa Conservation Commission. IIHR Report No. 215, Iowa Institute of Hydraulic Research, University of Iowa, Iowa
Stanford JA, Ward JV (1993) An ecosystem perspective of alluvial rivers: connectivity and hyporheic corridor. J North Am Benthol Soc 12(1):48–60
Stewardson M (2005) Downstream geometry of stream reaches. J Hydrol 306(1–4):97–111
Thomas A, Sharma PK (1998) The shift of Ravi River and the geomorphological features along its course in Amritsar and Gurdaspur districts of Punjab. J Indian Soc Remote Sens 26(12):57–68
Tockner K, Ward JV, Arscott DB, Edwards PJ, Kollmann J, Gurnell AM, Petts GE, Maiolini B (2003) The Tagliamento River: a model ecosystem of European importance. Aquat Sci 65(3):239–253
Toms River Corridor Task Force (2004) A regional natural resources protection plan for the toms river corridor. Jackson and Manchester Townships, Ocean County, New Jersey

US EPA (1992) Streamwalk manual. Water Division Region 10, United States Environment Protection Agency, Seattle

van den Berg JH (1995) Prediction of alluvial channel pattern of perennial rivers. Geomorphology 12:259–279

Vermont Agency of Natural Resource (2005) Riparian buffers and corridors. Technical papers. Waterbury, Vermont

Vermont Department of Environmental Conservation (2013) River, river corridor, floodplain management programs. Biennial Report to the General Assembly Pursuant to Act 110, Vermont

Verry ES, Hornbeck JW, Dolloff CA (eds) (2000) Riparian management in forests to the continental Eastern United States. Lewis Publishers, Boca Raton, Florida

Wohl E (2004) Limits of downstream hydraulic geometry. Geology 32(10):897–900

Wenger S (1999) A review of the scientific literature on riparian buffer width, extent and vegetation. Office of Public Service and Outreach, Institute of Ecology, University of Georgia, Athens, Georgia

Wegner S, Fowler L (2000) Protecting stream and river corridors: creating effective local riparian buffer ordinances. Public Policy Research Series, Carl Vinson Institute of Government, University of Georgia, Georgia

Williams GP (1986) River meanders and channel size. J Hydrol 88:147–164

Winterbottom SJ (2000) Medium and short-term channel planform changes on Rivers Tay and Tummel, Scotland. Geomorphology 34:195–208

Yang CT (1972) Unit stream power and sediment transport. ASCE J Hydraulics Div 98:1805–1826

Yang CT, Stall JB (1974) Unit stream power for sediment transport in natural rivers. University of Illinois Urbana-Champaign Water Resources Center Report UILU-WRC-74-0088 (Research Report 88), Urbana

10

Assessing Influence of Erosion and Accretion on Landscape Diversity in Sundarban Biosphere Reserve, Lower Ganga Basin: A Geospatial Approach

Mehebub Sahana and Haroon Sajjad

Abstract

Sundarban Biosphere Reserve (SBR) is located in world's largest sediment depocenter of Ganga-Brahmaputra-Meghna (GBM) deltaic coast of India. Unprecedented increase in the frequency of tropical cyclone, sea level rising and changes in shoreline has dynamically and significantly increased the threat to the world's largest mangrove habitation. Spatio-temporal variation of water level regimes is an important factor for estuarine and tidal-fluvial dynamics of deltaic islands in SBR. This article examines the land use/land cover dynamic and landscape diversity due to erosion and accretion processes in Sundarban deltaic region. Landsat MSS (1975), Landsat TM (1990, 2000) and Landsat 8 OLI (2015) were used for assessing land use land cover change, landscape metric, shoreline changes, and tidal-fluvial dynamics in the study area. Land use/land cover maps were prepared using supervised classification scheme and maximum likelihood method. Digital Shoreline Analysis System (DSAS) extension tool of Arc GIS was used to assess the shoreline change rate. On the basis of land use/land cover map, Shannon's diversity index (SHDI) was estimated to understand the landscape fragmentation due to tidal-fluvial dynamics and estuarine processes within the biosphere region. The study revealed that the land use/land cover of the Sundarban Biosphere Reserve has been diversely changed during the study period. Northern part of the SBR experienced maximum diversity of landscape. The findings revealed that there has been dramatic increase in settlement, swamp, and water-logged area and a decrease in vegetation/plantation in the study area. A remarkable change was noticed in the area under water-logging in the upper part of the Biosphere Reserve. This change is attributed to river erosion and inclusion of sea water into the agricultural fields. The overall erosion rate in the study area has been 5.98 km^2/year during 1975–2015. Marked variations were observed in erosion rate in different in different blocks and islands. Southern inhabited islands were more prone to erosion than the uninhabited islands. The outcome of this study may help in management and

M. Sahana · H. Sajjad (✉)
Department of Geography, Faculty of Natural Sciences, Jamia Millia Islamia, New Delhi, India
e-mail: haroon.geog@gmail.com

B. C. Das et al. (eds.), *Quaternary Geomorphology in India*,
Geography of the Physical Environment, https://doi.org/10.1007/978-3-319-90427-6_10

planning for estuarine dynamics, river bank erosion and accretion of Sundarban Biosphere Reserve.

Keywords
Land use/land cover · Erosion accretion
Landscape diversity · Sundarban Biosphere Reserve

10.1 Introduction

The coastal regions of the world are most sensitive entities due to their tidal-fluvial dynamics and estuarine processes. These regions are likely to be affected more in view of increasing impact of climate change. Hence, it is essential to make a systematic assessment of physical and biological factors and their impact on deltaic islands to conserve and restore the tidal-fluvial and estuarine ecosystems (Yu et al. 2000). Variability of hydrological regimes of river floodplains is a fundamental phenomenon for land use/land cover dynamics in coastal ecosystem (Poff et al. 2010; Bunn and Arthington 2002). Tide induced inundation dynamics affects the process of coastal erosion and deposition. The biotic and abiotic composition of fragile ecosystem, tidal freshwater, oligohaline marshes and salt marshes depend on these fluvial tidal processes (Sharpe and Baldwin 2013; Cornu and Sadro 2002). Further anthropogenic intervention in coastal ecosystems causes of physical and ecological degradation (Kingsford 2000). The Sundarban Biosphere Reserve (hereafter SBR) is a natural region which is considered as the world's largest Reserve (10,200 km^2) of mangrove ecosystems and is an important biodiversity hotspot (Purkait 2007). Tidal-fluvial dynamics and geomorphological attributes makes this fragile landscape very sensitive and vulnerable. Morphologically fluvial deposition of Ganga and Brahmaputra Rivers has major contribution towards landscape evolution of this region. From the beginning this region are affected by coastal and fluvial hydrodynamic processes, long shore current, anthropogenic thrusting and extreme climate event. Continuous erosion and deposition have reshaped the marginal shorelines in this active estuarine delta (Chakrabarti 1995; Jana et al. 2012; Addo 2015).

Sundarban area is characterized river channels and creeks of varying widths, from a few meters to several kilometers. Mangroves not only helps in protecting coastline from degradation, but also acts as flourishing grounds for coastal fishes (Goodbred et al. 2003). The mangrove ecosystem helps in providing food and livelihood to a large section of local population living in the transition zone of the SBR. The rich biodiversity of SBR plays a vital role in carbon absorption and thus acts as a carbon sink. It also protects from extreme climate event and thus helps in reducing vulnerability. However, the mangrove forests in SBR are extremely vulnerable to multi hazard events like climate change from last few decades (Sharma et al. 2010). Growing population is putting pressure on its bio-resources and freshwater inflows in SBR. Large areas of this ecosystem have been converted into agricultural land over the past two hundred years and more recently into artificial prawn cultivation farm (Raha et al. 2014). Exploited of wood, prawns, fish, and fodder has extensively degraded the reserve. The construction of embankments, dams, and barrages has control flood at a large scale in freshwater flow in the upstream areas of SBR. It has seriously affected the base of biodiversity which has resulted in an increment in the salinity content and extensive sedimentation (Chaudhuri and Choudhury 1994). Threats to such ecosystems arise from changes in global climate, especially rise in erosion, changing shoreline, sea level rise. Therefore, proper planning and management is essential for conserving freshwater and biological resources in SBR (Islam and Gnauck 2008).

Remote sensing data and geographical information system have been extensively used for the assessment of environmental protection, space management and environmental degradation. For these purposes different methodologies, matrices, statistical techniques have been developed and

improved in geospatial environment (Bia^{3}ousz et al. 2010). Land use land cover change analysis is a significant assessment of landscape environment since land use land cover change is always associated with anthropogenic activities (Abrishamkesh et al. 2011). In recent years landscape matrices are frequently used to quantify change in landscape patterns (Gustafson 1998). Landscape diversity index, evenness index, patch index, edge density and landscape shape index are important factors for assessing landscape characteristics (Uuemaa et al. 2009; Sahana et al. 2018a). Landscape matrix is mainly used to assess three function of land use/land cover structure. Shannon's diversity index (SHDI) and Simpson's diversity Index (SIDI) was sued in this study as the indicators of landscape metrics to assess the diversity in land use/land cover changes and ecological degradation as a consequence. The study also analyzed the influence of erosion and accretion on landscape diversity in coastal deltaic ecosystem of Sundarban biosphere reserve.

10.2 Study Area

The Sundarban is situated in the coastal region of Ganga-Brahmaputra deltaic island of Indian subcontinent. The entire Sundarban is spread over India and Bangladesh where 60% of Sundarban are in Bangladesh. Most of the lower part of Gangetic delta is composed of immature deltaic island with slit, sand and clay deposition. The Indian part of Sundarban is spread over 19 administrative block in north and south 24 Parganas district of west Bengal (Fig. 10.1). The lower part of the Sundarban region is extremely low-lying area and flat surface. Ingress of salt water, high coastal erosion and dune retreatment are common features in the study area. River banks are subjected to flood and erosion due to meandering of rivers and strong micro tides (Purkait 2007; Paul 2002; Das 2006). The delta building process is still active in the lower islands and the regions of neo-tectonic activity. Over all Sundarban biosphere reserve in Indian part is tilted toward north west to south east direction and most of the river carries sediment and deposit towards eastern part of the region (Bandyopadhyay 2007). Low-lying delta, salt marshes, sand flat, sand dunes, meandering channels, chars, and bars inter tidal deposition are the main characters of the entire Sundarban region. The average height of the Sundarban region varies between 2 to 6 m for south and north (Das 2006; Islam and Gnauck 2008). The Sundarban biosphere reserve has 4.37 million populations with 975 persons/km population density (Hazra et al. 2010; Ghosh 2012). Most of the population resides in rural areas and thrives on coastal agriculture and fisheries (Jana et al. 2012; Bandyopadhyay et al. 2014).

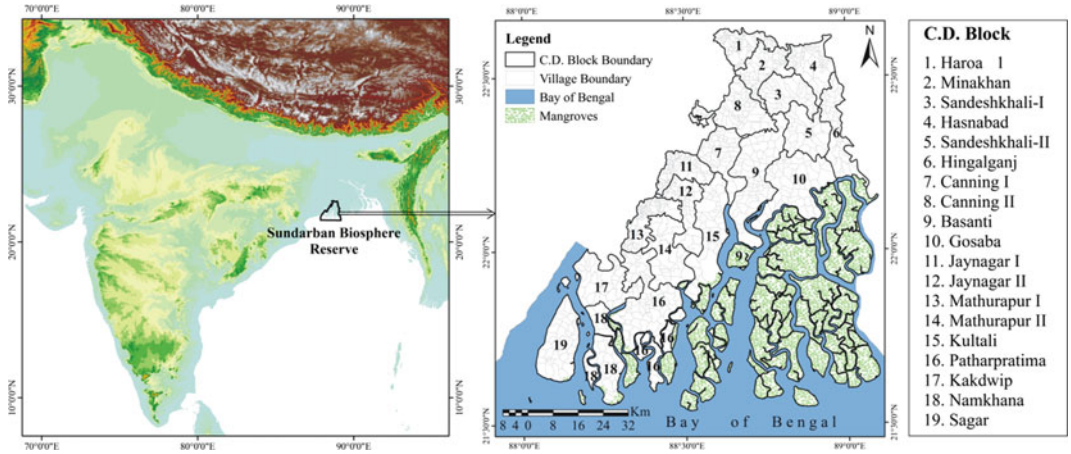

Fig. 10.1 Location of Sundarban Biosphere Reserve

Tropical cyclones frequently hit this region. Earthen embankments in the habited islands protect the salt water inclusion during the tidal surge (Bandyopadhyay 1997; Hazra et al. 2010; Ghosh 2012; Mallick and Vogt 2015). The tidal range varied from 3 to 5 m normally and sometimes reaches 7 and 8 m during spring time. Tidal rush affect low lying flat coastal zones greatly in southern of the Sundarban causing huge coastal erosion and complete destruction of coastal islands (Purkait 2007; Das 2006). The deep water channels in the upper part cause meandering of river system and regulate erosion and deposition activities within estuary (Paul 2002; Jana et al. 2012). Many intertidal mud flat, sand and swampy areas have been utilized for agricultural activities since last two centuries. Besides of these physical consequences most of the inhabited islands suffer from inadequate infrastructural facilities. Erosion is a major threat for the communities living in coastal islands. Fishing and tourism activities further create pressure on coastal track in the northern part of Sundarban (Mukherjee 2002; Basu 2013).

10.3 Materials and Methods

Landsat MSS (1975), Landsat Thematic Mapper (1990, 2000) and Landsat 8 OLI (2015) were used to assess land use/land cover change and its impact on the ecological status of Sundarban Biosphere Reserve. Land use/land cover maps were generated by supervised classification technique and maximum likelihood method. A stratified random sample technique technique was used to validate the classification (Anderson et al. 2001; Sahana et al. 2018b). The classification accuracy was determined through confusion matrix and kappa coefficient. Land use/ land cover classification showed 87.6, 91.3 and 94.9% overall accuracy and 0.89, 0.92, and 0.96 Kappa coefficient values for 1975, 1990, 2000, and 2015 respectively.

The land use/land cover change of the study area was estimated by using change detection techniques by following equation (Puyravaud 2003):

$$R = \left[\frac{1}{t_1 - t_2}\right] \times \left[\ln\left(\frac{C_1}{C_2}\right)\right], \tag{10.1}$$

where, R = rate of land use/land cover change and $C1$ and $C2$ = area under different land use/land cover classes t_1 and t_2 = time period.

10.3.1 Landscape Diversity and Ecological Degradation

The land use/land cover change is a major contributor to bring the change in ecological condition of an area (Bai et al. 2013). The relation between ecological process and land use/ land cover change is derived by various matrices and models. In the present study Shannon's diversity index (SHDI) and Simpson's diversity Index (SIDI) have been used to calculate diversity and evenness respectively within the landscape (Nagendra 2004). SHDI and SIDI were calculated with below equation

$$\text{SHDI} = \sum_{k=1}^{m} (P_k) \log_2 (P_k) \tag{10.2}$$

$$\text{SIDI} = 1 - \sum_{k=1}^{m} P_i^2, \tag{10.3}$$

where P_k the proportion of the landscape occupied by land use type k and m is the number of land use type present in the landscape and is the natural logarithm of the proportion P_i.

SHDI describes overall landscape structure and diversity. The SHDI is a sensitive index to analyze the landscape structure, diversity and heterogeneity in different time periods. The higher SHDI value indicates heterogeneous land use pattern and the higher degree of landscape fragmentation. The percentage of variation of land use land cover classes was calculated and the relationship between the SHDI and landscape diversity assessed (Bai et al. 2008).

10.3.2 Erosion and Accretion in Tidal Fluvial System

Shoreline experiences dynamics changing characteristics due to numerous natural processes and anthropogenic activities. Tidal process, erosion, accretion, sea level rising, wave, and ocean current are the important forces to cause coastal shoreline changes. Coastal shoreline is subjected to erosion and accretion.

Cloud free multi-temporal Landsat imageries were used in accordance with the date and time of high tide to determine the rate of shoreline change. The shoreline was extracted through raster to vector process in Arc GIS software. Digital Shoreline Analysis System (DSAS) extension tool of Arc GIS was used to assess the shoreline change rate (Himmelstoss 2009). Different methods were used by several scholars to calculate the shoreline change such as average of rates (AOR), end point rate (EPR), linear regression (LR), net shoreline movement (NSM), and jackknife (JK) (Hegde and Reju 2007). We applied liner regression to estimate rate of shoreline change over 377 transect drown on 200 m interval for 753 of km coastline Douglas and Crowell (2000) and Himmelstos (2009) also used the same procedure. Each grid was divided into four categories of risk based on shoreline changes.

Net areal changes of land have been analyzed by superimposing the vector layers of different geomorphic units during 1975 and 2015 using satellite images. Below equation was used to delineate the net erosion rate during the study period.

$$\text{Net erosion} = (\text{area eroded} - \text{area deposited})$$

Block-wise rate of erosion

$$\text{ER} = (a_1 - a_2)/t$$

10.4 Result and Discussion

10.4.1 Land Use Land Cover Changes and Ecological Degradation

Land use and land cover maps of Sundarban Biosphere Reserve for 1975, 1990, 2000, and 2015 are shown in Fig. 10.2. The statistics of land use/land cover classes during 1975 and 2015 were calculated and are presented in Table 10.1. Area under mangrove forest in SBR decreased from 22.9% in 1975 to 19.8% in 2015. Strangely during 1975–2015 a total 302.9 km of mangrove forest has been lost over the study periods. But the rate of decline is not static during 1975–1990 the lost of forest cover was 54.7 km^2 with the rate of (2.5%), during 1990–2000 the lost of total forest cover was 116.6 km^2 at the rate of (5.4%) and latest during 2000–2015 the forest cover was lost by 131.7 km^2 at the rate of (6.5%).

A rapid increase in settlement, swamp and waterlogged area and a decrease in vegetation/plantation area were noticed during last 40 years. One of the most conspicuous changes was noticed in waterlogged of upper part of the biosphere reserve which has gone up from 2.7 in 1975 to 9.5% in 2015. The increase in this class of land cover is due to river erosion and inclusion of sea water into the agricultural field particularly in the northern part of the study area. The study further indicates that settlement area has increased from 1.7% in 1975 to 4.8% in 2015 and thus putting pressure on natural recourses of the study area. Reckless cutting of open forest in transition and buffer zones is primarily attributed to this change of land transformation. The area under crop land slightly increased at the rate of 0.5% during 1975 and 1990 but decreased continuously during 1990 to 2015. This is mainly due to inclusion of salinity and coastal erosion in lower part of the reserve while a large scale

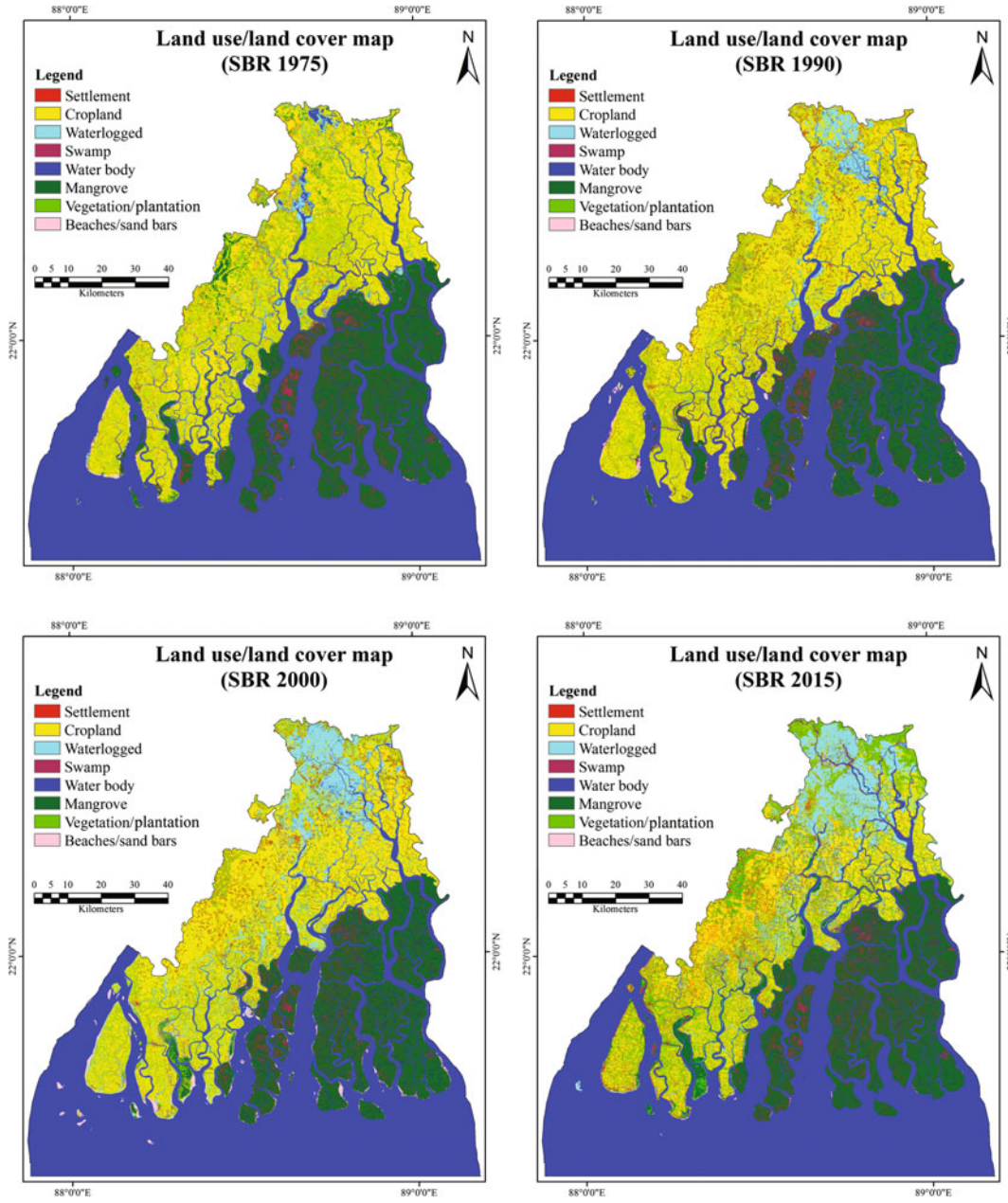

Fig. 10.2 Land use/land cover map of SBR for 1975, 1990, 2000 and 2015

agricultural land was converted into waterlogged area for fishing purpose in the upper part of the Reserve. Area under beaches and sand bars decreased significantly during 2000 and 2015 due to plantation for checking coastal erosion and restoration of mangrove forest (Table 10.2 and Fig. 10.2). Land use/land cover change analysis shows that the total area under swamp has increased from 3.2% in 1975 to 4.1% in 2015 (Table 10.2). The findings revealed that the agricultural area has decreased due to salinization and it has been converted to the waterlogged area

Table 10.1 Land use/land cover of SBR during 1975, 1990, 2000 and 2015

LULC classes	Area 1975		Area 1990		Area 2000		Area 2015	
	Area (km^2)	Area (%)	Area (km^2)	Area (%)	Area (km^2)	Area (%)	Area (km^2)	Area (%)
Water bodies	3343.3	34.7	3307	34.3	3217.8	33.4	3143.2	32.6
Waterlogged	263.2	2.7	377.1	3.9	652.6	6.8	910.2	9.5
Swamp	310.3	3.2	333.1	3.5	360.1	3.7	397.1	4.1
Vegetation/plantation	1202	12.5	1020.6	10.6	946.8	9.8	861.7	8.9
Mangroves	2208.2	22.9	2153.5	22.4	2036.9	21.2	1905.3	19.8
Beaches/sand bars	33.8	0.4	59.3	0.6	60.5	0.6	45.6	0.5
Crop land	2107.1	21.9	2118.1	22	2002.7	20.8	1901	19.7
Settlement	162.9	1.7	261.2	2.7	352.8	3.7	466.6	4.8

Table 10.2 Land use/land cover change

LULC classes	Change (1975–1990)		Change (1990–2000)		Change (2000–2015)	
	Change (km^2)	Change (%)	Change (km^2)	Change (%)	Change (km^2)	Change (%)
Water bodies	−36.2	−1.1	−89.2	−2.7	−74.6	−2.3
Waterlogged	113.9	43.3	275.5	73.1	257.6	39.5
Swamp	22.8	7.3	27.0	8.1	37.0	10.3
Vegetation/plantation	−181.4	−15.1	−73.8	−7.2	−85.1	−9.0
Mangroves	−54.7	−2.5	−116.6	−5.4	−131.7	−6.5
Beaches/sand bars	25.4	75.2	1.2	2.1	−14.9	−24.6
Crop land	11.0	0.5	−115.4	−5.4	−101.7	−5.1
Settlement	98.3	60.3	91.6	35.1	113.8	32.3

and at some places into the prawn cultivation. Mangrove islands facing south are submerging into sea due to strong coastal erosion.

10.4.2 Landscape Matrix and Spatiotemporal Diversity

The landscape diversity and evenness index are mostly used to assessing the richness and evenness of component within an ecological system. Change in landscape is affecting the ecosystem and heterogeneity in the land use patterns. Decrease in area under forest cover and increase in waterlogged area have affected landscape heterogeneity in SBR. The estuarine and creeks have created the landscape patches within the land use/land cover system. Heterogeneity in agricultural landscape is attributed to increase in settlement in northern part of the Reserve. Shannon's Diversity Index (SHDI) and Simpson's Evenness Index (SIDI) for Sundarban biosphere reserve was determine for the period of 1975, 1990, 2000, and 2015. Both diversity and evenness have increased within land use/land cover during 1975–2015. The higher SDHI value indicated high heterogeneity high SIDI values showed high evenness in the land use/land cover patterns (Table 10.3). The uninhabited islands are more diverse than the inhabited islands. High erosion rate was observed in those blocks where SDHI and SIDI values were high.

Table 10.3 SDHI and SIDI vale of Sundarban biosphere reserve

Year	SDHI	SIDI
1975	1.118	0.531
1990	1.293	0.629
2000	1.472	0.718
2015	1.568	0.752

Increase of SDHI is a symbol of increase of landscape patches or proportional distribution of area among patches and land fragmentation.

10.4.3 Erosion and Accretion Dynamics of Sundarban Tidal Fluvial Region

Monitoring of changes in erosion and accretion assumes greater significance in examining the influence of climate change and sea level rise on the coastal ecosystem. Information related to shoreline change can help to further coastal planning and adaptation to climate change. Continuous coastal erosion is reshaping the coastal islands of Sundarban biosphere reserve. Hydraulic system in the study area is eroded due to continuous erosion caused by tidal and wave intensity. The eroded materials were carried out by the tide and deposited in the tidal sheltered of the Bay of Bengal.

The rate of coastal erosion accretion and increased of waterlogged area have been measure for the time period of 1975–2015. The average rate of erosion in SBR was found to be 5.98 km^2/year. Marked variation in the erosion rate was observed in different block and islands (Table 10.4). The uninhabited islands (3.33 km^2/year) have recorded more erosion rate than the inhabited island (2.65 km^2/year) mainly due to protection measures in the form of artificial seawalls and embankments. Further erosion is most dominated in the edge of southern eastern island of the biosphere (Fig. 10.3). Extreme coastal islands like Bhanga duani, Mousani, Dalhousi or Bulcherry, Ghoramara are more prone to coastal erosion. Basically the sandy beaches, mud flats, salt flats and weak coastal zone were severely affected by coastal erosion. Table 10.4 shows area under erosion, accretion and water logging in various different block lying in Sundarban Biosphere Reserve. The erosion rate is much higher in the islands located in the southern part of Sundarban area which is evident from the Figs. 10.4 and 10.5. Namkhana, Pathar patima, sagar, and Gosaba are mostly affected block due to erosion where the rate of erosion is more than 200 m^2. The blocks located in the northern part of the Reserve are affected by water logging due to inclusion of sea water into agricultural land and convert into artificial prawn cultivation. (Fig. 10.4). Haroa, Minakhan, Sandeshkhali-I, Hasnabad, Sandeshkhali-II are mostly affected by the increase of waterlogged area but this area are mostly used by the prawn cultivation by the initiative of various government agencies and NGOs.

10.4.4 Change in Shape and Patterns of Coastal Islands in Deltaic Sundarban

Of the total 377 transects profile over the entire coastline of Sundarban region, 268 transects fall under erosion zone and 109 transects came under accretion zone. The overall coastal shoreline change analysis revealed a range of erosion rate between 0.02 and 149.7 m/y within all grids. The maximum accretion rate was of the order of 37.7 m/y while lowest accretion rate was found to be 0.08 m/y. Generally entire coastline of the study area is dominated by erosion. Only 152.6 km (20.3%) was influenced by accretion (Fig. 10.5). It is further revealed from the Figs. 10.4 and 10.5 that most of southern island is prone to erosion. Lohachara Island has already been vanished from the coast. Ghoramara Island, Jambudwip Island, Holliday Island, Bulcherry Island, and Bhangaduni Island have been subjected to erosion since 1975. Uninhabited islands are more affected by erosion while most of the accretion is occurred within the inhabited islands in eastern part of Sundarban region.

Table 10.4 Block wise erosion and accretion between 1975 and 2015

Dist	Block	Block area (km^2)	Area affected by erosion accretion and water logging (1975–2015)			Rate of change ($meter^2$/year)			Change %		
			Erosion (m^2)	Accretion (m^2)	Waterlogged area (m^2)	Erosion	Accretion	Waterlogged area	Erosion	Accretion	Waterlogged area
N 24 Parganas	Haroa	136	1995	0	48559	50	0.0	1214	1.5	0.00	35.7
	Minakhan	167	3959	0	59600	99	0.0	1490	2.4	0.00	35.7
	Sandeshkhali-I	176	9074	10	66546	227	0.3	1664	5.2	0.01	37.8
	Hasnabad	175	4780	25	50648	119	0.6	1266	2.7	0.01	28.9
	Sandeshkhali-II	196	8541	24	64672	214	0.6	1617	4.4	0.01	33.0
	Hingalganj	195	8170	1	27108	204	0.0	678	4.2	0.00	13.9
S 24 Parganas	Canning I	200	507	97	27439	13	2.4	686	0.3	0.05	13.7
	Canning II	228	994	13	57053	25	0.3	1426	0.4	0.01	25.0
	Basanti	416	5774	94	53064	144	2.3	1327	1.4	0.02	12.8
	Gosaba	344	12227	61	28401	306	1.5	710	3.6	0.02	8.3
	Jaynagar I	138	0	1	565	0	0.0	14	0.0	0.00	0.4
	Jaynagar II	172	8	8	12389	0	0.2	310	0.0	0.00	7.2
	Mathurapur I	156	0	0	1079	0	0.0	27	0.0	0.00	0.7
	Mathurapur II	239	1266	78	20034	32	1.9	501	0.5	0.03	8.4
	Kultali	312	2724	153	31803	68	3.8	795	0.9	0.05	10.2
	Patharpratima	476	5325	245	28457	133	6.1	711	1.1	0.05	6.0
	Kakdwip	243	5821	25	7934	146	0.6	198	2.4	0.01	3.3
	Namkhana	246	18921	90	7153	473	2.2	179	7.7	0.04	2.9
	Sagar	258	15837	174	5904	396	4.4	148	6.1	0.07	2.3
Uninhabited		4266	133232	330	1019	3331	8.3	25	3.1	0.01	0.0
Inhabited		5364	105925	1099	598409	2648	27.5	14960	2.0	0.02	11.2
SBR		9630	239157	1429	599427	5979	35.7	14986	2.5	0.01	6.2

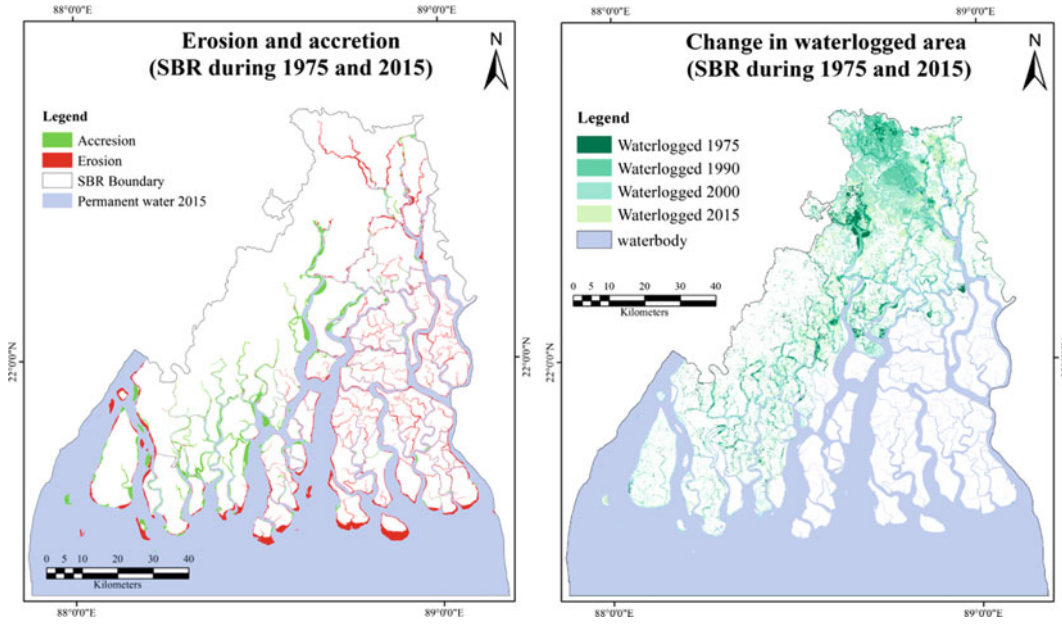

Fig. 10.3 Erosion and accretion and change in waterlogged area in SBR during 1975 and 2015

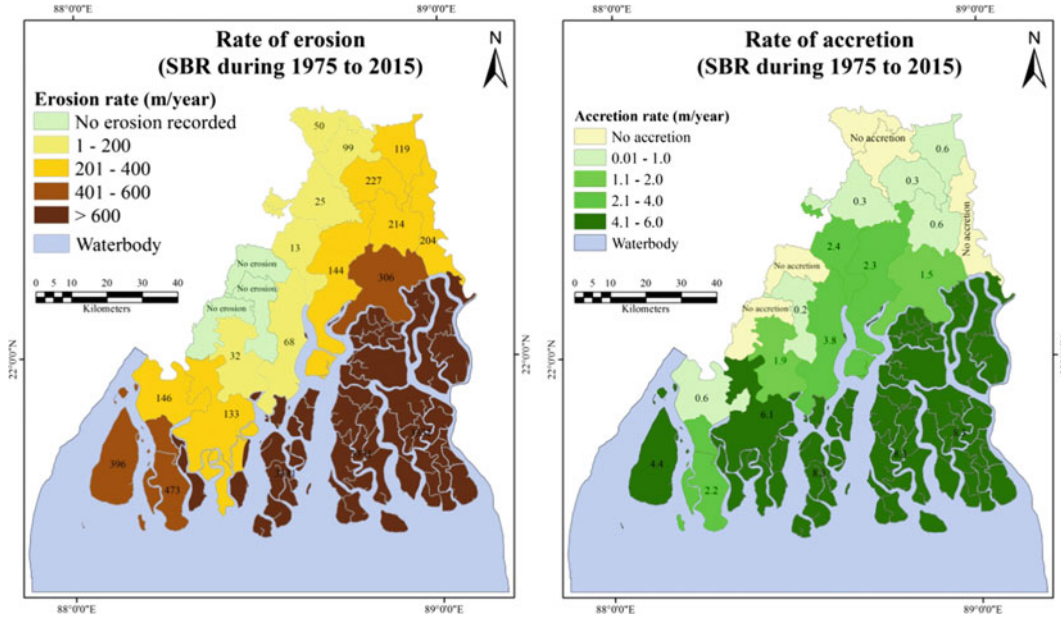

Fig. 10.4 Block (community development block) wise rate of erosion and accretion

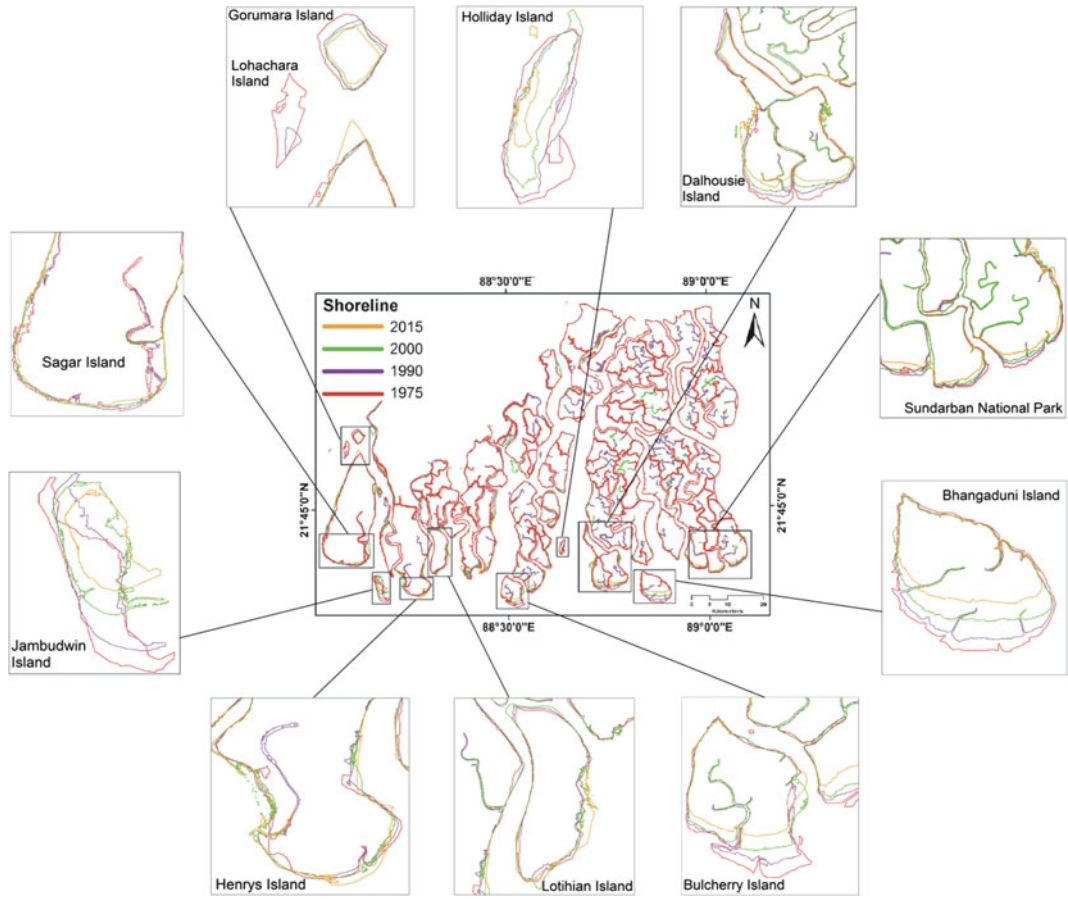

Fig. 10.5 Change in deltaic island of lower Ganga river basin in Indian Sundarban during 1975, 1990, 2000 and 2015

10.5 Conclusion

The Sundarban Biosphere Reserve has changed continuously due to physical and anthropogenic factors. One side the natural processes like high tide rush, relative sea level rise, tropical cyclone, long shore current are continuously change the shape of deltaic island, mangrove swamp, sandy coastal areas on other side infrastructural and development activity like construction of embankment, transformation of island to agri-culture land, river bank dwelling, cutting of mangrove forest are affecting the entire biosphere reserve. The southern islands especially some islands in Sagar, Namkhana and Pathar Patima block have seriously affected by erosion and inclusion of salt water. The extreme edge of the island situated in the southern part of Sundarban Biosphere Reserve are mostly low-lying islands in the mouth reaches of tidal estuaries. The morphological shape of southern islands and the shoreline of these islands are more expose to tidal process, land loss and changing shoreline is a major environmental crisis of this island in Sundarban region. The waterlogged area has increased in the upper part of the Biosphere Reserve due to practice of prawn cultivation for the last 25 years. This commercial cultivation has increased the salinity problem and ecological degradation in the northern part of the Biosphere Reserve. The present methodology used for this

study is providing a logical concept for land fragmentation and diversity of coastal landscape. The methodology and findings of this study may help in providing solution to coastal erosion and accretion.

N.B. In Chap. 11 of this volume, land use, land cover and landform of Sundarbans are identified using satellite standard FCC. Readers can get more about the topic from following chapter.

References

Addo KA (2015) Assessment of the Volta delta shoreline change. J Coast Zone Manage 18(3):1–6. https://doi.org/10.4172/jczm.1000408

Ali A (1996) Vulnerability of Bangladesh to climate change and sea level rise through tropical cyclones and storm surges. Water Air Soil Pollut 94:171–179

Abrishamkesh S, Gorji M, Asadi H (2011) Long-term effects of land use on soil aggregate stability. Int Agrophys 25:103–108

Anderson BJR, Hardy EE, Roach JT, Witmer RE (2001) A land use and land cover classification system for use with remote sensor data. Available from: http://landcover.usgs.gov/pdf/anderson.pdf

Bandyopadhyay S (1997) Natural environmental hazard and their management case study of Sagar Island India. Singap J Trop Geogr 18:20–25. https://doi.org/10.1111/1467-9493.00003

Bandyopadhyay S (2007) Evolution of the Ganga Brahmaputra delta: a review. Geogr Rev India 69 (3):235–268

Bandyopadhyay S, Bandyopadhyay MK (1996) Restrogradation of the Western Ganga-Brahmaputra delta (India and Bangladesh): possible reasons. Natl Geogr 31(1&2):105–128

Bandyopadhyay S, Nandy S (2011) Trends of sea level rise in Hugli estuary, India. Indian J Geomarine Sci 40:802–812

Bandyopadhyay S, Mukherjee D, Bag S, Pal DK, Rudra K (2004) 20th Century evolution of banks and Islands of the Hugli estuary. In: Singh S, Sharma HS, De SK (eds) West Bengal, India: evidence from maps, images and GPS survey, geomorphology and environment. ACB Publications, Kolkata, pp 235–263

Bandyopadhyay J, Mondal I, Samanta N (2014) Shore line shifting of Namkhana Island of Indian Sundarban, South 24 Parganas, West Bengal, India. Using remote sensing and GIS techniques. Int J Eng Sci Res Technol 3(5):162–169

Bai XY, Wang SJ, Xiong KN (2013) Assessing spatial-temporal evolution processes of karst rocky desertification land: indications for restoration strategies. Land Degrad Dev 24(1):47–56

Bai ZG, Dent DL, Olsson L, Schaepman ME (2008) Proxy global assessment of land degradation. Soil Use Manag 24(3):223–234

Basu R (2013) Constraints of biodiversity conservation in the Fragile ecosystems: the case of Sundarban Region in Ganga Delta of India. SIJ Trans Adv Space Res Earth Explor (ASREE) 1(1):26–31

Bia³ousz S, Chmiel J, Fija³kowska A, Ró¿ycki S (2010) The use of satellite imagery and GIS tools in the soil-landscape unit update process- example of small scalestudies (in Polish). Archives Photogrammetry, CartographyRemote Sensing, Land Cover and Landscape Diversity Analysis in the West Polesie Biosphere Reserve 21(15):21–32

Bouwer LM, Crompton RP, Faust E, Ho¨ppe P, Jr Pielke RA (2007) Confronting disaster losses. Science 318:753

Bunn SE, Arthington AH (2002) Basic principles and ecological consequences of altered flow regimes for aquatic biodiversity. Environ manag 30(4):492–507

Census of India (2011) Primary census abstract, census of India, Govt of India

Chakrabarti P (1995) Evolutionary history of the coastal quaternaries of the Bengal plain, India. Proc Indian Nat Sci Acad 61A(5):343–354

Chakraborty S (2013) Delineation of morpho-structural changes of some selected islands in the Ganga delta region, West Bengal, India: a spatio-temporal change detection analysis using GIS and Remote sensing. Int J Sci Nat 4(3):499–507

Chaudhuri AB, Choudhury A (1994) Mangroves of the Sundarban, vol. I, India. The IUCN Wetlands Programme, Bangkok, IUCN

Cornu CE, Sadro S (2002) Physical and functional responses to experimental marsh surface elevation manipulation in Coos Bay's South Slough. Restor Ecol 10(3):474–486

Das PK (1994) Prediction of storm surges in the Bay of Bengal. Proc Indian Natl Sci Acad 60:513–533

Das GK (2006) Sunderbans environment and ecosystem. Sarat Book Distributors, Kolkata, pp 30–73

Das S, Choudhury MR, Das S, Khan S (2013) Monitoring shore line and Inland changes by using multi-temporal satellite data and risk assessment: a case study of Ghoramara Island West Bengal. Int J Geosci Technol 1(1):1–20

Douglas BC, Crowell M (2000) Long-term shoreline position prediction and error propagation. J Coas Research 145–152

Gayathri R, Murty PLN, Bhaskaran PK, Kumar TS (2016) A numerical study of hypothetical storm surge and coastal inundation for AILA cyclone in the Bay of Bengal. Environ Fluid Mech 16(2):429–452

Ghosh A (2012) Living with changing climate Impact, vulnerability and adaptation challenges in Indian Sundarbans. In: Chaudhuri J (ed) Centre for Science And Environment, New Delhi, p 91

Gonnert G, Dube SK, Murty T, Siefert W (2001) Global storm surges: theory, observations and applications. Die Kueste, p 623

Goodbred SL Jr, Kuehl SA, Steckler MS, Sarker MH (2003) Controls on facies distribution and stratigraphic preservation in the Ganges-Brahmaputra delta sequence. Sed Geol 155:301–316

Gustafson EJ (1998) Minireview: quantifying landscape spatial pattern: what is the state of the art? Ecosystems 1(2):143–156

Hazra S, Samanta K, Mukhopadhyay A, Akhand A (2010) Temporal change detection (2001–2008) study of Sundarban (final report). School of Oceanographic Studies, Jadavpur University, Jadavpur

Himmelstoss EA (2009) DSAS 4.0—Installation instructions and user guide. In: Thieler ER, Himmelstoss EA, Zichichi JL, Ergul A, (Eds) The digital shoreline analysis system (DSAS) version 4.0—an arcGIS extension for calculating shoreline change: US geological survey open-file Report 2008–1278, ver. 4.2. p 81. http://pubs.usgs.gov/of/2008/1278/

Islam SN, Gnauck A (2007) Increased salinity in the Ganges delta and impacts on coastal environment in Bangladesh. proceeding of logistics and economic of resource and energy-saving in industries, 12–15 September ISPC. Saratov State Technical University, Saratov, Russia, pp 244–248

Islam SN, Gnauck A (2008) Mangrove wetland ecosystems in Ganges-Brahmaputra delta in Bangladesh. Front Earth Sci China 2(4):439–448. https://doi.org/10.1007/s11707-008-0049-2

Jana A, Sheena S, Biswas A (2012) Morphological change study of Ghoramara Island, Eastern India using multi temporal satellite data. Res J Recent Sci 1 (10):72–81

Kingsford RT (2000) Ecological impacts of dams, water diversions and river management on floodplain wetlands in Australia. Austral Ecol 25(2):109–127

Mallick B, Vogt J (2015) Societal dealings with cyclone in Bangladesh: a proposal of vulnerability atlas for sustainable disaster risk reduction. J Coast Zone Manage 18(3):1–11. https://doi.org/10.4172/jczm.1000409

Mukherjee KN (2002) Sundarban histogenesis, hazards and nemeses, changing environmental scenario of the Indian Sundarban. ACB Publication, Kolkata, pp 263–280

Nagendra H, Munroe DK, Southworth J (2004) From pattern to process: landscape fragmentation and the analysis of land use/land cover change

Paul AK (2002) Coastal geomorphology and environment: Sundarban coastal plain, Kathi coastal plain, Subarnarekha delta plain. ACB Publications, Kolkata, pp 131–559

Poff NL, Zimmerman JK (2010) Ecological responses to altered flow regimes: a literature review to inform the science and management of environmental flows. Freshw Biol 55(1):194–205

Purkait B (2007) Coastal responses to wave dynamics operative in Sagar Island, West Bengal, Unpublished progress report of GSI for FSP 2003–04

Raha AK (2014) Sea level rise and submergence of Sundarban Islands: a time series study of estuarine dynamics. J Ecol Environ Sci ISSN 0976–9900

Sahana M, Sajjad H, Ahmed R (2015) Assessing spatio-temporal health of forest cover using forest canopy density model and forest fragmentation approach in Sundarban reserve forest India. Model Earth Syst Environ 1(4):49

Sahana M, Ahmed R, Sajjad H (2016) Analyzing land surface temperature distribution in response to land use/land cover change using split window algorithm and spectral radiance model in Sundarban Biosphere Reserve India. Model Earth Syst Environ 2(2):81

Sahana M, Hong H, Sajjad H (2018a) Analyzing urban spatial patterns and trend of urban growth using urban sprawl matrix: a study on Kolkata urban agglomeration, India. Sci Total Environ 628–629:1557–1566

Sahana M, Hong H, Sajjad H, Liu J, Zhu AX (2018b) Assessing deforestation susceptibility to forest ecosystem in Rudraprayag district, India using fragmentation approach and frequency ratio model. Sci Total Environ Elsevier 627:1264–1275. https://doi.org/10.1016/j.scitotenv.2018.01.290

Sharma RK, Jhala YV, Qureshi Q, Vattakaven J, Gopal R, Nayak K (2010) Evaluating capture-recapture population and density estimation of tigers in a population with known parameters. Anim Conserv 1:94–103

Sharpe PJ, Baldwin AH (2013) Wetland plant species richness across estuarine gradients: the role of environmental factors and the mid domain effect. Aquat Bot 107:23–32

Uuemaa E, Marc A, Jüri R, Riho M, Ülo M (2009) Landscape metrics and indices: an overview of their use in landscape research. Living Rev Landscape Res 3(1):1–28

Hegde VA, Reju RV (2007) Development of coastal vulnerability index for Mangalore coast, India. J Coas Research 1106–1111

Yu ZK, Geyer RK, Maki CG (2000) MDM2-dependent ubiquitination of nuclear and cytoplasmic P53. Oncogene 19(51):5892

An Inventory for Land Use Land Cover and Landform Identification from Satellite Standard FCC: A Study in the Active Ganga Delta

11

Sunando Bandyopadhyay and Nabendu Sekhar Kar

Abstract

Using the Namkhana region of West Bengal (21° 30′–21° 50′N, 88° 10′–88° 22′E; 670 km^2) as a proxy for the Indian Sundarban, a standard False Colour Composite (FCC) generated from Resourcesat-2 LISS-3 data of 1st January 2014 is used for Ground Truth Verification (GTV) and preparing an inventory of land use, land cover and landform of the region. Photo and spectral characteristics of the land use and land cover types are recorded for eight classes: cropland, fallow, mangroves, orchards, clear water, turbid water, muds and sands. Similarly, photo characteristics of thirteen landform types were also brought out. These include: alluvial plain, channel bar, coastal dune, coastal bar, mangrove swamp, meander, mudflat, palaeochannel, sandy beach, sea, shore zone, swamp and tidal channel. The study should benefit similar works carried out in other areas of Sundarban.

Keywords

Indian Sundarban · Land use land cover classification · Landform classification Satellite data inventory

11.1 Introduction

Land use refers to the way in which the Earth's surface is modified and utilised by the humans. It is largely determined by the functional role of a given land parcel for subsistence and/or economic activities. Land cover stands for the surface characteristics of the Earth, generally unchanged by the humans. Because land use and land cover attributes are sometimes overlapping, separating one from another in a map is often impractical. These two broad aspects of land characteristics are generally grouped together in a 'land use land cover' (LULC) database and map. Landform, on the other hand, represents surface configuration of the Earth that is shaped by the geomorphic processes working on different types of formations. During the last few decades, satellite data of the Earth's surface have become widely available and turned out to be an indispensable tool for LULC extraction on various scales. Satellite images are also widely used for landform identification. The synoptic views provided by the satellite images on

S. Bandyopadhyay
Department of Geography, University of Calcutta, Kolkata 700019, West Bengal, India
e-mail: sunando@live.com

N. S. Kar (✉)
Department of Geography, Shahid Matangini Hazra Government College for Women, Purba Medinipur 721649, West Bengal, India
e-mail: naba1224@gmail.com

B. C. Das et al. (eds.), *Quaternary Geomorphology in India*,
Geography of the Physical Environment, https://doi.org/10.1007/978-3-319-90427-6_11

LULC and landforms are especially useful in study of deltaic islands that are often remote and difficult to access. Taking the Namkhana area as a representative for the deltaic region of Indian Sundarban, this work attempts to provide an inventory for LULC and landform classification from a standard False Colour Composite (FCC) generated from LISS-3 data of Resourcesat-2 satellite.

N.B. Readers are referred to go through Chap. 10 of this volume for further understanding of tidal-fluvial dynamics of deltaic islands and estuarine processes in Indian Sundarban of Lower Ganga River Basin.

11.2 Study Area

The Namkhana region falls in the tidally active lower Ganga–Brahmaputra delta, called Sundarban. In its western (Indian) section, the drainage consists of bidirectional macrotidal creeks and inlets that have lost connection to upcountry rivers due to delta abandonment and are mostly maintained by the tides (Bandyopadhyay et al. 2014). Beginning from the late eighteenth century, the mangrove islands of the region were started to be reclaimed by placing marginal embankments that prevented tidewaters to get in. This stopped the process of deltaic accretion in the island interiors, keeping them forever lower than the highest tide levels. Up till now, about 56% (5366 km^2) of the former tidal wetlands are reclaimed and turned to rice farms and homesteads in the Indian districts of North and South 24-Parganas, West Bengal. The surface sediments of the area are mostly constituted by Holocene silt and clay, with sand in channels and beaches. Notable environmental hazards of the region include coastal flooding due to breach in embankments during equinoctial tides and tropical storms. Besides this, coastal erosion occurs due to abandoned nature of the western Ganga–Brahmaputra delta, especially in the southern seaboard sections like Namkhana. Saline contamination of groundwater is also common. Sea level rise that varies between 4.61 mm $year^{-1}$ at the apex of the Hugli estuary (relative value) to 0.41 mm $year^{-1}$ (absolute value) in the offshore Bay of Bengal adds to the vulnerability of the region to coastal erosion and flooding (Bandyopadhyay et al. 2014; http://sealevel.colorado.edu).

The *Raiyatwari* rule of 1905—a land tenure act in British India—was officially inaugurated with reclamation of the southwestern portion of the 670-km^2 Namkhana region (Ascoli 1921). Bounded by the Baratala on the west and the Saptamukhi on the east (21° 30′–21° 50′N, 88° 10′–88° 22′E; Fig. 11.1), this region is chosen for the present work because it comprises of both forested and reclaimed areas—the two basic types of LULC categories seen in the Sunadarban. With its southern limit facing the Bay of Bengal, Namkhana also represents a region that transforms from an exposed seaboard locality in its south to an interior estuarine environment in the north. Among the islands that constitute the region, Namkhana and Mousuni are mostly reclaimed, while Lothian, Prentice and Jambu are under forests. Several other smaller tidal islets are also found in this estuarine complex, most of which remain non-reclaimed.

11.3 Previous Works

Preparation of land cover and land use inventories in the Sundarban was previously attempted by Nayak and Shaikh (1995) and Nanda et al. (2001) on a regional scale. Although there are quite a few subsequent studies that attempted to classify LULC in various parts of Sundarban (Bandyopadhyay 1997; Nayak 2004; Gopinath and Seralathan 2005; Jayappa et al. 2006; Hazra et al. 2010; Samanta and Hazra 2012; Mondal and Bandyopadhyay 2014; Thomas et al. 2014; Mondal et al. 2015; Kar and Bandyopadhyay 2015), none covered the Namkhana region in detail. Landform identification through FCCs was also not attempted per se.

In the above perspective, the objective of the present study is to generate a detailed inventory of LULC and landform identification keys for the Namkhana region from satellite standard FCCs, which will generally be applicable to the Indian Sundarban region.

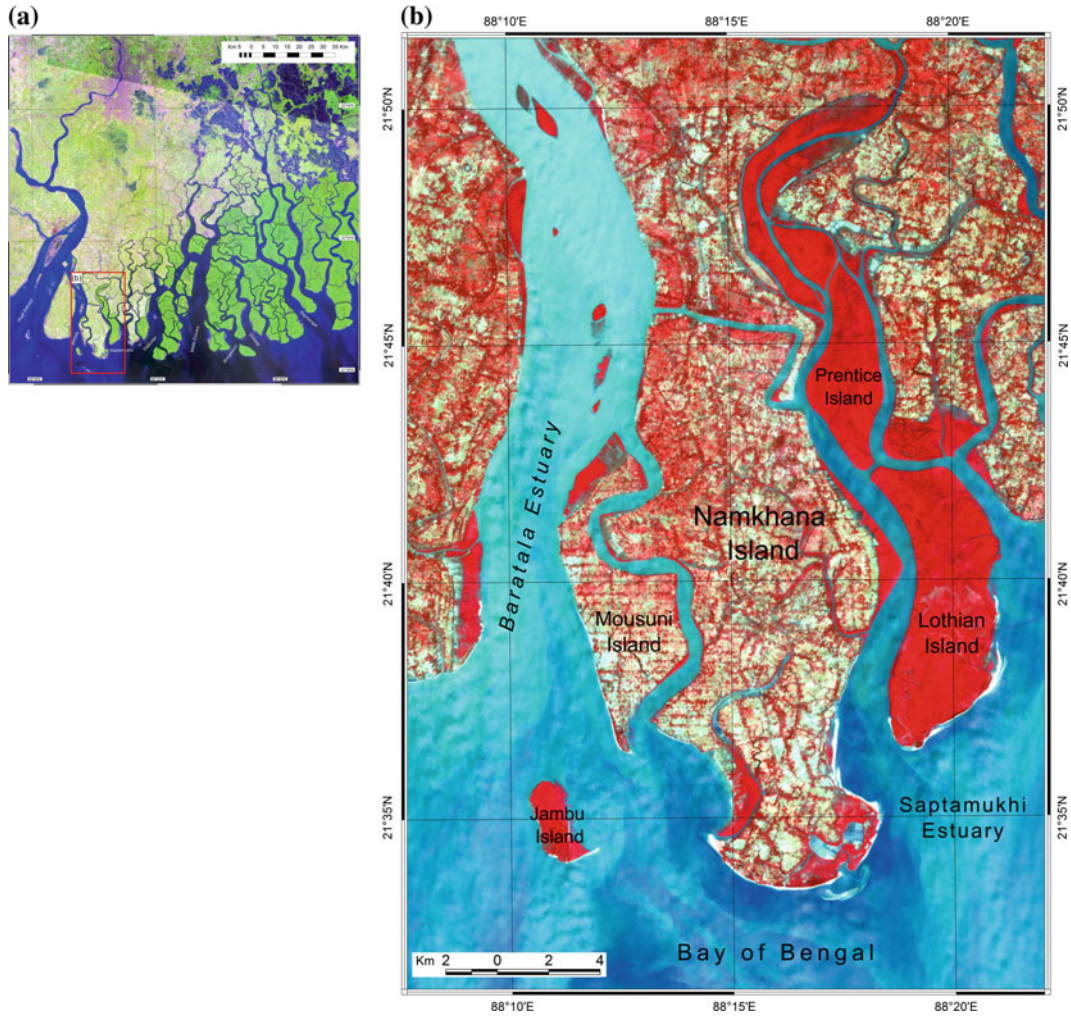

Fig. 11.1 Namkhana region (**b**) is situated between Baratala and Saptamukhi estuaries in the western part of Indian Sundarban (**a**)

11.4 Data Base and Methodology

The study is done with Resourcesat-2 LISS-3 data (Path: 108, Row: 56) of 1st January 2014, using PCI Geomatica 2012 software. First, a standard FCC is prepared and extensive Ground Truth Verification (GTV) is carried out with it using a Garmin eTrex-10 Global Navigational Satellite System receiver, which provides an accuracy level of ±5 m. This helped to sort out the major LULC classes seen in the region and to identify their photo characteristics in the standard FCC, in respect of tone, texture, shape, size, pattern and association. Subsequently, a supervised Maximum Likelihood Classification is run with the LULC classes already selected for the region to get their spectral characteristics. These include: mean and standard deviation of digital numbers across the four LISS-3 bands of green (0.52–0.59 μm), red (0.62–0.68 μm), near infrared (0.77–0.86 μm) and shortwave infrared (1.55–1.70 μm). The overall accuracy of the classification was 76% (Fig. 11.2). In addition to this, major landform types were also observed during the GTV sessions. Based on this, another

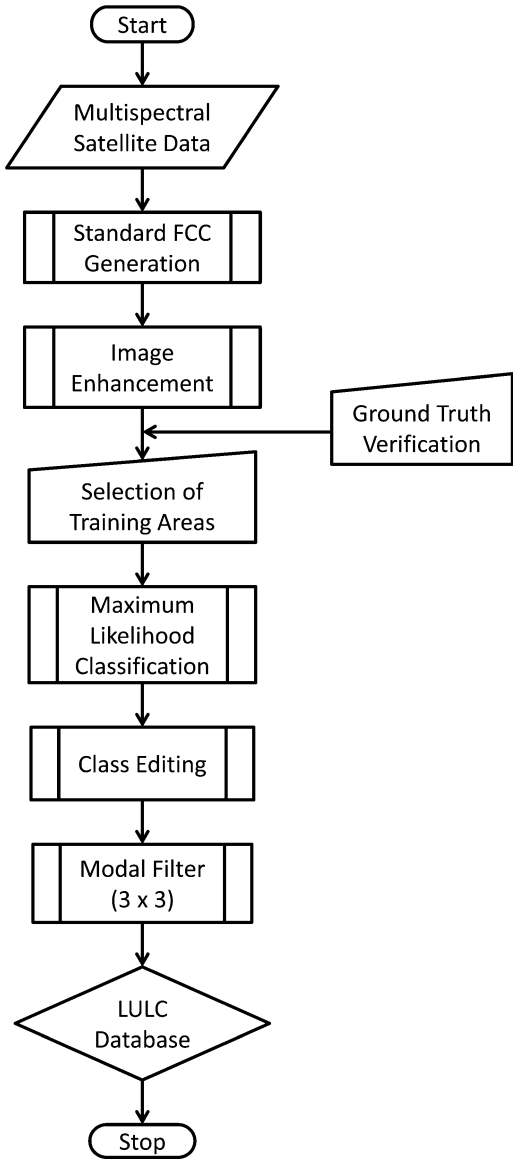

Fig. 11.2 Flowchart showing main components of the workflow for LULC database derivation

inventory is prepared to identify the major landforms from a standard FCC.

For LULC categories, an inventory is prepared here based on the NRSC/ISRO (2011) and SAC (SAC-ISRO 2010) schemes of broad LULC classes. For landforms, the classification is developed specifically for the Sundarban region.

11.5 Results

Eight LULC classes are identified from the analysis: cropland, fallow, mangroves, muds, orchards, clear water, turbid water and sands (Figs. 11.3 and 11.4). Table 11.1 summarises the results and LULC class identification keys on standard FCCs. The classes may be described as follows.

(1) *Cropland*: Represents area under crops. Summer paddy (*aman*) is extensively cultivated all over the alluvial plains. Farming of winter crops (*rabi*: paddy and vegetables) are confined only close to the sources of water. The areas under cropland and fallow land together account for the total area under agriculture and extension of one grows at the expense of the other.

(2) *Fallows* are almost absent towards the end of *aman* season in November. In winter (January), however, this class covers most of the interior plains barring isolated pockets close to the freshwater ponds and canals.

(3) *Mangroves* are found in reserved forests of the forest-covered islands (mangrove swamps). Principal species of mangroves seen in the Namkhana area include *Exocoercea agallocha, Phoenix paludosa*, *Avicenna* sp., etc.

(4) *Muds*: Muddy area, mainly associated with tidal flats of coasts and estuaries as well as waterlogged areas of alluvial plains and dune slacks. This LU/LC class is distinct from the landform class of 'Mudflats', which is restricted mainly to the coastal areas.

(5) *Orchards*: This category represents (a) the village orchards associated with rural habitations. They basically include woody trees like mango (*Mangifera indica*), jackfruit (*Artocarpus heterophyllus*), banyan (*Ficus benghalensis*), etc. and groves of bamboos (*Bambusoideae* sp.). The rural homesteads, courtyards and tiny ponds are often difficult to distinguish from this amalgamation at the resolution of LISS-3 (c. 24 m). This class is

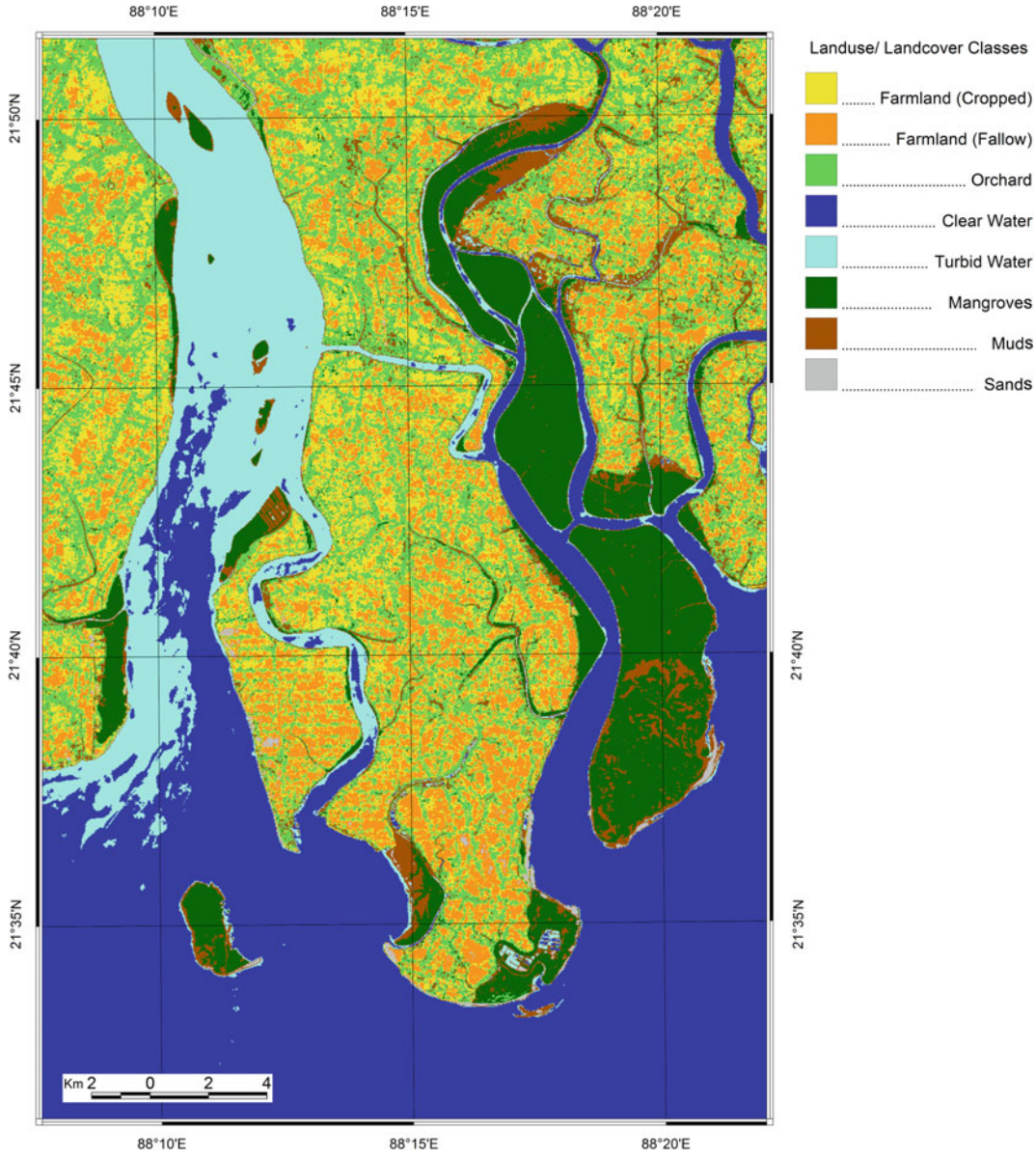

Fig. 11.3 LULC map of Namkhana region prepared from Resourcesat-2 LISS-3 data of 1st January 2014

also seen as (b) coastal afforestation projects on frontal dunes involving *Casuarina equisetifolia*.

(6) *Sands*: Areas occupied by beaches, frontal dunes and bare interior dunes where sands dominate.

(7) *Water (Turbid)*: Any depression that mainly contains stagnant water with low suspended sediments: palaeochannels, impounded canals and creeks, village ponds and near-shore seawater.

Fig. 11.4 Major LULC classes of Namkhana region identified from satellite data and GTV

(8) *Water (Clear)*: Any depression that mainly contains flowing water with high suspended sediments: active canals, creeks, seawater away from the shore.

Thirteen landform types were identified in the Namkhana region. These include alluvial plain, channel bar, coastal dune, coastal bar, mangrove swamp, meander, mudflat, palaeochannel, sandy beach, sea, shore zone swamp and tidal channel (Fig. 11.5). Table 11.2 summarises the identification keys for the major landforms of the study area in standard FCCs, verified by ground survey. A brief description of the landforms identified from the Namkhana region is given below.

(1) *Alluvial Plain*: An embanked and reclaimed tract formed from the deposition of

Table 11.1 LISS-3 (Resourcesat-2) data interpretation key for land use/land cover feature identification in Baratala–Saptamukhi estuarine complex (based on GTV of standard FCC)

LU/LC class	Colour/signature statistics[a]	Tone	Texture	Shape	Size	Pattern	Association
(1) Cropland	Pink (nascent growth) to red (mature growth) Green band: 88 (σ3.7) Red band: 50 (σ3.2) NIR band: 71 (σ6.2) SWIR band: 60 (σ4.8) No of training pixels: 634	Light to medium	Smooth to coarse	Irregular, at places patchy	Small to medium (January), large to very large (November)	Continuous to disjointed	Fallow land, water body and orchards
(2) Fallow	Yellowish grey (dry) to greenish grey (moist) Green band: 96 (σ2.5) Red band: 63 (σ2.4) NIR band: 61 (σ2.7) SWIR band: 88 (σ6.5) No of training pixels: 3873	Light to medium	Medium to coarse: Occurring mainly due to differences in ground moisture content as well as coexistence of small patches of different LU classes	Irregular, at places patchy	Very small to small (November), large to very large (January)	Continuous to disjointed	Cropland, water body and orchards
(3) Mangroves	Red Green band: 82 (σ2.3) Red band: 43 (σ1.4) NIR band: 69 (σ4.8)	Medium	Fine (smooth)	Well-defined ovals and smooth-edged polygons. Tend to be surrounded by water	Small to medium	Continuous	Waterbody and mudflat

(continued)

Table 11.1 (continued)

LU/LC class	Colour/signature statistics[a]	Tone	Texture	Shape	Size	Pattern	Association
	SWIR band: 35 (σ2.7) No of training pixels: 1005						
(4) Muds	Grey, grey–brown Green band: 91 (σ2.8) Red band: 52 (σ2.3) NIR band: 46 (σ5.0) SWIR band: 29 (σ6.7) No of training pixels: 2489	Medium to dark	Fine	Linear in coastal locations; elsewhere irregular in appearance resembling sharp-edged polygons	Small to medium	Continuous	Waterbody, mangroves and sandy area
(5) Orchards	Red, brownish red Green band: 81 (σ3.2) Red band: 44 (σ3.0) NIR band: 56 (σ4.4) SWIR band: 47 (σ5.7) No of training pixels: 4419	Medium to dark	Coarse to very coarse: Mainly because of mixing of many species of vegetation with different crown density and reflectivity	Circular, oval and linear. Branching and/or interlacing where grow on natural levees, embankments and interior dunes	Small to very large	Continuous, sometimes patchy	Cropland, fallow land and water body
(6) Sands	Bluish white to yellowish white Green band: 151 (σ12.3) Red band: 113 (σ11.5)	Light	Fine	Linear in coastal areas (beaches and frontal dunes). Oval to elongated oval in interior areas (reactivated sand)	Small to medium	Continuous	Waterbody and mudflat

(continued)

Table 11.1 (continued)

LU/LC class	Colour/signature statistics[a]	Tone	Texture	Shape	Size	Pattern	Association
	NIR band: 100 (σ10.5) SWIR band: 138 (σ13.2) No of training pixels: 596						
(7) Water: turbid	Cyan Green band: 115 (σ1.8) Red band: 70.4 (σ2.0) NIR band: 38.9 (σ4.7) SWIR band: 8.5 (σ5.9) No of training pixels: 17,284	Light	Very fine	Liner (canals) meandering and branching (rivers), rectangular and oval (ponds), large polygons that tend to occupy one or more side(s) of an image (sea)	Very small (village tank) to very large (sea)	Continuous	Associated with all other LU/LC classes
(8) Water: clear	Blue–black (clear) Green band: 108.7 (σ5.1) Red band: 57.6 (σ4.5) NIR band: 24.6 (σ1.8) SWIR band: 8.3 (σ2.6) No of training pixels: 10,217	Dark	Very fine	As above	As above	Continuous	Associated with all other LU/LC classes

[a]Includes mean digital number of training pixels across four LISS-3 bands with standard deviation (σ). Based on 1st January 2014 data

Fig. 11.5 Major landforms of Namkhana region identified from satellite data and GTV

sediments from tidal creeks. Used for extensive summer cropping (*aman*) and winter cropping (*rabi*) in isolated patches close to water sources. Standing water may also be noticed in images of post-monsoon season. Therefore, signature may reflect any of the three ground conditions: fallow, cropped or waterlogged.

(2) *Channel Bar*: A flat-topped ridge-like accumulation of alluvium in the channel, along the banks, or at the mouth of a creek. May be formed of sand (high reflection) or mud (low to diminutive reflection). Mud bars are often colonised by vegetation like mangroves in intertidal areas.

(3) *Coastal Dune*: A mobile or stationary linear mound of windblown sands found along coasts and in the shore zone. The frontal dunes formed in the backshore are often active and devoid of any vegetation. At places, they are stabilised by extensive casuarina afforestation.

Table 11.2 LISS-3 (Resourcesat-2) data interpretation key for landform feature identification in Baratala–Saptamukhi estuarine complex of Indian Sundarban (based on GTV of standard FCC)

LF class	Colour	Tone	Texture	Shape	Size	Pattern	Association
(1) Alluvial plain	*Fallow*: Yellowish grey (dry) to greenish grey (moist) *Cropped*: Pink (nascent growth) to red (dense growth) *Waterlogged*: Grey to brownish grey	*Fallow*: Light *Cropped*: Light *Waterlogged*: Dark	Coarse to very coarse: Many types of elements sometimes coexist in the alluvial plain, ranging from ponds to isolated homesteads. Differences in moisture content of soils also lead to a mosaic of tones and colours	Irregular, at places, patchy	Large to very large. Tends to be small in fragmented areas. This class is the most extensive landform feature of deltas and coastal interiors	Continuous to disjointed	Riverine channels, meander, natural levee and swamp
(2) Channel bar	*Sandbar*: White to bluish–white *Mud bar*: Grey *Vegetated mud bar*: Red	*Sandbar*: Light *Mud bar*: Medium *Vegetated mud bar*: Light to dark	Generally fine but may appear coarse if repeatedly intersected by creeks and waterways	Well-defined oval to elongated oval (mid-channel bar). Delta-shaped when attached to riverbank (point bar)	Small to very small	Continuous and well-defined	Riverine channels
(3) Coastal dune	*Frontal dunes*: White to yellowish white *Afforested frontal dunes*: Red	*Frontal dunes*: Light *Afforested frontal dunes*: Dark	Fine to medium	Linear/elongated. Interior dunes may show branching or interlacing occurrences	Large	Mostly continuous; disjointed in isolated occurrences	Sandy beach, shore zone and alluvial plain
(4) Coastal bar	Bluish–white, grey. Alternate bands of grey and white common in bars with ridge-and-runnel topography	Light	Medium to fine.	Circular to elongated oval	Small	Mostly disjointed	Sea
(5) Mangrove swamp	Red	Medium	Fine (or smooth)	Well-defined oval to elongated oval islands	Small to large	Continuous	Riverine channels, meander

(continued)

Table 11.2 (continued)

LF class	Colour	Tone	Texture	Shape	Size	Pattern	Association
							and mudflats
(6) Meander	Blue (sediment-free) to cyan (sediment-rich)	Light	Fine (or smooth)	Linear and smoothly curving from one side to the other (meandering)	Small (creeks) to very large (major streams)	Always continuous	Channel bar, alluvial plan and natural levee
(7) Mudflat	*Bare mudflat*: Grey, grey–brown. *Vegetated mudflat*: Reddish grey, brown	Medium, dark	Fine	Linear	Medium	Continuous	Sea, sandy beach and river channel
(8) Palaeochannel	Greenish grey, blush grey. Bright red if covered with water hyacinths	Medium to dark. In its subtle expression, slightly darker than surroundings (due to higher moisture content)	Fine to medium in general. Tends to be coarse if the palaeochannel bed is wide and characterised by diverse land use	Linear: May also display meandering and/or branching configuration	Small to large	Continuous	Alluvial plain
(9) Tidal channel	Blue (sediment-free) to cyan (sediment-rich)	Light	Fine (or smooth)	Linear, maybe branching and meandering	Small (creeks) to very large (major streams)	Always continuous	Channel bar, alluvial plain
(10) Sandy beach	White (dry), bluish white (moist)	Very light	Fine (or smooth)	Linear	Medium to large	Linear	Sea, mudflat and coastal dune

(continued)

Table 11.2 (continued)

LF class	Colour	Tone	Texture	Shape	Size	Pattern	Association
(11) Sea	Blue or blue–black (sediment-free) to cyan (sediment-rich)	Dark to light	Very fine	Massive: Tends to fully occupy one side of the image	Very large	Always continuous	Sandy beach, mudflat and offshore bar
(12) Shore zone	Yellowish grey (dry) to greenish grey (moist)	Light	Medium to coarse	Irregular and patchy	Medium to large	Continuous or fragmented	Riverine channels, coastal dune and swamp
(13) Swamp	Black, grey and blue	Dark	Fine to medium	Linear and circular with irregular outline	Small to medium	Continuous	Alluvial plain, shore zone and coastal dune

(4) *Coastal Bar*: Narrow and disjointed bodies of sand and/or mud running parallel to the mainland, mostly intertidal.
(5) *Mangrove Swamp*: A tidally flooded bottomland with more woody mangrove plants than a vegetated mudflat and better drainage than a bog.
(6) *Meander*: A meander is a large bend in the course of a channel. It usually has a steep bank on the outside of the bend and a gentler slope on the inside of the curve.
(7) *Mudflat*: Low-lying muddy land that gets inundated at high tide and becomes exposed at low tide. May possess some grasses like *Porteresia coarctata* (dhani grass).
(8) *Palaeochannel*: Remnant of a decayed or plugged creek that used to flow through the reclaimed alluvial plains. These old (palaeo) courses are often conspicuously indicated by linear water bodies, rarely surrounded by diminutive natural levees. However, in some cases, they are subtly connoted by linear and meandering/branching dark patches on otherwise featureless interior plains.
(9) *Tidal Channel*: A bidirectional natural stream of tidewater connected to the sea or a creek.
(10) *Sandy Beach*: The intertidal zone above the low water line at the land–sea interface, marked by an accumulation of sand that has been deposited by the tide or waves.
(11) *Sea*: The continuous body of saltwater covering most of the Earth's surface, regarded as a geophysical entity distinct from Earth and sky.
(12) *Shore Zone*: The land along the edge of the sea: the littoral zone. Morphologically akin to bare (fallow) alluvial plain.
(13) *Swamp*: A lowland region saturated with water, commonly occurs in alluvial plains and shore zones. Presence of aquatic vegetation common.

11.6 Concluding Notes

The LULC and landform inventories proposed here are derived from the Namkhana area. However, because the land use, land cover and landform characteristics are mostly the same in the rest of Indian Sundarban, they can be used for the entire region as well as in similar areas of the world. The spectral characteristics of the four LISS-3 bands correspond well to Bands 2–5 of Landsat TM/ETM+ sensors and Bands 3–6 of Landsat OLI sensor, both extensively used by planners and researchers. Therefore, the proposed inventory, based on photo as well as spectral characteristics, should be equally useful in any work that involves the above Landsat bands.

References

Ascoli FD (1921) A Revenue History of Sundarban, vol 2. West Bengal District Gazetteers, Kolkata, 218 p. 2002 reprint

Bandyopadhyay S (1997) Coastal erosion and its management in Sagar Island, South 24 Parganas, West Bengal. Indian J Earth Sci 24(3–4):51–69

Bandyopadhyay S, Kar NS, Das J, Sen J (2014) River systems and water resources of West Bengal: a review. Geol Soc India Spl Publ 3:63–84

Gopinath G, Seralathan P (2005) Rapid erosion of the coast of Sagar island, West Bengal, India. Environ Geol 48:1058–1067

Hazra S, Samanta K, Mukhopadhyay A, Akhand A (2010) Final report on temporal change detection (2001–2008): study of Sundarban. School of Oceanographic Studies, Jadavpur University, 127 p. Retrieved on 2016-02-04 from: http://www.iczmpwb.org/main/pdf/ebooks/WWF_FinalReportPDF.pdf

Jayappa KS, Mitra D, Mishra AK (2006) Coastal geomorphological and land-use and land-cover study of Sagar. Int J Remote Sens 27(17):3671–3682

Kar NS, Bandyopadhyay S (2015) Tropical storm Aila in Gosaba block of Indian Sundarban: remote sensing based assessment of impact and recovery. Geogr Rev India 77(1):40–54

Mondal I, Bandyopadhyay J (2014) Coastal zone mapping through geospatial technology for resource management of Indian Sundarban, West Bengal, India. Int J Remote Sens Appl 4(2):103–112

Mondal I, Bandyopadhyay J, Chakrabarti P, Santra D (2015) Morphodynamic change of Fraserganj and Bakkhali coastal stretch of Indian Sundarban, South 24 Parganas, West Bengal, India. Int J Remote Sens Appl 5:1–10

Nanda JB, Mukherjee K, Bhattacharyya S, Chauhan HB, Nayak S (2001) Landuse mapping of the West Bengal coastal regulation zone. Space Application Centre, Indian Space Research Organisation, Ahmedabad, p 72

Nayak S (2004) Role of remote sensing to integrated coastal zone management. In: Altan O (ed) Proceedings

of 20th ISPRS congress, technical commission 7, pp 1232–1243. Retrieved on 2016-02-04 from: www.isprs.org/proceedings/XXXV/congress/comm7/papers/235.pdf

Nayak S, Shaikh MG (1995) Coastal land use mapping of West Bengal coast for brackish water aquaculture site selection. Space Application Centre, Indian Space Research Organisation, Ahmedabad, p 13

NRSC/ISRO: National Remote Sensing Centre / Indian Space Research Organisation (2011) Natural Resource Census: land use land cover database, Tech Rep v. 1, land use and land cover monitoring division, 9 p. Retrieved on 2016-02-04 from: http://bhuvan.nrsc.gov.in/gis/thematic/tools/document/LULC/PB.pdf

SAC-ISRO: Space Application Centre – Indian Space Research Organisation (2010) National Wetland Atlas—West Bengal. Ministry of Environment and Forest. Ahmedabad. Retrieved on 2016-02-04 from: www.envfor.nic.in/downloads/public-information/NWIA_WB_Atlas.pdf

Samanta K, Hazra S (2012) Landuse/landcover change study of Jharkhali island Sundarbans. Int J Geomat Geosci 3(2):299–203

Thomas JV, Arunachalam S, Jaiswal R, Diwakar PG, Kiranc B (2014) Dynamic land use and coastline changes in active estuarine regions—a study of Sundarban delta. The International Archives of the Photogrammetry, Remote Sensing and Spatial Information Sciences, XL-8. ISPRS Tech Com VIII Symp, Hyderabad: 133–139. Retrieved on 2016-04-17 from: http://eproofing.springer.com/books_v2/mainpage.php?token=ut24s3XxTlqU9v8K1apOxFjATFG1s_kTYN9ep2A3zGc

Index

B. C. Das et al. (eds.), *Quaternary Geomorphology in India*,
Geography of the Physical Environment, https://doi.org/10.1007/978-3-319-90427-6